Royal Norwegian Council
for Scientific and Industrial Research
(NTNF)

NORSAR

NORSAR Scientific Report No. 2-92/93

Semiannual Technical Summary

1 October 1992 — 31 March 1993

Kjeller, July 1993

NORSAR Scientific Report No. 2-92/93

Semiannual Technical Summary

1 October 1992 — 31 March 1993

Kjeller, July 1993

ICLASSIFIED
Y CLASSIFICATION OF THIS PAGE

REPORT DOCUMENTATION PAGE

ORT SECURITY CLASSIFICATION **NCLASSIFIED**	1b RESTRICTIVE MARKINGS **NOT APPLICABLE**
URITY CLASSIFICATION AUTHORITY **OT APPLICABLE**	3 DISTRIBUTION / AVAILABILITY OF REPORT **APPROVED FOR PUBLIC RELEASE** **DISTRIBUTION UNLIMITED**
LASSIFICATION / DOWNGRADING SCHEDULE **OT APPLICABLE**	
ORMING ORGANIZATION REPORT NUMBER(S) ntific Report 2-92/93	5. MONITORING ORGANIZATION REPORT NUMBER(S) Scientific Report 2-92/93
ME OF PERFORMING ORGANIZATION F/NORSAR — 6b OFFICE SYMBOL *(If applicable)*	7a. NAME OF MONITORING ORGANIZATION HQ/AFTAC/TTS
DRESS (City, State, and ZIP Code) Box 51)07 Kjeller, Norway	7b ADDRESS (City, State, and ZIP Code) Patrick AFB, FL 32925-6001
ME OF FUNDING / SPONSORING GANIZATION Advanced earch Projects Agency — 8b. OFFICE SYMBOL *(If applicable)* NMRO	9 PROCUREMENT INSTRUMENT IDENTIFICATION NUMBER
DRESS (City, State, and ZIP Code) 1 N. Fairfax Dr. #717 gton, VA 22203-1714	10 SOURCE OF FUNDING NUMBERS

PROGRAM ELEMENT NO	PROJECT NO	TASK NO	WORK UNIT ACCESSION NO.
R&D	NORSAR Phase 3	SOW Task 5.0	Seq.no. 003A2

LE *(Include Security Classification)*

IANNUAL TECHNICAL SUMMARY, 1 OCTOBER 1992 - 31 MARCH 1993 (UNCLASSIFIED)

RSONAL AUTHOR(S)

PE OF REPORT	13b. TIME COVERED	14. DATE OF REPORT (Year, Month, Day)	15. PAGE COUNT
ntific Summary	FROM 1 Oct 92 TO 31 Mar 93	Jul 1993	142

PLEMENTARY NOTATION

OT APPLICABLE

COSATI CODES			18. SUBJECT TERMS *(Continue on reverse if necessary and identify by block number)*
ELD	GROUP	SUB-GROUP	**NORSAR, Norwegian Seismic Array**
8	11		

STRACT *(Continue on reverse if necessary and identify by block number)*

This Semiannual Technical Summary describes the operation, maintenance and research activities at the Norwegian Seismic Array (NORSAR), the Norwegian Regional Seismic Array (NORESS), the Arctic Regional Seismic Array (ARCESS) and the experimental Spitsbergen regional array for the period 1 October 1992 -31 March 1993. Statistics are also presented for additional seismic stations, which through cooperative agreements with institutions in the host countries provide continuous data to the NORSAR Data Processing Center (NPDC). These stations comprise the Finnish Experimental Seismic Array (FINESA), the German Experimental Seismic Array (GERESS), and an experimental regional seismic array in Apatity, Russia.

(cont.)

STRIBUTION / AVAILABILITY OF ABSTRACT UNCLASSIFIED/UNLIMITED ☐ SAME AS RPT. ☐ DTIC USERS	21. ABSTRACT SECURITY CLASSIFICATION
IAME OF RESPONSIBLE INDIVIDUAL Michael C. Baker	22b. TELEPHONE (Include Area Code) (407) 494-7665 — 22c. OFFICE SYMBOL AFTAC/TTS

ORM 1473, 84 MAR — 83 APR edition may be used until exhausted. All other editions are obsolete.

SECURITY CLASSIFICATION OF THIS PAGE
UNCLASSIFIED

Abstract (cont.)

This Semiannual Report also presents statistics from operation of the Intelligent Monitoring System (IMS). The IMS has been operated in an experimental mode, and the performance has been very satisfactory. Since October 1991, a new version of the IMS that accepts data from an arbitrary number of arrays and single 3-component stations has been operated.

The NORSAR Detection Processing system has been operated throughout the period with an average uptime of 97.8% as compared to 96.7% for the previous reporting period. A total of 1733 seismic events have been reported in the NORSAR monthly seismic bulletin. The performance of the continuous alarm system and the automatic bulletin transfer by telex to AFTAC has been satisfactory. The system for direct retrieval of NORSAR waveform data through an X.25 connection has been tested successfully for acquiring such data by AFTAC. Processing of requests for full NORSAR and regional array data on magnetic tapes has progressed according to established schedules. There have been no modifications made to the NORSAR data acquisition system.

On-line detection processing and data recording at the NORSAR Data Processing Center (NDPC) of NORESS, ARCESS, FINESA and GERESS data have been conducted throughout the period. Data from two experimental small-aperture arrays at sites in Spitsbergen and Apatity, Kola Peninsula, have been recorded and processed in an experimental mode. Monthly processing statistics for the arrays as well as results of the IMS analysis for the reporting period are given.

Maintenance activities in the period comprise preventive/corrective maintenance in connection with all the NORSAR subarrays, NORESS and ARCESS. In addition, the maintenance center has been involved with occasional maintenance of equipment for FINESA. Other activities have involved testing of the NORSAR communications systems and work in connection with the experimental small-aperture arrays in Spitsbergen and the Kola Peninsula.

Starting 1 October 1991, an effort began to carry out a complete technical refurbishment of the NORSAR array. This project is funded jointly by AFTAC, ARPA and NTNF. During the reporting period, efforts have focused upon evaluation and laboratory testing of technical options for field instrumentation, in particular state-of-the-art A/D converters, data acquisition and synchronization devices. During the reporting period, we have also been testing several such systems under realistic operating conditions in the field. When these studies have been completed, a recommendation for a system to be installed will be presented to the funding agencies.

Summaries of six scientific contributions are presented in Chapter 7 of this report.

Section 7.1-7.3 describe the basic principles and give examples of application of a promising new approach to automatic analysis of events from sites with recurring seismic activity. This method, which we have called "intelligent post-processing of seismic events" is particularly well suited to implement as a post-event processing technique in the Intelligent Monitoring System.

Section 7.1 describes the basic principles of this approach. From experience with analyst review of events automatically defined by the Intelligent Monitoring System (IMS), we have realized that the quality of the automatic event locations can be significantly improved if the event intervals are reprocessed with signal processing parameters tuned to phases from events in the given region. The tuned processing parameters are obtained from off-line analysis of events located in the region of interest. The primary goal of such intelligent post-processing is to provide event definitions of a quality that minimizes the need for subsequent analysis and review.

The first step in this post-processing is to subdivide the area to be monitored in order to identify sites of interest. Clearly, calibration will be easiest and potential savings in manpower are largest for areas with high, recurring seismic activity. We have identified 8 mining sites in Fennoscandia/W. Russia/Estonia and noted that 65.6 per cent of the events of $M_L > 2.0$ in this region can be associated with one of these sites. This result is based on 1 1/2 years of data.

Section 7.2 describes the second step in the post-processing approach. This second step is to refine the phase arrival time and azimuth estimates using frequency filters and processing parameters that are tuned to the initial event location provided by the IMS. We have studied, as a first example, a set of 58 events from the Khibiny Massif in the Kola peninsula. Very accurate locations of these events has been provided by the Kola Regional Seismological Centre. Our refinement of phase arrival times for these events, as recorded in Apatity and at ARCESS, have given quite remarkable results. Using the autoregressive likelihood technique of Pisarenko et al (1987) we have been able to estimate onset times automatically to an accuracy (standard deviation) of about 0.05 s for P-phases and 0.15-0.20 s for S-phases. These accuracies are as good as for analyst picks, and are considerably better than in the current SigPro analysis.

Section 7.3 describes the third step in the post-processing approach. This third step in the post-processing is a recomputation of the location estimate, using the refined arrival times and broad-band azimuths associated with a fixed frequency band (tied to the initial IMS location). Again using the set of 58 known Khibiny Massif events as a reference, we have investigated the accuracy of the LocSat location procedure using varying amounts of regional corrections. Using a depth constrained to 0, we find that the epicenter can be estimated to 2-3 km accuracy (median value), with "worst case" error less than 10 km, even without any regional corrections. It is noted that the method needs to be tested for additional target sites before firm conclusions can be drawn.

Section 7.4 describes a four-month monitoring experiment, using the Continuous Threshold Monitoring technique applied to the Novaya Zemlya test site. Data from the NORESS, ARCESS and FINESA regional arrays were used. Starting 1 December 1992, we have been compiling daily statistics of all peaks on the threshold diagram exceeding $m_b = 2.75$, and associating these peaks to regional or teleseismic events whenever possible. In addition, we are analyzing smaller peaks (below $m_b = 2.75$) that can possibly be associated with Novaya Zemlya epicenters.

We have conducted extensive analysis of the $m_b = 2.5$ seismic event at Novaya Zemlya at 09.29.25 GMT on 31 December 1992. This event was detected by ARCESS (P and S), Spitsbergen (P and S), NORESS (P) and Apatity (S). In addition, the Kola Regional Seismological Centre provided readings for the station Amderma (Pg and Sn) made from analog recordings. Our results indicate that the epicenter was slightly to the north of the northern Novaya Zemlya test site. However, there are some uncertainties in the travel time tables, and an on-site location cannot entirely be ruled out.

Section 7.5 contains some initial processing results from the Spitsbergen array. Preliminary analysis of data from this new small-aperture (1km) array on the Arctic island of Spitsbergen has revealed a large variation in signal and noise amplitudes across the array.. Further investigations are needed in order to determine the reason for this variation, and it may prove necessary to redeploy one or more of the array sensors. Site B2 in this array exhibits a particularly favorable signal focusing for nearly all arrival azimuths. Initial studies of the noise characteristics show that the noise is quite stable over time, especially at high frequencies. Also, the noise amplitudes at high frequencies seem to be similar across the array, in contrast to the large variation seen at low frequencies.

Section 7.6 contains results from an evaluation of the most recent version of the Intelligent Monitoring System (IMS). In order to assess the performance of IMS, the automatic results for a one-week test period were carefully and thoroughly reviewed. The conclusion is that the overall performance of IMS has improved considerably from previous versions and can now be rated as very satisfactory, but also that there is still room for some improvements. Nearly 80% of the events automatically declared by IMS were judged to be acceptable in the sense that they correspond to real seismic events for which only relatively minor modifications were made during the analyst review process. The majority of the remaining 20% were judged to be false events, and some modifications to IMS are proposed that may help in reducing the number of such events. Using various reference bulletins, it was found that some events were missed by IMS, even if data were available to IMS that should allow it to associate phases and form events. An evaluation of the manual corrections made to the automatically determined onset times shows that there is a potential for improving these by, e.g., implementing in IMS new procedures for onset time estimation like those described in section 7.2.

AFTAC Project Authorization	:	T/9141/B/PKP
ARPA Order No.	:	4138 AMD # 16
Program Code No.	:	0F10
Name of Contractor	:	Royal Norwegian Council for Scientific and Industrial Research (NTNF)
Effective Date of Contract	:	1 Oct 1988
Contract Expiration Date	:	30 Sep 1993
Project Manager	:	Frode Ringdal (06) 81 71 21
Title of Work	:	The Norwegian Seismic Array (NORSAR) Phase 3
Amount of Contract	:	$ 9,954,194
Contract Period Covered by Report	:	1 October 1992 - 31 March 1993

This research was supported by the Advanced Research Projects Agency of the Department of Defense and was monitored by AFTAC, Patrick AFB, FL32925, under contract no. F08606-89-C-0005.

NORSAR Contribution No. 492

Table of Contents

1 Summary

This Semiannual Technical Summary describes the operation, maintenance and research activities at the Norwegian Seismic Array (NORSAR), the Norwegian Regional Seismic Array (NORESS, the Arctic Regional Seismic Array (ARCESS) and the experimental Spitsbergen regional array for the period 1 October 1992 -31 March 1993. Statistics are also presented for additional seismic stations, which through cooperative agreements with institutions in the host countries provide continuous data to the NORSAR Data Processing Center (NPDC). These stations comprise the Finnish Experimental Seismic Array (FINESA), the German Experimental Seismic Array (GERESS), and an experimental regional seismic array in Apatity, Russia.

This Semiannual Report also presents statistics from operation of the Intelligent Monitoring System (IMS). The IMS has been operated in an experimental mode, and the performance has been very satisfactory. Since October 1991, a new version of the IMS that accepts data from an arbitrary number of arrays and single 3-component stations has been operated.

The NORSAR Detection Processing system has been operated throughout the period with an average uptime of 97.8% as compared to 96.7% for the previous reporting period. A total of 1733 seismic events have been reported in the NORSAR monthly seismic bulletin. The performance of the continuous alarm system and the automatic bulletin transfer by telex to AFTAC has been satisfactory. The system for direct retrieval of NORSAR waveform data through an X.25 connection has been tested successfully for acquiring such data by AFTAC. Processing of requests for full NORSAR and regional array data on magnetic tapes has progressed according to established schedules. There have been no modifications made to the NORSAR data acquisition system.

On-line detection processing and data recording at the NORSAR Data Processing Center (NDPC) of NORESS, ARCESS, FINESA and GERESS data have been conducted throughout the period. Data from two experimental small-aperture arrays at sites in Spitsbergen and Apatity, Kola Peninsula, have been recorded and processed in an experimental mode. Monthly processing statistics for the arrays as well as results of the IMS analysis for the reporting period are given.

Maintenance activities in the period comprise preventive/corrective maintenance in connection with all the NORSAR subarrays, NORESS and ARCESS. In addition, the maintenance center has been involved with occasional maintenance of equipment for FINESA. Other activities have involved testing of the NORSAR communications systems and work in connection with the experimental small-aperture arrays in Spitsbergen and the Kola Peninsula.

Starting 1 October 1991, an effort began to carry out a complete technical refurbishment of the NORSAR array. This project is funded jointly by AFTAC, ARPA and NTNF. During the reporting period, efforts have focused upon evaluation and laboratory testing of technical options for field instrumentation, in particular state-of-the-art A/D converters, data acquisition and synchronization devices. During the reporting period, we have also

been testing several such systems under realistic operating conditions in the field. When these studies have been completed, a recommendation for a system to be installed will be presented to the funding agencies.

Summaries of six scientific contributions are presented in Chapter 7 of this report.

Section 7.1-7.3 describe the basic principles and give examples of application of a promising new approach to automatic analysis of events from sites with recurring seismic activity. This method, which we have called "intelligent post-processing of seismic events" is particularly well suited to implement as a post-event processing technique in the Intelligent Monitoring System.

Section 7.1 describes the basic principles of this approach. From experience with analyst review of events automatically defined by the Intelligent Monitoring System (IMS), we have realized that the quality of the automatic event locations can be significantly improved if the event intervals are reprocessed with signal processing parameters tuned to phases from events in the given region. The tuned processing parameters are obtained from off-line analysis of events located in the region of interest. The primary goal of such intelligent post-processing is to provide event definitions of a quality that minimizes the need for subsequent analysis and review.

The first step in this post-processing is to subdivide the area to be monitored in order to identify sites of interest. Clearly, calibration will be easiest and potential savings in manpower are largest for areas with high, recurring seismic activity. We have identified 8 mining sites in Fennoscandia/W. Russia/Estonia and noted that 65.6 per cent of the events of $M_L > 2.0$ in this region can be associated with one of these sites. This result is based on 1 1/2 years of data.

Section 7.2 describes the second step in the post-processing approach. This second step is to refine the phase arrival time and azimuth estimates using frequency filters and processing parameters that are tuned to the initial event location provided by the IMS. We have studied, as a first example, a set of 58 events from the Khibiny Massif in the Kola peninsula. Very accurate locations of these events has been provided by the Kola Regional Seismological Centre. Our refinement of phase arrival times for these events, as recorded in Apatity and at ARCESS, have given quite remarkable results. Using the autoregressive likelihood technique of Pisarenko et al (1987) we have been able to estimate onset times automatically to an accuracy (standard deviation) of about 0.05 s for P-phases and 0.15-0.20 s for S-phases. These accuracies are as good as for analyst picks, and are considerably better than in the current SigPro analysis.

Section 7.3 describes the third step in the post-processing approach. This third step in the post-processing is a recomputation of the location estimate, using the refined arrival times and broad-band azimuths associated with a fixed frequency band (tied to the initial IMS location). Again using the set of 58 known Khibiny Massif events as a reference, we have investigated the accuracy of the LocSat location procedure using varying amounts of regional corrections. Using a depth constrained to 0, we find that the epicenter can be estimated to 2-3 km accuracy (median value), with "worst case" error less than 10 km, even without any regional corrections. It is noted that the method needs to be tested for additional target sites before firm conclusions can be drawn.

Section 7.4 describes a four-month monitoring experiment, using the Continuous Threshold Monitoring technique applied to the Novaya Zemlya test site. Data from the NORESS, ARCESS and FINESA regional arrays were used. Starting 1 December 1992, we have been compiling daily statistics of all peaks on the threshold diagram exceeding $m_b = 2.75$, and associating these peaks to regional or teleseismic events whenever possible. In addition, we are analyzing smaller peaks (below $m_b = 2.75$) that can possibly be associated with Novaya Zemlya epicenters.

We have conducted extensive analysis of the $m_b = 2.5$ seismic event at Novaya Zemlya at 09.29.25 GMT on 31 December 1992. This event was detected by ARCESS (P and S), Spitsbergen (P and S), NORESS (P) and Apatity (S). In addition, the Kola Regional Seismologicai Centre provided readings for the station Amderma (Pg and Sn) made from analog recordings. Our results indicate that the epicenter was slightly to the north of the northern Novaya Zemlya test site. However, there are some uncertainties in the travel time tables, and an on-site location cannot entirely be ruled out.

Section 7.5 contains some initial processing results from the Spitsbergen array. Preliminary analysis of data from this new small-aperture (1km) array on the Arctic island of Spitsbergen has revealed a large variation in signal and noise amplitudes across the array. Further investigations are needed in order to determine the reason for this variation, and it may prove necessary to redeploy one or more of the array sensors. Site B2 in this array exhibits a particularly favorable signal focusing for nearly all arrival azimuths. Initial studies of the noise characteristics show that the noise is quite stable over time, especially at high frequencies. Also, the noise amplitudes at high frequencies seem to be similar across the array, in contrast to the large variation seen at low frequencies.

Section 7.6 contains results from an evaluation of the most recent version of the Intelligent Monitoring System (IMS). In order to assess the performance of IMS, the automatic results for a one-week test period were carefully and thoroughly reviewed. The conclusion is that the overall performance of IMS has improved considerably from previous versions and can now be rated as very satisfactory, but also that there is still room for some improvements. Nearly 80% of the events automatically declared by IMS were judged to be acceptable in the sense that they correspond to real seismic events for which only relatively minor modifications were made during the analyst review process. The majority of the remaining 20% were judged to be false events, and some modifications to IMS are proposed that may help in reducing the number of such events. Using various reference bulletins, it was found that some events were missed by IMS, even if data were available to IMS that should allow it to associate phases and form events. An evaluation of the manual corrections made to the automatically determined onset times shows that there is a potential for improving these by, e.g., implementing in IMS new procedures for onset time estimation like those described in section 7.2.

2 NORSAR Operation

2.1 Detection Processor (DP) operation

There have been 58 breaks in the otherwise continuous operation of the NORSAR online system within the current 6-month reporting interval. The uptime percentage for the period is 97.8 as compared to 96.7 for the previous period.

Fig. 2.1.1 and the accompanying Table 2.1.1 both show the daily DP downtime for the days between 1 October 1992 and 31 March 1993. The monthly recording times and percentages are given in Table 2.1.2.

The breaks can be grouped as follows:

a)	Hardware failure	3
b)	Stops related to program work or error	2
c)	Hardware maintenance stops	0
d)	Power jumps and breaks	0
e)	TOD error correction	5
f)	Communication lines	48

The total downtime for the period was 119 hours and 3 minutes. The mean-time-between-failures (MTBF) was 3.6 days, as compared to 2.0 for the previous period.

J. Torstveit

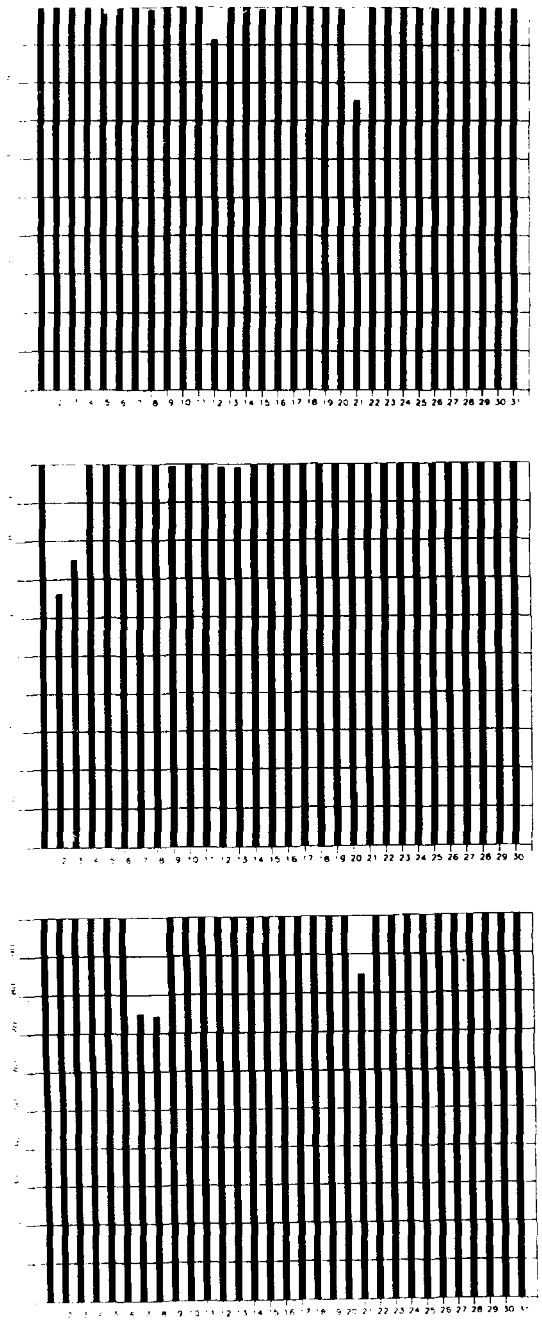

Fig. 2.1.1. Detection Processor uptime for October (top), November (middle) and December (bottom) 1992.

NORSAR Sci. Rep. 2-92/93 May 1993

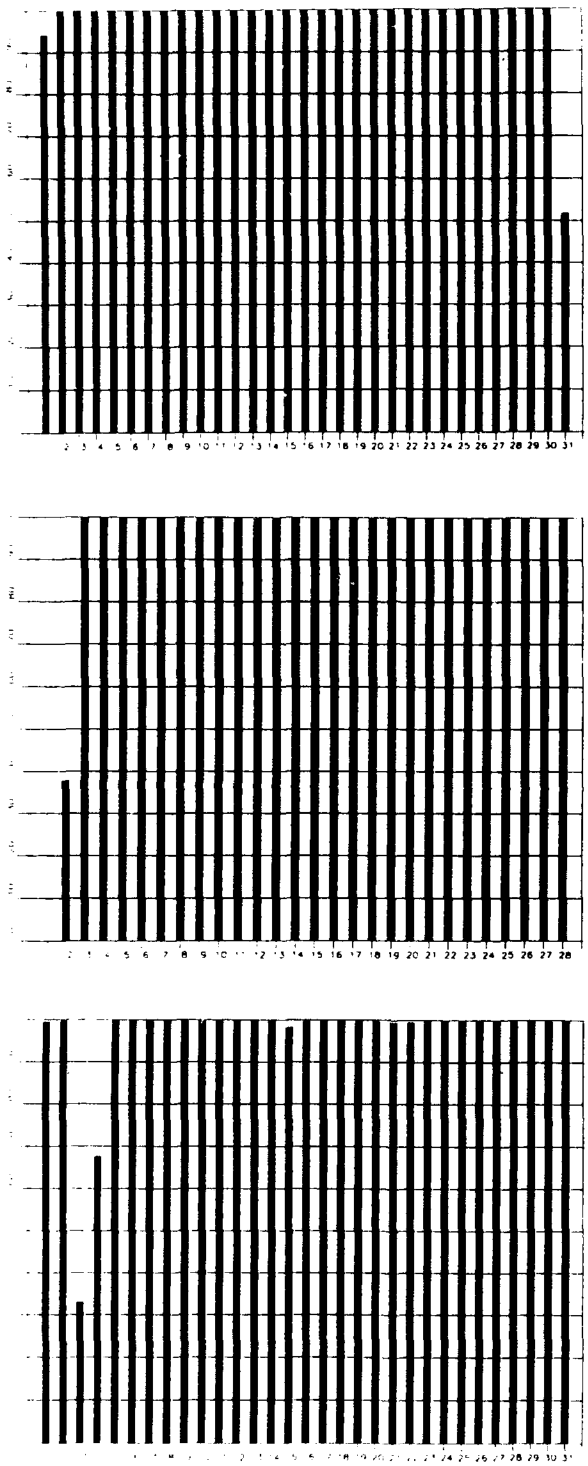

Fig. 2.1.1. Detection Processor uptime for January (top), February (middle) and March (bottom) 1993.

Date	Time	Cause
12 Oct	0939 - 1140	Software work
21 Oct	0720 - 1315	Line failure
02 Nov	1605 -	Line failure
03 Nov	- 0555	
07 Dec	1801 -	Line failure
08 Dec	- 0606	
21 Dec	0423 - 0802	Line failure
01 Jan	1007 - 1131	Software work
31 Jan	0906 - 1448	Hardware failure
31 Jan	1808 -	Hardware failure
01 Feb	-	Hardware failure
02 Feb	- 1455	Hardware failure
03 Mar	0759 -	Line failure
04 Mar	- 0747	
15 Mar	1248 - 1314	Hardware failure

Table 2.1.1. The major downtimes in the period 1 October 1992 - 31 March 1993.

Month	DP Uptime Hours	DP Uptime %	No. of DP Breaks	No. of Days with Breaks	DP MTBF* (days)
Oct 92	735.24	98.84	11	9	2.6
Nov 92	705.09	97.94	14	11	2.0
Dec 92	728.10	97.87	4	4	6.1
Jan 93	723.57	97.31	8	7	3.4
Feb 93	724.51	97.43	4	4	6.0
Mar 93	700.45	97.34	17	13	1.6
		97.79	58	48	3.6

*Mean-time-between-failures = total uptime/no. of up intervals.

Table 2.1.2. Online system performance, 1 October 1992 - 31 March 1993.

2.2 Array communications

General

Table 2.2.1 reflects the performance of the communications system throughout the reporting period.

The most prominent events which have affected the different systems have been: loss of synch, bad cable, spikes on data, PCM irregularities, Digital Access Cross Connection System (DACCS), SLEM, line outage and 2701 data adapter.

Detailed Summary

October (weeks 40-44), 28.9-1.11.92

NTA/Lillestrøm replaced the carrier frequency system pertaining to 01A-06C (-02C), with pulse code modulation equipment (PCM) between Lillestrøm and Hamar 1 Oct 93. An attempt to replace the 02C system was also made, but without success.

01A, which had been down since 18 June, was back in operation 23 Oct with satisfactory performance.

8 Oct 01B started with deteriorated data (spikes) and excessive error rate, after the original SLEM was reinstalled. Between 9 and 12 Oct the subarray was out of operation. During a subarray visit 15 Oct a SLEM failure occurred and after this the system was down throughout October.

02C continued to cause us trouble after NTA's first attempt to replace the carrier system with PCM equipment (1 Oct). Although it was (according to NTA/Lillehammer) changed back to the original system the same day. Between 2 and 7 Oct the subarray was affected by different irregularities related to the communication path, and was more or less out of operation until 12 Oct, when it was demasked. On 28 Oct 02C was again affected in connection with NTA work in Oslo.

Other subarrays which were affected in October were 03C and 06C; 03C between 4 and 6 Oct and 06C between 22 and 26 Oct.

All systems were affected 21 Oct between 0720 and 1316 GMT.

Average outages for October, individual weeks 40-44

Week 40 (-01A,02C)	:	0.003%
Week 41 (-01A,02C)	:	0.001%
Week 42 (-01A,01B,02C)	:	0.002%
Week 43 (N/A)	:	--
Week 44-01B,02C,06C)	:	0.003%

November (weeks 45-48), 2-29.11.92

01B resumed operation 11 Nov (week 46) after having been down since 8 Oct, due to a SLEM failure.

In the same period 02C and 04C were also affected. 02C had synch problems, and the 04C irregularity was caused by NTA/Hamar.

02B was affected between 12 and 16 Nov and from 17 through 30 Nov due to a bad communications cable. Also the 02C synch problem continued week 46 (39.5% down), and week 47 (17.4% down).

06C was affected week 48 (38.1% down), probably by a line outage. A Modcomp restart caused 06C reinitialization.

Average outages in November, individual weeks:

Week 45 (-01B,02C,04Cl)	:	0.002%
Week 46 (-01B,02B,02Cl)	:	0.0006%
Week 47 (-02B,02C)	:	0.003%
Week 48(-02B,06C)	:	0.002%

December (weeks 49-53), 30.11.92-3.1.93

02B went down week 46 due to a bad communications cable located in a swampy area, with snow depths exceeding 1.5 meters. A cable repair was therefore difficult according to NTA/Hamar. They suggested, however, a start date mid-January 93. 21 December, after 1 a.m. all systems were affected 4 hours caused by an NTA system irregularity.

Average outage in December, individual weeks:

Week 49 (-02B)	:	0.0008%
Week 50 (-02B)	:	0.0003%
Week 51 (-02B)	:	0.001%
Week 52 (-02B)	:	2.380%
Week 53 (-02B)	:	0.0008%

January (weeks 1-4), 4-31.1.93

NTA/Hamar finally finished the repair of the 02B communications cable on 29 Jan 93. The subarray had been out of operation since week 46/92.

After a few days' observation of the performance, the subarray communications were accepted. Communications errors were not discovered between 29 Jan 0945 GMT and 31 Jan approx 1800 GMT, which was the approximate hour that the communication adapter 2701 stopped, and the data transfer between the Modcomp and the IBM 4381 machine was suspended. The 2701 remained down throughout 31 Jan.

Average outages in January, individual weeks:

Week 1 (-02B)	:	0.002%
Week 2 (-02B	:	0.002%
Week 3 (-02B)	:	0.001%
Week 4 (-,02B)	:	0.001%

February (weeks 5-8), 1-28.2.93

The 2701 communications adapter which failed 31 Jan 93 approx. 1800 GMT was repaired 3 Feb, and the NORSAR system started again 1455 GMT. After restart all systems performed satisfactorily.

Average outages in February, individual weeks:

Week 5	:	0.002%
Week 6	:	0.002%
Week 7	:	0.002%
Week 8	:	0.002%

March (weeks 9-12), 1-28.3.92

3 March a DACCS (Data Access Cross Connection System) failed at the NTA/Lillestrøm premises and affected all NORSAR subarray communications systems (01A-06C). According to NTA/Lillestrøm all the systems (-02C) were in operation approx 2100 hrs GMT. On 4 March at 0544 GMT, an attempt to start NORSAR was made, but without success. The TOD (Time Code Generator), which was replaced 3 March, was reinstalled. 0747 GMT a new ONLINE start was successful, but 02C was still inoperative.

During the period misalignment of received data and TOD generator clock pulses have resulted in several Modcomp restarts. 4 March 02C, which remained down after the NTA/DACCS failure in Lillestrøm, was loop-tested between Kjeller and Sjusjøen. No errors were observed.

15 March a NORSAR ONLINE stop occurred at 1248 hrs GMT, up 25 min 42 sec later.

16 March a new stop occurred at 1256 GMT, and the system was down for about 5 min 42 seconds.

18 March NTA/Hamar carried out scheduled work on the 02C PCM system between the Nes peninsula and Sjusjøen.

22 March deteriorated data (spikes) were observed on 01A, 02B and 02C. At the same time a 2-second misalignment of received NORSAR data and TOD clock pulses were detected. In order to find out if the seriously deteriorated data had created a situation in the Modcomp which resulted in the misalignment, the three subarrays were omitted. In response to a request, NTA/Hamar informed us that an attenuator had been removed in connection with changing the path between Løten and 06C from PCM cable to radiolink. After having reinstalled the attenuator, NORSAR performance was significantly improved.

Average outages in March, individual weeks:

Week 9 (-02C)	:	0.002%
Week 10 (-02C)	:	0.001%
Week 11 (all)	:	0.022%
Week 12 (all)	:	0.522%

O.A. Hansen

Subarrays	Oct (5)	Nov (4)	Dec (5)	Jan (4)	Feb (4)	Mar (4	Average
	28.9-1.11.93	2-29.11.93	30.11.92-3.1.93	4-31.1.93	1-28.2.93	1-28.3.93	1/2 year
01A	0.010 1)	0.004	0.001 13)	0.008	0.001	0.225	0.047
01B	0.030 2)	0.0005 8)	0.0009 14)	0.0007	0.0006	0.002	0.006
02B	0.0007 3)	0.001 9)	100.0 N/A	92.755 N/A	0.002	0.329	0.003 20)
02C	0.005 4)	0.002 10)	0.001 15)	0.002	0.002	0.010 19)	0.004
03C	0.002 5)	0.0004	0.001 16)	0.001	0.0004	0.011	0.003
04C	0.001 6)	0.0001 11)	0.001 17)	0.001	0.004	0.009	0.003
06C	0.002 7)	0.002 12)	0.003 18)	0.003	0.002	0.369	0.063
AVER	0.007	0.001	0.001 21)	0.016 22)	0.002	0.136	0.018

Figures representing error rate (in per cent) followed by number 1), 2), etc., are related to legend below.

Table 2.2.1. Communications performance. The numbers represent error rates in per cent based on total transmitted frames/week (28 Sep 92 - 28 Mar 93).

1), 4)	one week (43/44)
9), 10)	one week (45/48)
2), 8), 19)	average 2 weeks (40,41/47,48) (11,12/93)
7), 11),12)	average 3 weeks (40,41,42/46,47,48/45,46,47)
3), 5), 6)	average 4 weeks (40,41,42,44)
13), 14), 15), 16)	average 4 weeks (49,50,51,53)
17), 18)	average 4 weeks (49,50,51,53)
20)	average 4 months (Oct, Nov 92/ Feb, Mar 93)
21)	average 6 subarrays (01A,02B, 02C-06C)
22)	average 6 subarrays (01A,02B, 02C-06C)

2.3 NORSAR Event Detection operation

In Table 2.3.1 some monthly statistics of the Detection and Event Processor operation are given. The table lists the total number of detections (DPX) triggered by the on-line detector, the total number of detections processed by the automatic event processor (EPX) and the total number of events accepted after analyst review (teleseismic phases, core phases and total).

	Total DPX	Total EPX	Accepted events		Sum	Daily
			P-phases	Core Phases		
Oct 92	13450	1812	241	131	372	12.0
Nov 92	12175	1324	189	50	239	8.0
Dec 92	13752	1512	189	61	250	8.1
Jan 93	11324	1265	148	74	222	7.2
Feb 93	11450	1241	225	61	286	10.2
Mar 93	13000	1505	257	107	364	11.7
			1249	484	1733	9.5

Table 2.3.1. Detection and Event Processor statistics, 1 October 1992 - 31 March 1993.

NORSAR Detections

The number of detections (phases) reported by the NORSAR detector during day 275, 1992, through day 090, 1993, was 74,237, giving an average of 412 detections per processed day (180 days processed). Table 2.3.2 shows daily and hourly distribution of detections for NORSAR.

T. Schøyen

NAO .DPX Hourly distribution of detections

Day	00	01	02	03	04	05	06	07	08	09	10	11	12	13	14	15	16	17	18	19	20	21	22	23	Sum	Date
275	10	7	9	9	6	16	12	0	11	5	3	2	21	14	6	9	11	14	6	12	4	7	6	14	214	Oct 01 Thursday
276	8	5	5	9	14	4	0	12	1	2	8	6	11	13	16	5	12	25	15	15	14	35	30	19	284	Oct 02 Friday
277	14	16	14	19	16	22	13	14	12	14	9	15	14	17	17	19	17	38	29	22	17	30	30	37	465	Oct 03 Saturday
278	32	28	21	13	19	25	25	24	23	14	11	7	11	6	15	40	14	8	15	17	13	11	14	25	431	Oct 04 Sunday
279	11	16	14	6	12	10	25	20	2	7	13	14	2	17	11	4	8	9	15	18	13	13	13	16	289	Oct 05 Monday
280	6	22	23	19	12	14	7	4	10	21	30	18	14	4	10	23	16	27	13	15	21	17	24	15	385	Oct 06 Tuesday
281	15	21	14	16	17	11	12	12	30	15	27	8	25	14	6	22	7	9	13	19	24	15	9	14	375	Oct 07 Wednesday
282	21	12	21	18	14	12	137	116	13	12	16	6	17	13	17	8	19	12	14	22	9	10	21	16	576	Oct 08 Thursday
283	17	18	12	6	10	10	12	4	8	11	24	6	26	16	14	17	23	23	79	116	96	24	25	25	622	Oct 09 Friday
284	276	79	16	35	21	105	142	221	169	160	48	19	21	13	12	13	16	19	15	23	20	23	31	24	1521	Oct 10 Saturday
285	21	18	19	23	12	23	24	20	15	28	16	19	14	11	18	21	26	24	17	33	12	24	10	35	483	Oct 11 Sunday
286	17	12	10	17	14	11	16	13	6	4	0	1	6	13	20	5	14	12	15	20	19	12	19	16	292	Oct 12 Monday
287	21	20	16	15	19	16	14	9	12	12	9	24	20	27	12	19	18	21	25	16	18	22	31	26	442	Oct 13 Tuesday
288	23	27	16	18	23	26	7	11	20	10	21	12	17	9	29	19	8	12	14	14	15	14	13	18	396	Oct 14 Wednesday
289	27	23	16	18	19	22	11	11	18	30	17	35	18	13	21	6	18	15	23	72	13	14	22	13	495	Oct 15 Thursday
290	14	11	13	10	20	14	16	4	7	7	3	21	18	10	13	15	10	12	13	18	24	7	12	17	309	Oct 16 Friday
291	19	14	22	26	21	18	15	11	32	20	6	14	23	7	20	30	12	17	13	14	15	18	14	12	413	Oct 17 Saturday
292	14	20	11	15	13	23	30	19	12	18	12	32	19	37	14	38	34	28	19	18	23	14	16	13	492	Oct 18 Sunday
293	13	16	20	17	18	18	9	7	7	5	2	5	18	15	10	19	10	10	12	17	16	10	15	11	300	Oct 19 Monday
294	12	18	13	19	31	16	15	15	7	15	5	15	13	11	23	20	23	11	8	5	17	15	19	12	358	Oct 20 Tuesday
295	13	8	13	13	13	12	5	15	21	25	21	21	53	18	13	13	6	7	3	6	10	9	11	12	341	Oct 21 Wednesday
296	14	13	15	9	7	7	16	10	1	21	6	21	21	16	21	23	8	20	22	29	28	19	19	29	395	Oct 22 Thursday
297	30	34	34	29	25	23	21	23	18	37	31	21	21	24	18	22	17	25	20	14	16	41	13	38	595	Oct 23 Friday
298	36	23	11	15	19	8	12	16	10	12	24	20	18	23	16	16	17	25	23	19	20	20	12	16	431	Oct 24 Saturday
299	18	14	15	14	12	24	15	18	16	20	14	8	16	6	11	18	13	13	23	9	18	14	28	30	387	Oct 25 Sunday
300	12	17	11	13	13	8	8	7	10	12	14	21	22	2	11	10	4	18	7	13	7	10	17	17	284	Oct 26 Monday
301	23	24	28	22	21	20	8	9	7	9	6	21	11	3	15	23	12	7	12	17	16	13	17	15	359	Oct 27 Tuesday
302	26	15	25	12	22	15	12	6	4	3	23	16	9	13	12	22	18	13	24	12	23	28	24	24	401	Oct 28 Wednesday
303	24	13	25	21	28	14	17	17	9	19	4	16	8	10	8	14	13	14	15	21	15	17	16	13	371	Oct 29 Thursday
304	13	14	9	20	16	14	21	10	10	17	11	2	21	17	15	7	11	5	13	11	17	21	15	17	327	Oct 30 Friday
305	14	26	17	24	16	20	21	15	13	9	12	18	11	9	27	19	18	19	21	13	20	17	21	32	432	Oct 31 Saturday
306	26	33	34	27	30	24	17	39	32	28	35	18	25	34	28	15	15	22	19	18	17	20	20	18	594	Nov 01 Sunday
307	17	31	20	23	13	20	15	10	9	7	9	7	13	11	12	14	3	0	0	0	0	0	0	0	234	Nov 02 Monday
308	0	0	0	0	0	8	27	17	17	10	14	11	19	11	26	17	17	16	12	18	22	16	16	19	313	Nov 03 Tuesday
309	19	21	27	27	30	13	20	14	20	10	12	12	12	17	13	12	21	18	21	22	16	22	33	15	447	Nov 04 Wednesday
310	20	16	20	26	12	13	4	7	3	11	4	14	13	8	25	22	13	15	15	19	22	16	18	19	355	Nov 05 Thursday
311	16	27	7	13	25	18	9	9	10	18	15	15	12	16	12	26	29	17	20	26	28	28	22	29	447	Nov 06 Friday
312	36	43	32	30	10	21	28	21	21	21	22	16	19	15	32	24	22	18	21	16	22	24	16	23	553	Nov 07 Saturday
313	15	13	15	13	20	22	21	20	18	28	22	20	23	20	19	17	28	27	21	25	25	28	20	26	506	Nov 08 Sunday
314	30	22	29	28	16	17	10	14	13	18	13	8	12	15	13	7	12	22	18	19	6	16	19	20	397	Nov 09 Monday
315	22	18	17	19	16	13	13	11	19	18	31	19	11	18	20	15	14	19	17	21	29	17	28	23	448	Nov 10 Tuesday
316	20	19	19	21	18	16	15	20	16	8	13	8	15	15	20	13	14	15	14	28	16	12	17	23	395	Nov 11 Wednesday
317	16	18	21	17	13	15	7	8	6	4	7	6	9	23	12	22	17	9	18	17	23	16	21	22	347	Nov 12 Thursday
318	21	27	22	19	25	25	15	11	9	10	14	8	23	5	9	15	12	13	10	18	14	20	14	27	386	Nov 13 Friday
319	20	14	25	27	24	24	23	20	29	18	13	19	25	15	17	22	15	15	19	17	19	22	5	22	469	Nov 14 Saturday
320	9	9	13	21	19	12	14	14	19	10	11	11	10	11	12	8	12	13	21	14	9	8	5	12	297	Nov 15 Sunday
321	14	21	32	21	15	21	10	5	8	5	11	13	9	3	9	20	13	25	28	17	17	22	20	28	387	Nov 16 Monday
322	28	19	18	20	19	11	18	15	11	4	3	10	25	13	19	15	8	10	9	9	16	9	13	10	332	Nov 17 Tuesday
323	20	11	11	19	6	2	8	2	7	2	19	9	27	6	19	9	17	15	15	20	21	20	25	15	325	Nov 18 Wednesday
324	17	28	27	26	22	17	14	6	10	5	5	8	12	13	18	12	13	15	14	6	15	13	16	16	348	Nov 19 Thursday
325	19	15	16	19	18	18	16	6	14	8	14	8	22	10	14	12	12	6	15	17	19	18	14	16	346	Nov 20 Friday
326	26	19	23	30	19	18	17	20	22	19	24	12	21	31	12	21	14	11	18	15	18	16	21	19	466	Nov 21 Saturday
327	14	16	26	12	31	12	15	13	20	9	15	21	18	15	8	24	11	17	15	16	26	16	24	29	423	Nov 22 Sunday
328	18	19	19	25	18	11	9	7	6	5	7	6	8	11	12	19	11	8	7	15	12	15	18	17	303	Nov 23 Monday
329	18	33	23	23	22	20	12	10	9	6	12	18	6	18	20	13	13	19	12	12	19	8	11	27	384	Nov 24 Tuesday
330	15	9	12	19	20	26	25	13	12	21	28	17	14	11	17	21	21	19	13	12	18	22	22	26	433	Nov 25 Wednesday

Table 2.3.2 (Page 1 of 4)

NAO .DPX Hourly distribution of detections

Day	00	01	02	03	04	05	06	07	08	09	10	11	12	13	14	15	16	17	18	19	20	21	22	23	Sum	Date		
331	13	24	19	12	12	11	16	5	2	5	14	12	21	9	26	21	9	13	10	10	15	19	25	24	347	Nov 26	Thursday	
332	24	10	25	14	20	8	15	20	7	10	15	21	15	10	13	20	19	21	24	22	20	38	25	19	435	Nov 27	Friday	
333	22	20	50	36	19	19	19	17	15	20	12	14	24	26	17	22	26	17	17	22	28	27	26	21	536	Nov 28	Saturday	
334	30	18	23	21	28	15	20	13	38	13	17	17	22	21	14	21	28	26	22	20	17	21	16	21	502	Nov 29	Sunday	
335	26	18	22	28	16	20	21	13	7	13	14	9	4	15	18	19	20	20	19	17	16	16	25	22	418	Nov 30	Monday	
336	27	13	16	23	16	15	16	3	4	13	13	18	10	11	14	14	22	17	20	13	10	19	21	25	373	Dec 01	Tuesday	
337	36	29	26	23	18	18	26	12	6	22	15	19	11	11	21	15	9	20	21	13	11	21	18	14	435	Dec 02	Wednesday	
338	17	13	25	15	26	15	8	12	10	11	12	16	10	6	21	15	16	22	16	20	18	20	13	17	374	Dec 03	Thursday	
339	19	17	23	17	14	17	11	10	16	16	29	25	14	5	19	12	17	20	15	18	16	16	17	13	396	Dec 04	Frida''	
340	15	19	13	13	19	17	34	15	25	17	12	23	17	17	17	21	18	10	22	11	19	19	17	23	433	Dec 05	Saturoay	
341	29	25	18	19	18	29	25	23	25	11	18	13	25	18	13	14	18	21	22	26	20	30	28	20	508	Dec 06	Sunday	
342	24	26	30	25	20	19	16	9	6	5	12	12	9	19	12	11	12	24	0	0	0	0	0	0	291	Dec 07	Monday	
343	0	0	0	0	0	0	13	25	9	5	13	5	8	14	15	9	11	23	15	18	15	19	26	25	268	Dec 08	Tuesday	
344	20	27	22	20	30	31	19	16	12	10	18	9	6	8	19	23	14	15	15	19	25	13	10	24	425	Dec 09	Wednesday	
345	28	22	22	22	14	10	11	15	2	4	10	15	13	7	11	12	8	5	17	12	8	12	10	10	300	Dec 10	Thursday	
346	16	14	12	2	7	4	6	9	8	6	11	11	11	22	13	21	21	15	24	27	14	15	19	21	329	Dec 11	Friday	
347	22	30	26	36	26	56	29	15	24	27	24	15	22	20	32	26	17	26	23	17	30	25	31	24	623	Dec 12	Saturday	
348	27	29	40	29	30	27	18	27	32	16	9	14	24	22	19	21	25	23	11	14	21	19	30	25	552	Dec 13	Sunday	
349	26	15	21	25	20	24	13	17	9	10	7	16	10	25	13	27	21	24	23	17	11	27	23	20	444	Dec 14	Monday	
350	28	31	19	26	23	23	11	14	5	14	21	8	19	17	11	9	17	15	17	17	16	15	11	6	393	Dec 15	Tuesday	
351	14	27	15	7	22	12	9	7	4	7	5	13	11	7	11	24	17	10	17	12	6	5	14	17	293	Dec 16	Wednesday	
352	12	13	14	16	23	10	13	13	7	11	18	10	21	17	19	12	16	23	13	13	9	15	10	11	339	Dec 17	Thursday	
353	22	8	19	24	17	12	9	5	9	5	11	14	23	4	7	16	21	20	11	14	10	19	21	9	330	Dec 18	Friday	
354	14	16	14	16	10	17	9	16	20	17	11	15	23	13	18	18	13	9	13	11	15	11	19	13	351	Dec 19	Saturday	
355	11	17	13	13	10	14	9	9	8	13	12	14	16	12	9	11	14	9	13	19	7	46	13	13	325	Dec 20	Sunday	
356	14	14	11	11	10	0	0	0	14	7	15	16	13	18	19	16	20	12	13	8	12	14	24	23	304	Dec 21	Monday	
357	26	20	28	19	27	35	25	10	12	12	5	11	12	10	12	12	19	19	10	26	18	13	21	32	434	Dec 22	Tuesday	
358	19	23	39	39	25	26	26	30	26	20	14	27	28	15	19	6	18	17	8	10	14	5	3	8	465	Dec 23	Wednesday	
359	22	16	28	14	17	22	21	17	13	14	20	18	25	13	22	22	15	20	15	20	17	27	14	28	460	Dec 24	Thursday	
360	18	23	14	25	23	26	22	25	23	18	21	18	28	14	18	15	11	9	10	18	9	11	19	15	433	Dec 25	Friday	Frste
361	26	30	29	28	25	30	30	19	20	20	15	25	33	19	25	19	20	20	20	31	31	36	27	31	609	Dec 26	Saturday	Andre
362	26	28	22	18	23	21	20	17	28	18	23	23	17	21	32	31	35	19	23	30	25	29	35	26	590	Dec 27	Sunday	
363	18	22	19	23	31	18	22	14	20	17	27	15	17	12	15	15	19	22	12	16	25	17	17	26	459	Dec 28	Monday	
364	22	12	31	27	21	19	21	11	14	21	17	16	14	18	11	16	15	20	16	19	13	21	26	29	450	Dec 29	Tuesday	
365	32	35	23	44	22	18	23	14	8	18	14	41	29	20	26	32	29	9	31	20	31	23	27	26	595	Dec 30	Wednesday	
366	29	43	26	30	35	27	26	27	24	26	31	28	20	25	23	25	41	28	31	19	34	44	33	29	704	Dec 31	Thursday	
1	38	27	25	26	33	15	22	23	42	20	2	6	24	22	14	13	18	14	18	20	14	20	14	16	486	Jan 01	Friday	Frste
2	15	9	13	11	18	8	5	9	23	4	15	15	10	18	15	24	27	24	18	12	21	19	34	26	393	Jan 02	Saturday	
3	28	15	31	31	22	24	19	20	25	21	19	21	15	18	22	14	14	16	11	17	14	14	14	6	451	Jan 03	Sunday	
4	8	28	17	18	6	11	13	16	4	9	8	6	6	5	7	12	14	11	8	13	9	10	18	13	270	Jan 04	Monday	
5	13	22	11	14	16	12	9	11	19	14	24	11	16	15	10	18	19	15	15	18	15	25	31	16	389	Jan 05	Tuesday	
6	21	12	11	12	5	3	10	4	10	12	5	8	14	12	11	16	20	30	27	18	23	16	19	15	334	Jan 06	Wednesday	
7	30	14	20	24	20	20	13	10	10	6	20	23	23	11	22	20	21	15	17	29	20	17	12	10	427	Jan 07	Thursday	
8	23	15	9	9	14	7	17	8	5	7	5	13	18	8	12	5	8	11	4	13	10	19	4	13	257	Jan 08	Friday	
9	7	3	7	16	10	14	10	9	6	16	5	18	13	16	29	15	8	22	19	20	24	20	24	24	355	Jan 09	Saturday	
10	21	16	31	22	23	17	26	14	27	23	14	16	11	23	32	39	22	31	18	17	17	27	21	17	525	Jan 10	Sunday	
11	21	25	18	17	28	18	13	11	6	6	6	10	3	7	10	10	4	9	5	7	7	15	13	6	275	Jan 11	Monday	
12	3	13	8	1	11	3	10	3	6	6	5	9	11	6	6	9	7	18	22	11	8	9	24	21	230	Jan 12	Tuesday	
13	13	19	16	14	12	18	10	12	14	11	11	19	21	20	17	19	16	24	20	27	18	23	18	18	410	Jan 13	Wednesday	
14	26	26	20	22	20	19	20	17	16	18	18	7	19	16	27	23	19	11	22	19	20	15	13	15	448	Jan 14	Thursday	
15	7	7	13	5	19	22	13	8	12	11	21	21	27	8	17	4	19	12	11	13	9	10	16	14	319	Jan 15	Friday	
16	15	19	15	7	2	4	1	5	3	3	7	5	11	8	9	17	18	15	15	17	35	15	17	13	276	Jan 16	Saturday	
17	21	20	19	26	14	23	19	37	18	20	18	9	4	3	5	3	3	6	6	2	0	6	1	1	284	Jan 17	Sunday	
18	3	13	1	3	0	2	0	1	2	4	4	11	9	15	11	14	9	23	16	24	13	14	18	19	229	Jan 18	Monday	
19	14	22	28	16	18	17	10	8	8	10	13	13	26	13	14	14	11	9	10	19	16	18	17	46	390	Jan 19	Tuesday	
20	26	22	30	32	41	24	24	12	9	12	21	28	19	17	24	25	9	20	18	26	28	23	20	20	530	Jan 20	Wednesday	

Table 2.3.2. (Page 2 of 4)

NAO .DPX Hourly distribution of detections

Day	00	01	02	03	04	05	06	07	08	09	10	11	12	13	14	15	16	17	18	19	20	21	22	23	Sum	Date	
21	10	9	7	6	8	13	2	12	8	10	12	15	15	25	22	6	15	24	13	17	11	19	12	15	306	Jan 21	Thursday
22	7	15	11	11	10	4	1	2	5	3	5	4	8	4	4	5	14	9	14	18	6	17	21	14	212	Jan 22	Friday
23	25	21	25	27	27	20	23	21	12	33	31	24	29	21	22	28	23	22	22	14	22	12	25	14	543	Jan 23	Saturday
24	23	27	29	27	16	18	15	17	22	23	17	26	9	25	16	23	15	20	14	17	21	27	13	19	479	Jan 24	Sunday
25	20	22	16	13	26	19	13	18	12	13	8	3	7	12	11	7	13	12	10	13	10	14	12	15	319	Jan 25	Monday
26	21	21	15	14	17	16	19	17	17	9	31	16	11	22	13	10	15	18	17	15	26	18	26	12	416	Jan 26	Tuesday
27	29	23	11	21	17	19	21	15	14	10	14	16	20	21	27	22	17	24	11	14	8	15	19	16	424	Jan 27	Wednesday
28	17	14	18	20	16	10	7	6	1	3	12	42	7	15	13	60	9	18	9	21	10	22	17	9	376	Jan 28	Thursday
29	18	12	21	15	15	19	11	9	16	23	22	17	19	16	25	21	16	34	30	41	35	33	28	27	523	Jan 29	Friday
30	26	22	20	22	19	25	17	20	18	23	25	16	11	21	17	20	21	20	15	17	27	16	24	24	486	Jan 30	Saturday
31	16	22	20	12	25	35	20	18	20	2	0	0	0	0	0	11	9	11	1	0	0	0	0	0	222	Jan 31	Sunday
32	0	0	0	0	0	0	0	0	0	0	0	0	0	0	0	0	0	0	0	0	0	0	0	0	0	Feb 01	Monday
33	0	0	0	0	0	0	0	0	0	0	0	0	0	0	0	14	21	13	19	21	13	22	14	12	149	Feb 02	Tuesday
34	25	16	12	24	24	7	6	3	4	11	11	3	2	9	6	7	9	10	2	5	6	8	11	9	230	Feb 03	Wednesday
35	10	12	17	8	5	8	12	7	9	6	16	13	12	14	8	9	11	12	14	20	14	21	12	20	290	Feb 04	Thursday
36	20	10	22	23	8	16	15	19	9	15	10	9	11	12	11	16	13	7	11	17	26	15	18	15	348	Feb 05	Friday
37	23	31	16	13	13	14	17	19	13	8	12	11	12	20	12	19	13	17	20	17	12	24	14	13	383	Feb 06	Saturday
38	22	20	12	15	21	25	27	23	33	17	19	27	27	30	28	25	19	18	19	14	17	18	28	23	527	Feb 07	Sunday
39	17	24	27	22	25	17	11	15	13	21	15	14	19	12	14	12	18	16	11	14	8	15	21	17	398	Feb 08	Monday
40	21	13	12	16	16	8	7	8	12	6	2	16	19	14	10	12	14	10	3	5	9	15	5	14	267	Feb 09	Tuesday
41	12	15	15	18	20	10	3	4	12	10	11	32	29	1	15	10	9	11	3	8	6	17	13	8	292	Feb 10	Wednesday
42	15	13	8	13	12	9	8	10	11	4	8	18	26	7	12	27	18	21	24	27	17	19	18	21	366	Feb 11	Thursday
43	14	12	22	22	18	16	18	13	22	14	19	15	33	14	10	16	18	20	28	18	22	25	27	20	456	Feb 12	Friday
44	32	18	19	27	21	30	22	15	16	12	22	19	25	21	27	29	20	27	32	18	27	27	32	28	566	Feb 13	Saturday
45	31	28	32	30	36	35	28	42	40	36	36	34	26	15	27	22	24	29	26	20	24	29	20	16	686	Feb 14	Sunday
46	14	24	23	25	21	18	9	16	20	12	15	13	49	23	22	19	26	23	17	19	23	24	25	17	497	Feb 15	Monday
47	32	20	22	29	19	9	10	13	11	22	20	24	17	10	13	21	17	16	13	16	31	19	16	23	443	Feb 16	Tuesday
48	39	18	32	16	20	20	15	22	15	14	22	19	17	29	18	24	26	19	22	22	19	11	17	17	493	Feb 17	Wednesday
49	17	19	36	22	17	16	18	13	8	10	14	29	24	19	16	30	17	29	19	25	19	25	16	22	480	Feb 18	Thursday
50	25	17	25	19	26	15	8	9	12	12	14	5	10	7	10	5	10	19	16	16	25	20	22	19	366	Feb 19	Friday
51	30	28	23	19	34	25	22	23	23	36	23	31	25	18	18	19	20	13	13	12	22	6	12	6	501	Feb 20	Saturday
52	5	9	2	7	11	11	16	9	24	19	17	7	18	13	12	18	22	18	20	23	17	23	28	23	372	Feb 21	Sunday
53	34	27	20	18	32	28	10	22	15	18	10	15	12	9	16	14	14	25	18	15	10	15	15	15	427	Feb 22	Monday
54	18	17	21	15	18	21	14	16	15	29	7	15	48	18	15	22	25	22	15	9	24	23	24	29	480	Feb 23	Tuesday
55	28	18	19	31	20	17	15	17	14	22	17	17	13	15	30	13	33	29	31	27	19	27	15	18	505	Feb 24	Wednesday
56	23	17	22	22	23	20	17	21	16	20	13	18	26	15	21	19	12	19	19	26	21	19	19	25	473	Feb 25	Thursday
57	32	23	32	22	24	28	15	17	13	15	15	11	24	37	8	11	20	21	25	24	17	20	31	11	496	Feb 26	Friday
58	23	18	23	19	26	15	18	4	20	18	23	19	20	20	21	17	12	22	30	20	21	16	30	20	475	Feb 27	Saturday
59	24	16	23	27	25	20	26	23	16	28	24	14	16	20	23	18	19	23	20	15	17	15	22	17	491	Feb 28	Sunday
60	23	34	15	15	11	16	4	22	7	5	2	10	21	40	2	15	10	12	14	16	25	9	23	14	365	Mar 01	Monday
61	26	14	10	23	18	26	8	5	10	7	5	15	10	22	7	18	10	15	15	15	19	8	13	18	337	Mar 02	Tuesday
62	13	29	20	21	24	11	8	2	21	0	0	0	0	0	0	0	17	0	0	0	0	0	0	0	166	Mar 03	Wednesday
63	0	0	0	0	0	0	12	10	12	17	10	26	21	10	30	22	22	14	18	17	21	15	15	14	306	Mar 04	Thursday
64	23	16	16	23	20	23	15	20	22	16	22	25	25	12	21	13	13	30	17	22	26	14	14	14	462	Mar 05	Friday
65	19	29	18	23	20	21	14	18	19	11	16	27	17	10	19	21	18	15	13	16	26	22	15	13	440	Mar 06	Saturday
66	28	16	24	16	35	17	18	21	27	21	15	13	11	16	27	19	22	16	25	19	25	32	36	27	526	Mar 07	Sunday
67	23	25	29	32	32	19	21	15	17	15	13	14	26	15	20	13	21	19	24	21	14	21	20	21	490	Mar 08	Monday
68	17	24	24	25	21	22	0	0	0	0	0	0	0	0	0	0	0	0	0	0	0	0	0	0	133	Mar 09	Tuesday
69	0	0	0	0	0	0	0	0	0	0	0	0	0	0	0	0	0	0	0	0	0	0	0	0	0	Mar 10	Wednesday
70	9	15	14	14	17	10	19	11	22	16	19	13	28	10	21	16	17	15	13	12	20	19	15	18	383	Mar 11	Thursday
71	30	21	15	14	25	19	12	13	11	17	2	11	12	11	9	11	22	18	16	18	17	27	15	24	390	Mar 12	Friday
72	30	28	41	31	24	33	16	27	15	27	27	24	17	23	22	24	27	22	31	25	26	35	29	25	629	Mar 13	Saturday
73	38	27	24	30	27	27	23	24	21	16	28	25	24	24	24	22	26	25	19	12	13	24	17	36	576	Mar 14	Sunday
74	16	17	29	28	31	8	0	0	0	0	0	0	0	0	0	0	0	0	0	0	0	0	0	0	129	Mar 15	Monday
75	30	12	19	22	18	17	10	6	18	9	16	13	18	18	13	16	11	15	24	17	18	25	21	25	411	Mar 16	Tuesday
76	25	24	25	23	24	25	17	13	8	8	16	6	17	18	16	19	19	20	13	21	13	14	28	18	430	Mar 17	Wednesday

Table 2.3.2. (Page 3 of 4)

NAO .DPX Hourly distribution of detections

Day	00	01	02	03	04	05	06	07	08	09	10	11	12	13	14	15	16	17	18	19	20	21	22	23	Sum	Date
77	10	18	25	20	19	15	14	20	10	7	10	16	16	22	25	21	15	15	15	12	8	15	12	11	371	Mar 18 Thursday
78	12	10	12	7	8	6	18	11	6	7	9	12	29	8	7	13	15	11	13	16	27	11	17	18	303	Mar 19 Friday
79	18	20	24	16	12	25	21	19	22	30	26	31	26	25	12	21	25	33	20	17	27	34	16	22	542	Mar 20 Saturday
80	16	34	26	14	25	22	17	24	16	20	15	20	19	13	13	26	18	20	14	15	16	21	20	24	468	Mar 21 Sunday
81	19	15	23	13	12	24	14	8	17	13	4	18	6	8	23	4	10	11	21	18	17	21	31	23	373	Mar 22 Monday
82	18	30	33	32	24	20	20	12	14	13	15	7	14	15	11	20	18	18	18	17	15	18	25	22	449	Mar 23 Tuesday
83	16	17	22	25	28	18	18	11	13	10	13	20	26	14	21	15	11	20	9	10	8	18	14	12	389	Mar 24 Wednesday
84	14	10	10	17	17	17	17	15	15	15	10	18	9	27	16	14	14	19	13	16	11	13	8	17	352	Mar 25 Thursday
85	24	10	22	20	14	16	3	22	7	19	21	6	37	6	15	8	15	11	16	14	14	17	12	21	370	Mar 26 Friday
86	8	15	15	17	20	16	23	22	20	28	10	16	18	19	29	19	22	29	24	18	32	20	20	24	484	Mar 27 Saturday
87	27	33	37	33	36	27	42	29	21	29	16	24	21	19	18	19	25	24	29	19	13	15	21	30	607	Mar 28 Sunday
88	14	38	31	22	35	11	20	14	16	11	8	11	10	14	14	17	18	14	13	22	16	16	15	14	414	Mar 29 Monday
89	21	26	21	29	23	7	11	19	13	3	25	12	20	11	10	11	16	17	14	21	15	11	12	19	387	Mar 30 Tuesday
90	12	23	33	24	23	8	20	10	8	9	24	7	34	21	10	20	11	17	26	16	12	20	16	17	411	Mar 31 Wednesday

NAO	00	01	02	03	04	05	06	07	08	09	10	11	12	13	14	15	16	17	18	19	20	21	22	23		
Sum	3799	3525	3537	3476	3413	3151	2971	2794	2668	2618	2621	2725	3110	2654	2884	3057	2929	3097	2996	3176	3130	3261	3294	3351	74237	Total sum
180	21	20	20	19	19	18	17	16	15	15	15	15	17	15	16	17	16	17	17	18	17	18	18	19	412	Total average
126	19	18	19	18	18	15	14	12	11	11	13	14	17	13	15	15	15	16	16	18	17	17	17	18	377	Average workdays
54	27	22	22	22	21	23	22	23	24	22	18	18	18	18	19	21	19	20	19	17	19	21	20	21	493	Average weekends

Table 2.3.2. Daily and hourly distribution of NORSAR detections. For each day is shown number of detections within each hour of the day and number of detections for that day. The end statistics give total number of detections distributed for each hour and the total sum of detections during the period. The averages show number of processed days, hourly distribution and average per processed day. (Page 4 of 4)

3 Operation of regional arrays

3.1 Recording of NORESS data at NDPC, Kjeller

Table 3.1.1 lists the main outage times and reasons.

The average recording time was 99.69% as compared to 98.55% during the previous reporting period.

Date	Time	Cause
11 Nov	1925 - 1941	Transmission line failure
31 Dec	2310 - 0000	Software work
08 Mar	1200 - 1216	Hub maintenance
15 Mar	0934 - 0952	Transmission line failure

Table 3.1.1. Interruptions in recording of NORESS data at NDPC, 1 October 1992 - 31 March 1993.

Monthly uptimes for the NORESS on-line data recording task, taking into account all factors (field installations, transmissions line, data center operation) affecting this task were as follows:

October	:	99.97
November	:	99.96
December	:	99.89
January	:	100.00
February	:	100.00
March	:	99.91

Fig. 3.1.1 shows the uptime for the data recording task, or equivalently, the availability of NORESS data in our tape archive, on a day-by-day basis, for the reporting period.

J. Torstveit

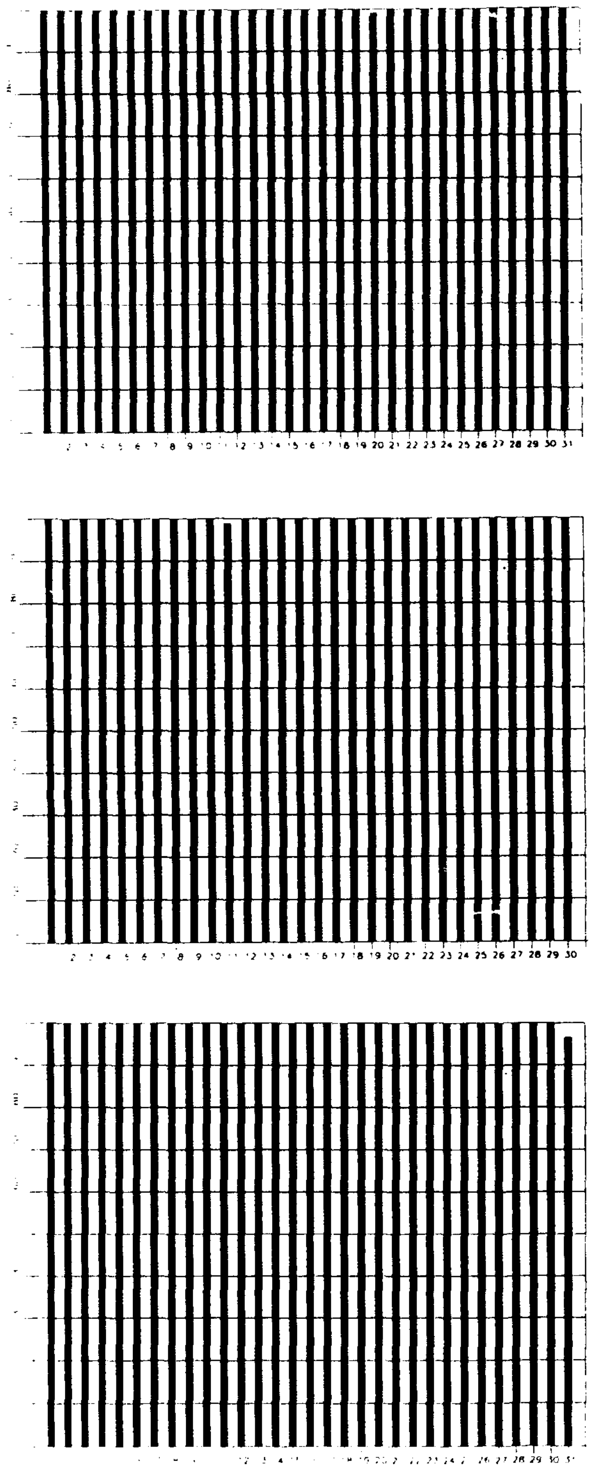

Fig. 3.1.1. NORESS data recording uptime for October (top), November (middle) and December (bottom) 1992.

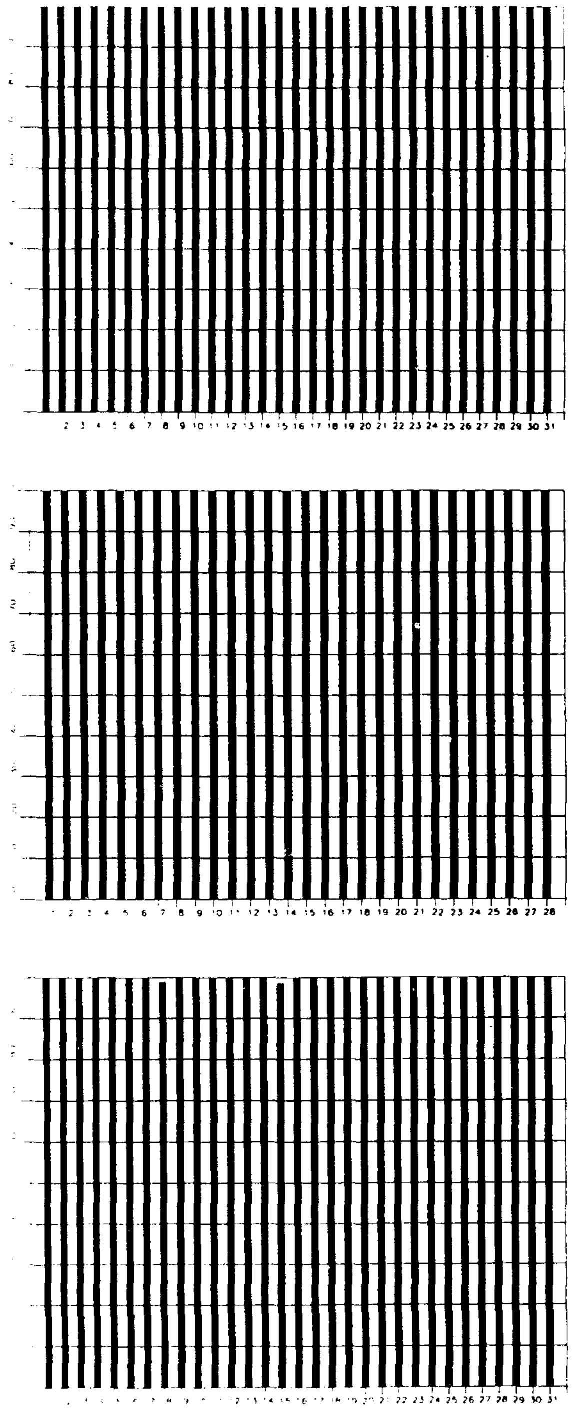

Fig. 3.1.1. (cont.) NORESS data recording uptime for January (top), February (middle) and March (bottom) 1993.

3.2 Recording of ARCESS data at NDPC, Kjeller

Table 3.2.1 lists the main outage times and reasons.

The average recording time was 99.61% as compared to 99.25% for the previous reporting period.

Date	Time	Cause
27 Nov	2123 - 2214	Hardware failure NDPC
28 Nov	2153 - 2230	Hardware failure NDPC
16 Dec	1057 - 1147	Hardware failure NDPC
18 Dec	0641 - 0912	Software work
31 Dec	2311 - 0000	Software work
01 Feb	1821 - 1927	Satellite link failure
01 Feb	2054 -	Satellite link failure
02 Feb	- 0516	

Table 3.2.1. The main interruptions in recording of ARCESS data at NDPC, 1 October 1992 - 31 March 1993.

Monthly uptimes for the ARCESS on-line data recording task, taking into account all factors (field installations, transmissions line, data center operation) affecting this task were as follows:

October	:	99.99%
November	:	99.78%
December	:	99.41%
January	:	100.00%
February	:	98.49%
March	:	99.98%

Fig. 3.2.1. shows the uptime for the data recording task, or equivalently, the availability of ARCESS data in our tape archive, on a day-by-day basis, for the reporting period.

J. Torstveit

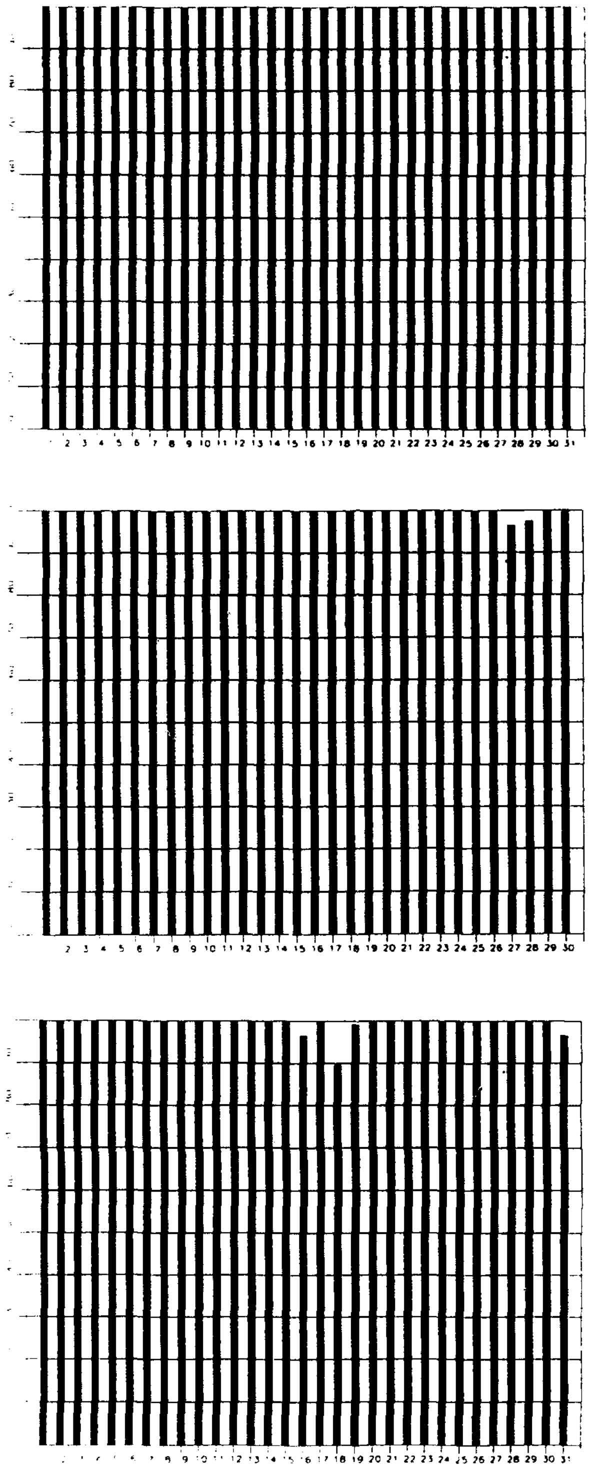

Fig. 3.2.1. ARCESS data recording uptime for October (top), November (middle) and December (bottom) 1992.

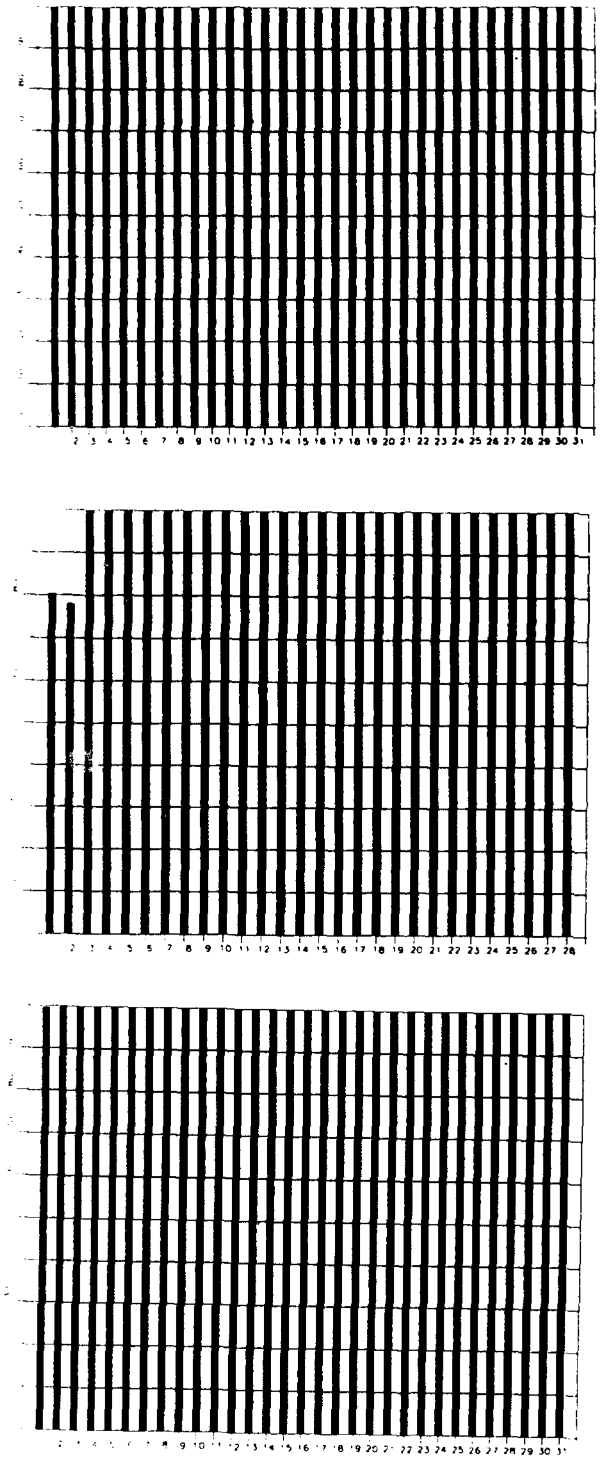

Fig. 3.2.1. ARCESS data recording uptime for January (top), February (middle) and March (bottom) 1993.

3.3 Recording of FINESA data at NDPC, Kjeller

The average recording time was 98.78% as compared to 93.75% for the previous period. As can be seen from Table 3.3.1 below, the main reason for the downtime is transmission line failure.

Date	Time	Cause
23 Oct	0434 - 0935	Transmission line failure
10 Dec	0547 - 1314	Transmission line failure
18 Dec	1337 - 1422	Transmission line failure
18 Dec	1427 - 1447	Transmission line failure
21 Dec	1021 - 1035	Transmission line failure
26 Jan	1636 - 1651	Transmission line failure
26 Jan	2104 - 2137	Transmission line failure
27 Jan	1255 -	Software work in Helsinki
28 Jan	- 1440	
29 Jan	2316 -	Hardware failure NDPC
30 Jan	- 0030	
31 Jan	2213 -	Transmission line failure
01 Feb	- 0712	Transmission line failure
10 Mar	1043 - 1057	Transmission line failure
10 Mar	1334 - 1349	Transmission line failure
10 Mar	1525 - 1544	Transmission line failure

Table 3.3.1. The main interruptions in recording of FINESA data at NDPC, 1 October 1992 - 31 March 1993.

Monthly uptimes for the FINESA on-line data recording task, taking into account all factors (field installations, transmission lines, data center operation) affecting this task were as follows:

October	:	99.13%
November	:	99.98%
December	:	98.79%
January	:	95.99%
February	:	98.91%
March	:	99.87%

Fig. 3.3.1 shows the uptime for the data recording task, or equivalently, the availability of FINESA data in our tape archive, on a day-by-day basis, for the reporting period.

J. Torstveit

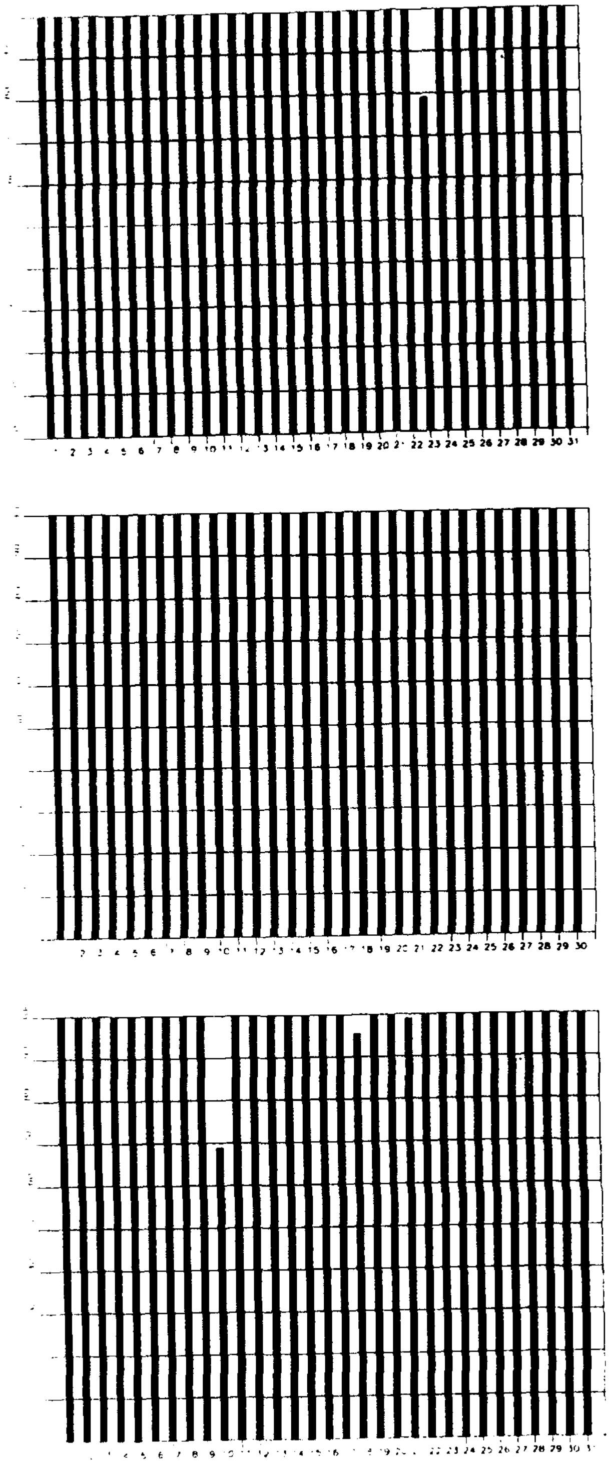

Fig. 3.3.1. FINESA data recording uptime for October (top), November (middle) and December (bottom) 1992.

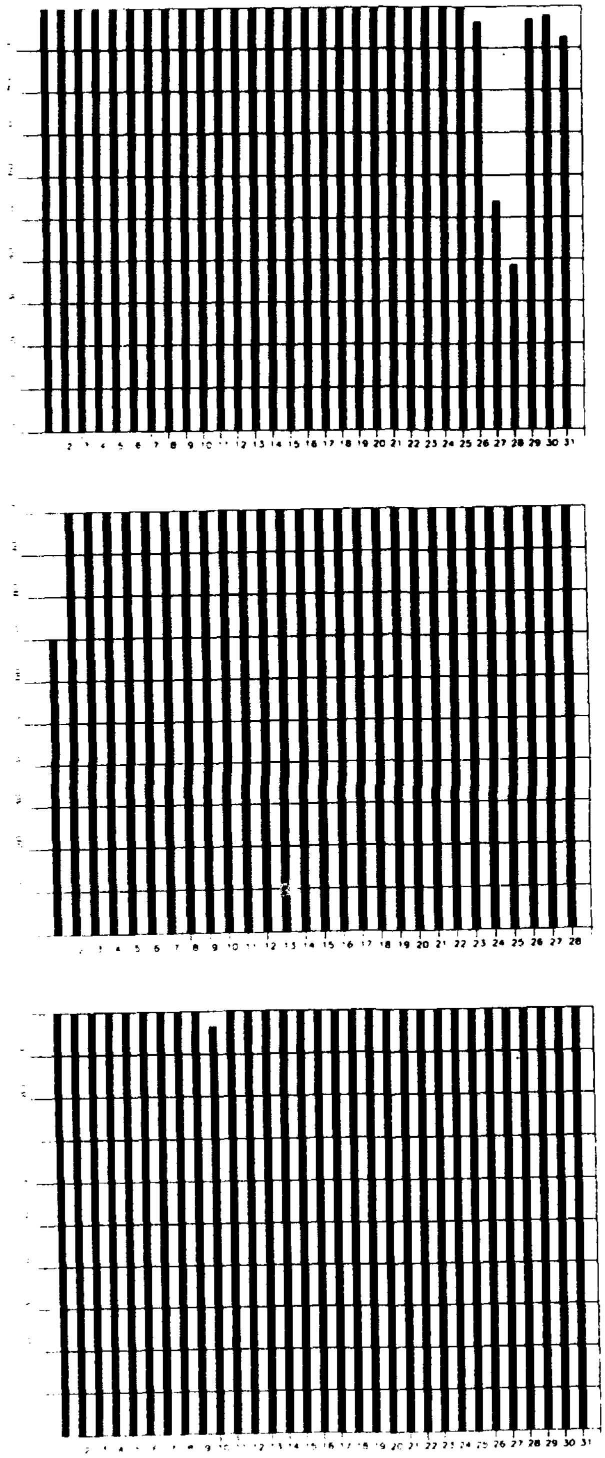

Fig. 3.3.1. FINESA data recording uptime for January (top), February (middle) and March (bottom) 1993.

3.4 Event detection operation

This section reports results from one-array automatic processing using signal processing recipes and "ronapp" recipes for the ep program (NORSAR Sci. Rep. No 2-88/89).

Three systems are in parallel operation to associate detected phases and locate events:

1. The ep program with "ronapp" recipes is operated independently on each array to obtain simple one-array automatic solutions.
2. The Generalized Beamforming method (GBF) (see F. Ringdal and T. Kværna (1989), A mulitchannel processing approach to real time network detection, phase association and threshold monitoring, BSSA Vol 79, no 6, 1927-1940) processes the four arrays jointly and presents locations of regional events.
3. The IMS system is operated on the same set of arrivals as ep and GBF and reports also teleseismic events in addition to regional ones.

IMS results are reported in section 3.5 and GBF results in section 3.6.

In addition to these three event association processes, we are running test versions of the so-called Threshold Monitoring (TM) process. This is a process that monitors the seismic amplitude level at the four regional arrays continuously in time to estimate the upper magnitude limit of an event that might go undetected by the network. The current TM process is beamed to several sites of interest, including the Novaya Zemlya test site. Simple displays of so-called threshold curves reveal instants of particular interest; i.e., instants when events above a certain magnitude threshold may have occurred in the target region. Results from the three processes described above are used to help resolve what actually happened during these instances.

NORESS detections

The number of detections (phases) reported from day 275, 1992, through day 090, 1993, was 36,783 giving an average of 202 detections per processed day (182 days processed).

Table 3.4.1 shows daily and hourly distribution of detections for NORESS.

Events automatically located by NORESS

During days 275, 1992, through 090, 1993, 2074 local and regional events were located by NORESS, based on automatic association of P- and S-type arrivals. This gives an average of 11.4 events per processed day (183 days processed). 63% of these events are within 300 km, and 88% of these events are within 1000 km.

ARCESS detections

The number of detections (phases) reported during day 275, 1992, through day 090, 1993, was 91,474, giving an average of 503 detections per processed day (182 days processed).

Table 3.4.2 shows daily and hourly distribution of detections for ARCESS.

Events automatically located by ARCESS

During days 275, 1992, through 090, 1993, 3359 local and regional events were located by ARCESS, based on automatic association of P- and S-type arrivals. This gives an average 18.5 events per processed day (182 days processed). 43% of these events are within 300 km, and 84% of these events are within 1000 km.

FINESA detections

The number of detections (phases) reported during day 275, 1992, through day 090, 1993, was 58,399, giving an average of 321 detections per processed day (182 days processed).

Table 3.4.3 shows daily and hourly distribution of detections for FINESA.

Events automatically located by FINESA

During days 275, 1992, through 090, 1993, 2835 local and regional events were located by FINESA, based on automatic association of P- and S-type arrivals. This gives an average of 15.6 events per processed day (182 days processed). 65% of these events are within 300 km, and 87% of these events are within 1000 km.

GERESS detections

The number of detections (phases) reported from day 275, 1992, through day 090, 1993, was 7,456, giving an average of 182 detections per processed day (41 days processed).

Table 3.4.4 shows daily and hourly distribution of detections for GERESS.

Events automatically located by GERESS

During days 275, 1992, through 090, 1993, 717 local and regional events were located by GERESS, based on automatic association of P- and S-type arrivals. This gives an average of 17.5 events per processed day (41 days processed). 72% of these events are within 300 km, and 90% of these events are within 1000 km.

Apatity detections

The number of detections (phases) reported from day 275, 1992, through day 090, 1993, was 90,712, giving an average of 501 detections per processed day (181 days processed).

As described in earlier reports, the data from Apatity is transferred by one-way (simplex) radio links to Apatity city. The transmission suffers from radio disturbances that result in a large number of small data gaps and spikes in the data. Although the communication protocol may correct such errors by requesting retransmission of data, this cannot be done at Apatity. For such error corrections, a two-way radio link is needed (duplex radio). Some of the detections are consequently due to bad data spikes. However, it should be noted that noise from cultural activities and from the nearby lakes cause most of the unwanted detections. These unwanted detections are "filtered" in the signal procesing, as they give seismic velocities that are outside accepted limits for regional and teleseismic phase velocities.

Table 3.4.5 shows daily and hourly distribution of detections for Apatity.

Events automatically located by Apatity

During days 275, 1992, through 090, 1993, 2691 local and regional events were located by Apatity, based on automatic association of P- and S-type arrivals. This gives an average of 15.0 events per processed day (180 days processed). 31% of these events are within 300 km, and 66% of these events are within 1000 km.

Spitsbergen detections

The number of detections (phases) reported from day 275, 1992, through day 090, 1993, was 19,359, giving an average of 150 detections per processed day (129 days processed).

Table 3.5.6 shows daily and hourly distribution of detections for Spitsbergen.

Events automatically located by Spitsbergen

The installation at Spitsbergen is not completed, and automatic processing for location of events has only been done for experimental purposes. See also section 7.5.

J. Fyen

NRS .FKX Hourly distribution of detections

Day	00	01	02	03	04	05	06	07	08	09	10	11	12	13	14	15	16	17	18	19	20	21	22	23	Sum	Date	
275	3	3	3	8	0	10	9	2	10	4	2	9	13	17	9	11	6	11	6	8	0	1	2	5	152	Oct 01	Thursday
276	5	2	1	1	8	1	2	4	1	10	5	14	5	6	13	6	4	9	8	3	12	3	5	2	130	Oct 02	Friday
277	2	4	1	3	0	6	13	5	2	4	9	9	10	8	17	15	15	10	14	4	2	21	15	2	191	Oct 03	Saturday
278	3	2	2	3	2	2	0	2	2	7	5	3	9	5	2	20	1	2	2	2	4	8	0	11	99	Oct 04	Sunday
279	0	1	7	1	10	1	4	1	2	3	11	9	7	18	6	3	8	5	6	18	10	2	2	3	138	Oct 05	Monday
280	1	3	2	0	5	1	3	1	6	16	17	10	17	5	13	14	7	8	2	8	15	1	2	7	164	Oct 06	Tuesday
281	2	3	1	3	1	4	3	4	13	17	21	7	16	13	6	22	8	8	0	0	14	2	2	2	172	Oct 07	Wednesday
282	3	3	3	5	4	0	3	0	3	8	6	4	9	7	14	3	12	3	1	4	3	12	3	3	116	Oct 08	Thursday
283	6	1	1	0	2	0	4	7	1	9	13	10	10	5	8	5	3	2	5	3	3	11	0	3	112	Oct 09	Friday
284	3	5	4	3	4	6	3	3	4	7	19	8	4	5	1	4	8	2	4	5	4	5	0	3	114	Oct 10	Saturday
285	8	4	1	5	1	4	4	1	3	8	12	11	11	3	2	4	2	2	3	14	4	3	6	8	124	Oct 11	Sunday
286	2	4	2	6	3	3	3	6	4	3	1	7	4	12	17	6	7	6	15	7	7	3	3	2	133	Oct 12	Monday
287	4	0	3	7	7	1	2	4	3	5	0	15	8	22	6	1	5	6	1	0	0	6	4	1	111	Oct 13	Tuesday
288	6	3	2	1	5	4	3	5	6	1	15	9	12	11	15	12	0	3	1	1	9	5	3	4	136	Oct 14	Wednesday
289	2	6	5	2	6	3	3	5	4	1	10	4	5	17	14	1	2	9	3	6	3	13	12	9	145	Oct 15	Thursday
290	4	5	6	1	3	3	7	2	3	3	4	9	13	6	4	11	9	6	3	12	10	8	2	1	135	Oct 16	Friday
291	0	6	13	6	1	3	3	9	9	5	2	6	3	1	5	10	2	1	5	7	6	3	3	0	109	Oct 17	Saturday
292	1	3	1	3	5	8	10	4	5	7	8	23	10	10	2	24	17	5	8	4	4	6	5	2	175	Oct 18	Sunday
293	2	0	11	4	5	1	1	3	0	0	0	0	0	0	0	0	0	0	0	0	0	0	0	0	27	Oct 19	Monday
294	0	0	0	0	0	0	0	0	0	0	0	0	1	15	14	20	21	5	2	1	4	8	3	3	97	Oct 20	Tuesday
295	3	1	7	1	3	1	3	3	5	4	8	3	17	11	16	7	9	5	2	4	2	3	3	1	122	Oct 21	Wednesday
296	5	1	7	5	0	2	10	11	1	20	6	17	25	14	21	9	6	10	13	13	11	11	8	23	249	Oct 22	Thursday
297	12	14	16	11	7	8	7	16	5	28	14	10	11	15	8	7	5	9	1	7	4	10	0	16	241	Oct 23	Friday
298	11	9	4	8	12	3	10	14	11	13	11	12	14	15	13	8	6	15	7	11	4	6	3	7	227	Oct 24	Saturday
299	5	4	1	2	2	4	6	6	3	7	2	3	8	8	4	11	5	0	10	1	5	0	6	3	106	Oct 25	Sunday
300	2	3	1	3	4	3	2	3	2	3	8	7	12	3	4	11	1	12	5	4	8	2	1	3	107	Oct 26	Monday
301	2	3	7	7	4	6	1	5	13	11	0	6	6	16	16	11	9	5	1	3	5	2	2	0	141	Oct 27	Tuesday
302	1	2	6	5	4	1	4	4	1	11	13	9	6	17	15	2	8	3	4	2	9	3	8	5	143	Oct 28	Wednesday
303	3	1	1	3	5	4	4	7	0	6	6	23	8	7	5	18	6	6	15	3	13	4	3	4	155	Oct 29	Thursday
304	6	5	2	16	5	11	9	5	3	4	9	10	15	9	10	13	3	3	3	5	2	11	5	0	164	Oct 30	Friday
305	4	8	3	3	2	7	4	4	3	4	5	14	3	7	9	4	6	4	1	5	6	5	5	1	117	Oct 31	Saturday
306	5	6	6	8	2	6	7	7	4	3	5	5	4	11	1	7	4	10	9	3	3	11	1	1	129	Nov 01	Sunday
307	8	13	4	9	8	6	7	0	3	4	5	3	4	9	9	6	5	4	9	6	8	3	4	3	140	Nov 02	Monday
308	9	8	3	1	2	3	0	1	6	2	8	2	9	7	22	11	7	2	3	3	3	3	1	1	117	Nov 03	Tuesday
309	6	1	13	2	11	1	2	2	5	0	7	13	14	12	6	15	8	7	10	4	12	5	6	6	168	Nov 04	Wednesday
310	12	6	3	5	5	1	4	5	4	12	4	5	11	16	12	8	2	6	3	15	7	3	7	1	157	Nov 05	Thursday
311	2	3	2	1	12	5	8	8	1	7	4	14	5	9	6	11	1	10	4	12	8	6	2	4	145	Nov 06	Friday
312	5	9	7	6	2	2	15	3	8	4	3	4	8	4	2	14	7	7	3	5	10	6	21	3	158	Nov 07	Saturday
313	11	7	7	12	15	7	7	1	6	12	6	4	2	1	16	18	13	9	13	14	8	2	20	18	229	Nov 08	Sunday
314	20	10	17	19	13	8	3	5	4	4	6	5	11	12	22	3	3	13	7	3	5	1	0	7	201	Nov 09	Monday
315	6	7	4	7	4	2	4	1	4	13	8	14	13	18	10	10	1	1	1	1	10	3	5	9	156	Nov 10	Tuesday
316	7	8	4	0	3	2	1	12	2	2	4	3	6	19	13	5	3	6	2	4	3	6	4	3	122	Nov 11	Wednesday
317	2	0	0	7	4	3	3	4	2	5	7	6	17	18	15	21	1	10	1	7	8	2	4	2	149	Nov 12	Thursday
318	1	4	1	9	3	0	7	5	1	2	7	10	20	12	3	2	5	7	7	6	10	12	11	1	146	Nov 13	Friday
319	8	1	0	1	4	5	6	5	7	2	1	6	4	4	9	6	4	2	2	0	4	9	3	1	94	Nov 14	Saturday
320	2	1	1	2	3	4	10	5	10	4	3	1	5	3	6	2	0	2	9	8	5	2	1	8	97	Nov 15	Sunday
321	2	4	6	1	5	8	4	2	4	6	5	6	7	10	11	12	3	3	8	7	4	2	6	7	133	Nov 16	Monday
322	6	0	5	8	3	4	5	5	9	6	4	11	22	13	20	20	3	12	6	5	10	5	2	1	185	Nov 17	Tuesday
323	7	2	0	4	9	3	4	3	5	4	13	4	19	16	27	5	15	3	0	4	16	7	11	1	182	Nov 18	Wednesday
324	2	8	5	6	4	3	4	3	1	0	7	2	12	13	17	8	4	6	3	1	2	2	1	1	115	Nov 19	Thursday
325	3	4	2	2	2	4	3	1	3	4	6	2	11	12	8	1	6	2	4	9	5	16	3	4	117	Nov 20	Friday
326	6	4	1	8	2	8	6	6	5	6	1	2	11	13	1	10	1	3	9	2	3	4	5	10	127	Nov 21	Saturday
327	3	2	8	1	6	2	1	9	3	6	8	7	1	3	3	5	8	10	3	2	7	0	2	7	107	Nov 22	Sunday
328	6	2	9	11	7	1	9	3	3	4	1	5	6	10	12	7	6	2	4	3	5	5	6	9	136	Nov 23	Monday
329	4	9	0	7	5	2	4	2	8	4	4	6	8	11	15	13	8	8	6	2	10	6	2	5	149	Nov 24	Tuesday
330	2	3	4	0	9	7	6	2	5	3	14	8	5	8	12	12	6	5	6	1	2	4	3	6	133	Nov 25	Wednesday

Table 3.4.1. (Page 1 of 4)

NRS .FKX Hourly distribution of detections

Day	00	01	02	03	04	05	06	07	08	09	10	11	12	13	14	15	16	17	18	19	20	21	22	23	Sum	Date	
331	4	1	3	7	6	3	4	3	3	6	5	14	13	9	20	6	4	1	2	6	5	3	6	1	135	Nov 26 Thursday	
332	9	0	3	2	5	2	1	10	5	3	9	21	8	9	10	5	10	7	8	6	11	9	12	8	173	Nov 27 Friday	
333	4	3	18	8	2	5	9	1	6	4	3	6	7	3	5	4	3	3	3	4	2	0	8	4	115	Nov 28 Saturday	
334	3	2	3	8	8	4	6	5	9	4	4	5	6	9	7	2	12	5	4	6	11	5	6	9	143	Nov 29 Sunday	
335	3	6	5	5	2	3	5	7	1	4	3	5	3	16	18	7	8	1	2	10	2	2	2	3	123	Nov 30 Monday	
336	8	1	3	1	1	3	1	2	1	0	5	5	9	12	26	2	1	5	2	3	8	1	0	5	105	Dec 01 Tuesday	
337	0	2	1	1	1	3	2	0	1	4	4	9	6	14	15	4	1	1	8	0	6	1	2	4	90	Dec 02 Wednesday	
338	3	2	2	2	2	2	0	1	1	1	3	7	8	14	10	5	2	2	3	3	6	5	8	4	96	Dec 03 Thursday	
339	2	2	1	2	2	6	1	0	6	2	7	18	15	11	12	0	1	1	6	4	1	2	1	2	105	Dec 04 Friday	
340	1	5	2	0	1	4	9	1	0	6	5	4	1	9	3	3	4	2	4	0	2	1	3	4	74	Dec 05 Saturday	
341	6	5	1	7	3	2	8	2	1	0	1	2	7	2	4	3	5	6	2	4	5	4	3	4	87	Dec 06 Sunday	
342	3	4	10	13	15	2	4	4	1	1	5	5	5	17	15	13	5	4	6	11	6	9	9	7	174	Dec 07 Monday	
343	8	6	9	2	9	3	2	10	1	8	8	1	8	11	25	2	2	2	3	6	9	3	3	5	146	Dec 08 Tuesday	
344	4	3	14	14	6	6	5	6	1	5	4	3	10	20	11	11	14	2	3	5	11	3	4	8	173	Dec 09 Wednesday	
345	8	8	5	12	4	8	6	3	2	6	2	10	16	9	26	5	2	2	4	10	4	3	2	6	163	Dec 10 Thursday	
346	0	2	5	2	1	2	1	4	3	6	5	12	2	8	6	8	3	4	4	12	9	2	0	1	102	Dec 11 Friday	
347	8	4	5	13	11	39	21	14	8	9	0	6	14	7	18	5	6	14	16	26	20	33	33	21	351	Dec 12 Saturday	
348	21	12	6	8	12	35	51	56	34	18	17	8	21	16	15	52	57	28	11	4	2	8	8	11	511	Dec 13 Sunday	
349	7	11	3	9	5	1	3	8	3	1	1	14	9	9	18	12	2	3	3	8	10	3	2	1	146	Dec 14 Monday	
350	0	2	1	4	5	3	2	1	1	2	4	10	11	15	8	6	4	5	3	3	6	1	1	3	101	Dec 15 Tuesday	
351	4	3	4	4	4	5	3	1	2	4	7	14	12	11	8	22	8	2	3	3	12	1	0	0	137	Dec 16 Wednesday	
352	7	1	1	2	10	4	0	3	9	5	8	5	18	14	33	7	9	10	5	9	6	1	3	2	172	Dec 17 Thursday	
353	2	5	3	10	4	1	0	4	2	3	3	6	14	3	4	1	6	7	3	1	6	3	4	1	96	Dec 18 Friday	
354	4	5	2	1	3	1	3	6	3	5	2	1	6	12	17	1	1	8	3	11	3	6	8	4	116	Dec 19 Saturday	
355	7	6	6	10	2	8	3	9	9	2	3	8	5	2	14	18	13	15	28	27	21	45	20	33	314	Dec 20 Sunday	
356	40	38	46	37	43	28	24	26	18	6	7	8	6	13	25	51	56	38	31	5	4	6	5	5	566	Dec 21 Monday	
357	11	9	15	19	23	24	7	22	24	4	8	19	23	31	24	26	32	46	57	60	57	78	67	62	748	Dec 22 Tuesday	
358	52	59	68	69	44	40	44	44	26	10	20	13	13	10	45	70	77	48	32	11	7	3	2	3	810	Dec 23 Wednesday	
359	13	2	2	1	3	9	5	4	4	4	4	20	12	1	7	17	10	6	7	10	8	3	5	4	161	Dec 24 Thursday	
360	4	3	7	8	0	9	9	6	8	6	19	7	17	7	4	5	2	3	5	0	1	1	7	4	142	Dec 25 Friday	Frste
361	16	5	11	5	42	66	48	39	80	72	35	45	39	71	67	69	78	68	60	62	87	87	61	31	1244	Dec 26 Saturday	Andre
362	36	8	7	5	3	3	12	36	36	9	11	5	5	5	48	91	81	74	85	36	13	9	8	3	629	Dec 27 Sunday	
363	11	7	4	2	8	6	10	9	10	27	24	6	7	28	46	28	36	41	36	16	21	21	20	12	436	Dec 28 Monday	
364	28	26	19	6	9	8	7	14	9	7	5	16	10	12	8	3	2	15	40	46	55	39	34	30	448	Dec 29 Tuesday	
365	54	99	64	68	77	28	17	21	6	6	7	16	9	9	59	91	55	69	20	13	7	9	5	8	817	Dec 30 Wednesday	
366	3	8	1	4	9	2	8	15	1	13	5	5	7	6	6	2	5	6	3	7	16	20	7	4	163	Dec 31 Thursday	
1	4	6	9	6	7	9	17	42	59	33	6	5	6	16	9	14	11	11	7	1	2	5	0	3	268	Jan 01 Friday	Frste
2	5	6	1	2	3	5	0	2	9	2	1	2	3	5	6	8	19	6	1	1	5	1	9	1	103	Jan 02 Saturday	
3	3	1	3	1	5	2	6	7	4	4	8	1	10	15	0	0	1	14	16	13	9	10	16	26	175	Jan 03 Sunday	
4	37	33	20	8	0	3	2	4	3	5	7	10	6	3	15	6	1	3	6	2	5	3	1	0	183	Jan 04 Monday	
5	1	4	0	2	3	2	4	2	8	4	16	2	5	9	7	4	7	2	11	5	5	1	1	1	106	Jan 05 Tuesday	
6	1	3	4	2	0	2	1	1	3	3	7	6	8	6	12	6	3	9	5	6	2	3	4	9	106	Jan 06 Wednesday	
7	12	6	3	12	46	33	10	10	8	10	16	12	17	13	11	15	0	10	4	9	10	4	6	1	278	Jan 07 Thursday	
8	4	0	1	3	1	4	8	0	5	3	3	9	7	9	7	1	4	6	1	7	5	13	6	6	113	Jan 08 Friday	
9	4	4	3	10	7	9	0	3	0	5	7	9	1	5	7	3	0	0	2	1	3	2	3	7	95	Jan 09 Saturday	
10	3	0	4	3	7	5	4	5	4	1	5	3	5	2	6	4	3	3	2	4	0	1	9	3	86	Jan 10 Sunday	
11	5	2	1	4	8	1	1	3	2	1	2	13	8	5	11	3	1	3	3	4	1	8	12	2	104	Jan 11 Monday	
12	2	3	1	1	2	2	1	2	1	4	5	7	4	8	9	5	1	4	4	0	2	1	1	6	76	Jan 12 Tuesday	
13	2	7	7	1	2	9	6	0	1	9	10	7	12	20	9	8	3	5	2	8	3	0	0	0	131	Jan 13 Wednesday	
14	4	2	4	2	2	5	5	3	8	8	14	13	9	4	12	15	8	3	1	3	2	1	5	8	141	Jan 14 Thursday	
15	1	7	5	3	9	9	10	0	10	0	12	15	22	8	14	5	7	1	5	0	6	1	2	2	154	Jan 15 Friday	
16	2	1	7	1	3	4	1	0	0	1	0	3	7	2	2	2	4	1	4	2	0	6	6	0	59	Jan 16 Saturday	
17	3	4	2	3	3	2	2	6	4	6	7	3	1	0	2	4	1	3	3	1	1	4	1	2	68	Jan 17 Sunday	
18	1	2	2	0	0	1	0	1	0	2	5	6	8	5	6	3	3	5	5	4	8	9	2	8	86	Jan 18 Monday	
19	35	70	52	53	20	11	6	8	14	9	16	13	16	11	31	21	8	16	9	10	24	44	52	54	603	Jan 19 Tuesday	
20	30	16	14	20	25	9	5	7	1	3	8	22	13	15	16	13	10	5	3	3	10	5	2	2	257	Jan 20 Wednesday	

Table 3.4.1. (Page 2 of 4)

NRS .FKX Hourly distribution of detections

Day	00	01	02	03	04	05	06	07	08	09	10	11	12	13	14	15	16	17	18	19	20	21	22	23	Sum	Date	
21	6	1	1	2	0	0	2	0	7	3	2	4	14	16	27	10	4	2	6	4	4	11	3	4	133	Jan 21	Thursday
22	2	0	1	2	0	1	0	1	2	1	4	2	4	9	3	4	1	7	3	9	5	1	2	3	67	Jan 22	Friday
23	10	4	5	5	11	18	24	16	14	24	35	35	17	15	29	15	12	10	9	0	5	4	4	3	324	Jan 23	Saturday
24	7	3	1	7	4	4	1	3	7	1	5	5	10	11	4	3	7	2	5	2	1	4	3	3	103	Jan 24	Sunday
25	1	5	0	1	6	4	1	1	4	5	4	3	9	8	6	3	3	9	4	4	6	3	4	3	97	Jan 25	Monday
26	6	7	4	7	11	9	7	6	2	3	22	8	3	18	15	20	24	17	25	21	24	20	20	9	308	Jan 26	Tuesday
27	8	7	4	13	11	9	4	3	2	7	9	12	10	17	9	15	11	10	4	26	29	33	26	24	303	Jan 27	Wednesday
28	12	18	31	43	24	16	20	12	11	4	13	23	4	23	16	44	17	17	32	41	25	31	43	50	570	Jan 28	Thursday
29	64	49	44	44	46	44	17	20	19	13	17	16	22	14	16	7	23	41	53	85	77	71	47	39	888	Jan 29	Friday
30	16	7	8	3	3	11	5	5	5	10	10	7	10	8	5	6	2	3	3	1	14	2	0	5	149	Jan 30	Saturday
31	2	1	3	4	3	4	5	9	10	1	4	8	5	2	4	1	2	1	2	4	1	3	1	2	82	Jan 31	Sunday
32	1	3	1	9	5	2	0	0	4	7	3	12	10	10	6	4	0	4	9	18	15	13	23	15	174	Feb 01	Monday
33	20	15	24	19	17	11	2	5	3	4	7	10	7	17	15	9	9	7	6	1	6	5	3	1	223	Feb 02	Tuesday
34	5	3	1	5	5	2	0	1	2	3	6	4	10	3	11	10	8	2	1	1	4	2	4	2	95	Feb 03	Wednesday
35	1	3	8	2	3	5	6	1	2	2	7	9	15	13	14	7	5	0	2	4	1	2	8	17	137	Feb 04	Thursday
36	15	14	23	22	19	3	6	6	7	6	4	5	15	17	19	20	21	16	25	23	18	33	40	37	414	Feb 05	Friday
37	27	26	28	27	46	71	42	30	7	5	23	12	3	6	2	7	4	8	12	18	30	28	37	47	546	Feb 06	Saturday
38	40	89	80	75	60	37	40	37	58	66	34	18	13	15	7	15	5	3	5	2	3	4	11	6	723	Feb 07	Sunday
39	6	7	12	9	15	14	8	6	6	2	14	10	16	13	11	8	2	5	8	4	14	8	10	8	216	Feb 08	Monday
40	16	21	13	17	22	12	11	9	9	3	3	8	17	10	19	13	9	3	2	6	14	7	6	4	254	Feb 09	Tuesday
41	11	0	9	5	17	9	2	3	12	6	10	21	28	15	11	18	8	5	3	14	8	17	16	13	261	Feb 10	Wednesday
42	12	12	4	5	17	32	14	10	12	2	8	12	13	9	8	12	7	7	5	14	11	1	0	3	230	Feb 11	Thursday
43	2	4	1	3	7	5	4	3	8	9	9	11	19	12	14	11	7	15	10	4	11	4	12	3	188	Feb 12	Friday
44	9	9	10	9	10	21	6	12	18	11	34	44	18	8	7	2	13	8	12	12	15	24	30	15	357	Feb 13	Saturday
45	21	41	46	61	62	68	59	65	51	18	15	6	5	8	9	3	8	8	9	3	2	3	6	4	581	Feb 14	Sunday
46	7	7	4	6	5	1	0	4	10	2	6	5	22	11	14	12	10	3	1	13	5	2	10	2	162	Feb 15	Monday
47	8	7	10	10	4	8	3	6	5	14	17	25	7	22	7	6	11	8	16	0	2	2	9	3	210	Feb 16	Tuesday
48	5	2	7	3	3	4	3	4	1	3	8	5	12	16	8	11	5	10	6	0	12	3	2	3	136	Feb 17	Wednesday
49	2	3	7	0	11	3	7	3	2	3	8	7	16	17	4	4	5	7	1	4	10	4	1	3	132	Feb 18	Thursday
50	0	5	4	1	8	10	0	1	6	2	3	12	6	8	7	7	5	2	7	2	3	3	6	4	112	Feb 19	Friday
51	3	4	10	10	21	16	57	72	58	38	18	12	5	5	8	4	5	3	1	1	0	2	3	2	358	Feb 20	Saturday
52	0	2	2	3	3	1	5	2	4	5	5	1	0	1	0	1	2	3	4	3	2	6	3	2	60	Feb 21	Sunday
53	10	13	9	8	11	12	2	10	6	5	3	9	9	16	11	9	9	3	9	2	9	2	2	5	184	Feb 22	Monday
54	1	1	3	3	7	7	1	1	6	5	4	13	29	10	4	13	7	13	3	3	3	10	5	5	157	Feb 23	Tuesday
55	3	6	3	5	3	2	2	10	4	9	6	9	10	6	17	8	8	10	3	5	12	8	9	1	159	Feb 24	Wednesday
56	6	4	1	5	7	9	13	2	7	12	3	7	23	10	10	9	4	5	12	8	5	4	2	2	170	Feb 25	Thursday
57	3	3	2	0	2	6	0	1	1	7	7	7	15	16	4	14	9	2	5	7	12	1	7	4	135	Feb 26	Friday
58	4	3	4	2	3	3	4	1	6	6	7	9	13	1	1	3	5	2	5	1	3	1	1	0	88	Feb 27	Saturday
59	3	2	2	5	2	3	4	4	8	1	1	6	7	0	9	8	8	2	3	3	2	3	4	2	92	Feb 28	Sunday
60	0	8	6	3	8	0	3	9	3	4	1	4	20	24	5	10	5	8	10	6	9	9	5	5	165	Mar 01	Monday
61	7	7	1	2	5	4	6	5	3	7	6	12	13	24	8	18	5	5	7	6	5	11	5	8	180	Mar 02	Tuesday
62	38	17	14	17	13	20	4	3	4	7	5	5	15	17	9	13	13	3	2	10	12	8	1	6	256	Mar 03	Wednesday
63	1	0	2	7	1	11	3	6	4	13	8	15	17	11	19	14	6	3	1	3	12	1	3	4	165	Mar 04	Thursday
64	4	3	2	0	5	2	4	7	7	3	13	10	14	4	19	8	6	9	11	7	11	3	4	5	161	Mar 05	Friday
65	8	21	5	5	3	0	7	5	8	4	6	12	6	2	6	3	7	6	6	0	7	6	1	3	137	Mar 06	Saturday
66	7	2	2	8	8	2	10	1	5	6	2	5	3	2	4	8	1	7	6	6	6	3	1	9	114	Mar 07	Sunday
67	2	3	11	5	5	1	4	5	6	8	1	9	18	10	6	8	10	8	12	3	11	0	3	0	149	Mar 08	Monday
68	2	9	7	1	14	8	5	2	8	7	17	22	17	21	12	11	10	10	6	7	4	5	7	8	220	Mar 09	Tuesday
69	2	8	1	3	5	3	3	6	4	10	7	9	19	31	8	21	10	23	3	10	11	1	11	3	212	Mar 10	Wednesday
70	13	4	6	2	7	2	6	1	12	8	15	18	30	10	10	19	14	6	11	4	4	8	9	9	228	Mar 11	Thursday
71	12	11	16	17	25	17	12	14	4	8	13	9	13	13	3	18	21	2	5	8	17	6	11	10	285	Mar 12	Friday
72	6	4	2	7	2	3	3	9	9	7	11	6	14	10	4	9	0	6	7	7	2	3	5	8	144	Mar 13	Saturday
73	3	4	8	3	0	1	4	4	9	10	10	4	3	2	5	5	3	12	11	9	5	7	4	14	140	Mar 14	Sunday
74	3	17	16	17	2	7	3	2	2	5	3	5	7	10	9	9	13	8	12	4	11	3	1	2	171	Mar 15	Monday
75	3	3	20	3	4	5	3	1	13	2	2	15	19	0	0	5	12	8	9	5	8	2	3	9	154	Mar 16	Tuesday
76	5	4	2	3	5	2	0	4	4	14	15	6	15	18	14	20	15	12	3	2	14	9	3	5	194	Mar 17	Wednesday

Table 3.4.1. (Page 3 of 4)

NRS .FKX Hourly distribution of detections

Day	00	01	02	03	04	05	06	07	08	09	10	11	12	13	14	15	16	17	18	19	20	21	22	23	Sum	Date
77	6	3	4	0	9	5	5	11	7	1	4	6	5	12	23	16	7	8	5	2	9	3	4	8	163	Mar 18 Thursday
78	6	3	3	4	7	6	12	2	3	1	4	5	29	9	12	1	11	10	3	5	12	1	0	0	149	Mar 19 Friday
79	4	7	3	9	20	36	13	3	16	13	3	14	4	5	7	5	8	10	2	5	1	5	6	5	204	Mar 20 Saturday
80	3	5	1	3	9	9	3	8	2	5	2	11	5	7	4	3	4	2	4	1	4	6	4	0	105	Mar 21 Sunday
81	1	5	10	11	9	10	4	2	3	8	6	15	5	7	19	10	5	7	13	6	10	4	8	10	188	Mar 22 Monday
82	3	7	5	2	3	4	4	2	9	5	5	9	9	11	6	5	12	10	8	2	7	7	6	5	146	Mar 23 Tuesday
83	11	1	2	12	11	6	5	5	3	7	3	9	13	6	12	14	4	11	7	6	6	5	28	19	206	Mar 24 Wednesday
84	14	15	11	15	15	10	0	6	3	3	6	13	12	14	3	11	5	11	3	6	13	2	4	11	206	Mar 25 Thursday
85	7	1	3	11	6	12	9	21	2	6	8	36	42	9	16	8	7	9	16	13	15	12	8	7	284	Mar 26 Friday
86	8	10	7	6	20	10	9	11	11	39	23	16	18	14	9	22	8	7	7	6	7	4	8	10	290	Mar 27 Saturday
87	15	7	15	12	17	14	16	66	52	15	7	2	8	12	7	7	4	6	7	2	3	3	5	8	310	Mar 28 Sunday
88	2	22	11	4	12	6	4	4	6	4	9	5	10	7	10	11	9	13	4	13	3	3	5	2	179	Mar 29 Monday
89	5	1	4	4	8	1	2	13	11	6	16	6	12	10	8	6	5	5	8	20	20	11	6	3	191	Mar 30 Tuesday
90	6	4	4	11	6	5	3	8	16	14	13	15	27	16	7	14	10	13	10	6	16	1	8	8	241	Mar 31 Wednesday

NRS	00	01	02	03	04	05	06	07	08	09	10	11	12	13	14	15	16	17	18	19	20	21	22	23		
Sum	1400	1391	1438	1373	1432	1579	1380	1256	1312	1375	1709	1443	1972	1990	2030	2121	1530	1592	1387	1442	1392	1612	1273	1354	36783	Total sum
182	8	8	8	8	9	8	7	8	8	7	8	9	11	11	12	11	9	8	8	8	9	8	7	7	202	Total average
128	8	8	8	8	8	6	5	5	5	6	7	10	12	12	13	11	8	8	8	8	10	7	7	7	196	Average workdays
54	8	8	7	8	9	12	12	13	13	11	9	9	8	8	8	11	9	8	9	7	7	8	8	7	217	Average weekends

Table 3.4.1. Daily and hourly distributions of NORESS detections. For each day is shown number of detections within each hour of the day, and number of detections for that day. The end statistics give total number of detections distributed for each hour and the total sum of detections during the period. the averages show number of processed days, hourly distribution and average per processed day. (Page 4 of 4)

FRS .FKX Hourly distribution of detections

Day	00	01	02	03	04	05	06	07	08	09	10	11	12	13	14	15	16	17	18	19	20	21	22	23	Sum	Date		
275	15	13	10	19	8	17	20	19	22	6	11	16	22	24	32	12	16	23	14	22	4	12	12	26	395	Oct	01	Thursday
276	2	14	5	1	10	15	16	24	39	13	37	34	35	15	24	15	25	25	7	29	12	23	14	21	455	Oct	02	Friday
277	4	8	7	4	7	11	25	20	9	21	13	32	17	16	17	11	24	15	13	12	10	7	18	24	345	Oct	03	Saturday
278	3	8	5	2	5	13	8	11	2	13	7	3	23	63	19	18	2	6	16	12	14	13	17	8	291	Oct	04	Sunday
279	0	5	10	10	8	9	15	14	12	18	26	20	12	14	11	9	18	16	15	5	16	5	10	29	307	Oct	05	Monday
280	13	7	1	14	8	15	18	19	13	11	34	21	30	19	22	16	21	12	6	19	24	12	18	18	391	Oct	06	Tuesday
281	11	4	10	8	8	10	18	18	38	17	19	19	27	16	11	28	22	16	13	13	13	13	19	8	379	Oct	07	Wednesday
282	4	4	15	19	13	13	11	17	14	28	8	28	10	19	11	7	17	11	11	12	8	10	11	15	316	Oct	08	Thursday
283	24	16	10	9	9	11	14	15	5	16	27	22	36	16	32	24	7	43	34	13	12	19	24	31	469	Oct	09	Friday
284	7	5	7	5	10	8	10	6	17	15	9	22	10	3	15	18	8	10	14	10	15	5	19	21	269	Oct	10	Saturday
285	12	26	25	36	46	30	12	7	6	4	8	7	1	8	11	6	9	12	8	25	8	14	10	22	353	Oct	11	Sunday
286	19	7	12	15	37	29	31	20	21	21	13	20	29	54	39	39	45	48	48	40	61	19	43	23	733	Oct	12	Monday
287	21	14	8	8	6	13	25	27	11	25	21	24	32	32	27	9	21	28	3	18	12	14	17	24	440	Oct	13	Tuesday
288	4	11	11	10	15	20	20	29	25	26	25	34	97	104	155	212	217	209	175	161	127	210	238	150	2285	Oct	14	Wednesday
289	124	114	178	44	25	80	15	18	24	26	35	29	21	35	34	11	20	12	14	29	29	31	22	26	996	Oct	15	Thursday
290	10	17	18	13	12	28	19	15	25	8	43	33	39	60	79	166	148	130	41	23	15	12	25	38	1017	Oct	16	Friday
291	13	26	44	117	227	192	91	9	20	30	18	28	51	93	191	205	180	156	134	79	105	114	91	127	2341	Oct	17	Saturday
292	94	112	134	119	107	102	63	21	7	7	14	17	18	33	29	48	55	65	69	78	58	27	14	43	1334	Oct	18	Sunday
293	35	32	24	52	51	42	30	22	12	12	20	26	41	16	24	22	42	152	167	147	88	37	12	19	1125	Oct	19	Monday
294	30	64	79	58	103	100	66	28	4	12	11	18	17	26	23	19	46	8	14	20	21	10	6	26	809	Oct	20	Tuesday
295	12	11	1	6	10	19	22	17	22	15	25	24	30	23	15	21	10	10	10	12	10	14	8	74	421	Oct	21	Wednesday
296	184	113	9	7	13	17	11	5	12	25	30	23	28	33	24	24	34	30	87	146	161	140	120	73	1349	Oct	22	Thursday
297	17	19	43	129	182	176	135	54	16	46	32	36	46	41	57	124	118	102	57	52	48	47	29	37	1643	Oct	23	Friday
298	19	13	8	12	19	8	16	18	23	16	20	31	18	11	12	21	13	3	15	14	9	16	8	35	378	Oct	24	Saturday
299	12	21	24	12	8	9	6	10	23	10	1	15	1	10	32	29	9	8	11	39	48	89	111	113	651	Oct	25	Sunday
300	64	7	6	12	9	16	21	11	23	11	21	13	33	33	28	48	37	30	17	19	7	11	7	26	510	Oct	26	Monday
301	17	4	7	8	6	9	15	8	35	18	30	37	33	54	74	92	113	104	113	108	112	94	79	57	1227	Oct	27	Tuesday
302	36	30	15	17	15	19	43	16	20	33	34	13	48	22	34	51	67	78	54	59	64	74	93	90	1025	Oct	28	Wednesday
303	105	108	89	90	53	75	57	26	15	25	15	18	12	19	12	14	15	17	6	8	16	14	20	22	851	Oct	29	Thursday
304	12	13	15	36	14	33	25	27	20	17	19	23	29	16	19	18	15	14	5	20	15	16	21	18	460	Oct	30	Friday
305	8	7	8	6	21	28	39	32	18	19	22	17	6	24	21	23	19	19	11	9	9	12	25	25	428	Oct	31	Saturday
306	22	37	37	21	22	14	29	10	20	15	14	10	10	32	53	58	69	136	110	92	138	160	130	110	1349	Nov	01	Sunday
307	71	58	35	13	11	13	15	8	11	20	13	17	17	23	32	16	25	13	16	10	19	12	11	17	496	Nov	02	Monday
308	15	10	6	7	24	8	10	11	27	23	17	17	23	22	21	25	18	12	18	16	9	6	8	20	373	Nov	03	Tuesday
309	9	11	8	6	7	13	13	7	18	20	11	15	21	10	17	7	12	7	9	19	10	7	11	15	283	Nov	04	Wednesday
310	9	6	3	2	3	5	10	12	11	23	14	29	30	27	18	17	4	9	12	34	21	21	46	40	406	Nov	05	Thursday
311	42	49	65	63	59	39	41	37	43	32	46	38	35	30	48	48	65	84	77	63	25	21	4	14	1068	Nov	06	Friday
312	5	5	11	6	18	36	56	64	59	27	28	47	65	85	96	85	33	90	81	60	62	65	61	60	1205	Nov	07	Saturday
313	62	50	31	15	13	6	8	4	8	8	10	5	5	2	14	9	5	5	14	19	13	15	11	12	344	Nov	08	Sunday
314	7	6	3	13	5	6	12	9	5	13	16	9	22	13	17	15	8	14	9	14	13	18	6	13	266	Nov	09	Monday
315	3	10	5	8	8	4	10	6	22	8	34	24	17	10	22	7	14	15	5	10	10	12	13	25	302	Nov	10	Tuesday
316	10	10	4	9	4	12	5	15	13	24	19	13	25	20	12	13	15	14	9	15	10	12	6	15	304	Nov	11	Wednesday
317	3	7	3	5	5	17	17	18	18	18	22	21	28	33	12	14	10	19	4	19	11	16	16	18	354	Nov	12	Thursday
318	14	14	15	6	7	3	21	6	20	23	23	24	40	22	7	12	13	13	10	7	10	9	10	15	344	Nov	13	Friday
319	8	7	6	7	7	6	16	2	16	17	19	31	22	23	10	20	6	4	12	14	7	5	13	10	288	Nov	14	Saturday
320	4	4	15	26	24	15	22	34	53	56	50	20	35	52	55	60	52	79	86	60	41	6	5	33	887	Nov	15	Sunday
321	5	12	3	5	9	8	12	23	22	23	9	21	12	14	13	11	11	18	11	14	8	3	18	12	297	Nov	16	Monday
322	10	7	8	6	12	5	11	13	25	16	16	16	28	18	11	10	5	19	9	18	8	8	10	25	314	Nov	17	Tuesday
323	12	2	3	3	15	17	14	15	13	28	25	18	39	22	25	10	26	18	8	15	4	21	17	18	388	Nov	18	Wednesday
324	8	12	5	14	6	6	18	17	35	28	19	16	26	20	13	16	6	13	8	11	12	9	4	36	358	Nov	19	Thursday
325	5	8	14	2	11	21	12	7	18	25	29	26	24	31	21	19	18	17	23	25	13	25	28	29	451	Nov	20	Friday
326	24	21	23	27	30	22	14	8	25	27	50	20	28	16	12	10	7	12	8	4	5	9	20	38	460	Nov	21	Saturday
327	14	10	11	6	9	7	9	6	11	13	12	10	8	14	14	21	20	28	42	63	67	83	79	79	636	Nov	22	Sunday
328	69	82	79	63	56	45	32	12	14	10	19	7	22	10	18	13	20	12	11	13	14	14	18	23	676	Nov	23	Monday
329	22	21	8	9	1	6	8	5	7	8	17	31	23	14	18	7	15	11	12	8	8	15	10	32	316	Nov	24	Tuesday
330	13	6	2	10	7	4	20	2	8	14	44	26	15	16	16	13	13	14	18	22	17	14	12	16	342	Nov	25	Wednesday

Table 3.4.2 (Page 1 of 4)

FRS .FKX Hourly distribution of detections

Day	00	01	02	03	04	05	06	07	08	09	10	11	12	13	14	15	16	17	18	19	20	21	22	23	Sum	Date		
331	5	9	7	4	17	3	8	7	13	14	19	24	18	12	15	11	20	5	14	16	17	21	6	25	310	Nov 26	Thursday	
332	16	8	17	7	15	7	7	18	13	15	16	27	25	25	22	3	13	24	13	15	17	8	2	20	353	Nov 27	Friday	
333	11	7	8	16	5	4	11	12	14	6	34	14	32	16	28	53	61	20	18	14	9	9	1	24	427	Nov 28	Saturday	
334	13	3	10	8	15	7	13	6	14	12	5	14	19	15	10	45	16	54	24	53	42	39	16	17	470	Nov 29	Sunday	
335	17	21	16	14	11	12	8	6	13	26	19	14	37	7	23	9	26	26	10	10	3	5	4	27	364	Nov 30	Monday	
336	10	5	5	6	11	5	7	11	21	20	17	21	25	20	13	19	14	13	16	11	14	27	10	29	350*	Dec 01	Tuesday	
337	5	1	6	12	4	10	10	16	12	21	21	32	16	18	23	10	17	8	12	9	9	24	11	16	323	Dec 02	Wednesday	
338	2	2	3	3	4	9	11	12	23	23	25	18	26	10	24	20	13	14	11	17	23	14	13	15	335	Dec 03	Thursday	
339	13	11	10	7	14	8	18	29	29	20	18	16	38	17	23	11	9	16	8	14	14	9	18	20	390	Dec 04	Friday	
340	15	10	6	10	11	7	19	11	7	18	23	28	12	4	11	7	10	6	11	11	6	2	9	16	270	Dec 05	Saturday	
341	5	11	10	9	2	9	7	9	4	7	6	5	8	7	21	12	8	13	9	15	9	6	21	15	228	Dec 06	Sunday	
342	5	6	12	5	10	14	15	15	8	10	17	12	12	17	13	16	18	23	24	15	12	14	6	13	312	Dec 07	Monday	
343	10	4	7	10	15	7	8	13	20	10	27	29	37	18	30	18	32	17	20	18	31	15	22	29	447	Dec 08	Tuesday	
344	21	18	10	6	11	15	16	11	16	17	23	32	34	17	15	21	11	15	9	9	16	13	10	20	386	Dec 09	Wednesday	
345	1	9	4	10	7	10	12	11	5	6	16	13	11	16	8	15	4	13	8	10	17	11	16	17	250	Dec 10	Thursday	
346	7	8	14	2	7	9	12	23	23	15	18	41	15	22	13	24	1	3	12	6	1	6	13	11	306	Dec 11	Friday	
347	8	8	12	6	3	27	11	17	7	5	14	21	9	12	22	10	2	5	6	8	6	9	7	16	251	Dec 12	Saturday	
348	11	2	6	8	2	5	8	21	14	17	23	21	18	22	30	21	18	36	26	41	27	23	24	17	441	Dec 13	Sunday	
349	9	7	5	14	6	8	13	28	24	12	8	24	19	11	7	11	4	14	7	12	7	18	12	19	299	Dec 14	Monday	
350	9	12	5	8	17	13	15	27	27	23	5	23	35	16	17	11	12	16	22	25	8	13	10	16	385	Dec 15	Tuesday	
351	10	5	13	12	7	14	12	19	22	24	25	0	12	19	8	14	17	20	11	9	7	3	4	24	311	Dec 16	Wednesday	
352	2	8	6	8	17	14	17	11	14	19	13	20	28	10	12	13	21	21	10	28	11	6	13	21	343	Dec 17	Thursday	
353	13	7	6	17	8	11	18	2	0	20	20	24	35	7	15	9	2	18	12	14	14	12	3	11	298	Dec 18	Friday	
354	7	15	6	9	1	63	9	6	13	8	6	15	22	12	8	4	7	2	4	7	11	9	12	16	272	Dec 19	Saturday	
355	3	4	4	4	1	2	1	7	5	7	0	3	3	2	2	1	8	5	3	5	4	13	5	6	98	Dec 20	Sunday	
356	2	4	4	5	7	7	2	5	3	5	6	8	8	6	7	4	7	3	3	11	0	1	9	17	134	Dec 21	Monday	
357	8	8	10	6	8	14	6	6	12	11	13	11	19	12	11	13	13	3	7	5	12	5	6	17	236	Dec 22	Tuesday	
358	8	2	5	5	10	5	15	8	15	10	15	19	16	8	6	12	7	3	10	6	7	7	5	13	217	Dec 23	Wednesday	
359	14	5	8	1	3	12	9	7	21	2	3	19	17	5	6	5	3	8	8	5	11	4	4	2	182	Dec 24	Thursday	
360	4	3	3	7	8	2	8	7	11	10	9	3	20	2	3	4	8	7	7	2	4	6	7	2	147	Dec 25	Friday	Frste
361	6	3	1	3	3	10	11	8	7	8	11	19	8	5	1	6	2	3	8	13	8	9	12	4	169	Dec 26	Saturday	Andre
362	6	4	0	1	4	9	9	12	9	5	5	7	5	4	6	6	15	4	0	9	3	11	15	9	158	Dec 27	Sunday	
363	4	4	4	11	8	7	10	5	10	15	19	12	7	15	6	15	4	6	3	10	14	2	5	14	210	Dec 28	Monday	
364	1	12	9	6	1	4	6	4	2	6	7	14	6	9	13	13	7	4	3	7	4	10	4	19	171	Dec 29	Tuesday	
365	7	5	2	4	8	5	22	19	29	12	21	39	23	17	12	28	7	11	8	27	14	12	7	13	352	Dec 30	Wednesday	
366	6	6	9	8	13	11	10	13	16	15	7	17	11	9	12	5	10	19	6	6	11	9	6	1	236	Dec 31	Thursday	
1	3	7	3	3	14	6	8	7	9	4	8	4	4	12	6	15	1	4	4	3	3	9	7	12	156	Jan 01	Friday	Frste
2	7	7	2	8	12	6	5	2	8	5	6	6	8	7	4	7	3	0	1	2	4	3	5	5	123	Jan 02	Saturday	
3	0	3	5	1	2	6	0	3	1	4	3	8	6	6	2	6	13	17	6	6	26	13	5	14	156	Jan 03	Sunday	
4	2	12	8	11	6	11	11	15	15	18	13	11	10	6	6	7	11	3	14	14	11	13	5	14	247	Jan 04	Monday	
5	0	7	8	4	5	4	2	12	9	8	14	14	4	6	9	6	5	7	1	5	5	14	5	14	168	Jan 05	Tuesday	
6	8	7	5	10	6	3	12	7	13	15	19	19	19	16	12	6	12	6	6	15	7	3	12	30	268	Jan 06	Wednesday	
7	3	5	2	3	7	9	10	10	11	18	12	19	27	17	9	14	8	17	14	9	14	25	17	35	315	Jan 07	Thursday	
8	25	30	30	14	14	6	21	17	22	12	9	16	16	17	23	4	10	14	10	10	6	12	5	15	358	Jan 08	Friday	
9	5	7	6	8	7	4	4	10	3	3	5	14	6	4	7	6	7	7	3	5	3	5	5	18	152	Jan 09	Saturday	
10	9	5	4	4	4	8	5	6	9	5	15	6	9	2	9	14	6	8	12	5	16	13	11	19	204	Jan 10	Sunday	
11	5	2	1	9	8	11	7	19	27	15	13	20	19	16	11	10	3	2	2	9	14	19	11	9	262	Jan 11	Monday	
12	9	4	3	5	18	12	9	23	13	26	17	9	19	13	1	8	9	4	5	5	5	2	1	8	228	Jan 12	Tuesday	
13	4	6	3	5	8	3	9	6	5	12	10	9	24	9	8	7	14	16	27	37	43	49	57	61	432	Jan 13	Wednesday	
14	60	44	49	51	61	57	46	55	45	32	20	35	42	39	54	60	71	68	62	73	54	57	56	63	1254	Jan 14	Thursday	
15	60	68	68	48	56	32	35	39	43	24	39	39	48	34	31	20	17	7	11	13	13	11	9	22	787	Jan 15	Friday	
16	3	5	12	5	11	14	12	8	17	11	15	28	29	14	14	12	11	6	11	4	8	1	7	20	278	Jan 16	Saturday	
17	10	5	4	8	4	3	10	3	5	3	10	9	16	19	14	20	8	12	24	28	26	17	11	14	283	Jan 17	Sunday	
18	15	20	9	12	20	5	16	13	17	30	24	14	27	12	15	12	19	11	12	19	14	11	13	29	389	Jan 18	Monday	
19	21	16	27	19	18	15	7	19	21	20	31	16	41	35	18	38	30	42	41	60	65	59	57	85	801	Jan 19	Tuesday	
20	96	115	118	123	108	99	82	53	46	64	76	67	66	42	25	23	33	22	10	15	11	16	26	35	1371	Jan 20	Wednesday	

Table 3.4.2. (Page 2 of 4)

FRS .FKX Hourly distribution of detections

Day	00	01	02	03	04	05	06	07	08	09	10	11	12	13	14	15	16	17	18	19	20	21	22	23	Sum	Date		
21	13	11	15	14	9	9	6	9	19	19	15	23	29	28	23	13	5	7	10	11	8	14	2	34	346	Jan	21	Thursday
22	8	12	7	13	10	1	12	11	19	22	23	17	31	26	7	14	8	18	12	8	0	10	17	19	325	Jan	22	Friday
23	10	13	17	17	39	55	51	60	43	49	58	60	54	40	45	60	51	55	63	46	52	44	54	61	1097	Jan	23	Saturday
24	45	50	51	66	70	82	59	76	91	93	70	61	81	80	86	94	74	88	102	94	94	76	70	67	1820	Jan	24	Sunday
25	60	43	40	37	46	47	51	52	64	61	58	55	43	57	56	49	42	53	59	58	48	31	25	25	1160	Jan	25	Monday
26	12	14	7	11	10	6	18	10	9	13	13	20	10	19	4	5	14	13	9	8	13	9	4	18	269	Jan	26	Tuesday
27	7	10	10	16	5	10	12	8	7	12	21	23	20	25	18	18	12	7	9	13	12	16	9	27	327	Jan	27	Wednesday
28	12	5	12	7	4	21	17	5	8	15	26	29	22	16	15	16	18	11	18	17	10	11	13	36	364	Jan	28	Thursday
29	22	9	15	7	9	4	10	9	16	21	19	16	40	20	18	11	5	8	14	10	11	11	1	30	336	Jan	29	Friday
30	5	8	4	7	8	11	9	4	15	6	25	9	14	12	9	4	11	6	16	11	17	7	4	23	245	Jan	30	Saturday
31	1	13	1	2	8	6	3	7	3	5	1	4	5	6	3	4	4	6	4	12	2	1	7	10	118	Jan	31	Sunday
32	7	4	5	7	5	7	15	2	11	13	3	5	10	5	3	6	1	8	3	1	1	0	0	0	122	Feb	01	Monday
33	0	0	0	0	0	13	19	19	14	8	10	15	4	12	4	6	13	9	5	9	2	7	5	10	184	Feb	02	Tuesday
34	5	4	5	11	14	10	11	10	5	4	18	7	12	8	4	4	7	4	4	3	3	1	4	12	170	Feb	03	Wednesday
35	4	6	5	7	5	12	4	9	15	8	25	34	30	35	16	39	30	34	65	70	65	40	31	30	619	Feb	04	Thursday
36	17	17	29	53	74	94	117	98	76	55	70	52	54	55	39	29	37	24	7	6	7	4	5	8	1027	Feb	05	Friday
37	8	3	4	2	8	3	6	10	3	5	5	12	6	3	13	7	4	5	10	10	7	3	8	12	157	Feb	06	Saturday
38	3	7	3	10	12	13	13	34	31	48	48	50	59	72	114	142	164	196	189	204	190	176	228	34	2040	Feb	07	Sunday
39	0	0	0	0	0	0	0	0	0	0	0	0	0	0	0	0	0	0	0	3	5	5	3	11	27	Feb	08	Monday
40	1	4	7	8	3	3	9	4	17	10	14	15	18	17	20	6	10	7	13	10	20	11	13	24	264	Feb	09	Tuesday
41	20	13	8	5	14	13	10	10	11	10	17	24	30	22	6	11	23	14	18	14	17	22	33	29	394	Feb	10	Wednesday
42	9	15	3	9	7	7	4	9	13	16	16	13	22	13	6	9	10	13	11	4	8	5	6	7	235	Feb	11	Thursday
43	5	4	8	3	4	8	3	3	14	21	16	16	21	27	14	7	14	3	10	10	10	9	20	24	274	Feb	12	Friday
44	16	4	5	19	8	8	10	10	16	7	19	21	23	17	5	7	10	8	5	5	12	4	18	16	273	Feb	13	Saturday
45	6	8	4	7	8	9	4	11	6	6	7	6	7	4	6	7	6	4	13	11	10	13	16	12	191	Feb	14	Sunday
46	11	8	2	10	6	6	2	7	13	16	13	21	31	26	59	7	11	14	5	8	9	6	11	15	317	Feb	15	Monday
47	10	9	12	14	7	17	22	6	22	9	12	11	15	23	13	7	16	11	6	4	13	10	10	18	297	Feb	16	Tuesday
48	21	25	29	27	38	29	26	24	21	16	21	27	32	19	10	13	23	18	35	43	48	56	47	53	701	Feb	17	Wednesday
49	45	44	39	25	29	30	53	47	37	36	45	60	50	43	40	39	49	53	49	52	45	50	41	75	1076	Feb	18	Thursday
50	69	62	81	68	72	73	64	66	77	69	71	46	70	57	62	27	43	43	36	47	41	42	42	72	1400	Feb	19	Friday
51	64	58	71	78	86	85	99	82	86	67	79	75	97	62	92	80	74	84	109	92	106	105	96	106	2033	Feb	20	Saturday
52	123	98	97	95	105	100	78	70	52	53	52	35	38	25	36	34	20	20	25	19	22	22	22	34	1275	Feb	21	Sunday
53	27	20	26	26	26	35	30	19	29	30	24	17	30	11	29	22	13	8	12	18	16	14	10	23	515	Feb	22	Monday
54	13	4	10	9	10	10	9	13	12	28	16	5	23	27	12	15	7	6	22	11	8	9	3	23	305	Feb	23	Tuesday
55	4	13	9	9	6	5	7	4	5	12	16	11	18	5	20	11	14	8	7	9	13	14	12	19	251	Feb	24	Wednesday
56	8	14	9	4	8	8	8	9	13	20	8	15	20	11	14	13	8	14	13	11	19	15	14	22	298	Feb	25	Thursday
57	21	17	11	15	15	14	21	10	21	22	24	21	30	30	27	7	9	16	22	12	9	8	17	20	419	Feb	26	Friday
58	15	4	7	7	6	11	12	9	14	15	15	15	30	9	4	10	19	14	16	7	20	4	10	19	292	Feb	27	Saturday
59	10	3	7	9	15	7	8	12	27	25	5	6	14	14	29	68	87	81	50	50	57	64	64	76	788	Feb	28	Sunday
60	54	50	44	31	29	21	33	21	25	26	17	12	17	14	8	14	12	8	6	8	8	9	2	10	479	Mar	01	Monday
61	6	16	11	16	16	9	15	16	19	6	24	12	29	9	15	22	15	15	8	10	16	19	12	11	347	Mar	02	Tuesday
62	10	15	6	15	6	7	12	10	8	6	22	10	18	11	8	5	8	5	6	7	3	7	2	8	215	Mar	03	Wednesday
63	3	4	4	6	2	18	2	3	11	15	2	16	20	19	10	17	18	15	16	18	38	48	52	64	421	Mar	04	Thursday
64	56	81	78	89	71	74	69	54	70	38	44	36	44	35	38	37	18	19	14	16	8	12	9	15	1025	Mar	05	Friday
65	1	19	8	18	12	5	20	13	18	18	32	36	20	6	12	7	11	15	9	13	11	14	17	32	367	Mar	06	Saturday
66	16	4	15	11	16	24	28	27	26	30	39	26	30	34	46	26	29	36	26	40	24	25	20	35	633	Mar	07	Sunday
67	19	9	8	11	9	6	8	10	17	9	15	14	9	16	19	17	11	4	15	11	4	9	17	22	289	Mar	08	Monday
68	3	9	1	4	7	16	13	8	38	17	14	19	18	13	20	13	13	9	11	7	11	7	4	19	294	Mar	09	Tuesday
69	2	2	2	3	5	6	7	5	5	4	6	6	26	11	5	4	8	4	11	12	12	13	22	29	210	Mar	10	Wednesday
70	35	33	36	56	48	36	33	16	33	17	21	28	38	16	23	38	61	61	64	62	80	72	80	88	1075	Mar	11	Thursday
71	104	93	94	70	79	79	80	74	78	70	73	61	73	86	66	68	61	62	66	61	74	65	65	62	1764	Mar	12	Friday
72	35	33	33	45	28	22	20	28	21	26	15	23	31	24	15	12	12	14	13	9	21	12	6	16	514	Mar	13	Saturday
73	9	3	8	9	8	4	8	14	15	19	11	20	10	12	12	13	4	9	13	10	14	13	11	22	271	Mar	14	Sunday
74	9	8	5	12	7	2	12	13	7	13	17	10	18	25	15	14	15	12	9	10	17	8	7	15	280	Mar	15	Monday
75	7	8	3	8	9	6	9	18	29	11	13	25	23	15	11	9	11	11	7	17	10	12	4	27	303	Mar	16	Tuesday
76	7	5	6	7	4	12	7	7	21	14	28	18	33	21	11	15	18	16	23	9	16	13	7	16	334	Mar	17	Wednesday

Table 3.4.2 (Page 3 of 4)

FRS .FKX Hourly distribution of detections

Day	00	01	02	03	04	05	06	07	08	09	10	11	12	13	14	15	16	17	18	19	20	21	22	23	Sum	Date
77	12	5	7	3	9	9	21	26	13	11	25	20	20	20	11	34	15	13	10	13	11	13	7	21	349	Mar 18 Thursday
78	16	3	15	9	10	9	16	17	20	26	29	16	38	9	16	13	16	20	15	12	12	11	10	7	365	Mar 19 Friday
79	5	15	11	8	14	6	24	13	18	20	23	33	11	8	16	20	14	4	3	15	4	10	5	25	325	Mar 20 Saturday
80	10	15	2	9	8	14	6	7	4	4	3	15	8	11	12	6	3	15	14	14	12	5	22	13	232	Mar 21 Sunday
81	8	7	5	16	7	14	11	16	16	15	18	13	13	17	22	24	13	23	17	19	5	11	16	19	345	Mar 22 Monday
82	6	8	6	15	9	10	12	10	23	20	25	26	26	24	21	23	19	10	9	17	14	15	21	18	387	Mar 23 Tuesday
83	15	14	10	16	9	20	19	15	16	27	11	20	25	31	24	12	17	6	7	20	15	9	22	15	395	Mar 24 Wednesday
84	8	10	8	6	11	12	24	23	11	9	8	20	17	26	16	12	11	17	7	12	15	17	11	27	338	Mar 25 Thursday
85	12	5	8	8	9	12	17	23	18	25	31	15	60	28	14	14	6	12	14	13	9	11	18	26	408	Mar 26 Friday
86	7	5	9	8	7	8	15	22	23	33	21	25	22	16	13	8	14	12	10	12	8	6	8	14	326	Mar 27 Saturday
87	7	4	6	5	12	5	4	13	6	19	16	5	5	9	9	6	10	8	11	5	19	10	7	17	218	Mar 28 Sunday
88	4	18	9	8	12	31	18	23	14	12	12	22	26	24	17	15	18	11	12	2	12	9	27	8	364	Mar 29 Monday
89	10	14	14	10	22	25	29	35	38	42	31	31	32	29	26	15	20	15	24	15	24	11	20	9	541	Mar 30 Tuesday
90	3	9	7	24	16	15	21	6	22	15	14	15	19	13	17	25	10	11	16	7	16	13	19	8	341	Mar 31 Wednesday
FRS	00	01	02	03	04	05	06	07	08	09	10	11	12	13	14	15	16	17	18	19	20	21	22	23		
Sum	3280	3138	3033	3171	3450	3625	3589	3155	3556	3455	3783	3845	4531	3925	4064	4180	4107	4330	4053	4263	4079	3943	3953	4966	91474	Total sum
182	18	17	17	17	19	20	20	17	20	19	21	21	25	22	22	23	23	24	22	23	22	22	22	27	503	Total average
128	19	18	17	17	18	19	20	17	20	19	21	22	27	22	21	21	22	22	20	22	20	19	19	26	486	Average workdays
54	15	15	16	18	21	22	19	17	18	18	19	20	21	21	25	28	25	28	28	28	28	27	28	31	538	Average weekends

Table 3.4.2. Daily and hourly distributions of ARCESS detections. For each day is shown number of detections within each hour of the day, and number of detections for that day. The end statistics give total number of detections distributed for each hour and the total sum of detections during the period. the averages show number of processed days, hourly distribution and average per processed day. (page 4 of 4)

FIN .FKX Hourly distribution of detections

Day	00	01	02	03	04	05	06	07	08	09	10	11	12	13	14	15	16	17	18	19	20	21	22	23	Sum	Date	
275	7	11	12	17	7	5	7	2	17	9	7	15	20	12	6	9	2	7	9	10	14	5	7	9	226	Oct 01	Thursday
276	10	7	7	3	5	6	2	5	5	15	12	16	17	16	6	2	7	7	2	9	3	3	2	0	167	Oct 02	Friday
277	2	4	3	5	0	4	0	5	41	32	8	8	4	14	15	14	12	5	4	0	3	3	3	0	189	Oct 03	Saturday
278	0	1	2	9	4	10	22	12	12	10	10	5	2	3	5	6	11	13	3	3	6	9	13	7	178	Oct 04	Sunday
279	10	6	11	13	6	14	10	6	19	9	4	6	15	11	4	7	6	6	10	9	2	10	7	8	209	Oct 05	Monday
280	13	5	15	21	21	2	4	3	12	11	17	14	21	5	9	10	5	4	15	20	17	9	24	16	293	Oct 06	Tuesday
281	16	14	7	14	12	3	4	9	13	13	19	14	34	10	12	15	5	2	7	9	7	3	8	3	253	Oct 07	Wednesday
282	11	3	6	11	24	7	4	9	9	16	11	13	26	11	41	21	25	10	15	17	4	5	4	6	309	Oct 08	Thursday
283	13	10	9	16	18	8	11	4	5	6	14	14	21	11	21	5	2	5	6	7	3	3	3	4	219	Oct 09	Friday
284	2	1	4	5	10	7	7	3	4	9	5	4	9	10	12	1	0	5	5	1	3	2	5	5	119	Oct 10	Saturday
285	7	6	4	1	1	0	10	3	3	5	0	4	5	4	11	11	8	10	8	13	10	5	10	18	157	Oct 11	Sunday
286	10	20	14	8	4	14	21	8	12	16	7	17	8	15	7	6	5	7	9	9	14	11	9	11	262	Oct 12	Monday
287	13	12	16	14	5	0	3	2	4	14	4	15	12	31	13	13	4	6	6	3	9	6	6	3	214	Oct 13	Tuesday
288	7	9	7	10	4	2	6	3	6	23	26	20	40	30	35	31	39	44	29	44	27	31	31	34	538	Oct 14	Wednesday
289	40	35	31	38	40	20	8	5	5	7	22	14	18	28	21	12	23	5	8	13	9	8	15	9	434	Oct 15	Thursday
290	13	13	20	5	18	7	10	6	8	14	12	13	23	26	16	27	14	20	13	15	3	3	8	7	314	Oct 16	Friday
291	10	13	14	9	20	8	6	3	7	9	5	7	18	8	4	7	1	3	1	0	4	7	2	4	170	Oct 17	Saturday
292	5	4	11	8	4	5	3	3	3	1	3	12	4	12	0	20	14	5	6	16	6	6	5	9	165	Oct 18	Sunday
293	5	11	7	11	5	3	1	2	4	6	8	12	15	9	3	14	4	3	6	9	17	20	15	12	202	Oct 19	Monday
294	15	21	14	9	8	4	3	11	11	10	3	16	3	10	16	7	9	3	3	4	9	5	10	5	209	Oct 20	Tuesday
295	5	10	6	13	6	4	1	3	12	14	5	23	18	13	8	7	16	4	10	9	16	20	11	17	251	Oct 21	Wednesday
296	22	20	6	40	21	9	8	4	11	28	13	25	18	37	28	26	24	32	32	47	52	46	63	69	681	Oct 22	Thursday
297	25	14	13	15	4	0	0	0	0	10	15	22	17	18	4	10	2	12	8	3	6	12	11	28	249	Oct 23	Friday
298	17	44	75	46	21	9	5	7	11	12	16	26	13	37	70	96	65	83	70	23	42	12	23	14	837	Oct 24	Saturday
299	71	31	58	66	16	32	8	8	8	5	2	5	22	20	9	49	107	68	88	39	21	114	51	53	951	Oct 25	Sunday
300	20	11	51	102	99	58	18	9	11	7	13	25	17	29	33	12	31	40	47	79	79	92	108	47	1038	Oct 26	Monday
301	64	73	19	16	2	4	0	3	3	9	1	27	13	18	12	8	5	2	2	8	5	8	8	8	318	Oct 27	Tuesday
302	8	11	20	8	31	17	14	16	10	20	25	27	29	19	27	28	78	26	41	69	67	74	72	68	805	Oct 28	Wednesday
303	40	12	7	18	4	11	33	36	9	6	23	12	3	12	18	6	6	2	4	11	9	5	9	2	298	Oct 29	Thursday
304	3	4	3	11	12	8	6	2	3	11	12	9	25	13	10	11	7	17	44	28	8	5	6	12	270	Oct 30	Friday
305	10	9	5	12	5	15	1	0	3	3	3	10	4	1	13	13	4	5	11	6	5	3	4	5	150	Oct 31	Saturday
306	4	4	2	3	6	19	5	8	7	6	13	3	6	9	7	24	3	7	10	11	20	11	4	2	194	Nov 01	Sunday
307	10	9	4	11	6	6	6	6	11	4	4	11	18	11	11	7	9	2	10	15	13	9	13	9	215	Nov 02	Monday
308	17	8	12	8	11	6	6	4	11	8	9	11	14	10	5	4	9	7	2	13	12	14	23	34	258	Nov 03	Tuesday
309	21	30	26	19	15	10	13	3	4	11	16	20	24	12	18	15	20	10	9	15	8	3	7	7	336	Nov 04	Wednesday
310	7	8	8	6	5	3	1	2	4	18	7	31	25	12	5	8	6	5	17	11	15	12	14	5	235	Nov 05	Thursday
311	7	9	19	18	15	9	2	14	14	11	14	22	21	24	8	13	3	7	8	7	11	7	3	7	273	Nov 06	Friday
312	8	4	7	8	6	7	3	1	3	5	25	16	1	4	14	12	29	39	41	41	47	21	12	17	371	Nov 07	Saturday
313	16	13	15	24	22	21	8	11	13	13	13	10	6	13	15	24	22	22	31	23	26	34	42	31	468	Nov 08	Sunday
314	15	3	6	4	8	2	5	4	8	8	13	9	18	17	11	5	4	9	6	3	7	11	10	8	194	Nov 09	Monday
315	10	11	9	14	8	3	7	3	6	12	11	20	22	20	5	7	3	4	4	9	12	7	8	8	223	Nov 10	Tuesday
316	6	11	14	8	7	5	3	6	6	15	16	11	18	17	12	2	1	4	2	12	6	9	6	4	201	Nov 11	Wednesday
317	10	10	10	18	7	10	19	7	12	17	7	24	21	17	4	13	7	8	5	7	7	6	13	5	264	Nov 12	Thursday
318	10	12	6	8	5	9	10	2	6	13	6	24	31	21	9	4	6	4	7	5	7	9	5	2	221	Nov 13	Friday
319	4	4	4	6	3	4	3	1	8	2	3	6	3	2	6	2	4	3	6	4	2	7	5	1	93	Nov 14	Saturday
320	5	5	6	2	0	0	4	5	8	9	4	4	25	10	3	6	4	1	2	9	5	2	10	11	140	Nov 15	Sunday
321	5	6	6	8	5	4	1	12	7	8	2	22	14	9	11	2	7	10	5	11	8	5	13	14	195	Nov 16	Monday
322	9	9	10	10	10	9	5	7	15	2	7	23	27	17	6	9	5	15	9	16	8	7	13	19	267	Nov 17	Tuesday
323	11	16	10	15	11	9	3	3	8	12	9	20	35	19	7	10	14	7	8	7	8	15	18	9	284	Nov 18	Wednesday
324	11	19	10	9	13	13	6	12	14	10	11	25	19	21	9	7	8	7	4	4	0	7	9	10	258	Nov 19	Thursday
325	8	15	10	9	5	2	2	11	7	8	20	20	18	26	6	3	2	6	5	9	10	11	11	5	229	Nov 20	Friday
326	11	3	8	10	19	17	8	9	4	6	10	8	10	9	7	9	5	2	6	2	3	6	4	7	183	Nov 21	Saturday
327	5	4	11	7	16	7	6	9	14	12	8	13	12	22	32	32	37	26	30	22	25	28	33	18	429	Nov 22	Sunday
328	26	27	22	21	18	10	17	11	12	11	13	20	26	23	26	21	30	17	21	31	24	41	45	57	570	Nov 23	Monday
329	35	38	14	10	4	7	1	4	11	9	12	25	17	13	4	1	15	5	8	8	6	5	3	9	264	Nov 24	Tuesday
330	6	8	8	5	7	2	5	5	9	3	30	22	13	27	8	6	10	3	8	5	6	8	6	12	222	Nov 25	Wednesday

Table 3.4.3 (Page 1 of 4)

FIN .FKX Hourly distribution of detections

Day	00	01	02	03	04	05	06	07	08	09	10	11	12	13	14	15	16	17	18	19	20	21	22	23	Sum	Date	
331	6	7	6	7	8	3	3	21	7	6	11	22	19	16	9	1	9	4	9	9	19	6	13	8	229	Nov 26 Thursday	
332	8	8	13	7	9	3	0	6	14	14	13	15	22	15	12	8	7	3	3	5	4	20	12	4	225	Nov 27 Friday	
333	5	4	8	7	6	9	12	1	8	5	0	7	11	6	5	3	1	5	3	1	3	1	4	4	119	Nov 28 Saturday	
334	1	2	2	11	12	1	5	4	8	7	4	8	6	5	6	3	3	5	5	5	2	5	9	8	127	Nov 29 Sunday	
335	4	5	7	3	6	0	7	5	6	14	5	7	14	22	19	5	7	3	3	2	2	7	8	8	169	Nov 30 Monday	
336	9	12	11	10	9	2	8	5	8	13	14	24	29	16	5	9	11	3	7	7	8	6	13	14	253	Dec 01 Tuesday	
337	11	7	5	6	6	7	9	14	22	19	14	19	12	15	5	3	8	8	5	6	10	11	18	21	261	Dec 02 Wednesday	
338	7	9	7	5	3	2	13	6	12	15	10	24	18	14	16	12	14	14	16	11	12	14	20	8	282	Dec 03 Thursday	
339	8	14	19	19	31	13	8	6	7	13	27	30	34	19	5	4	10	7	2	9	7	10	18	19	339	Dec 04 Friday	
340	11	35	23	21	17	20	22	18	8	13	18	10	15	10	6	5	10	12	13	12	14	11	6	19	349	Dec 05 Saturday	
341	27	29	14	29	14	11	23	15	17	10	10	6	13	5	12	12	13	6	14	12	21	14	13	10	350	Dec 06 Sunday	
342	12	14	16	9	10	4	6	6	7	9	7	10	13	29	11	8	6	2	8	11	13	9	10	12	242	Dec 07 Monday	
343	9	22	17	16	16	6	6	11	6	6	21	19	19	16	9	18	12	25	13	7	20	19	19	14	346	Dec 08 Tuesday	
344	22	28	20	8	14	16	3	13	8	13	17	21	31	35	11	14	31	22	18	26	26	12	19	30	458	Dec 09 Wednesday	
345	18	16	17	14	10	5	0	0	0	0	0	0	0	6	10	11	11	10	5	16	12	10	12	22	205	Dec 10 Thursday	
346	16	24	23	30	36	11	16	12	20	29	22	33	22	19	6	8	4	5	10	6	9	17	14	10	402	Dec 11 Friday	
347	8	16	6	18	12	26	4	4	5	0	3	6	8	3	16	8	1	5	2	7	1	7	4	6	176	Dec 12 Saturday	
348	30	12	8	13	6	2	1	4	8	4	3	5	8	6	4	7	2	7	8	9	6	9	10	10	182	Dec 13 Sunday	
349	9	8	17	8	8	3	1	14	7	11	6	13	13	16	5	6	9	12	7	5	6	9	6	12	211	Dec 14 Monday	
350	9	6	5	6	10	0	3	7	6	3	15	16	32	19	8	7	14	5	6	8	11	8	6	7	217	Dec 15 Tuesday	
351	15	7	12	15	6	4	3	4	6	18	12	4	18	23	9	11	3	5	8	5	4	11	8	14	225	Dec 16 Wednesday	
352	8	13	5	9	6	7	1	7	8	13	15	23	42	15	6	21	19	10	11	7	20	35	27	10	338	Dec 17 Thursday	
353	8	7	15	13	5	2	2	1	13	12	11	25	32	8	0	9	3	6	6	8	8	7	18	8	227	Dec 18 Friday	
354	4	1	5	9	9	16	6	11	14	24	31	21	42	25	12	15	19	23	18	21	7	18	20	18	389	Dec 19 Saturday	
355	6	18	12	26	13	14	11	18	8	11	14	14	15	14	17	16	19	23	18	27	18	38	29	20	419	Dec 20 Sunday	
356	24	44	42	27	18	2	4	10	7	10	9	11	24	9	6	5	4	5	11	13	21	31	41	37	415	Dec 21 Monday	
357	42	41	68	28	13	14	4	7	6	13	12	13	25	38	26	15	14	27	2	9	9	8	18	15	467	Dec 22 Tuesday	
358	12	13	11	12	5	6	1	6	13	11	23	24	15	21	9	9	23	40	35	32	30	48	23	27	449	Dec 23 Wednesday	
359	33	46	53	58	19	6	9	4	23	24	17	16	10	9	3	2	6	8	15	14	8	7	15	6	411	Dec 24 Thursday	
360	7	2	5	5	8	8	3	2	7	9	11	2	16	6	2	5	2	2	6	3	1	3	8	23	146	Dec 25 Friday	Frste
361	5	11	3	11	5	15	17	4	4	3	1	7	15	22	7	12	27	25	14	20	32	30	59	40	389	Dec 26 Saturday	Andre
362	50	64	42	70	58	53	55	45	17	2	5	3	9	4	10	72	87	83	50	57	60	82	86	55	1119	Dec 27 Sunday	
363	25	14	7	20	17	16	12	11	23	29	23	5	9	10	5	5	11	7	11	10	14	20	15	10	329	Dec 28 Monday	
364	9	12	14	18	14	9	5	7	7	12	20	18	17	12	6	4	9	5	11	10	20	41	37	32	349	Dec 29 Tuesday	
365	34	38	43	58	50	57	43	35	12	18	22	22	24	11	11	28	15	26	47	59	78	89	104	89	1013	Dec 30 Wednesday	
366	94	89	77	78	88	87	92	69	33	12	20	9	13	24	35	90	78	80	77	64	45	48	42	36	1380	Dec 31 Thursday	
1	32	28	30	24	32	24	22	19	20	9	14	17	25	11	12	14	14	13	6	6	7	14	12	13	418	Jan 01 Friday	Frste
2	18	16	13	5	10	5	4	6	7	3	4	4	10	4	6	12	9	2	4	6	9	1	6	7	171	Jan 02 Saturday	
3	5	6	11	9	8	5	3	5	9	4	5	1	1	3	9	4	11	14	6	8	13	16	11	8	175	Jan 03 Sunday	
4	8	22	11	12	8	14	6	11	15	27	31	30	34	26	13	32	51	52	37	19	21	46	16	6	548	Jan 04 Monday	
5	4	7	8	9	8	10	6	1	12	13	18	22	6	12	6	5	10	6	7	4	8	9	7	7	205	Jan 05 Tuesday	
6	5	6	4	11	6	6	9	12	54	37	35	42	70	19	6	5	2	15	2	19	4	21	27	19	436	Jan 06 Wednesday	
7	10	9	14	13	10	10	2	12	26	20	24	35	33	51	43	12	95	100	19	18	16	10	11	10	603	Jan 07 Thursday	
8	11	16	37	41	52	54	62	44	55	30	42	45	27	15	10	7	16	8	3	7	7	10	7	17	623	Jan 08 Friday	
9	7	6	6	1	5	9	10	5	6	5	3	12	5	3	10	10	8	3	8	8	6	2	2	8	148	Jan 09 Saturday	
10	4	3	3	6	2	1	3	4	6	8	8	5	3	5	10	5	10	3	9	10	10	11	17	14	160	Jan 10 Sunday	
11	10	11	13	16	8	5	8	6	11	13	31	15	29	15	13	9	9	6	7	5	6	10	7	12	275	Jan 11 Monday	
12	10	14	5	13	10	11	9	6	12	8	6	20	25	22	10	20	5	6	17	9	8	6	6	16	274	Jan 12 Tuesday	
13	10	11	8	9	13	8	10	6	6	21	13	23	18	19	12	5	6	8	8	9	10	5	6	14	258	Jan 13 Wednesday	
14	7	12	13	7	8	4	5	10	12	25	21	22	39	19	14	9	16	6	9	7	13	6	9	16	309	Jan 14 Thursday	
15	6	11	13	9	9	20	3	7	15	13	22	25	35	15	4	12	13	3	11	10	18	11	22	21	328	Jan 15 Friday	
16	24	13	8	17	6	7	8	7	3	6	2	17	12	5	13	4	5	6	2	3	11	4	3	3	189	Jan 16 Saturday	
17	8	8	8	9	10	18	9	20	22	11	19	12	11	8	6	3	3	6	13	11	6	9	4	23	257	Jan 17 Sunday	
18	17	22	19	24	14	12	7	12	10	13	9	28	21	15	12	8	4	6	1	9	5	7	10	7	292	Jan 18 Monday	
19	7	11	9	16	9	11	6	5	17	13	9	22	28	25	14	13	5	7	7	6	9	20	21	21	311	Jan 19 Tuesday	
20	22	15	31	30	22	49	29	16	15	14	13	12	23	15	15	2	7	9	6	2	4	6	6	4	367	Jan 20 Wednesday	

Table 3.4.3 (Page 2 of 4)

FIN .FKX Hourly distribution of detections

Day	00	01	02	03	04	05	06	07	08	09	10	11	12	13	14	15	16	17	18	19	20	21	22	23	Sum	Date
21	9	4	6	4	7	7	9	10	12	18	14	16	21	15	15	10	8	2	4	4	3	6	5	6	215	Jan 21 Thursday
22	15	6	6	13	18	24	7	4	7	29	18	21	43	19	23	25	19	32	35	33	34	25	58	32	546	Jan 22 Friday
23	4	37	28	15	27	37	21	9	18	33	17	16	23	6	17	14	15	14	14	6	10	13	8	12	414	Jan 23 Saturday
24	18	14	5	9	17	14	4	11	12	10	6	6	3	4	4	7	11	2	13	8	5	14	5	7	209	Jan 24 Sunday
25	11	16	12	17	10	7	3	4	9	15	5	24	16	19	24	5	8	4	9	6	6	8	9	6	253	Jan 25 Monday
26	10	10	8	4	4	5	6	5	8	10	11	17	23	14	13	6	2	6	6	9	9	1	17	10	214	Jan 26 Tuesday
27	18	21	31	31	13	15	7	16	16	10	12	17	23	0	0	0	0	0	0	0	0	0	0	0	230	Jan 27 Wednesday
28	0	0	0	0	0	0	0	0	0	0	0	0	0	0	3	16	13	4	23	32	18	14	12	14	149	Jan 28 Thursday
29	15	9	17	11	8	15	10	15	9	12	25	12	38	23	17	22	11	11	4	13	5	9	6	2	319	Jan 29 Friday
30	7	2	7	4	8	4	2	7	5	7	26	6	10	22	13	7	2	7	2	2	4	3	3	3	163	Jan 30 Saturday
31	1	3	2	9	10	4	5	1	2	1	1	3	2	3	2	3	0	4	4	5	6	4	2	0	77	Jan 31 Sunday
32	0	0	0	0	0	0	0	1	6	6	6	14	9	16	6	4	7	9	9	6	4	10	8	6	127	Feb 01 Monday
33	4	8	10	12	7	7	4	6	16	4	6	16	7	22	10	8	11	8	3	6	10	12	9	8	214	Feb 02 Tuesday
34	4	8	10	14	15	13	5	11	12	4	13	25	31	6	9	6	11	5	2	8	9	7	24	27	279	Feb 03 Wednesday
35	16	8	14	8	10	9	4	8	11	7	2	24	40	24	11	13	11	10	6	9	5	7	44	27	328	Feb 04 Thursday
36	15	14	12	8	11	5	9	11	7	13	18	25	27	17	15	13	12	17	15	19	5	9	5	9	311	Feb 05 Friday
37	5	20	26	27	34	32	31	20	19	15	37	18	3	12	20	15	23	17	47	42	45	46	40	54	648	Feb 06 Saturday
38	60	53	76	97	97	66	57	69	70	64	33	8	6	7	4	7	6	7	6	7	24	8	9	4	845	Feb 07 Sunday
39	5	5	11	12	11	7	4	3	6	6	9	9	24	14	7	7	5	10	16	17	7	27	17	7	246	Feb 08 Monday
40	8	5	7	8	6	4	1	3	11	11	7	8	42	20	29	9	20	7	3	11	13	11	8	6	258	Feb 09 Tuesday
41	7	9	16	9	13	11	9	3	15	21	25	28	21	27	32	21	23	20	19	16	30	31	61	71	538	Feb 10 Wednesday
42	48	76	76	64	37	20	23	39	72	41	16	21	22	23	10	6	6	5	7	9	7	10	8	8	654	Feb 11 Thursday
43	10	11	12	14	7	5	8	2	8	14	22	22	33	22	19	24	8	5	8	12	14	11	8	9	308	Feb 12 Friday
44	14	5	10	12	5	12	38	12	8	5	19	5	11	5	8	5	9	9	8	4	4	5	4	1	218	Feb 13 Saturday
45	4	4	5	13	2	4	4	9	7	2	4	3	5	3	5	4	9	10	9	11	14	6	16	4	157	Feb 14 Sunday
46	8	9	8	9	4	3	3	4	9	11	8	10	24	24	10	9	12	13	2	11	8	5	8	13	225	Feb 15 Monday
47	9	9	12	22	6	5	5	5	12	18	8	15	11	27	7	12	9	9	9	5	11	10	11	11	258	Feb 16 Tuesday
48	15	13	13	21	11	6	8	20	7	4	12	17	22	25	4	5	10	11	10	14	3	11	24	6	292	Feb 17 Wednesday
49	11	15	20	25	9	5	14	12	11	13	22	20	19	19	12	13	8	9	4	11	19	13	26	20	350	Feb 18 Thursday
50	24	26	32	20	17	6	10	8	16	16	18	23	27	25	13	10	5	10	3	13	9	14	7	5	357	Feb 19 Friday
51	6	8	12	6	16	4	11	10	8	11	10	19	17	15	7	13	16	7	9	14	6	12	20	23	280	Feb 20 Saturday
52	24	24	21	18	22	23	21	31	27	26	33	11	14	9	9	18	22	26	38	45	40	53	41	52	648	Feb 21 Sunday
53	47	53	44	49	22	15	21	12	11	4	11	19	15	12	14	5	15	10	10	9	11	13	11	11	444	Feb 22 Monday
54	12	11	7	7	8	6	3	5	7	11	10	16	23	14	16	7	9	4	8	8	6	12	10	8	228	Feb 23 Tuesday
55	7	7	15	6	7	5	3	10	5	13	11	12	16	30	12	10	7	5	9	9	9	2	9	12	231	Feb 24 Wednesday
36	6	9	3	5	5	4	3	13	9	15	10	12	26	15	7	6	10	6	10	8	10	10	8	3	213	Feb 25 Thursday
57	4	10	7	18	9	5	6	5	5	21	29	18	17	21	6	12	10	15	7	4	8	11	11	6	265	Feb 26 Friday
58	11	15	16	7	7	18	5	11	10	0	9	12	14	6	12	12	13	11	15	6	12	18	19	11	270	Feb 27 Saturday
59	12	5	14	21	6	3	6	8	8	3	7	2	4	3	9	12	4	1	15	11	12	11	10	15	202	Feb 28 Sunday
60	7	9	14	19	10	6	3	11	7	18	6	12	33	21	13	20	8	10	9	15	16	22	28	20	337	Mar 01 Monday
61	12	18	16	14	8	5	2	16	8	14	7	24	21	22	10	10	9	17	14	20	24	8	24	23	346	Mar 02 Tuesday
62	16	13	22	11	11	5	8	8	15	18	24	21	17	17	12	9	17	9	18	27	17	14	13	13	355	Mar 03 Wednesday
63	14	16	15	9	11	12	3	4	10	15	13	15	18	17	9	13	10	4	7	12	10	9	7	10	263	Mar 04 Thursday
64	6	9	4	9	4	8	3	13	14	18	26	20	34	9	7	8	6	10	8	10	5	6	6	8	251	Mar 05 Friday
65	9	15	11	8	9	11	8	5	12	10	13	22	6	7	14	6	10	16	11	10	15	18	7	17	270	Mar 06 Saturday
66	17	14	9	13	13	9	19	13	9	10	13	2	9	10	13	19	16	19	17	16	11	8	12	13	304	Mar 07 Sunday
67	7	7	11	12	10	7	5	7	8	8	2	12	16	19	9	10	3	12	11	9	6	5	10	6	212	Mar 08 Monday
68	10	7	6	4	7	7	3	7	13	13	11	4	19	13	9	5	4	8	11	4	6	7	5	16	199	Mar 09 Tuesday
69	7	4	7	7	12	4	4	6	9	7	8	21	18	15	4	4	6	6	9	9	6	6	13	12	204	Mar 10 Wednesday
70	14	8	7	8	6	6	7	7	13	18	23	18	25	14	12	15	20	7	9	5	10	2	4	7	265	Mar 11 Thursday
71	4	7	14	8	10	5	7	11	13	17	23	36	21	22	6	10	13	3	10	7	2	8	8	9	274	Mar 12 Friday
72	7	2	13	13	6	2	10	7	4	9	6	8	5	3	5	11	7	6	2	3	0	2	2	2	135	Mar 13 Saturday
73	5	5	4	4	1	3	4	4	4	8	3	1	5	5	4	4	7	5	13	1	7	12	7	7	123	Mar 14 Sunday
74	9	5	4	10	4	2	5	7	4	8	9	14	7	19	6	9	7	6	8	8	10	5	6	14	186	Mar 15 Monday
75	6	12	5	6	4	2	3	4	5	3	4	24	16	11	3	8	1	3	7	7	9	8	6	16	173	Mar 16 Tuesday
76	15	6	9	13	9	5	1	6	5	6	17	12	19	14	14	7	11	11	17	7	15	10	12	11	252	Mar 17 Wednesday

Table 3.4.3 (Page 3 of 4)

FIN .FKX Hourly distribution of detections

Day	00	01	02	03	04	05	06	07	08	09	10	11	12	13	14	15	16	17	18	19	20	21	22	23	Sum	Date
77	12	12	13	12	11	10	5	19	17	13	10	14	23	17	13	13	9	2	8	8	6	11	15	22	295	Mar 18 Thursday
78	15	9	12	13	8	11	12	7	9	15	15	16	27	17	12	7	8	11	13	14	17	6	2	9	285	Mar 19 Friday
79	12	9	9	15	10	10	9	5	19	9	11	11	7	8	5	13	6	5	25	29	62	46	31	33	399	Mar 20 Saturday
80	20	36	26	30	19	10	5	5	2	3	1	3	1	4	11	6	8	7	12	4	5	7	10	6	241	Mar 21 Sunday
81	12	13	7	13	3	9	2	5	5	5	5	9	15	8	12	8	5	13	12	15	9	10	14	19	228	Mar 22 Monday
82	15	16	10	12	10	8	6	5	7	6	10	17	19	12	11	17	12	8	7	6	5	5	11	6	241	Mar 23 Tuesday
83	9	9	6	15	7	2	5	5	6	14	7	16	18	18	10	11	12	7	7	12	12	8	18	7	241	Mar 24 Wednesday
84	10	8	12	14	10	10	7	6	4	9	10	18	16	22	17	10	7	9	7	4	11	12	14	21	268	Mar 25 Thursday
85	16	15	8	25	16	1	6	15	2	17	18	10	26	17	6	6	2	16	12	17	12	18	10	32	323	Mar 26 Friday
86	24	23	9	28	20	11	9	8	12	9	12	9	20	11	11	10	17	9	18	65	71	67	71	73	617	Mar 27 Saturday
87	58	57	81	66	53	36	29	29	10	7	13	5	6	12	6	17	18	6	18	18	12	18	12	15	602	Mar 28 Sunday
88	19	22	6	10	9	6	4	7	10	9	8	21	9	20	76	19	9	15	19	21	15	9	11	14	368	Mar 29 Monday
89	17	8	20	12	6	6	2	12	14	5	14	12	17	6	8	10	9	8	10	17	9	24	14	6	266	Mar 30 Tuesday
90	6	8	6	9	12	13	0	5	9	17	9	79	51	32	8	5	18	8	8	21	20	10	11	9	374	Mar 31 Wednesday
FIN	00	01	02	03	04	05	06	07	08	09	10	11	12	13	14	15	16	17	18	19	20	21	22	23		
Sum	2534	2657	2700	2928	2370	1930	1630	1698	2031	2192	2325	2888	3359	2780	2152	2156	2343	2170	2265	2449	2460	2700	2914	2768	58399	Total sum
182	14	15	15	16	13	11	9	9	11	12	13	16	18	15	12	12	13	12	12	13	14	15	16	15	321	Total average
128	14	15	15	16	12	9	8	9	11	13	14	19	22	18	12	11	12	11	11	13	13	14	16	15	320	Average workdays
54	14	14	15	17	14	13	11	10	11	10	10	9	10	9	10	14	15	13	15	14	15	17	16	16	313	Average weekends

Table 3.4.3. Daily and hourly distributions of FINESA detections. For each day is shown number of detections within each hour of the day, and number of detections for that day. The end statistics give total number of detections distributed for each hour and the total sum of detections during the period. the averages show number of processed days, hourly distribution and average per processed day. (page 4 of 4)

GER .FKX Hourly distribution of detections

Day	00	01	02	03	04	05	06	07	08	09	10	11	12	13	14	15	16	17	18	19	20	21	22	23	Sum	Date
21	0	0	0	0	0	0	0	0	0	0	0	0	0	0	0	0	0	0	0	0	0	0	0	0	0	Jan 21 Thursday
22	0	0	0	0	0	0	0	0	0	0	0	0	0	0	0	0	0	0	0	0	0	0	0	0	0	Jan 22 Friday
23	0	0	0	0	0	0	0	0	0	0	0	0	0	0	0	0	0	0	0	0	0	0	0	0	0	Jan 23 Saturday
24	0	0	0	0	0	0	0	0	0	0	0	0	0	0	0	0	0	0	0	0	0	0	0	0	0	Jan 24 Sunday
25	0	0	0	0	0	0	0	0	0	0	0	0	0	0	0	0	0	0	0	0	0	0	0	0	0	Jan 25 Monday
26	0	0	0	0	0	0	0	0	0	0	0	0	0	0	0	0	0	0	0	0	0	0	0	0	0	Jan 26 Tuesday
27	0	0	0	0	0	0	0	0	0	0	0	0	0	0	0	0	0	0	0	0	0	0	0	0	0	Jan 27 Wednesday
28	0	0	0	0	0	0	0	0	0	0	0	0	0	0	0	0	0	0	0	0	0	0	0	0	0	Jan 28 Thursday
29	0	0	0	0	0	0	0	0	0	0	0	0	0	0	0	0	0	0	0	0	0	0	0	0	0	Jan 29 Friday
30	0	0	0	0	0	0	0	0	0	0	0	0	0	0	0	0	0	0	0	0	0	0	0	0	0	Jan 30 Saturday
31	0	0	0	0	0	0	0	0	0	0	0	0	0	0	0	0	0	0	0	0	0	0	0	0	0	Jan 31 Sunday
32	0	0	0	0	0	0	0	0	0	0	0	0	0	0	0	0	0	0	0	0	0	0	0	0	0	Feb 01 Monday
33	0	0	0	0	0	0	0	0	0	0	0	0	0	0	0	0	0	0	0	0	0	0	0	0	0	Feb 02 Tuesday
34	0	0	0	0	0	0	0	0	0	0	0	0	0	0	0	0	0	0	0	0	0	0	0	0	0	Feb 03 Wednesday
35	0	0	0	0	0	0	0	0	0	0	0	0	0	0	0	0	0	0	0	0	0	0	0	0	0	Feb 04 Thursday
36	0	0	0	0	0	0	0	0	0	0	0	0	0	0	0	0	0	0	0	0	0	0	0	0	0	Feb 05 Friday
37	0	0	0	0	0	0	0	0	0	0	0	0	0	0	0	0	0	0	0	0	0	0	0	0	0	Feb 06 Saturday
38	0	0	0	0	0	0	0	0	0	0	0	0	0	0	0	0	0	0	0	0	0	0	0	0	0	Feb 07 Sunday
39	0	0	0	0	0	0	0	0	0	0	0	0	0	0	0	0	0	0	0	0	0	0	0	0	0	Feb 08 Monday
40	0	0	0	0	0	0	0	0	0	0	0	0	0	0	0	0	0	0	0	0	0	0	0	0	0	Feb 09 Tuesday
41	0	0	0	0	0	0	0	0	0	0	0	0	0	0	0	0	0	0	0	0	0	0	0	0	0	Feb 10 Wednesday
42	0	0	0	0	0	0	0	0	0	0	0	0	0	0	0	0	0	0	0	0	0	0	0	0	0	Feb 11 Thursday
43	0	0	0	0	0	0	0	0	0	0	0	0	0	0	0	0	0	0	0	0	0	0	0	0	0	Feb 12 Friday
44	0	0	0	0	0	0	0	0	0	0	0	0	0	0	0	0	0	0	0	0	0	0	0	0	0	Feb 13 Saturday
45	0	0	0	0	0	0	0	0	0	0	0	0	0	0	0	0	0	0	0	0	0	0	0	0	0	Feb 14 Sunday
46	0	0	0	0	0	0	0	0	0	0	0	0	0	0	0	0	0	0	0	0	0	0	0	0	0	Feb 15 Monday
47	0	0	0	0	0	0	0	0	0	0	0	0	0	0	0	0	0	0	0	0	0	0	0	0	0	Feb 16 Tuesday
48	0	0	0	0	0	0	0	0	0	0	0	0	0	0	0	0	0	0	0	0	0	0	0	0	0	Feb 17 Wednesday
49	0	0	0	0	0	0	0	0	0	0	0	0	0	0	0	0	0	0	0	0	0	0	0	0	0	Feb 18 Thursday
50	17	12	14	18	23	4	9	10	15	12	22	24	21	19	15	9	17	12	10	6	6	3	4	3	305	Feb 19 Friday
51	3	5	5	3	3	1	2	7	7	5	46	17	9	3	7	5	6	13	18	15	11	18	12	33	254	Feb 20 Saturday
52	12	16	21	21	12	14	6	9	4	2	1	34	68	20	3	0	0	1	4	3	4	2	1	3	261	Feb 21 Sunday
53	9	7	2	4	8	3	4	6	6	7	9	8	12	16	6	2	6	3	15	10	3	1	6	4	157	Feb 22 Monday
54	0	1	0	3	1	3	3	4	11	7	9	9	15	6	1	3	0	4	1	2	2	2	2	1	90	Feb 23 Tuesday
55	0	1	2	3	0	1	1	3	4	5	21	14	21	21	17	3	10	5	1	6	8	1	4	4	156	Feb 24 Wednesday
56	0	0	3	3	5	6	0	4	7	15	18	26	6	13	8	14	2	2	3	2	2	3	1	5	148	Feb 25 Thursday
57	2	5	1	0	9	7	0	0	1	4	22	19	8	8	7	1	2	11	4	4	11	5	5	8	144	Feb 26 Friday
58	6	1	3	3	1	5	2	3	19	6	10	8	17	2	2	1	11	2	9	5	4	11	0	1	132	Feb 27 Saturday
59	4	1	1	4	2	2	5	1	5	0	10	7	11	6	5	4	1	2	8	6	1	6	1	1	94	Feb 28 Sunday
60	1	4	3	1	2	3	0	7	9	5	18	6	11	5	7	4	11	10	3	6	6	5	6	1	134	Mar 01 Monday
61	1	5	1	5	4	1	1	0	11	12	16	9	16	7	6	9	7	6	4	9	8	3	8	3	152	Mar 02 Tuesday
62	0	4	0	4	0	3	1	5	9	9	15	9	15	13	5	5	8	2	2	8	2	3	1	4	127	Mar 03 Wednesday
63	3	1	2	8	2	5	2	7	5	5	16	11	23	16	6	9	1	6	6	6	13	4	0	6	163	Mar 04 Thursday
64	3	2	1	5	5	2	12	8	12	13	14	12	17	13	10	2	7	8	5	3	1	8	5	3	171	Mar 05 Friday
65	8	8	9	12	4	2	6	5	5	0	11	12	16	6	8	7	3	4	2	2	3	3	1	8	145	Mar 06 Saturday
66	3	2	0	9	2	7	3	10	5	16	13	18	8	0	3	6	1	4	2	1	3	6	7	6	135	Mar 07 Sunday
67	0	1	5	1	2	2	2	8	8	7	15	6	6	10	5	10	0	7	2	5	6	1	2	2	113	Mar 08 Monday
68	3	5	2	6	12	4	2	1	8	7	24	11	19	12	18	5	6	2	6	0	2	5	1	3	164	Mar 09 Tuesday
69	6	2	1	3	5	0	1	5	12	5	10	5	16	7	6	10	13	10	2	4	4	2	8	0	137	Mar 10 Wednesday
70	5	1	2	2	4	1	2	2	9	10	23	15	17	9	11	2	14	9	8	5	6	1	18	5	181	Mar 11 Thursday
71	7	9	2	7	11	10	3	10	16	16	24	30	35	10	12	10	10	11	11	7	1	5	4	5	266	Mar 12 Friday
72	7	1	5	7	0	9	6	2	14	11	37	14	4	28	34	16	7	9	10	9	9	10	8	2	259	Mar 13 Saturday
73	5	2	6	9	1	2	0	5	7	4	2	11	5	10	6	10	0	2	2	2	5	9	4	3	112	Mar 14 Sunday
74	2	8	1	7	4	4	4	3	2	7	15	12	9	10	11	13	22	9	6	3	0	2	3	12	169	Mar 15 Monday
75	1	8	2	3	1	0	3	9	6	20	10	14	16	16	12	8	12	1	7	8	8	2	22	7	196	Mar 16 Tuesday
76	8	7	6	30	22	12	7	7	10	19	36	22	32	24	33	21	9	14	16	10	3	5	0	2	355	Mar 17 Wednesday

Table 3.4.4 (Page 1 of 2)

GER .FKX Hourly distribution of detections

Day	00	01	02	03	04	05	06	07	08	09	10	11	12	13	14	15	16	17	18	19	20	21	22	23	Sum	Date
77	10	10	8	14	15	14	6	11	18	24	22	29	14	13	14	21	12	6	14	6	4	0	6	12	303	Mar 18 Thursday
78	2	6	8	6	2	4	7	3	8	18	33	14	14	10	7	5	8	10	0	13	5	6	5	3	197	Mar 19 Friday
79	6	3	1	1	3	8	8	5	5	10	2	15	0	3	2	9	9	8	6	7	4	6	9	15	145	Mar 20 Saturday
80	5	2	3	4	6	8	0	3	4	4	8	12	4	8	9	2	3	1	4	3	5	8	7	3	116	Mar 21 Sunday
81	1	3	4	4	4	3	0	4	3	8	18	18	20	6	9	22	8	11	12	5	7	10	4	12	196	Mar 22 Monday
82	1	5	8	2	7	7	10	12	10	22	18	20	18	11	6	13	4	6	11	2	5	1	3	2	204	Mar 23 Tuesday
83	6	1	2	2	8	10	4	15	3	15	15	21	14	15	4	5	7	1	12	2	5	0	10	4	181	Mar 24 Wednesday
84	5	1	8	3	2	11	5	4	7	6	21	17	17	9	6	8	6	12	8	1	9	3	6	7	182	Mar 25 Thursday
85	4	3	2	4	5	1	2	6	16	10	25	14	24	16	7	4	5	11	3	1	3	8	5	4	183	Mar 26 Friday
86	0	2	1	1	0	5	3	3	0	4	2	1	3	5	0	2	2	1	0	5	4	1	3	2	50	Mar 27 Saturday
87	1	2	0	6	6	0	14	10	9	5	1	23	1	5	10	6	4	1	1	10	5	5	1	7	133	Mar 28 Sunday
88	5	17	4	4	11	5	5	14	6	6	20	18	6	13	4	7	4	6	2	2	3	5	6	4	177	Mar 29 Monday
89	7	4	3	1	2	4	4	6	7	16	14	10	12	8	16	14	6	5	9	7	2	6	5	0	168	Mar 30 Tuesday
90	3	7	6	5	9	1	2	8	10	11	19	16	13	17	8	15	3	3	3	7	10	2	0	2	180	Mar 31 Wednesday

GER	00	01	02	03	04	05	06	07	08	09	10	11	12	13	14	15	16	17	18	19	20	21	22	23		
Sum	186	200	173	254	238	205	166	254	344	400	698	627	631	464	378	334	280	263	264	231	217	202	220	227	7456	Total sum
41	5	5	4	6	6	5	4	6	8	10	17	15	15	11	9	8	7	6	6	6	5	5	5	6	182	Total average
29	4	5	4	5	6	5	4	6	9	11	19	15	16	12	10	9	8	7	6	5	5	4	5	4	183	Average workdays
12	5	4	5	7	3	5	5	5	7	6	12	14	12	8	7	6	4	4	6	6	5	7	5	7	153	Average weekends

Table 3.4.4. Daily and hourly distributions of GERESS detections. For each day is shown number of detections within each hour of the day, and number of detections for that day. The end statistics give total number of detections distributed for each hour and the total sum of detections during the period. the averages show number of processed days, hourly distribution and average per processed day. Note that GERESS detection processing did not take place at NORSAR for the period 1 October 1992 through 18 February 1993 because of problems with the data transmission link. (Page 2 of 2)

APA .FKX Hourly distribution of detections

Day	00	01	02	03	04	05	06	07	08	09	10	11	12	13	14	15	16	17	18	19	20	21	22	23	Sum	Date
275	0	0	0	0	0	0	0	0	0	0	0	0	0	0	0	0	9	38	35	31	18	6	13	19	169	Oct 01 Thursday
276	6	9	10	15	30	29	45	38	50	24	0	48	45	46	45	25	21	30	16	26	11	14	20	20	623	Oct 02 Friday
277	10	16	20	25	28	28	22	27	24	16	15	24	31	31	35	35	8	22	5	9	7	5	1	7	451	Oct 03 Saturday
278	6	1	4	4	6	6	14	11	21	22	8	10	18	7	11	19	15	52	16	15	5	8	7	2	288	Oct 04 Sunday
279	2	18	9	27	20	39	45	51	46	51	45	50	43	38	41	39	28	22	16	25	8	6	6	4	679	Oct 05 Monday
280	3	10	14	19	37	30	48	55	46	72	39	41	60	36	44	30	28	30	20	20	11	3	9	8	713	Oct 06 Tuesday
281	2	5	6	24	39	41	77	84	128	138	84	40	50	42	6	15	29	26	15	6	12	14	7	1	891	Oct 07 Wednesday
282	8	3	13	22	36	40	75	30	67	59	46	50	54	44	43	52	46	49	53	43	37	22	39	35	966	Oct 08 Thursday
283	22	26	43	42	79	45	58	73	60	65	67	92	87	44	46	53	33	46	30	42	35	28	26	17	1159	Oct 09 Friday
284	26	23	24	31	32	37	38	43	28	45	24	40	32	24	36	29	20	15	23	27	23	23	27	21	691	Oct 10 Saturday
285	27	16	18	26	31	46	28	32	37	40	41	24	28	33	19	37	23	17	24	23	23	35	26	34	688	Oct 11 Sunday
286	22	24	26	31	57	33	46	55	50	45	41	37	53	53	40	35	24	31	33	31	30	22	29	15	863	Oct 12 Monday
287	23	29	34	33	45	41	52	57	36	57	46	40	62	47	14	57	45	35	35	35	30	31	22	22	928	Oct 13 Tuesday
288	21	36	25	38	51	46	58	58	51	33	49	52	50	49	36	27	12	22	26	32	22	21	12	10	837	Oct 14 Wednesday
289	16	14	18	13	34	19	46	27	18	40	38	34	33	41	21	24	30	25	21	27	22	8	14	19	602	Oct 15 Thursday
290	6	19	15	21	34	26	38	29	32	20	31	36	50	28	21	14	17	32	20	18	16	9	8	19	559	Oct 16 Friday
291	21	21	9	15	16	16	19	22	21	20	15	20	23	25	15	17	11	15	14	20	11	12	8	10	396	Oct 17 Saturday
292	7	12	13	28	7	18	15	25	11	17	15	11	7	18	22	27	13	16	12	14	32	12	8	19	379	Oct 18 Sunday
293	10	10	14	31	37	32	22	5	37	37	23	32	24	32	23	12	10	20	19	5	8	11	10	13	477	Oct 19 Monday
294	12	9	14	25	27	30	50	42	37	30	34	30	38	28	61	49	27	14	28	22	18	16	19	18	678	Oct 20 Tuesday
295	18	17	25	15	26	22	56	39	40	30	25	31	39	32	38	16	21	28	13	16	16	17	7	7	594	Oct 21 Wednesday
296	11	19	21	33	29	34	29	24	32	35	36	39	33	40	33	43	33	28	35	22	14	30	19	24	696	Oct 22 Thursday
297	14	31	24	48	58	44	43	38	32	55	22	37	48	33	31	22	6	42	15	20	25	21	21	34	764	Oct 23 Friday
298	18	10	20	29	14	4	0	0	0	2	12	30	26	20	21	22	24	56	22	51	46	43	25	58	553	Oct 24 Saturday
299	40	6	14	30	29	36	48	29	16	24	16	18	28	23	24	39	32	27	35	45	37	30	39	43	708	Oct 25 Sunday
300	27	25	37	27	71	41	45	48	44	39	40	43	41	35	35	26	34	51	22	18	9	12	27	57	854	Oct 26 Monday
301	75	59	56	52	37	50	49	55	47	32	34	27	36	41	27	72	79	71	55	45	54	29	28	53	1163	Oct 27 Tuesday
302	49	59	66	84	121	42	54	65	44	29	37	45	93	87	108	94	74	110	89	76	54	45	50	90	1665	Oct 28 Wednesday
303	73	29	44	34	52	63	53	53	15	41	41	43	71	80	52	68	84	63	92	65	24	27	50	22	1239	Oct 29 Thursday
304	16	17	35	45	43	41	49	33	45	30	32	39	51	33	65	90	83	71	44	44	39	19	42	3	1009	Oct 30 Friday
305	15	9	63	83	30	29	26	28	20	42	35	92	45	38	45	63	91	54	69	36	29	72	83	87	1184	Oct 31 Saturday
306	0	0	0	0	0	0	0	0	0	0	0	0	0	0	0	0	0	0	0	0	0	0	0	0	0	Nov 01 Sunday
307	0	0	0	0	0	0	0	0	23	83	104	122	71	100	101	85	96	97	115	114	100	55	43	24	1333	Nov 02 Monday
308	31	21	14	31	33	45	47	77	77	56	51	71	46	60	34	46	52	36	38	29	23	8	23	16	965	Nov 03 Tuesday
309	13	15	21	17	38	45	55	44	42	41	26	39	67	39	49	28	20	26	21	18	28	22	28	11	753	Nov 04 Wednesday
310	10	22	23	40	33	37	51	56	37	37	31	52	48	44	30	55	36	27	38	28	28	26	0	0	789	Nov 05 Thursday
311	0	0	0	0	0	0	0	22	33	31	36	56	46	43	42	51	54	52	42	48	17	23	11	29	636	Nov 06 Friday
312	8	12	16	10	11	14	31	43	9	17	16	12	23	17	19	29	18	16	6	16	15	19	16	13	406	Nov 07 Saturday
313	22	5	8	14	22	10	20	16	12	17	19	0	0	0	0	0	0	0	0	0	0	0	0	0	165	Nov 08 Sunday
314	0	0	0	0	0	0	0	9	15	17	17	30	13	13	16	12	13	12	14	17	21	22	16	10	267	Nov 09 Monday
315	13	20	13	28	38	23	44	37	43	31	25	34	13	30	30	34	24	18	20	13	14	24	16	18	603	Nov 10 Tuesday
316	20	11	30	21	70	39	60	51	45	41	46	40	45	38	37	33	40	67	33	19	18	24	11	19	858	Nov 11 Wednesday
317	18	14	38	20	45	32	35	48	44	35	36	42	42	25	19	58	27	17	24	14	20	12	13	14	692	Nov 12 Thursday
318	13	17	18	21	36	34	50	25	37	32	27	39	63	41	24	16	7	23	19	9	7	11	24	8	601	Nov 13 Friday
319	13	8	8	9	8	19	10	36	10	10	24	34	13	18	10	11	10	12	6	9	10	8	18	17	331	Nov 14 Saturday
320	5	5	10	12	6	10	19	15	14	14	14	13	12	6	8	10	12	13	13	10	8	15	8	18	270	Nov 15 Sunday
321	10	7	17	12	27	31	25	23	35	38	15	34	27	28	17	29	17	16	20	18	13	7	10	27	503	Nov 16 Monday
322	3	14	24	10	26	30	36	30	27	28	21	23	25	35	21	33	11	23	22	22	25	13	14	10	526	Nov 17 Tuesday
323	11	7	20	20	31	36	31	24	41	28	33	50	48	28	23	12	9	19	25	12	23	27	26	28	612	Nov 18 Wednesday
324	25	23	17	32	36	43	33	41	45	41	29	167	38	105	32	43	12	26	23	18	26	19	12	22	908	Nov 19 Thursday
325	18	20	26	29	30	37	43	41	26	0	0	0	0	0	0	0	0	0	0	0	0	0	0	0	270	Nov 20 Friday
326	0	0	0	0	0	0	0	2	19	39	12	24	43	34	30	29	34	20	25	36	25	20	29	15	436	Nov 21 Saturday
327	18	21	18	6	5	12	11	13	15	18	7	10	1	16	4	4	4	4	5	3	3	0	0	4	202	Nov 22 Sunday
328	8	8	12	10	16	24	25	30	29	12	10	19	23	33	34	18	33	26	29	20	33	24	32	21	529	Nov 23 Monday
329	17	12	21	35	49	35	24	48	24	44	11	30	34	39	18	26	31	33	16	16	16	13	20	14	626	Nov 24 Tuesday
330	6	13	19	20	27	32	29	23	24	17	34	17	26	31	32	15	19	30	25	13	25	12	11	17	517	Nov 25 Wednesday

Table 3.4.5 (Page 1 of 4)

APA .FKX Hourly distribution of detections

Day	00	01	02	03	04	05	06	07	08	09	10	11	12	13	14	15	16	17	18	19	20	21	22	23	Sum	Date		
331	15	8	10	17	28	30	27	26	34	31	36	41	31	21	26	41	30	20	20	10	14	13	17	12	558	Nov 26	Thursday	
332	21	16	16	22	22	23	26	60	23	22	16	33	38	38	32	18	29	21	29	20	11	24	9	16	585	Nov 27	Friday	
333	8	13	13	26	11	15	18	23	20	30	34	23	42	16	17	24	20	25	17	16	14	12	8	13	458	Nov 28	Saturday	
334	9	13	14	16	25	17	20	18	21	9	12	30	17	12	15	21	14	18	8	14	9	10	9	17	368	Nov 29	Sunday	
335	23	12	12	15	28	29	42	34	37	41	30	35	40	42	35	28	45	23	17	28	15	12	12	14	649	Nov 30	Monday	
336	6	12	10	33	38	25	39	41	38	26	44	35	44	26	28	47	27	20	13	20	28	26	16	16	658	Dec 01	Tuesday	
337	13	29	19	23	27	44	58	70	63	98	106	69	122	61	59	50	29	29	34	32	28	19	11	8	1101	Dec 02	Wednesday	
338	22	9	6	12	15	25	24	34	23	16	25	28	26	20	20	23	12	22	16	27	12	25	28	16	486	Dec 03	Thursday	
339	26	20	14	17	23	24	38	36	28	29	20	21	36	27	24	29	22	13	29	21	9	11	9	5	531	Dec 04	Friday	
340	2	2	1	4	6	12	19	14	2	20	12	1	26	23	7	5	6	5	7	11	0	4	2	3	194	Dec 05	Saturday	
341	3	5	6	8	1	4	14	13	3	3	4	8	5	12	5	1	6	8	6	5	1	2	3	15	141	Dec 06	Sunday	
342	16	3	18	10	20	23	26	23	24	16	16	15	22	14	16	15	20	13	6	8	5	6	3	3	341	Dec 07	Monday	
343	4	7	5	5	31	11	35	20	21	22	25	21	16	9	22	27	21	13	1	8	12	9	4	12	361	Dec 08	Tuesday	
344	22	9	7	23	24	24	19	13	23	9	15	19	21	15	17	14	15	16	15	6	14	5	15	12	372	Dec 09	Wednesday	
345	4	7	6	9	14	16	26	19	13	17	23	22	28	24	29	20	13	18	25	18	34	12	4	15	416	Dec 10	Thursday	
346	13	14	19	23	41	26	27	21	34	28	15	29	8	27	19	21	10	15	15	4	16	12	11	8	456	Dec 11	Friday	
347	10	4	4	4	4	9	4	13	6	5	19	20	5	7	12	11	5	6	9	9	15	4	4	2	191	Dec 12	Saturday	
348	4	0	4	7	1	6	13	18	6	7	11	14	9	6	9	11	17	10	11	11	5	3	12	4	199	Dec 13	Sunday	
349	7	5	5	5	8	21	25	26	22	26	19	17	30	35	23	24	23	13	11	13	10	12	6	12	398	Dec 14	Monday	
350	5	8	9	11	27	46	49	40	47	45	32	36	40	41	41	39	31	43	9	10	5	6	1	2	623	Dec 15	Tuesday	
351	0	11	5	8	13	10	9	21	16	12	12	18	13	10	11	15	15	14	7	10	15	19	31	23	318	Dec 16	Wednesday	
352	29	37	23	42	41	27	24	27	13	20	31	17	11	26	45	14	27	27	24	34	18	10	22	7	596	Dec 17	Thursday	
353	6	3	13	15	13	30	30	41	34	22	27	33	44	16	13	24	9	23	27	4	32	11	2	11	483	Dec 18	Friday	
354	5	9	10	22	21	23	27	29	28	18	18	32	37	16	20	36	44	47	43	40	36	55	60	44	720	Dec 19	Saturday	
355	51	80	96	100	103	69	37	52	58	32	55	55	61	41	34	29	42	39	9	12	19	31	11	39	1155	Dec 20	Sunday	
356	8	15	17	33	30	32	63	21	26	16	16	12	26	15	11	8	12	9	19	18	12	7	16	29	471	Dec 21	Monday	
357	11	16	12	6	15	17	12	10	19	25	11	10	10	23	6	13	9	8	24	8	5	6	11	4	291	Dec 22	Tuesday	
358	8	41	53	32	65	30	20	23	42	23	22	10	33	17	4	17	2	4	11	5	5	2	4	9	482	Dec 23	Wednesday	
359	7	5	8	4	10	21	21	11	20	12	10	10	25	18	14	34	12	5	5	11	8	8	2	11	292	Dec 24	Thursday	
360	17	21	6	6	19	15	15	29	24	13	8	10	35	14	12	15	7	13	10	12	10	4	5	7	327	Dec 25	Friday	Prste
361	38	26	17	0	7	8	27	38	67	48	69	72	30	30	45	57	66	60	59	44	51	39	25	24	947	Dec 26	Saturday	Andre
362	45	37	49	42	43	55	62	82	52	75	63	38	30	35	13	31	49	23	24	13	11	10	15	2	899	Dec 27	Sunday	
363	5	4	7	12	14	34	15	16	15	9	17	18	20	24	9	4	4	4	5	7	2	3	2	4	254	Dec 28	Monday	
364	3	4	7	6	9	14	13	15	27	27	116	35	45	45	65	92	92	76	43	34	10	14	19	37	848	Dec 29	Tuesday	
365	14	7	15	34	29	22	28	18	33	9	30	40	18	21	6	27	9	13	7	10	12	10	9	6	427	Dec 30	Wednesday	
366	13	10	26	11	21	16	25	27	15	16	5	5	9	7	2	10	4	4	10	7	14	12	17	14	300	Dec 31	Thursday	
1	8	1	3	3	1	1	3	5	1	12	4	2	7	11	4	11	10	22	16	14	28	19	3	17	206	Jan 01	Friday	Prste
2	19	55	27	19	9	11	8	20	13	4	12	13	11	13	7	6	2	16	33	46	20	22	36	44	466	Jan 02	Saturday	
3	66	50	66	74	51	38	48	31	16	15	19	17	8	14	7	12	10	13	5	8	4	9	5	9	595	Jan 03	Sunday	
4	3	8	5	11	8	17	12	16	12	22	16	12	9	16	12	10	23	7	12	2	4	1	2	10	250	Jan 04	Monday	
5	24	18	9	3	13	4	9	12	7	16	22	10	16	26	9	30	16	11	23	15	25	20	11	12	361	Jan 05	Tuesday	
6	21	13	15	5	13	5	15	27	41	22	12	17	15	12	6	7	8	6	6	6	5	0	6	19	302	Jan 06	Wednesday	
7	0	1	2	4	10	8	7	5	3	9	12	3	6	6	4	28	6	3	3	2	3	6	1	8	140	Jan 07	Thursday	
8	3	10	14	7	11	7	10	12	4	4	4	6	5	21	23	32	39	19	17	29	14	17	15	16	339	Jan 08	Friday	
9	6	23	13	13	10	9	12	20	30	24	20	36	25	15	17	31	41	26	9	0	4	1	10	4	399	Jan 09	Saturday	
10	5	13	23	25	23	18	19	18	12	14	24	21	30	23	31	10	18	11	5	5	7	8	4	3	370	Jan 10	Sunday	
11	6	6	3	7	18	7	15	14	19	12	12	12	25	30	27	29	23	33	17	24	11	17	1	2	370	Jan 11	Monday	
12	4	8	3	8	7	10	17	24	9	17	13	12	26	10	11	20	14	11	7	5	5	15	3	1	260	Jan 12	Tuesday	
13	2	7	20	12	7	32	27	19	18	31	19	7	22	16	5	4	0	0	0	0	0	12	6	7	273	Jan 13	Wednesday	
14	7	7	10	10	17	9	19	8	17	28	14	15	7	11	19	21	22	12	23	16	10	7	16	14	339	Jan 14	Thursday	
15	12	4	7	10	11	20	24	22	25	35	29	33	27	28	35	12	10	5	8	11	5	4	13	31	421	Jan 15	Friday	
16	14	30	26	37	41	28	31	36	37	41	27	37	31	21	25	26	31	25	29	30	21	24	27	22	697	Jan 16	Saturday	
17	20	20	36	26	27	17	36	27	26	21	14	13	2	4	5	10	2	5	5	7	0	1	2	3	329	Jan 17	Sunday	
18	8	13	8	4	12	18	13	18	20	19	14	16	27	16	9	23	20	22	9	1	12	5	11	25	343	Jan 18	Monday	
19	11	10	18	20	25	24	15	18	38	15	14	12	17	14	15	15	15	15	10	93	11	10	16	21	472	Jan 19	Tuesday	
20	25	20	11	8	37	22	18	20	16	27	26	24	55	25	18	22	24	21	9	24	23	2	12	38	527	Jan 20	Wednesday	

Table 3.4.5 (Page2 of 4)

APA .FKX Hourly distribution of detections

Day	00	01	02	03	04	05	06	07	08	09	10	11	12	13	14	15	16	17	18	19	20	21	22	23	Sum	Date		
21	28	9	13	15	20	11	14	11	20	19	8	23	18	34	17	17	11	12	8	8	7	8	6	19	356	Jan	21	Thursday
22	15	10	16	18	12	10	17	20	32	14	20	20	38	20	11	5	9	14	7	33	11	4	3	3	362	Jan	22	Friday
23	6	4	15	8	3	15	4	14	17	26	8	19	22	12	7	3	5	9	12	4	2	12	10	16	253	Jan	23	Saturday
24	15	6	2	2	4	5	10	9	34	13	13	6	18	26	16	14	7	13	9	21	5	7	6	9	270	Jan	24	Sunday
25	10	3	3	14	24	11	19	27	29	19	9	16	21	36	8	11	12	8	11	9	8	19	12	33	372	Jan	25	Monday
26	38	14	23	25	27	40	32	35	26	37	30	30	18	30	20	36	26	32	18	27	22	22	12	12	632	Jan	26	Tuesday
27	12	27	14	24	31	27	29	37	22	27	24	21	31	25	34	29	14	13	8	20	12	7	20	14	522	Jan	27	Wednesday
28	10	8	13	14	31	23	32	24	19	13	40	38	27	32	12	27	27	14	22	11	10	8	4	0	459	Jan	28	Thursday
29	32	27	12	14	21	9	21	23	13	17	31	8	33	10	16	6	7	5	19	5	5	16	2	10	362	Jan	29	Friday
30	14	12	12	13	16	11	4	16	10	2	16	5	26	11	3	3	0	5	12	4	13	0	1	8	217	Jan	30	Saturday
31	4	5	8	8	6	2	13	15	6	14	2	2	3	6	2	4	3	9	11	11	3	0	9	8	154	Jan	31	Sunday
32	4	3	6	9	20	20	21	44	23	22	8	8	8	9	9	29	36	40	68	81	85	94	117	80	844	Feb	01	Monday
33	0	0	0	0	0	0	26	49	33	34	19	23	30	29	25	24	19	14	10	4	5	1	8	6	359	Feb	02	Tuesday
34	3	6	9	18	14	15	24	35	8	18	33	23	29	27	11	13	24	15	9	3	13	2	3	13	368	Feb	03	Wednesday
35	3	15	7	10	7	15	8	11	14	20	12	14	16	23	11	22	19	20	16	18	21	13	12	13	340	Feb	04	Thursday
36	11	4	7	15	14	21	30	45	23	40	27	28	55	37	25	19	29	28	18	15	18	12	14	8	543	Feb	05	Friday
37	22	56	32	7	9	1	5	16	10	10	7	16	10	11	7	16	45	52	59	48	47	51	42	51	630	Feb	06	Saturday
38	40	36	46	16	10	6	7	27	16	5	3	3	10	12	5	14	12	3	4	5	7	4	3	4	298	Feb	07	Sunday
39	5	4	2	7	19	15	25	23	18	20	30	16	25	11	12	13	5	8	6	3	7	6	1	7	288	Feb	08	Monday
40	5	13	14	13	14	39	16	37	24	47	36	24	38	29	28	32	35	46	49	38	34	54	26	15	706	Feb	09	Tuesday
41	5	12	9	43	46	44	34	31	49	45	32	32	22	19	14	9	17	9	26	16	22	21	9	13	579	Feb	10	Wednesday
42	10	30	18	16	19	32	46	35	19	17	28	24	35	30	14	22	27	20	21	12	12	8	6	14	515	Feb	11	Thursday
43	21	26	62	44	64	74	80	51	53	40	62	32	35	23	26	16	6	14	8	14	11	7	0	10	779	Feb	12	Friday
44	9	2	3	19	6	4	6	11	7	10	16	15	19	24	7	3	4	14	2	5	7	7	7	0	207	Feb	13	Saturday
45	0	2	1	4	7	2	4	15	6	7	4	5	15	10	6	4	5	1	11	4	4	4	3	1	125	Feb	14	Sunday
46	3	1	6	9	17	18	30	29	24	20	18	24	26	16	14	12	12	16	19	12	12	4	1	6	349	Feb	15	Monday
47	1	0	9	12	20	30	31	31	20	25	23	34	24	33	18	10	13	17	3	6	22	18	5	6	411	Feb	16	Tuesday
48	13	45	31	38	21	26	26	26	22	29	15	24	38	27	24	14	11	25	24	30	15	22	13	20	579	Feb	17	Wednesday
49	14	22	16	9	33	27	38	28	36	29	34	18	19	19	28	21	27	20	34	35	18	10	16	21	572	Feb	18	Thursday
50	15	9	22	29	40	28	36	25	30	20	36	33	55	35	33	26	27	38	19	18	19	19	16	28	656	Feb	19	Friday
51	27	21	28	26	29	19	13	30	13	10	17	9	17	22	13	18	23	6	12	19	10	11	13	15	421	Feb	20	Saturday
52	14	7	9	14	11	11	10	14	14	16	10	11	21	14	20	21	21	20	19	22	13	13	19	15	359	Feb	21	Sunday
53	11	14	12	11	21	26	51	38	27	23	26	20	32	32	19	30	21	12	5	20	8	11	10	12	492	Feb	22	Monday
54	8	8	16	13	16	18	28	19	15	28	18	18	27	27	8	18	19	18	15	16	7	7	5	16	388	Feb	23	Tuesday
55	4	21	11	17	17	19	17	25	25	13	16	25	31	20	21	9	11	13	14	12	4	4	4	4	357	Feb	24	Wednesday
56	13	9	8	6	5	22	15	20	15	28	10	12	14	14	18	12	5	7	10	4	13	4	2	11	277	Feb	25	Thursday
57	8	4	20	20	23	24	38	36	33	39	42	41	49	29	40	20	23	33	37	34	16	11	22	12	654	Feb	26	Friday
58	8	7	4	3	10	3	8	8	17	19	11	17	25	7	3	3	8	10	2	1	5	2	0	2	183	Feb	27	Saturday
59	4	1	4	4	9	3	13	1	3	5	5	5	6	9	5	6	5	2	4	5	3	5	5	6	118	Feb	28	Sunday
60	8	6	4	12	19	12	17	20	20	16	13	21	32	18	6	4	11	9	4	6	11	11	2	4	286	Mar	01	Monday
61	7	8	1	7	22	24	30	23	37	20	18	23	31	21	17	11	8	17	14	9	18	8	5	16	395	Mar	02	Tuesday
62	11	1	13	9	24	28	23	18	13	20	17	11	24	31	11	16	15	13	7	6	6	7	4	5	333	Mar	03	Wednesday
63	3	3	12	10	27	46	28	13	27	22	10	28	26	28	21	12	11	24	8	10	17	16	15	9	426	Mar	04	Thursday
64	9	10	31	22	30	25	25	25	31	14	26	21	35	23	13	7	13	6	7	5	6	3	3	9	399	Mar	05	Friday
65	3	4	8	6	3	8	11	12	9	13	8	27	5	1	11	4	5	4	4	1	9	4	5	3	168	Mar	06	Saturday
66	3	6	1	4	14	4	17	9	3	11	4	4	8	6	5	4	8	5	2	2	2	2	2	6	132	Mar	07	Sunday
67	4	3	5	4	5	1	1	1	4	7	3	12	7	5	2	3	4	1	2	2	1	2	2	4	85	Mar	08	Monday
68	4	10	1	6	9	19	20	14	33	14	16	8	9	19	21	12	9	11	13	21	12	3	7	7	298	Mar	09	Tuesday
69	2	5	7	16	30	28	30	16	22	18	29	36	34	65	101	120	90	110	79	102	116	89	117	116	1378	Mar	10	Wednesday
70	76	55	62	73	62	38	13	12	24	15	35	21	20	21	17	13	37	28	52	38	26	36	24	36	834	Mar	11	Thursday
71	31	30	23	25	40	23	24	24	20	10	12	34	29	34	26	28	20	22	23	22	23	19	29	9	580	Mar	12	Friday
72	6	6	10	18	14	6	13	15	12	17	16	20	9	28	12	13	14	14	15	7	13	2	7	7	294	Mar	13	Saturday
73	5	1	9	8	12	7	10	1	9	21	4	12	2	2	9	12	6	15	18	15	21	11	16	20	246	Mar	14	Sunday
74	6	7	6	8	26	16	48	10	17	27	10	8	17	29	15	18	26	21	12	6	11	8	8	4	364	Mar	15	Monday
75	2	5	8	9	32	21	19	22	16	10	18	8	24	12	18	16	5	12	4	3	7	0	1	3	275	Mar	16	Tuesday
76	0	4	13	29	42	35	33	19	11	9	21	15	30	24	16	12	13	12	8	6	15	3	2	4	376	Mar	17	Wednesday

Table 3.4.5 (Page 3 of 4)

APA .FKX Hourly distribution of detections

Day	00	01	02	03	04	05	06	07	08	09	10	11	12	13	14	15	16	17	18	19	20	21	22	23	Sum	Date
77	14	10	13	13	32	17	31	35	25	14	20	17	10	23	16	23	1	3	6	10	10	1	3	3	350	Mar 18 Thursday
78	2	3	4	14	33	14	14	17	5	24	22	26	41	13	14	24	16	20	10	5	6	5	6	2	340	Mar 19 Friday
79	2	3	1	2	17	8	3	8	13	12	3	26	5	5	4	11	6	9	2	7	1	5	3	2	158	Mar 20 Saturday
80	2	13	4	7	4	8	8	7	5	7	3	11	6	5	8	9	3	3	1	6	4	0	7	8	139	Mar 21 Sunday
81	4	1	7	5	9	30	25	27	18	13	10	20	11	19	11	17	15	10	17	3	4	12	3	10	301	Mar 22 Monday
82	11	3	7	14	23	15	16	18	19	14	11	15	6	23	21	20	27	24	22	29	20	24	27	29	438	Mar 23 Tuesday
83	10	15	25	28	16	22	9	15	22	12	15	22	35	16	19	14	17	8	12	14	3	15	5	8	377	Mar 24 Wednesday
84	4	4	10	12	21	34	34	21	15	21	18	22	22	37	18	25	28	23	12	12	13	14	24	17	461	Mar 25 Thursday
85	10	7	8	18	20	22	25	52	19	15	49	30	44	15	37	36	34	13	10	16	4	11	10	20	525	Mar 26 Friday
86	9	13	12	6	6	8	3	10	15	21	23	24	10	2	2	12	10	13	10	4	13	13	12	15	266	Mar 27 Saturday
87	14	6	17	12	23	7	4	6	0	5	6	5	3	4	2	7	3	10	8	8	2	4	10	13	179	Mar 28 Sunday
88	9	20	3	17	33	19	10	26	20	20	18	12	11	13	18	7	15	15	15	8	5	16	15	7	352	Mar 29 Monday
89	7	18	23	21	19	24	14	12	11	101	29	15	14	16	17	16	8	17	14	7	21	16	9	7	456	Mar 30 Tuesday
90	19	6	6	25	55	149	126	13	8	12	22	7	16	8	11	4	4	8	4	7	2	7	1	6	526	Mar 31 Wednesday

APA	00	01	02	03	04	05	06	07	08	09	10	11	12	13	14	15	16	17	18	19	20	21	22	23		
Sum	2407	2485	2885	3363	4379	4198	4827	4836	4530	4577	4294	4666	5052	4523	3872	4223	3833	3929	3478	3359	2931	2618	2569	2878	90712	Total sum
181	13	14	16	19	24	23	27	27	25	25	24	26	28	25	21	23	21	22	19	19	16	14	14	16	501	Total average
128	13	13	16	19	27	27	31	29	28	28	27	28	32	29	25	26	23	23	21	20	17	15	14	16	548	Average workdays
53	15	15	17	18	16	15	17	20	17	18	17	20	19	16	14	17	17	18	15	15	13	14	14	16	389	Average weekends

Table 3.4.5. Daily and hourly distributions of Apatity detections. For each day is shown number of detections within each hour of the day, and number of detections for that day. The end statistics give total number of detections distributed for each hour and the total sum of detections during the period. the averages show number of processed days, hourly distribution and average per processed day. (page 4 of 4)

SPI .FKX Hourly distribution of detections

Day	00	01	02	03	04	05	06	07	08	09	10	11	12	13	14	15	16	17	18	19	20	21	22	23	Sum	Date
275	0	0	0	0	0	0	0	0	0	0	0	0	0	0	0	0	0	0	0	0	0	0	0	0	0	Oct 01 Thursday
276	0	0	0	0	0	0	0	0	0	0	0	0	0	0	0	0	0	0	0	0	0	0	0	0	0	Oct 02 Friday
277	0	0	0	0	0	0	0	0	0	0	0	0	0	0	0	0	0	0	0	0	0	0	0	0	0	Oct 03 Saturday
278	0	0	0	0	0	0	0	0	0	0	0	0	0	0	0	0	0	0	0	0	0	0	0	0	0	Oct 04 Sunday
279	0	0	0	0	0	0	0	0	0	0	0	0	0	0	0	0	0	0	0	0	0	0	0	0	0	Oct 05 Monday
280	0	0	0	0	0	0	0	0	0	0	0	0	0	0	0	0	0	0	0	0	0	0	0	0	0*	Oct 06 Tuesday
281	0	0	0	0	0	0	0	0	0	0	0	0	0	0	0	0	0	0	0	0	0	0	0	0	0	Oct 07 Wednesday
282	0	0	0	0	0	0	0	0	0	0	0	0	0	0	0	0	0	0	0	0	0	0	0	0	0	Oct 08 Thursday
283	0	0	0	0	0	0	0	0	0	0	0	0	0	0	0	0	0	0	0	0	0	0	0	0	0	Oct 09 Friday
284	0	0	0	0	0	0	0	0	0	0	0	0	0	0	0	0	0	0	0	0	0	0	0	0	0	Oct 10 Saturday
285	0	0	0	0	0	0	0	0	0	0	0	0	0	0	0	0	0	0	0	0	0	0	0	0	0	Oct 11 Sunday
286	0	0	0	0	0	0	0	0	0	0	0	0	0	0	0	0	0	0	0	0	0	0	0	0	0	Oct 12 Monday
287	0	0	0	0	0	0	0	0	0	0	0	0	0	0	0	0	0	0	0	0	0	0	0	0	0	Oct 13 Tuesday
288	0	0	0	0	0	0	0	0	0	0	0	0	0	0	0	0	0	0	0	0	0	0	0	0	0	Oct 14 Wednesday
289	0	0	0	0	0	0	0	0	0	0	0	0	0	0	0	0	0	0	0	0	0	0	0	0	0	Oct 15 Thursday
290	0	0	0	0	0	0	0	0	0	0	0	0	0	0	0	0	0	0	0	0	0	0	0	0	0	Oct 16 Friday
291	0	0	0	0	0	0	0	0	0	0	0	0	0	0	0	0	0	0	0	0	0	0	0	0	0	Oct 17 Saturday
292	0	0	0	0	0	0	0	0	0	0	0	0	0	0	0	0	0	0	0	0	0	0	0	0	0	Oct 18 Sunday
293	0	0	0	0	0	0	0	0	0	0	0	0	0	0	0	0	0	0	0	0	0	0	0	0	0	Oct 19 Monday
294	0	0	0	0	0	0	0	0	0	0	0	0	0	0	0	0	0	0	0	0	0	0	0	0	0	Oct 20 Tuesday
295	0	0	0	0	0	0	0	0	0	0	0	0	0	0	0	0	0	0	0	0	0	0	0	0	0	Oct 21 Wednesday
296	0	0	0	0	0	0	0	0	0	0	0	0	0	0	0	0	0	0	0	0	0	0	0	0	0	Oct 22 Thursday
297	0	0	0	0	0	0	0	0	0	0	0	0	0	0	0	0	0	0	0	0	0	0	0	0	0	Oct 23 Friday
298	0	0	0	0	0	0	0	0	0	0	0	0	0	0	0	0	0	0	0	0	0	0	0	0	0	Oct 24 Saturday
299	0	0	0	0	0	0	0	0	0	0	0	0	0	0	0	0	0	0	0	0	0	0	0	0	0	Oct 25 Sunday
300	0	0	0	0	0	0	0	0	0	0	0	0	0	0	0	0	0	0	0	0	0	0	0	0	0	Oct 26 Monday
301	0	0	0	0	0	0	0	0	0	0	0	0	0	0	0	0	0	0	0	0	0	0	0	0	0	Oct 27 Tuesday
302	0	0	0	0	0	0	0	0	0	0	0	0	0	0	0	0	0	0	0	0	0	0	0	0	0	Oct 28 Wednesday
303	0	0	0	0	0	0	0	0	0	0	0	0	0	0	0	0	0	0	0	0	0	0	0	0	0	Oct 29 Thursday
304	0	0	0	0	0	0	0	0	0	0	0	0	0	0	0	0	0	0	0	0	0	0	0	0	0	Oct 30 Friday
305	0	0	0	0	0	0	0	0	0	0	0	0	0	0	0	0	0	0	0	0	0	0	0	0	0	Oct 31 Saturday
306	0	0	0	0	0	0	0	0	0	0	0	0	0	0	0	0	0	0	0	0	0	0	0	0	0	Nov 01 Sunday
307	0	0	0	0	0	0	0	0	0	0	0	0	0	0	0	0	0	0	0	0	0	0	0	0	0	Nov 02 Monday
308	0	0	0	0	0	0	0	0	0	0	0	0	0	0	0	0	0	0	0	0	0	0	0	0	0	Nov 03 Tuesday
309	0	0	0	0	0	0	0	0	0	0	0	0	0	0	0	0	0	0	0	0	0	0	0	0	0	Nov 04 Wednesday
310	0	0	0	0	0	0	0	0	0	0	0	0	0	0	0	0	0	0	0	0	0	0	0	0	0	Nov 05 Thursday
311	0	0	0	0	0	0	0	0	0	0	0	0	0	0	0	0	0	0	0	0	0	0	0	0	0	Nov 06 Friday
312	0	0	0	0	0	0	0	0	0	0	0	0	0	0	0	0	0	0	0	0	0	0	0	0	0	Nov 07 Saturday
313	0	0	0	0	0	0	0		0	0	0	0	0	0	0	0	0	0	0	0	0	0	0	0	0	Nov 08 Sunday
314	0	0	0	0	0	0	0	0	0	0	0	0	0	0	0	0	0	0	0	0	0	0	0	0	0	Nov 09 Monday
315	0	0	0	0	0	0	0	0	0	0	0	0	0	0	0	0	0	0	0	0	0	0	0	0	0	Nov 10 Tuesday
316	0	0	0	0	0	0	0	0	0	0	0	0	0	0	0	0	0	0	0	0	0	0	0	0	0	Nov 11 Wednesday
317	0	0	0	0	0	0	0	0	0	0	0	0	0	0	0	0	0	0	0	0	0	0	0	0	0	Nov 12 Thursday
318	0	0	0	0	0	0	0	0	0	0	0	0	0	0	0	0	0	0	0	0	0	0	0	0	0	Nov 13 Friday
319	0	0	0	0	0	0	0	0	0	0	0	0	0	0	0	0	0	0	0	0	0	0	0	0	0	Nov 14 Saturday
320	0	0	0	0	0	0	0	0	0	0	0	0	0	0	0	0	0	0	0	0	0	0	0	0	0	Nov 15 Sunday
321	0	0	0	0	0	0	0	0	0	0	0	0	0	0	0	0	0	0	0	0	0	0	0	0	0	Nov 16 Monday
322	0	0	0	0	0	0	0	0	0	0	0	0	0	0	0	0	0	0	0	0	0	0	0	0	0	Nov 17 Tuesday
323	0	0	0	0	0	0	0	0	0	0	0	0	0	0	0	0	0	0	0	0	0	0	0	0	0	Nov 18 Wednesday
324	0	0	0	0	0	0	0	0	0	0	0	0	0	0	0	0	0	0	0	0	0	0	0	0	0	Nov 19 Thursday
325	0	0	0	0	0	0	0	0	0	0	0	0	0	0	0	0	0	0	0	0	0	0	0	0	0	Nov 20 Friday
326	0	0	0	0	0	0	0	0	0	0	0	0	0	0	0	0	0	0	0	0	0	0	0	0	0	Nov 21 Saturday
327	0	0	0	0	0	0	0	0	0	0	0	0	0	0	0	0	0	0	0	0	0	0	0	0	0	Nov 22 Sunday
328	3	13	7	12	6	20	2	5	10	11	4	1	28	9	12	9	11	5	14	12	21	14	14	13	256	Nov 23 Monday
329	15	25	17	10	5	3	13	9	9	1	8	7	18	5	9	5	6	34	8	9	13	2	15	12	258	Nov 24 Tuesday
330	21	9	7	11	4	4	23	7	16	7	26	10	8	16	16	6	4	5	2	5	3	2	3	9	224	Nov 25 Wednesday

Table 3.4.6 (Page 1 of 4)

Figs. 7.1.2-7.1.4 show the event distribution in Fennoscandia for all magnitudes, $M_L > 1$

SPI .FKX Hourly distribution of detections

Day	00	01	02	03	04	05	06	07	08	09	10	11	12	13	14	15	16	17	18	19	20	21	22	23	Sum	Date	
331	5	5	11	2	11	9	6	6	3	10	1	1	4	1	2	1	4	3	0	3	5	4	5	2	104	Nov 26 Thursday	
332	5	2	4	2	1	5	0	8	4	8	2	4	6	3	1	2	3	3	9	3	1	4	4	7	91	Nov 27 Friday	
333	2	3	4	8	0	4	1	6	6	7	5	8	5	3	9	7	2	7	9	3	6	3	4	1	113	Nov 28 Saturday	
334	1	5	7	3	6	0	3	11	5	4	9	3	7	9	5	1	3	0	2	4	1	2	1	1	93	Nov 29 Sunday	
335	0	2	1	0	2	4	1	0	0	9	2	3	1	1	1	2	1	6	0	0	4	3	2	6	51	Nov 30 Monday	
336	8	2	7	4	2	2	3	4	5	18	1	2	1	7	5	0	1	2	9	2	4	3	5	0	97*	Dec 01 Tuesday	
337	7	0	1	0	1	1	2	0	3	1	2	3	10	2	2	14	9	8	10	1	3	1	2	3	86	Dec 02 Wednesday	
338	0	0	1	0	1	2	0	0	0	0	2	0	1	0	2	0	2	0	2	8	3	3	1	0	28	Dec 03 Thursday	
339	2	2	0	0	0	1	1	2	1	0	2	5	0	2	12	3	2	1	1	0	0	1	3	1	42	Dec 04 Friday	
340	2	0	2	3	1	2	4	1	0	0	5	1	2	3	1	5	2	1	3	0	1	8	1	1	49	Dec 05 Saturday	
341	4	6	3	12	9	9	8	4	8	6	12	9	5	8	5	3	8	3	3	2	3	1	2	5	138	Dec 06 Sunday	
342	2	1	4	0	4	1	3	4	1	2	3	0	0	8	5	11	8	0	3	4	2	0	2	6	74	Dec 07 Monday	
343	11	11	12	5	19	6	9	9	4	8	2	4	7	6	4	1	3	10	4	13	1	9	18	2	178	Dec 08 Tuesday	
344	1	3	4	1	0	6	1	5	23	3	6	4	12	6	6	5	11	6	9	8	4	4	8	10	146	Dec 09 Wednesday	
345	4	6	2	7	8	1	2	4	15	15	16	10	7	4	5	17	10	23	9	5	24	24	6	9	233	Dec 10 Thursday	
346	1	12	27	10	7	4	13	13	8	8	14	3	16	3	12	1	12	1	1	5	7	6	5	3	192	Dec 11 Friday	
347	4	2	1	2	5	13	1	0	12	5	4	22	2	4	15	9	2	4	5	3	1	10	3	4	133	Dec 12 Saturday	
348	4	7	6	4	10	6	4	3	3	8	9	7	11	2	4	12	5	5	4	8	4	7	9	9	151	Dec 13 Sunday	
349	7	4	5	9	9	15	6	13	7	1	3	2	2	2	7	3	3	0	4	8	7	3	3	12	135	Dec 14 Monday	
350	8	7	2	0	9	8	3	4	20	3	4	5	4	4	2	2	1	4	4	4	1	2	2	3	106	Dec 15 Tuesday	
351	2	11	3	5	5	5	2	16	5	9	9	1	5	10	10	10	10	10	18	7	12	11	4	2	182	Dec 16 Wednesday	
352	2	8	1	7	6	8	4	17	31	15	18	43	32	18	16	14	28	24	32	29	18	23	16	10	420	Dec 17 Thursday	
353	17	6	8	8	22	7	6	20	11	8	6	8	3	9	6	13	9	14	8	6	2	10	11	7	225	Dec 18 Friday	
354	3	5	10	10	12	8	9	3	6	8	6	8	12	3	7	3	5	7	0	6	6	9	5	7	158	Dec 19 Saturday	
355	6	7	5	12	12	3	7	6	3	2	7	10	3	3	5	3	6	6	9	5	0	24	5	6	155	Dec 20 Sunday	
356	4	1	5	12	6	4	3	1	8	8	13	2	7	4	3	12	0	0	7	2	0	0	2	3	107	Dec 21 Monday	
357	7	1	11	0	1	10	1	4	2	1	9	5	4	5	1	11	3	2	1	0	3	6	7	6	101	Dec 22 Tuesday	
358	3	5	1	3	1	8	6	9	4	3	1	2	4	2	3	2	2	2	1	13	2	6	5	0	88	Dec 23 Wednesday	
359	4	5	7	3	0	14	5	17	9	2	10	0	7	1	5	7	5	8	5	2	4	9	5	2	136	Dec 24 Thursday	
360	0	1	1	13	1	1	0	8	2	4	4	1	4	8	6	21	2	1	1	0	2	6	1	4	92	Dec 25 Friday	Frste
361	0	0	0	3	3	1	3	0	1	3	1	11	0	0	0	3	7	4	6	2	7	3	48	15	121	Dec 26 Saturday	Andre
362	2	2	0	0	4	1	2	1	4	1	7	26	6	5	5	8	4	5	8	11	12	6	4	4	128	Dec 27 Sunday	
363	0	2	5	0	2	2	0	6	5	3	1	4	7	0	4	7	0	1	2	1	4	1	5	1	63	Dec 28 Monday	
364	1	11	6	2	2	1	3	0	0	0	4	8	4	6	2	2	0	4	1	0	5	2	3	14	81	Dec 29 Tuesday	
365	38	4	1	2	2	2	5	5	3	7	6	1	1	1	1	4	8	1	0	1	3	2	4	0	102	Dec 30 Wednesday	
366	0	1	1	1	1	2	5	0	10	5	1	9	2	4	2	0	1	2	3	5	5	4	8	1	73	Dec 31 Thursday	
1	1	7	2	2	2	3	0	0	1	1	3	1	1	14	2	1	1	6	2	2	6	2	2	1	63	Jan 01 Friday	Frste
2	7	0	0	4	6	1	5	1	10	13	12	1	3	4	3	3	6	2	10	2	1	10	2	1	107	Jan 02 Saturday	
3	0	0	0	0	0	0	0	0	0	0	0	3	5	8	5	4	1	0	5	1	1	10	3	1	47	Jan 03 Sunday	
4	1	0	2	0	5	2	1	5	1	4	0	0	1	0	0	10	3	3	4	0	0	3	0	0	45	Jan 04 Monday	
5	0	1	1	0	0	0	2	5	0	1	2	2	1	0	5	9	2	2	1	4	6	0	0	1	45	Jan 05 Tuesday	
6	1	3	4	0	2	5	4	4	1	2	0	8	3	1	9	1	3	1	2	0	7	8	2	11	82	Jan 06 Wednesday	
7	0	4	2	4	1	3	13	1	14	0	2	0	12	13	3	5	15	3	8	5	0	5	2	7	122	Jan 07 Thursday	
8	1	2	3	11	4	6	5	3	5	4	1	3	4	0	9	2	0	4	1	3	4	4	4	3	86	Jan 08 Friday	
9	4	4	4	7	6	3	5	8	16	1	6	1	1	4	2	9	1	7	5	3	2	1	0	1	101	Jan 09 Saturday	
10	7	6	3	9	8	4	4	16	2	2	1	5	14	11	9	9	7	3	7	6	12	8	5	5	163	Jan 10 Sunday	
11	10	5	4	6	10	7	7	7	13	5	5	8	4	6	10	7	5	3	8	8	2	5	3	5	153	Jan 11 Monday	
12	8	3	7	7	8	8	7	3	1	8	12	5	13	4	6	9	10	11	9	18	9	5	10	10	191	Jan 12 Tuesday	
13	21	22	12	9	22	3	10	16	12	6	19	11	15	30	11	22	16	40	28	29	16	26	23	14	433	Jan 13 Wednesday	
14	17	12	22	15	12	8	16	6	19	6	15	20	13	10	15	12	5	33	29	31	8	16	12	9	361	Jan 14 Thursday	
15	4	7	7	13	17	4	7	8	9	6	1	13	19	2	10	4	7	8	6	4	6	2	3	2	169	Jan 15 Friday	
16	6	4	4	3	4	2	3	2	0	5	7	3	7	2	2	3	11	4	8	5	11	1	6	2	105	Jan 16 Saturday	
17	0	3	0	1	2	5	3	5	2	7	4	2	2	0	4	1	0	2	2	0	3	9	2	3	62	Jan 17 Sunday	
18	4	5	5	3	3	4	7	1	5	6	5	2	4	11	4	6	13	4	3	5	4	7	1	2	114	Jan 18 Monday	
19	1	2	0	3	1	1	3	5	9	0	4	12	5	3	8	11	1	5	3	3	10	11	1	6	108	Jan 19 Tuesday	
20	3	0	7	4	3	7	1	2	0	1	2	1	1	2	1	0	5	3	2	0	6	0	12	17	80	Jan 20 Wednesday	

Table 3.4.6 (Page 2 of 4)

SPI .FKX Hourly distribution of detections

Day	00	01	02	03	04	05	06	07	08	09	10	11	12	13	14	15	16	17	18	19	20	21	22	23	Sum	Date	
21	2	7	2	4	1	2	1	2	1	10	1	5	5	7	1	3	3	0	6	2	1	1	0	0	67	Jan 21	Thursday
22	1	3	1	3	2	2	2	6	4	5	2	3	2	0	3	2	9	3	1	3	1	4	4	0	66	Jan 22	Friday
23	4	4	2	2	7	2	2	9	0	8	12	1	8	5	7	9	3	7	11	4	12	10	3	5	137	Jan 23	Saturday
24	2	5	9	3	3	1	5	5	6	6	0	5	3	8	6	1	5	3	7	5	0	10	8	2	108	Jan 24	Sunday
25	1	5	1	4	5	3	4	6	4	2	3	4	5	11	1	6	3	7	7	6	7	2	14	6	117	Jan 25	Monday
26	2	4	2	9	7	7	3	8	6	7	11	4	6	3	4	3	2	7	9	0	4	6	7	9	130	Jan 26	Tuesday
27	3	4	5	2	5	13	3	7	8	5	12	12	12	4	17	5	1	5	4	3	9	7	9	11	166	Jan 27	Wednesday
28	15	3	10	12	6	8	9	5	4	18	8	10	7	6	7	13	9	5	7	5	6	5	7	6	191	Jan 28	Thursday
29	1	4	0	6	2	1	3	4	8	4	11	0	6	1	8	79	67	36	1	6	5	10	5	10	278	Jan 29	Friday
30	12	4	9	6	0	2	2	0	18	0	6	0	3	2	27	2	2	1	3	14	2	12	9	2	138	Jan 30	Saturday
31	10	1	4	10	0	5	0	1	7	1	7	22	1	6	1	6	3	0	2	2	0	3	11	2	105	Jan 31	Sunday
32	2	8	1	6	3	2	0	3	7	2	4	8	3	8	9	0	2	2	0	2	0	2	0	2	76	Feb 01	Monday
33	4	1	2	4	3	5	7	2	1	4	0	4	2	1	0	4	6	1	6	2	5	3	0	6	73	Feb 02	Tuesday
34	2	0	6	3	2	0	5	5	1	0	3	0	0	4	0	5	9	12	0	5	2	2	12	0	78	Feb 03	Wednesday
35	3	0	3	1	0	2	0	2	2	0	0	1	4	2	5	2	1	2	2	1	4	2	4	3	46	Feb 04	Thursday
36	4	1	2	2	0	5	0	1	0	1	0	3	3	56	7	8	1	1	2	2	8	2	3	4	116	Feb 05	Friday
37	0	1	2	3	0	3	2	5	4	41	34	18	16	1	8	20	1	0	13	1	1	2	1	4	181	Feb 06	Saturday
38	0	0	1	11	0	0	3	2	0	37	1	23	37	31	6	24	2	3	1	3	3	1	2	5	196	Feb 07	Sunday
39	1	5	5	1	4	1	1	6	1	0	2	3	0	7	6	1	2	2	1	2	7	3	4	11	76	Feb 08	Monday
40	6	12	3	12	10	16	19	12	7	19	12	15	17	55	59	12	10	13	12	20	11	35	23	14	424	Feb 09	Tuesday
41	13	12	21	18	23	19	12	15	21	30	36	16	23	16	15	23	15	6	12	10	26	20	22	9	433	Feb 10	Wednesday
42	4	5	11	13	10	3	6	5	7	4	12	9	7	5	14	10	10	7	11	10	9	4	8	1	185	Feb 11	Thursday
43	5	10	2	5	13	4	3	5	4	6	9	1	4	2	3	12	5	43	37	6	4	8	5	3	199	Feb 12	Friday
44	0	4	0	2	1	3	1	1	49	7	4	17	26	14	0	1	1	3	8	6	3	3	8	0	162	Feb 13	Saturday
45	6	2	2	1	0	0	8	1	2	2	1	7	1	17	10	0	6	0	0	2	0	4	3	0	75	Feb 14	Sunday
46	0	1	0	0	0	3	0	0	12	1	0	0	3	1	1	4	5	5	1	2	0	3	2	3	47	Feb 15	Monday
47	0	1	3	0	0	0	9	4	4	4	1	4	2	0	7	4	1	1	3	1	1	0	2	6	58	Feb 16	Tuesday
48	1	0	4	3	1	1	2	1	3	2	1	4	14	0	1	2	4	0	2	8	4	8	0	0	66	Feb 17	Wednesday
49	2	1	2	1	1	3	8	2	0	9	2	1	6	0	1	0	5	1	4	1	1	1	3	3	58	Feb 18	Thursday
50	0	12	2	3	5	5	7	0	3	3	0	0	5	14	2	2	3	8	34	5	0	0	5	4	122	Feb 19	Friday
51	1	4	1	0	2	1	0	4	30	140	22	4	48	26	1	24	4	0	1	31	2	2	4	1	353	Feb 20	Saturday
52	2	2	1	0	1	2	0	2	0	5	24	64	83	10	62	7	2	4	0	10	1	2	19	8	311	Feb 21	Sunday
53	4	3	3	0	8	4	9	2	7	9	1	5	5	2	5	3	7	3	5	4	4	13	4	9	119	Feb 22	Monday
54	9	7	12	28	1	0	6	4	10	1	3	6	12	2	4	0	1	1	11	2	2	3	8	1	134	Feb 23	Tuesday
55	4	2	1	0	10	1	2	0	8	2	3	14	1	3	18	3	3	0	5	2	0	1	0	1	84	Feb 24	Wednesday
56	6	3	1	2	3	2	3	2	0	4	13	5	1	10	7	6	4	2	9	6	2	8	4	1	104	Feb 25	Thursday
57	1	4	0	3	4	3	3	6	0	0	2	1	1	4	4	0	10	1	1	3	2	0	6	1	60	Feb 26	Friday
58	0	0	0	0	4	4	6	6	11	5	1	8	3	1	15	5	3	4	4	0	1	0	11	0	92	Feb 27	Saturday
59	0	1	3	0	1	1	0	0	20	2	201	52	5	32	6	9	11	20	2	5	0	2	0	1	374	Feb 28	Sunday
60	3	1	8	1	2	0	0	11	2	1	2	3	2	10	9	2	4	0	0	0	60	0	5	1	127	Mar 01	Monday
61	3	2	10	2	0	3	2	3	3	2	1	1	5	2	4	7	0	1	0	0	1	0	0	3	55	Mar 02	Tuesday
62	4	0	3	9	2	2	7	0	13	0	0	0	0	0	0	0	0	0	1	4	0	4	0	0	49	Mar 03	Wednesday
63	1	3	9	0	3	14	14	6	1	0	22	15	5	5	11	8	0	5	8	0	6	5	12	4	157	Mar 04	Thursday
64	4	13	1	0	0	12	3	4	9	0	2	0	7	0	104	8	20	2	6	8	5	0	3	0	211	Mar 05	Friday
65	2	1	8	2	2	0	2	4	1	1	7	10	32	5	1	11	4	0	2	0	0	4	1	1	101	Mar 06	Saturday
66	13	2	3	0	3	0	6	0	0	28	132	56	32	8	10	24	15	2	0	0	4	11	0	1	350	Mar 07	Sunday
67	0	1	2	3	2	1	1	0	0	7	7	1	5	2	1	1	1	2	0	2	0	2	3	1	45	Mar 08	Monday
68	3	5	4	0	0	0	5	0	1	2	8	72	1	2	6	1	4	5	4	0	6	0	1	7	137	Mar 09	Tuesday
69	4	2	6	4	4	7	4	7	3	9	1	2	9	9	1	9	5	4	8	5	0	2	10	6	121	Mar 10	Wednesday
70	7	7	10	12	2	6	5	5	18	4	16	10	10	6	9	11	10	10	6	7	7	10	10	8	206	Mar 11	Thursday
71	12	8	13	13	12	12	16	21	16	18	14	37	6	12	16	6	77	121	8	8	17	7	12	8	490	Mar 12	Friday
72	10	5	11	7	8	10	6	9	11	10	8	3	15	16	20	10	9	19	5	11	13	4	10	6	236	Mar 13	Saturday
73	8	6	5	7	4	7	7	7	5	6	13	9	5	10	16	36	16	53	8	17	5	4	10	2	266	Mar 14	Sunday
74	3	1	5	3	2	1	0	14	9	9	3	13	5	6	4	3	3	16	2	1	4	0	3	4	114	Mar 15	Monday
75	2	12	0	4	3	5	4	6	1	0	2	3	2	11	23	1	4	0	6	3	3	1	19	6	121	Mar 16	Tuesday
76	0	2	4	1	7	5	0	1	11	4	4	2	2	1	10	13	1	11	6	2	0	1	0	2	90	Mar 17	Wednesday

Table 3.4.6 (Page 3 of 4)

SPI .FKX Hourly distribution of detections

Day	00	01	02	03	04	05	06	07	08	09	10	11	12	13	14	15	16	17	18	19	20	21	22	23	Sum	Date
77	3	0	1	0	2	2	4	1	4	0	1	0	10	0	0	6	1	2	0	7	0	3	2	2	51	Mar 18 Thursday
78	1	4	4	5	0	0	8	0	4	8	1	6	12	17	7	2	12	4	0	24	4	5	1	2	131	Mar 19 Friday
79	0	1	0	5	2	4	0	0	17	24	17	11	1	42	52	15	14	2	12	0	0	0	0	0	219	Mar 20 Saturday
80	5	2	1	0	1	1	0	4	2	2	2	0	15	5	3	2	9	24	27	5	0	0	3	0	113	Mar 21 Sunday
81	0	0	5	2	2	5	0	1	1	4	5	8	0	1	16	10	19	1	2	1	3	8	1	1	96	Mar 22 Monday
82	1	2	1	2	2	4	1	2	2	0	7	15	8	7	4	1	9	10	7	1	2	4	3	0	95	Mar 23 Tuesday
83	4	0	0	1	1	0	0	9	7	0	21	11	2	6	3	0	30	1	3	4	7	10	19	10	149	Mar 24 Wednesday
84	1	1	4	3	9	5	6	7	6	2	3	5	7	9	2	3	7	10	9	6	4	5	2	2	120	Mar 25 Thursday
85	1	4	2	2	2	0	1	2	3	3	5	14	10	12	7	18	3	2	1	10	0	1	0	4	107	Mar 26 Friday
86	1	0	1	0	0	0	1	0	8	4	16	2	5	11	7	8	0	1	3	2	1	2	1	11	85	Mar 27 Saturday
87	5	1	0	4	1	4	1	1	21	82	67	56	88	11	10	2	48	13	51	4	1	4	2	3	606	Mar 28 Sunday
88	7	7	3	2	8	0	0	8	2	3	2	47	11	9	8	3	8	2	10	16	1	0	0	0	157	Mar 29 Monday
89	1	2	8	2	0	0	4	56	2	3	45	2	2	0	39	6	64	4	10	3	5	2	0	5	265	Mar 30 Tuesday
90	0	2	9	11	7	3	1	4	0	0	4	3	17	2	37	65	36	2	0	11	3	5	0	0	222	Mar 31 Wednesday

SPI	00	01	02	03	04	05	06	07	08	09	10	11	12	13	14	15	16	17	18	19	20	21	22	23		
Sum	565	550	589	596	576	549	555	689	865	875	1466	1145	1124	941	1150	996	1005	931	827	711	647	697	735	575	19359	Total sum
129	4	4	5	5	4	4	4	5	7	7	11	9	9	7	9	8	8	7	6	6	5	5	6	4	150	Total average
91	5	5	5	5	5	5	5	6	6	5	6	7	6	6	9	7	8	8	6	6	6	5	6	5	140	Average workdays
38	4	3	3	4	3	3	3	4	8	11	23	13	14	9	9	8	6	6	7	5	3	5	6	3	163	Average weekends

Table 3.4.6. Daily and hourly distributions of Spitsbergen detections. For each day is shown number of detections within each hour of the day, and number of detections for that day. The end statistics give total number of detections distributed for each hour and the total sum of detections during the period. the averages show number of processed days, hourly distribution and average per processed day. (page 4 of 4)

3.5 IMS operation

The Intelligent Monitoring System (IMS) was installed at NORSAR in December 1989 and was operated at NORSAR from 1 January 1990 for automatic processing of data from ARCESS and NORESS. A second version of IMS that accepts data from an arbitrary number of arrays and single 3-component stations was installed at NORSAR in October 1991, and regular operation of the system comprising analysis of data from the 4 arrays ARCESS, NORESS, FINESA and GERESS started on 15 October 1991. As opposed to the first version of IMS, the one in current operation also locates events at teleseismic distance.

During this reporting period, two new data sources were made available to IMS: the array near Apatity on the Kola peninsula of Russia, and the array on Spitsbergen. The analysts had waveforms available from these two arrays from 11 December 1992. On 14 December 1992, phase detections from the Apatity array were included in the automatic phase association. The phase detections from the Spitsbergen array were made available to the analysts on 5 February 1993. These detections are not used in the automatic phase association, but can be added manually during analysis.

The operational stability of IMS has been very good during the reporting period. In fact the IMS event processor (pipeline) has had no downtime of its own; i.e., all data available to IMS have been processed by IMS.

Phase and event statistics

Table 3.5.1 gives a sumary of phase detections and events declared by IMS. From top to bottom the table gives the total number of detections by the IMS, the number of detections that are associated with events automatically declared by the IMS, the number of detections that are not associated with any events, the number of events automatically declared by the IMS, the total number of events defined by the analyst, and finally the number of events accepted by the analyst without any changes (i.e., from the set of events automatically declared by the IMS).

	Oct 92	Nov 92	Dec 92	Jan 93	Feb 93	Mar 93	Total
Phase detections	38026	26150	39885	40148	49504	50710	206397
- Associated phases	5835	5439	5936	5838	6127	8923	32263
- Unassociated phases	32191	20711	33949	34310	43377	41787	174134
Events automatically declared by IMS	1742	1671	1785	1755	1765	2554	9530
No. of events defined by the analyst	1275	1359	1136	1141	1430	2125	7191
No. of events accepted without modifications	1018	880	951	954	1105	1623	5513

Table 3.5.1. IMS phase detections and event summary

U. Baadshaug
B. Ferstad
B.Kr. Hokland
L.B. Loughran

3.6 GBF operation

Events automatically located by GBF

During days 275, 1992, through 090, 1993, 9280 local and regional events were located by GBF. This gives an average of 51.0 events per processed day (182 days processed). 70% of these events are within 300 km of nearest station, and 85% of these events are within 1000 km of the nearest station.

70.8% of these events were defined by 2 regional phases. Teleseismic phases are currently not used by GBF. 86.7% of all events had 3 defining phases or less.

T. Kværna

4 Improvements and Modifications

4.1 NORSAR

NORSAR data acquisition

No modification has been made to the NORSAR data acquisition system.

The data are recorded on a 30-hour circular disk buffer on the IBM system, and archived onto 1/2 inch magnetic tapes. In addition to this, the data are now regularly transmitted to a SUN system for recording on a 48-hour circular disk buffer.

NORSAR detection processing

The NORSAR detection processor has been running satisfactorily on the IBM 4381 computer during this reporting period.

Detection statistics are given in section 2. In addition to the detection processing done on IBM, the dp program is doing regular detection processing on a SUN system, using the unix-based circular disk buffer (see below). A detection SNR threshold of 20.0 triggers automatic saving of waveforms into CSS 3.0 data files.

NORSAR event processing

There have been no changes in the routine processing of NORSAR events, using the IBM system.

In parallel with the IBM processing, routine event processing is also done on a SUN computer using the "old" IBM time delay correction data base that has been converted to SUN/UNIX. The automatic solutions produced are equal to or better than the old system with a lower false alarm rate. Alert messages are sent to USGS for events above magnitude 5.5.

NORSAR refurbishment

As reported earlier, the main problem in this refurbishment is to find 24-bit A/D converters with low power consumption. We have received evaluation units from Refraction Technology, Teledyne Geotech and Science Horizons. During the reporting period, the available units have been extensively tested, and they appear to perform satisfactorily. Details on the refurbishment effort will be reported on separately.

4.2 Regional Arrays

Detection processing

The routine detection processing of the arrays is running satisfactorily on each of the array's SUN-3/280 acquisition systems. The same program is used for NORSAR, NOR-

ESS, ARCESS, FINESA, GERESS, Apatity and Spitsbergen, but with different "recipes". The beam table for NORESS and ARCESS is found in NORSAR Sci. Rep. No. 1-89/90. The beam table for FINESA and GERESS is found in NORSAR Sci. Rep. No. 1-90/91. The beam table for Apatity is found in NORSAR Sci. Rep. No. 1-92/93, and that for Spitsbergen is given in the present report (section 7.5).

Detection statistics are summarized in section 3.

Signal processing. Phase estimation

This process performs f-k and polarization analysis for each detection to determine phase velocity, azimuth and type of phase, and the results are put into the ORACLE detection data base for use by the IMS.

Event Processing. Plot and epicenter determination

A description of single-array event processing is found in NORSAR Sci. Rep. No. 2-88/89, and NORSAR Sci. Rep. No. 2-89/90.

J. Fyen

5 Maintenance Activities

5.1 Activities in the field and at the Maintenance Center

This section summarizes the activities at the Maintenance Center (NMC) Hamar, and NDPC activities related to monitoring and control of NORSAR, including monitoring of NORESS, ARCESS, FINESA, GERESS and Apatity.

Activities involve preventive and corrective maintenance, planning and installation of the Spitsbergen array (28 Oct - 7 Nov 92) and completion of the Apatity installation (22 Sep - 3 Oct 92).

NORSAR

Visits to subarrays in connection with:

- Test of SLEM equipment in order to locate a failure
- Reinstallation of SLEM used for test purposes
- Adjustment of gain SP/LP channels
- Adjustment of MP/FP
- Adjustment of DC offset SP channels
- Replacement of MP/FP motors incl. adjustments
- SLEM rest
- Replacement of BE-card
- Comm. cable test
- Modem and line test

NMC

- Preparations for the Spitsbergen installation
- NORSAR refurbishment preparations
- Other tasks related to repair of SLEM and related subarray equipment

NORESS

- Repair of C6, D6

Spitsbergen

- Installation of the Spitsbergen array (Oct/Nov 92)
- Installation of a second windmill and extra batteries (Feb 93)

Apatity

- Installation continued through 30 Sep 92 and was completed 3 Oct 92

Subarray/ area	Task	Date
NORSAR		
01B	Installation of 01A analog unit in 01B SLEM for test purposes (possible because 01A was still down)	6 Oct
01B	Spikes in data still required CTV engagement. A test with a data scope at the NDPC and the CTV modem (in C-loop) proved that the communications system was OK. A Digital Unit from the 01B SLEM was installed in the 01A SLEM for continued testing	12 Oct
01B	Visit to the SA in connection with installation of original SLEM with a new power unit. Power unit failed (lack of +15 Volt). No spare unit was available.	15 Oct
01A	Reinstalled the SLEM used for test purposes on 01B. Attempts to adjust the gain SP/LP resulted in improper data.	15 Oct
01A	A new visit to the subarray resulted in proper data and demasking of the array.	22 Oct
NPDC	Daily checks of the following arrays have been carried out, i.e., NORSAR, NORESS, ARCESS, FINESA and Apatity. SP/LP instruments have been calibrated. Free Period (FP) and Mass Pos. (MP) were measured. Those outside specifications adjusted (when feasible from NDPC).	Oct
NORSAR		
01B	SLEM brought to NMC for repair	9 Nov
01B	SLEM installed	11 Nov
02B	Found communication inoperative	20 Nov
04C	Replaced BE-card channel 1. Adjusted gain all SP/LP channels. Adjusted FP/MP all LP instruments	30 Nov
NDPC	Daily checks of the following arrays have been carried out, i.e., NORSAR, NORESS, ARCESS, FINESA, Apatity and Spitsbergen (partly). SP/LP instruments were calibrated weeks 45, 47 and 48. FP/MP were measured. Those outside specifications adjusted (when feasible from NDPC).	Nov

Subarray/ area	Task	Date
NMC	The staff have been engaged in preparations in connection with the refurbishment of the NORSAR array. In addition, installation of the Spitsbergen array (28 Oct - 7 Nov has been carried out.	Nov
NORSAR		
03C	Adjusted channel gain all SP/LP channels. Adjusted MP/FP V, NS, EW seismometers. Adjusted DC offset all SP channels.	2 Dec
04C	LP seismometer NS repaired	4 Dec
02B(tel)	Replaced the telemetry receiver station batteries.	4 Dec
NMC	The NMC staff continued with preparations for the refurbishment of the NORSAR array.	Dec
NDPC	Daily checks of the following arrays have been carried out, i.e., NORSAR, NORESS, ARCESS, FINESA, Apatity and Spitsbergen. SP/LP instruments were calibrated weeks 45, 49 - 52. FP/ MP were measured. Those outside specifications adjusted (when feasible from NDPC).	Dec
NORSAR		1993
02B	A SLEM reset carried out.	11 Jan
NMC	NORSAR refurbishment preparations continued.	Jan
NDPC	Daily checks of the following arrays have been carried out, i.e., NORSAR, NORESS, ARCESS, FINESA, Apatity and Spitsbergen. SP/LP instruments were calibrated (NORSAR). FP/ MP were measured. Those outside specifications adjusted (when feasible from NDPC).	Jan
Spitsbergen	A second windmill and extra batteries were mounted.	19 Feb
NMC	NORSAR refurbishment preparations continued.	Feb

Subarray/ area	Task	Date
NDPC	Daily checks of the following arrays have been carried out, i.e., NORSAR, NORESS, ARCESS, FINESA, Apatity and Spitsbergen. SP/LP instruments were calibrated (NORSAR). FP/ MP were measured. Those outside specifications adjusted (when feasible from NDPC).	
NORSAR		
02C	Replaced NS MP motor. Adjusted EW,NS Mass Position and Free Period (MP/FP).	11 Mar
02C	Replaced EW MP/FP motor and adjusted.	29 Mar
NORESS	Replaced C6.	23 Mar
	Final repair of D6. NORSAR refurbishment	31 Mar
NPDC	Daily checks of the following arrays have been carried out, i.e., NORSAR, NORESS, ARCESS, FINESA, Apatity and Spitsbergen. SP/LP instruments were calibrated (NORSAR). FP/ MP were measured. Those outside specifications adjusted (when feasible from NDPC).	

Table 5.1. Activities in the field and the NORSAR Maintenance Center, including NDPC activities related to NORSAR, NORESS, ARCESS, FINESA, GERESS, Apatity and Spitsbergen 1 Oct 92 - 31 Mar 93.

5.2 Array status

As of 31 March 1992 the following NORSAR channels deviated from tolerances:

01A	01	8 Hz filter
	02	8 Hz filter
	04	30 dB attenuation
02B	01	
	08	
	09	
02C	01	
	08	
03C	04	

O.A. Hansen

6 Documentation Developed

Fyen, J. and F. Ringdal (1993): Initial processing results from the Spitsbergen small-aperture array, in Semiannual Tech. Summ. 1 Oct 92 - 31 Mar 93, NORSAR Sci. Rep. 2-92/93, Kjeller, Norway.

Kværna, T. (1993): Intelligent post-processing of seismic events -- Part 2: Accurate determination of phase arrival times using autoregressive likelihood estimation, in Semiannual Tech. Summ. 1 Oct 92 - 31 Mar 93, NORSAR Sci. Rep. 2-92/93, Kjeller, Norway.

Kværna, T. and F. Ringdal (1993): Intelligent post-processing of seismic events -- Part 3: Precise relocation of events in a known target region, in Semiannual Tech. Summ. 1 Oct 92 - 31 Mar 93, NORSAR Sci. Rep. 2-92/93, Kjeller, Norway.

Kværna, T. and F. Ringdal (1993): Monitoring a moratorium: An experiment in continuous seismic threshold monitoring of the northern Novaya Zemlya test site, in Semiannual Tech. Summ. 1 Oct 92 - 31 Mar 93, NORSAR Sci. Rep. 2-92/93, Kjeller, Norway.

Kværna, T., U. Baadshaug and F. Ringdal (1993): Intelligent post-processing of seismic events -- Part 1: Basic approach, in Semiannual Tech. Summ. 1 Oct 92 - 31 Mar 93, NORSAR Sci. Rep. 2-92/93, Kjeller, Norway.

Mykkeltveit, S., U. Baadshaug, B.Kr. Hokland, T. Kværna and L.B. Loughran (1993): An evaluation of the performance of the Intelligent Monitoring System, in Semiannual Tech. Summ. 1 Oct 92 - 31 Mar 93, NORSAR Sci. Rep. 2-92/93, Kjeller, Norway.

Ruud, B.O., C.D. Lindholm and E.S. Husebye (1993): An exercise in automating seismic record analysis and network bulletin production, *Bull. Seism. Soc. Am.*, 83, 660-679.

Semiannual Tech. Summary, 1 Apr - 30 Sep 92, NORSAR Sci. Rep. 1-92/93, NORSAR, Kjeller, Norway.

7 Summary of Technical Reports / Papers Published

7.1 Intelligent post-processing of seismic events -- Part 1: Basic approach

Introduction

This is the first in a series of three contributions in this report addressing the topic of intelligent post-processing of seismic events. In this first contribution we discuss how to subdivide the area to be monitored in order to identify sites of particularly high seismic activity. We further introduce the basic idea behind this post-processing technique, which is to use as a starting point the initial event location provided by the Intelligent Monitoring System (IMS) and then use region-specific information to refine the solution. By applying this technique to areas with significant recurring seismic activity, such as mining sites, a considerable part of the analyst work can be eliminated.

Since 15 October 1991, the Intelligent Monitoring System (IMS, Bache et al, 1993) has been processing seismic data from four high-frequency arrays in northern Europe. These are NORESS and ARCESS in Norway, FINESA in Finland and GERESS in Germany. During October 1992 a small-aperture array was installed near Apatity on the Kola peninsula, and during late October/early November 1992 another small-aperture array on the island of Spitsbergen became operational. The data from these installations are now included in the IMS processing for the production of the event bulletin.

Since four of the arrays providing data to the IMS are located in Fennoscandia, see Fig. 7.1.1, the IMS event bulletin shows an excellent event detection capability for this region. Ringdal (1991) found that for Fennoscandia/NW Russia, a network consisting of NORESS, ARCESS and FINESA has a 90% detection capability close to M_L 2.0. Near the individual arrays, the detection capability is considerably better, and consequently a large number of events less than M_L 1.0 are detected.

IMS event statistics

The basic principle of the post-processing method is to start by subdividing the area to be monitored into smaller areas, and subsequently apply region-specific analysis to each such area. As an example, we will consider in some detail the statistics of events in Fennoscandia and NW Russia for the 18-month time period 10/15/91 - 04/15/93. We will only consider "well-defined" events; thus we ignore events with author identification "yes/no" and "ESAL/Poor_Loc" in the origin table.

For the time period 10/15/91 to 04/15/93 the IMS bulletin contains 19503 well-defined events. 65.6% (12799) of these events are located in the Fennoscandian/NW Russian region defined by the map of Fig. 7.1.2, 15.8% (3089) are located within 5 degrees of the GERESS array, and the remaining 18.5% (3615) are distributed around the rest of the world, mostly at teleseismic distances from the regional array network.

Figs. 7.1.2-7.1.4 show the event distribution in Fennoscandia for all magnitudes, $M_L > 1$ and $M_L > 2$, respectively. In each figure, we have marked the approximate geographical extent of 8 main mining areas. Table 7.1.1 lists these mining sites and gives details on the number and percentages of events associated to the sites at various magnitudes.

From the three figures and Table 7.1.1 we can make the following general observations:

- Out of the total 12799 events, 6317 (49.4 per cent) are above $M_L = 1$, and only 1131 (8.8 per cent) are above M_L 2.
- The total percentage of events associated with the 8 mining sites is 47.88% (all magnitudes), 56.66% ($M_L > 1.0$) and 65.61% ($M_L > 2.0$). Thus, these sites become more dominant for the largest events, in terms of relative number of events reported.
- Some mining sites have a relatively high proportion of large events ($M_L > 2.0$). This is particularly noticeable for the mining areas in Western Russia/Estonia. On the other hand, the Kiruna mine has the largest number of events altogether, but almost none of these are above M_L 2.

Being based on about 1 1/2 year of data, the statistics discussed here should be reasonably representative for the situation in the Fennoscandian/NW Russia region. Thus, analysis of recurring events from these mining areas is a significant workload for the analyst. An automatic method to improve the automatic analysis so as to obtain location precisions comparable with the analysts' results would be a significant development. In this and the next two sections of this report, we will show that such an improvement is possible for a well-calibrated mining area (the Khibiny Massif).

General outline of the method

Most automatic detection processor algorithms work without any ***a priori*** assumptions as to when and where a seismic event occurred. This is, of course, quite reasonable, and to some extent inevitable. The detector (SigPro) associated with the IMS works in this way. As a result, some of the SigPro output parameters, which later will be used by the IMS ESAL system, are less than optimum.

However, once an initial event location is given by the IMS, it is possible to use this initial location successively in an automatic iteration scheme. Each iteration gives a more precise location, which in turn allows the automatic program to place successively stronger constraints on the processing parameters.

As a first example (see Section 7.2), we can consider the estimation of signal arrival time. Given that an event has occurred in a certain area, the automatic program can select a set of optimum filter bands and beam parameters for this area, prior to reassessing the arrival time estimate. As shown in Section 7.2, this can lead to a remarkable improvement in timing precision. The examples given in Section 7.2 make use of an autoregressive likelihood technique (Pisarenko et al, 1987; Kushnir et al, 1990). It is noteworthy that this method seems to require that the search be limited to a relatively short time window in order to work well. If an initial location and origin time is known, we can obtain the required short

data in a low passband, e.g. 1 - 2 Hz, where S has a low SNR, and the first S-onset is in many cases missed. With this problem in mind we have found it difficult to justify a comtime window for the search. The method is therefore well suited to a post-processing application.

Another example is the estimation of azimuth from either arrays or three-component stations. The advantage of using a fixed frequency interval for broadband F-k analysis was convincingly demonstrated by Kværna and Ringdal (1986). Again, a prerequisite was the knowledge that the event in question was located in a certain known area.

Section 7.3 demonstrates that the approach of doing post-processing based on IMS initial solutions has the potential of providing an order-of-magnitude improvement in location precision, at least in certain cases such as the Khibiny Massif near the Apatity array. The improvement may be less if no network station is located close to the source, but it should still be significant. For example, the data from Kværna and Ringdal (1986) indicate that a single array (NORESS) would be capable of locating the Blåsjø explosions to within an accuracy of 10 km or better at a distance of 300 km. This is compared to the typical uncertainty of about 30 km in traditional single-array location estimates at this distance (Mykkeltveit and Ringdal, 1981).

In general, it is true that regional corrections are required in order to compute an optimum location. Again, the post-processing analysis is well suited toward this end, because the corrections can be tied to the general area, to which the initial IMS processing assigns the event.

In this context, it is important to note that no regional travel-time tables need to be involved as long as an adequate set of calibration events for the general area are available. The corrections for systematic bias may be made both to the phase arrival times and to the estimated azimuths. Again, this subject will be discussed in detail in Section 7.3, in connection with an applicaiton of the method to the Khibiny Massif area in the Kola peninsula.

T. Kværna
U. Baadshaug
F. Ringdal

References

Bache, T.C., S.R. Bratt, H.J. Swanger, G.W. Beall and F.K. Dashiell (1993): Knowledge-based interpretation of seismic data in the Intelligent Monitoring System, *Bull. Seism. Soc. Am.*, in press.

Kværna, T. and F. Ringdal (1986): Stability of various F-k estimation techniques, in *NORSAR Semiann. Rep. 1-86/87*, NORSAR, Kjeller, 29-40.

Kushnir, A.F., V.M. Lapshin, V.I. Pinsky and J. Fyen (1990): Statistically optimal event detection using small array data, *Bull. Seism. Soc. Am.*, 80, No. 6, Special Issue, 1934-1950.

Mykkeltveit, S and F. Ringdal (1981): Phase identificaiton and event location at regional distances using small-aperture array data, in *Identification of Seismic Sources -- Earthquake or Underground Explosions*, E.S. Husebye and S. Mykkeltveit, eds. Dordrecht, Holland, 467-481.

Pisarenko, V.F., A.F. Kushnir and I.V. Savin (1987): Statistical adaptive algorithms for estimation of onset moments of seismic phases, *Phys. Earth Planet. Int.*, 47, 4-10.

Ringdal, F. (1991): Regional detection performance during GSETT-2. Initial results for the Fennoscandian array network, in Semiannual Tech. Summ. 1 April - 30 September 1991, NORSAR Sci. Rep. 1-91/92, NORSAR, Kjeller, 127-133.

Region	All Mag		Mag > 1.0		Mag > 2.0	
	Number	*Percent*	*Number*	*Percent*	*Number*	*Percent*
Fennoscandia/NW Russia	12799	100.00	6317	49.36	1131	8.84
Estonia	1487	11.62	1159	18.36	225	19.89
Karelia	379	2.96	212	3.36	70	6.19
Khibiny	1374	10.74	1106	17.51	233	20.60
Kiruna	1953	15.26	634	10.04	11	0.97
Kostomuksha	69	0.54	69	1.09	47	4.16
Kovdor	112	0.88	99	1.57	34	3.01
Nikel	620	4.84	181	2.87	104	9.20
Siilinjaervi	134	1.05	119	1.88	18	1.59
Total for 8 mines	6128	47.88	3579	56.66	742	65.61

Table 7.1.1. Distribution of events in mining regions of Fennoscandia and NW Russia. Events with author identificantion "yes/no" and "ESAL/Poor_Loc" in the origin table are not included in the statistics.

Seismic stations

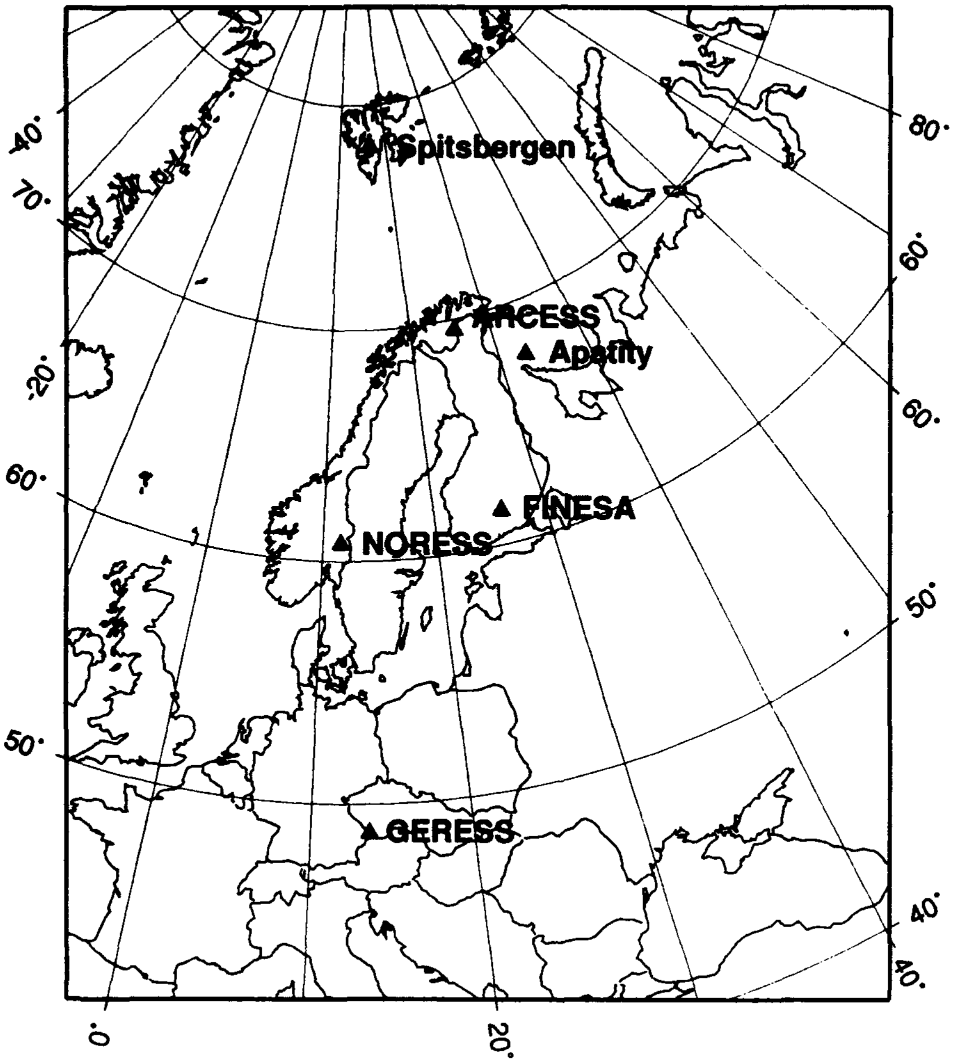

Fig. 7.1.1. Map showing the location of the regional arrays currently used by the Intelligent Monitoring System in operation at the NORSAR processing center.

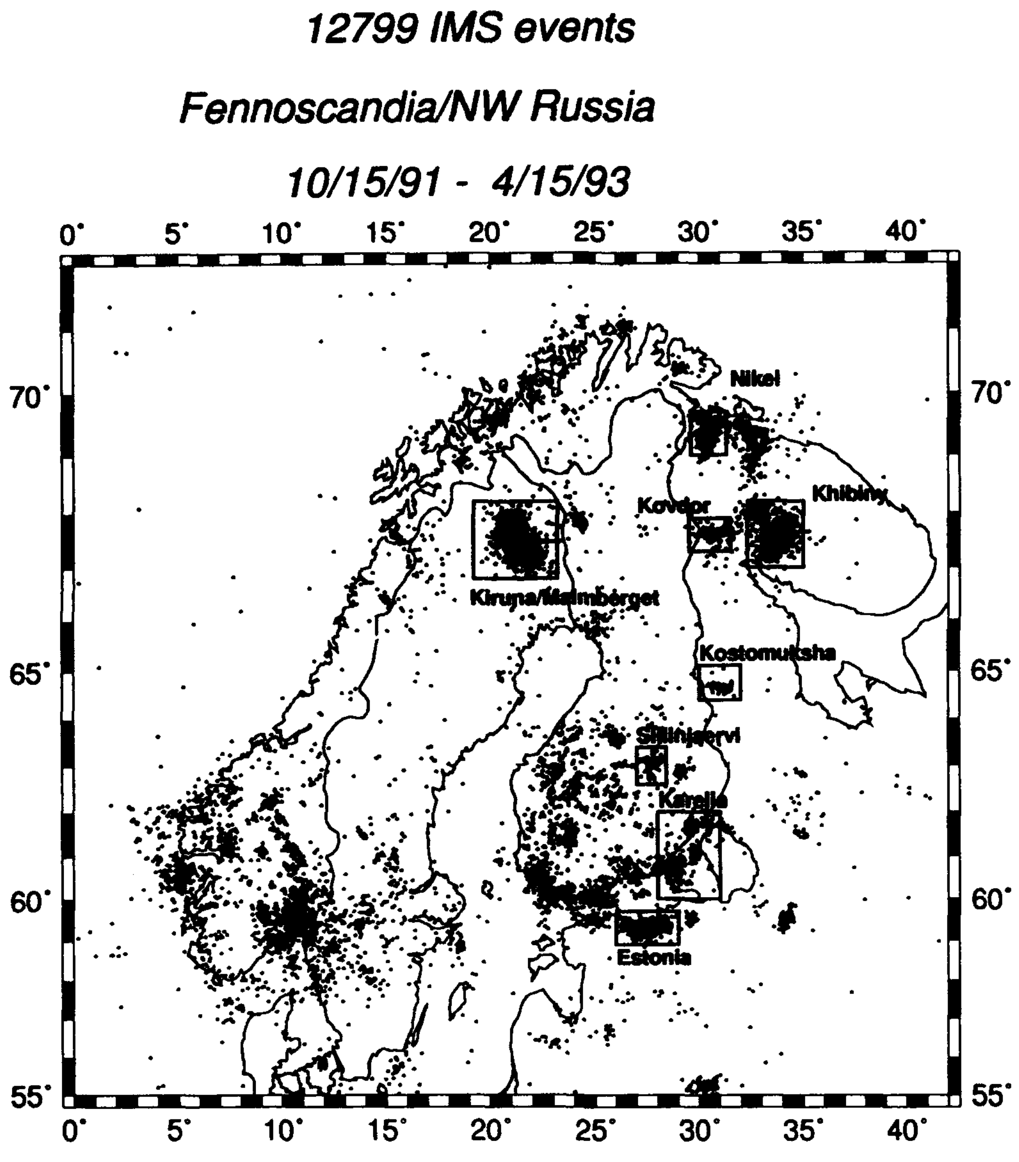

Fig. 7.1.2. Location of 12,799 events (all magnitudes) processed by the IMS for an 18-month period. Only event solutions of satisfactory quality have been included (see text for details). Note the concentration of events in selected mining areas.

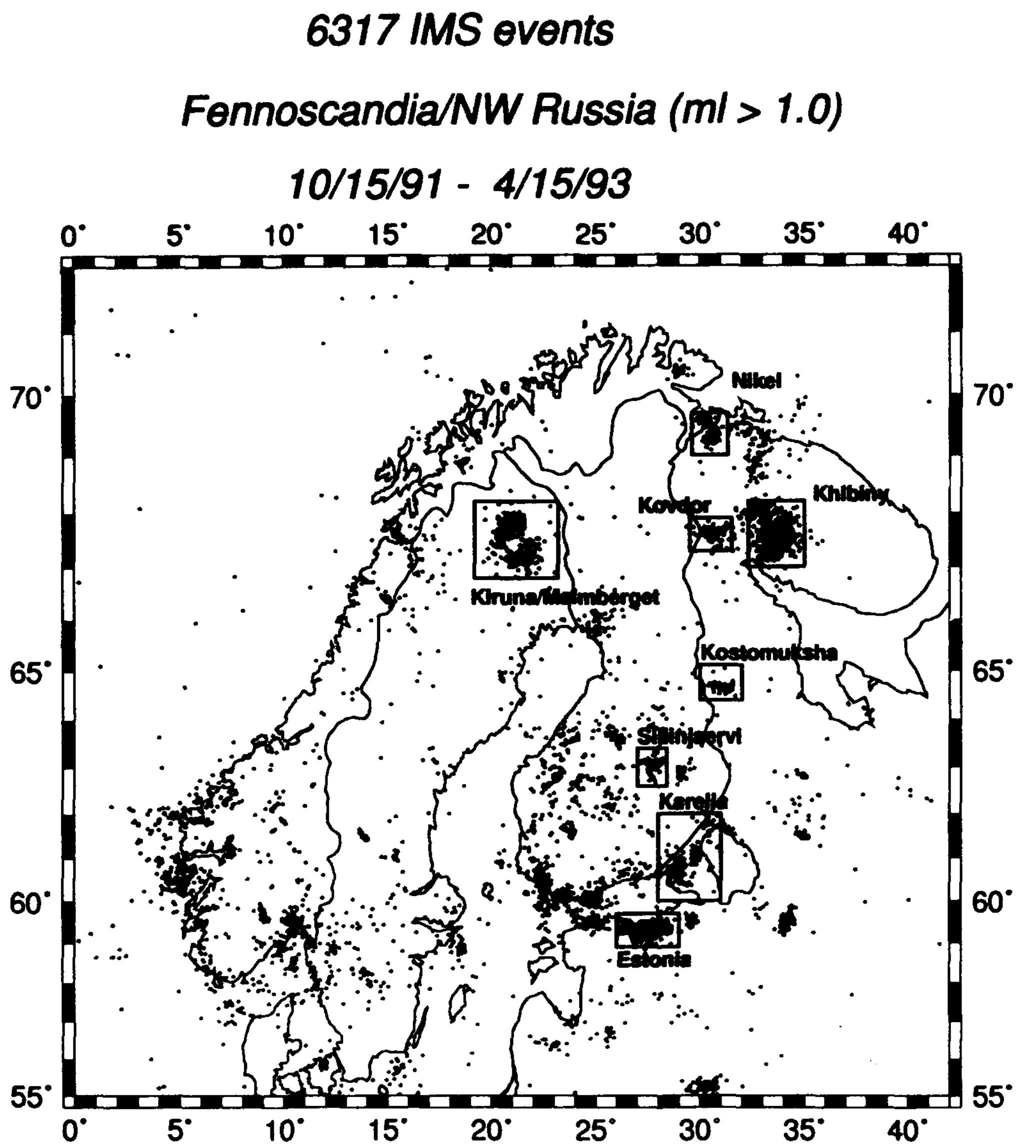

Fig. 7.1.3. Same as Fig. 7.1.2, but showing only events of $M_L > 1.0$. The total number of events is 6317 for the 18-month period.

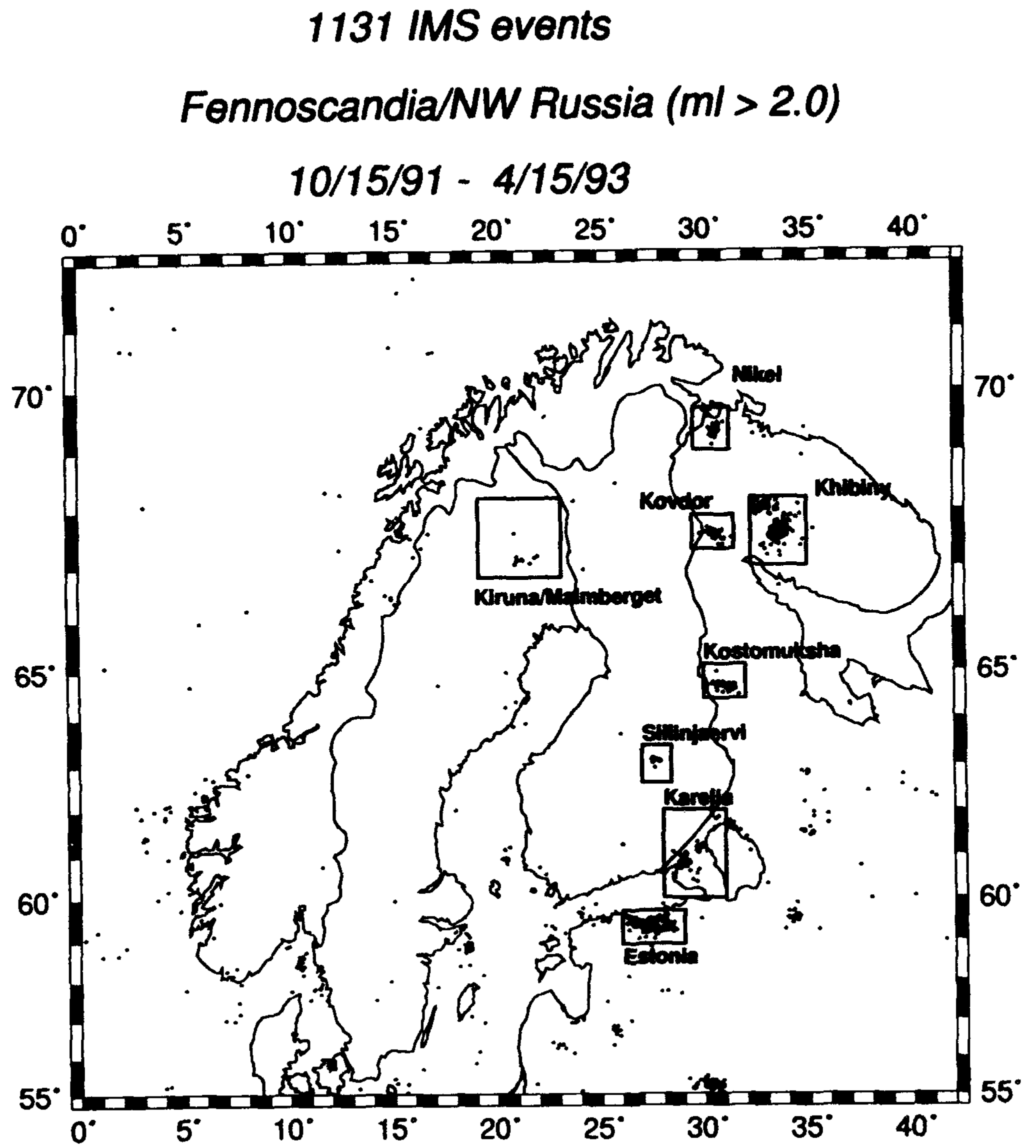

Fig. 7.1.4. Same as Fig. 7.1.2, but showing only events of $M_L > 2.0$. The total number of events is 1131 for the 18-month period.

7.2 Intelligent post-processing of seismic events -- Part 2: Accurate determination of phase arrival times using autoregessive likelihood estimation

Introduction

A precise estimation of the onset time of seismic phases is necessary to obtain an accurate event location. In the context of automatic processing of the regional arrays operated by NORSAR, a two-step procedure has been in use since the first regional array, NORESS, was established in 1985 (Mykkeltveit and Bungum, 1984). This procedure consist of first applying a series of STA/LTA detectors in parallel to a set of filtered beams. When one or more of the STA/LTA detectors exceed a predefined threshold, a phase detection is declared and a detection time is found. Subsequently, a time domain phase timing algorithm is applied to the filtered beam with the highest SNR, using the detection time as the starting value. A detailed description of this algorithm is found in Mykkeltveit and Bungum (1984).

These estimates of the onset times are used by the automatic phase association and event location procedure (ESAL) of the Intelligent Monitoring System (IMS) (Bache et al, 1993), and the fully automatic processing results are finally reviewed and corrected by the analyst using the Analyst Review Station (ARS) of the IMS. Through the analyst review we have experienced that in most cases the phase onsets need to be adjusted. In section 7.6 of this report, comparisons between the automatic and manual onset time estimates of various seismic phases are presented. For P-type phases the standard deviations of automatic - manual onset time generally varies between 0.5 and 0.7 seconds. It should be noticed that these estimates represent averages for all seismic phases for a one-week period, and thus include phases with very different SNR's, frequency characteristics and signatures. For phases with an high SNR and an instantaneous signature, the performance of the phase timing algorithm is significantly better. Nevertheless, one of the conclusions from the study presented in section 7.6 is that in order to improve the precision of the automatic event locations provided by the IMS and in order to reduce the analyst's workload, there is a strong need to improve the precision of the automatic onset time estimates.

In this study we will investigate the potential automatic use of an onset picker based on autoregressive likelihood estimation (Pisarenko et al, 1987, Kushnir et al, 1990). Both a single-component version (ESTON1) and a three-component version (ESTON3) of this method will be tested on data from events located in the Khibiny Massif on the Kola Peninsula of Russia, recorded at the Apatity array, the Apatity three-component station and the ARCESS array, see Fig. 7.2.1.

The Khibiny Massif events

Six apatite mines are located within an area of about 10 km^2 in the Khibiny Massif (see Fig. 7.2.1).A detailed description of these mines and the mining activity is found in Mykkeltveit (1992). The coordinates of the mines are given in Table 7.2.1. Notice that Mine I consists of both an underground mine and an open-pit mine. Although we have no explicit information on the exact sizes of these mines, interpretation of various maps suggest that the typical size is about 1 km^2. The Kola Regional Seismological Centre has since the beginning of 1991 provided NORSAR with information on mining blasts in the six Khibiny mines. The information provided contains an assignment of the relevant mine (I-VI), P (and normally also S) arrival times at the analog APA (Apatity) station (co-located with the three-component station), the amplitude and period of the signal, and the total charge size in tons. Detailed information on the 58 events used in this study is given in Table 7.2.2.

At the Apatity array (APA0) and the Apatity three-component station (APZ9) which are located within a distance range of 18 - 49 km from the different Khibiny mines, the seismograms show clear P (Pg), S (Sg or Lg) and Rg arrivals (see Figs. 7.2.2 and 7.2.3). At ARCESS which is located about 400 km from the mines, a clear Pn and emergent Pg, Sn and Lg phases are observed (see Fig. 7.2.4). Table 7.2.3 gives detailed information on the distances and azimuths from APZ9, APA0 and ARCESS to the six Khibiny mines.

Estimation of P arrival time

We will not go into any detail concerning the theory of the autoregressive likelihood technique for onset time estimation, but refer to Pisarenko et al (1987) and Kushnir et al (1990) for details. We will, however, concentrate on the practical aspects of implementing the method as part of an automatic processing sequence. The onset time procedure requires that we have available an approximate timing of the phase arrival, and the search for the exact onset is limited to an interval around the initial arrival time. The initial arrival time can be obtained in several ways:

- Pisarenko et al (1987) and Kushnir et al (1990) suggest that an optimal event detector based on an Bayesian approach using autoregressive modelling of the data should be used for phase detection and approximate timing.
- Another alternative, which we will use for P-phases at APA0 and ARCESS, is to take the onset time provided by the IMS as the initial estimate. This onset time is calculated using the algorithm described in the *Introduction*.
- A third alternative is to use the predicted phase arrival time, e.g., derived from an initial event location and origin time or from the expected pattern of phase arrivals from events in a given region. This is the approach to be used for both P- and S-phases at APZ9 and for S-phases at APA0.

The autoregressive likelihood estimator is based on regarding the signal onset time as the moment in time when the statistical features of the observed time series (single-component or three-component) are abruptly changed. The single-component method thus takes into account changes in both power and frequency content, and it is therefore important that the broadband signal waveforms are retained (no narrow bandpass filtering). In addition to taking into account changes in power and frequency content, the three-component method is also sensitive to changes in the polarization characteristics of the three-component data. From experimenting with both ESTON1 and ESTON3 we have found that in order to obtain stable estimates, the data should first be lowpass filtered and decimated according to the highest frequencies of the signals. For P-phases from the Khibiny events recorded at the Apatity stations and at ARCESS, signal frequencies up to the Nyquist frequency of 20 Hz are in almost all cases observed. Consequently, no lowpass filtering or decimation is applied to the data. However, a low-order prediction error filter, designed from a 25 second noise sample preceding the P-phase, is applied.

For the arrays APA0 and ARCESS, the slowness and azimuth of the P-phases are computed using broad-band f-k analysis (Kværna and Doornbos, 1986). Kværna and Ringdal (1986) showed that the key to obtain stable slowness and azimuth estimates of phases from a given region is to process the data in a fixed frequency band, using a fixed time window positioning. The time window positioning for the f-k analysis and the fact that the onset time is computed from a steered beam (with steering delays found from f-k analysis) make these two processes to be closely integrated. Through extensive testing we have found that for P-phases from the Khibiny mines recorded at APA0, the most stable slowness and azimuth estimates are obtained if the f-k spectrum is computed in the frequency band 4.0 - 10.0 Hz using the 9 SPZ-component sensors of the array. The time window has a length of 2 seconds and starts 0.3 seconds ahead of the P-arrival. For ARCESS the most stable estimates are obtained if all 25 SPZ-component sensors are processed in the frequency band 3.0 - 6.0 Hz using a 3 second time window starting 0.3 seconds ahead of the P-arrival. Further refinement can be made by including a procedure that checks the SNR in the predefined frequency band, and adjusts the frequency cutoffs in the case of low SNR.

For APA0 and ARCESS, the automatic algorithm used for estimating the P-onsets from events from the Khibiny Massif can be summarized in the following way:

- Use the P onset from the IMS as the initial arrival time estimate.
- Generate a beam with steering delays corresponding to the IMS f-k results and prewhiten the beam with a low order prediction error filter.
- Apply ESTON1 to the prewhitened beam in an interval of ±2 seconds around the initial onset estimate. A sliding window length of 1 second is used by ESTON1, and the autoregressive modelling is of order 3.
- Position the time window according to the onset time from ESTON1 and run the f-k analysis as outlined above.
- Generate a new beam with steering delays corresponding to the new f-k results and prewhiten the beam with a low order prediction error filter.
- Apply ESTON1 to the new prewhitened beam in an interval of ±2 seconds around the previous ESTON1 onset estimate.
- Position the time window according to the last onset time estimate from ESTON1 and run the f-k analysis once more as outlined above.

For the three-component station APZ9 the situation is somewhat different as this station is not part of the automatic IMS processing. APZ9 is, however, located only 18 km from APA0, and we therefore choose to use the onset time at APA0 as the initial arrival time estimate. The processing can be summarized as follows:

- Use the P onset at APA0 as the initial arrival time estimate.

- Prewhiten the Z-component APZ9 with a low order prediction error filter.
- Apply ESTON1 to the prewhitened Z-component APZ9 in an interval of ±5 seconds around the initial onset estimate from APA0. The sliding window length used by ESTON1 is 1 second and the autoregressive modelling is of order 3.
- Reestimate the onset time applying ESTON1 to the prewhitened z-component APZ9 in an interval of ±2seconds around the previous ESTON1 onset estimate.

Precision of automatic P-onsets using the single-component estimator (ESTON1)

The precision of the automatic P-onsets using ESTON1 has been assessed by two different methods. The first method is to compare the ESTON1 estimates to the best manual pick. The purpose of this approach is to obtain information on any bias in ESTON1 estimates, and also to check the consistency between the automatic and manual onset estimates. In the second method we estimate the standard deviation of the phase picks by looking at the consistency of the arrival time differences between phases from events located in the same mine, see Sereno (1990). In this way, an unbiased estimate of the standard deviation is found for both the automatic and manual picks.

In Fig. 7.2.5.a the time differences between the automatic onsets from IMS and the manual pick at APA0 are presented as a function of signal-to-noise ratio (SNR) on the prewhitened beam. The standard deviation of these differences is as high as 0.43 seconds. In comparison, the time difference between the automatic ESTON1 onsets and the manually picked onsets, given in Fig. 7.2.5.b has a standard deviation as low as 0.02 seconds, and has a systematic positive bias of 0.05 seconds, i.e. the ESTON1 onsets are consistently picked a bit late.

In Fig. 7.2.6 similar plots are presented for Pn phases recorded at ARCESS. The automatic onsets from IMS shows significantly less scatter ($\sigma = 0.13$ s) than for APA0. On the other hand, the automatic ESTON1 onsets has a somewhat larger scatter ($\sigma = 0.03$ s) and a somewhat larger positive bias (0.08 s) than at APA0. Nevertheless, the accuracy of the ESTON1 time picks appears to be significantly better than those of the current processing system.

To address possible dependency of ESTON1 on the signal-to-noise ratio, we have in Fig. 7.2.7 plotted the time difference between the automatic ESTON1 onsets and the manually picked onsets for both APA0 and APZ9. In this way, we get an overview of the scatter for SNR's ranging from about 3 to about 500. We find from this figure that the time differences seem to be almost independent of SNR, which again indicate that the ESTON1 onset estimator works well for quite low signal-to-noise ratios. For direct comparison, we have in Fig. 7.2.8 plotted the ARCESS data on the same scale, but for ARCESS no low SNR phases are observed, as all SNR's exceed 6. By SNR, we mean the maximum of the linear ratio STA/LTA (i.e., short term average divided by long term average.)

The results presented above show that an automatic onset time procedure for P-phases using ESTON1 can give a remarkable improvement in precision compared to the current algorithm used in the IMS. The ESTON1 onset estimator has a bias that is dependent on the dominant frequency of the signal. At the Apatity stations the average dominant P frequency is 13 Hz and the average bias is 0.05 s, whereas at ARCESS the average dominant P frequency is 6 Hz and the average bias is 0.08 s. The difference in bias can not be due to differences in sampling rate, since both APA0, APZ9 and ARCESS have a sampling frequency of 40 Hz. For the high frequency signals at the Apatity stations, the bias shows no clear dependency on SNR, at least not for SNR above 3. As expected, the results also suggest that the precision of ESTON1 increases with increasing signal frequencies. This can be inferred from the fact that the automatic P-onset estimates of the high-frequency signals at the Apatity stations are more consistent with the manual picks than the P-onsets at ARCESS, which generally have a lower dominant frequency. According to Pisarenko et al (1987) there are no analytical expressions for the theoretical biases and variances of ESTON1 and ESTON3, and it is therefore necessary to obtain empirical values. In any case, the biases and variances are less than 0.1 s for the P-phases considered in this study.

An unbiased estimate of the measurement variance is determined from the arrival time difference between two phase observations for repeated events in the same mine. Specifically:

$$\sigma^2_{1,pick} + \sigma^2_{2,pick} = \frac{\sum_{k=1}^{N_{mines}} \sum_{i=1}^{N_{obs}} [\Delta T_{obs_{ik}} - \langle \Delta T_{obs} \rangle_k]^2}{(N_{obs} - N_{mines})}$$

where σ_1^2 and σ_2^2 are the picking variances of each phase, $\Delta T_{obs_{ik}}$ is the *ith* observation of the arrival-time difference for the *kth* mine. $\langle \Delta T_{obs} \rangle_k$ is the mean arrival time difference for the *kth* mine. N_{obs} is the total number of observations (at all mines), and N_{mines} is the number of mines.

By computing the arrival-time differences between the P observations at the three stations APA0(1), APZ9(2) and ARCESS(3), we get three equations of the type above, with altogether three unknowns. These equations can easily be solved to obtain estimates of each individual variance value. For example, for the automatic picks we obtain:

$$\sigma_1^2 + \sigma_2^2 = (0.065)^2$$

$$\sigma_1^2 + \sigma_3^2 = (0.065)^2$$

$$\sigma_2^2 + \sigma_3^2 = (0.074)^2$$

which gives $\sigma_1 = 0.04$, $\sigma_2 = 0.05$ and $\sigma_3 = 0.05$ (see Table 7.2.4).

The standard deviations of both the manual picks and the automatic picks from ESTON1 are given in Table 7.2.4. All standard deviations are less than or equal to 0.06 s, and a part of this variability is likely due to the fact that the events of each mine are not located at the same spot, but are distributed within the mine. Under the assumption that each mine has an extent of 1 x 1 km (which is reasonable from interpretation from various maps), we have computed the maximum theoretical P travel-time difference between APA0 and APZ9 for the six Khibiny mines. The largest value is obtained for Mine I, where a 0.09 s travel-time difference is possible. The smallest values are found for Mine V and Mine VI, where a 0.04 s travel-time difference is possible. This clearly suggest that location variability within each mine can have a significant impact on the estimates of the picking precision. If we, however, assume that the distribution of the events within each mine increases all picking error estimates with a similar amount, a likely interpretation of the differences in picking precision between the three stations is as follows:

- The P picks at APZ9 are less precise than at APA0 due to generally lower SNR.
- The P picks at ARCESS are less precise than at APA0 due to generally lower dominant frequency of the signals.

The results of Table 7.2.4 show that the automatic ESTON1 method matches the human precision, and that for the relatively high SNR P arrivals analyzed in this study, the standard deviation of the automatic picks is well below 0.1 s.

Estimation of S arrival time at the Apatity stations

As seen from Fig. 7.2.2 and 7.2.3, the seismograms of the Khibiny events show clear P, S and Rg arrivals at the Apatity stations APA0 and APZ9. The S-onsets do, however, become more emergent with increasing source-receiver distance. The S-phases typically have the largest SNR on the transverse component, but they are also clearly observed on the radial and vertical components. For automatic estimation of S-onsets, we have experimented with both the single-component ESTON1 onset estimator applied to the transverse component, and the three-component ESTON3 onset estimator applied to the three-component data, and found that the ESTON3 method gave the best results. The most stable results were obtained if the data were first filtered in a relatively wide band between 2.0 and 8.0 Hz and then decimated to a sampling rate of 20 Hz.

The Rg arrivals occur very close in time to the S-onset. Moreover, the Rg phase is dispersive. We therefore did not succeed in estimating the Rg-onset in a reliable way with the autoregressive likelihood estimation technique. In order to design an automatic processing sequence for the Khibiny events at the Apatity stations APA0 and APZ9, we have utilized the expected pattern of phase observations from events in this region, and the procedure is as follows:

- Estimate P-onset as previously outlined
- Identify the peak of the Rg-phase from an STA envelope created from the filtered z-component (0.8 - 2.0 Hz). The search interval for the Rg maximum is currently limited to 20 seconds after the P-onset.

- For the APA0 array, the slowness and azimuth of the Rg phase is estimated using data in a 5 s window starting 3 s ahead of the Rg peak. A frequency band of 0.8 - 2.0 Hz is used in the f-k analysis.
- For estimation of S-onsets, the three-component data are first filtered and decimated as outlined above, and the ESTON3 estimator is then applied within a time interval that starts 2 s after the P-onset and stops at the time of the Rg peak. The sliding window length used by ESTON3 is 2 seconds and the autoregressive modelling is of order 3.
- For the APA0 array, the slowness and azimuth of the S phase is estimated using data in a 2 s window starting 0.3 s ahead of the S-onset. A frequency band of 2- 5 Hz is used in the f-k analysis.

Illustrations of the automatic processing sequence are shown if Figs. 7.2.9 and 7.2.10. Notice the clear peak of the ESTON3 likelihood function at the S-onset for both events.

Precision of automatic S-onsets using the three-component estimator (ESTON3)

When comparing the automatic ESTON3 onsets to the manually picked S-onsets at APA0, we find that the standard deviation of the time differences is 0.18 s and that the bias is 0.01 s. For APZ9 the standard deviation is 0.12 s and the bias is 0.04 s. Due to the relatively large scatter in the observations, this bias of 0.04 is not significantly different from 0.

To compute the measurement variance of the S-onset estimates, we have again investigated the consistency of the arrival time difference between two phase observations for repeated events in the same mine, according to equation 7.2.1. By using the P-onsets at both APA0, APZ9 and ARCESS as references, for which the measurement variances are known (see. Table 7.2.4), we can reliably estimate both the manual and the automatic S-onset variances at both APA0 and APZ9. The results are summarized in Table 7.4.5

We see from Table 7.4.5 that the picking uncertainty estimates based on all three reference P-phases are very consistent, indicating that the method for estimating uncertainty works well. The fact that the precision of the manual and automatic picks are about equal, indicates that the automatic S-onset algorithm using ESTON3 matches the human precision. Table 7.4.5 also show that the S-onsets at APZ9 ($\sigma = 0.13$ s) are generally more precise than at APA0 ($\sigma = 0.19$ s). We believe that this is due to the fact that the S-phases become more emergent with increasing source-receiver distance, as illustrated in Figs. 7.2.2 and 7.2.3. The six Khibiny mines are located within a distance range of 18 - 33 km from APZ9, and within a distance range of 32 - 49 km from APA0, see Table 7.2.3.

It would have been interesting to compare the precision of the automatic S-onsets from ESTON3 to the precision of the automatic S-onsets used by the IMS. We have, however, experienced that the continuous processing of the Apatity array data (APA0) has problems in detecting and estimating the onsets, slowness and azimuths of secondary phases that have little time separation and large differences in frequency content. The first S-detection of the Khibiny events recorded at APA0 is in almost all cases declared in a low frequency band, which is typical for detection of Rg. Consequently the onset routine prefilters the data in a low passband, e.g. 1 - 2 Hz, where S has a low SNR, and the first S-onset is in many cases missed. With this problem in mind we have found it difficult to justify a comparison between the automatic S-onsets from ESTON3 and the automatic S-onsets from the procedure providing data to the IMS.

Precision of azimuth estimates from broad-band f-k analysis

As described above, the estimation of onset time and the estimation of slowness and azimuth by f-k analysis are closely integrated processes. In one-array location of seismic events, the azimuth estimates are necessary to be able to compute an event location, and in the event location procedure of the IMS (Bratt and Bache, 1988) the phase azimuth estimates are required to be accompanied with an uncertainty estimate.

In Table 7.5.6, the mean and the standard deviation of the azimuth residuals relative to the Khibiny mine locations of the phases recorded at the arrays APA0 and ARCESS are presented. We see from the table that the P and Rg azimuths at APA0 have about the same standard deviation (3.9 and 3.4 degrees, respectively), but that the P azimuths have a systematic bias of 8.2 degrees. The Rg azimuth bias is as low as -1.8 degrees. The ARCESS P azimuths have a very low standard deviation (0.9 degrees), but a systematic bias of 4.6 is consistently observed. The S-azimuths at APA0 show a very large scatter. This show that if the Khibiny events are located without introducing corrections for the azimuth biases, the Rg azimuths should be given the smallest a priori uncertainty. If the systematic biases are removed, the a priori uncertainty of P and Rg at APA0 become comparable. With the systematic bias removed, the a priori uncertainty of ARCESS P is very small, but it should be noticed that in the event location procedure (Bratt and Bache, 1988) the a priori azimuth uncertainty is scaled by the source-receiver distance, such that an azimuth observation at 400 km distance with an uncertainty of 0.9 degrees (ARCESS P) is given less weight than an azimuth observation at 40 km distance with an uncertainty of 3.9 degrees (APA0 P).

Conclusions

The results presented in this study show that very precise automatic estimates of phase onsets from events in the Khibiny Massif can be obtained with the autoregressive likelihood estimation method. Implementation of the method requires that we have available approximate estimates of the phase arrival, and we have shown that such approximate estimates can be obtained from the IMS event definitions (phase association and event location) or from analysis of previous events in the region. In this way, the autoregressive likelihood estimation method can provide phase onsets that match the human precision. The uncertainties and biases of the automatic onset estimates of various phases at the Apatity stations and at ARCESS have been quantified, and the precision of the automatic phase picks shows very large improvement in comparison to the automatic phase onsets from the continuous processing providing input to the IMS.

In addition to the automatic onset estimation, we have estimated the phase azimuths and slowness using broad-band f-k analysis. This has been done using data in a fixed frequency band, using a fixed window positioning, as suggested by Kværna and Ringdal

(1986) for the purpose of obtaining increased stability. For P-phases recorded at ARCESS, the results are in accordance with those of Kværna and Ringdal (1986), where a scatter of only ±1 degree were observed at NORESS for Pn phases from repeated events at a distance of 300 km. Comparing to the overall azimuth uncertainty of phases recorded at ARCESS and NORESS (Sereno, 1990), we find that if the systematic biases are removed from our azimuth estimates, the event location precision can be significantly improved. Without introducing azimuth corrections, the Rg azimuths at APA0 show to be quite reliable.

We realize that in order to obtain accurate event locations, precise onset time and azimuth estimates are necessary, but not sufficient. If the theoretical travel-time model used in the event location deviates from the true travel-times, the precision of the event locations will be reduced. To overcome this, we will in Section 7.3 of this report discuss the introduction of travel-time corrections.

A natural extension to this study will be to investigate the performance of ESTON1 and ESTON3 applied to phases at the other stations of the network recording the Khibiny events. At NORESS and FINESA the detected Pn phases have quite low SNR, and it would be interesting to quantify the precision of the automatic onset estimates of these phases. It also remains to test and implement the automatic picking of Sn and Lg phases at ARCESS, NORESS and FINESA.

During the work with the autoregressive likelihood estimation method, we have experienced that the display of the likelihood functions, as illustrated in Figs. 7.2.9 and 7.2.10 can assist the analyst in picking correct phase onsets. In the context of interactive analysis of seismic data, we believe that the idea of making such likelihood functions available to the analyst should be pursued.

T. Kværna

References

Bache, T.C., S.R. Bratt, H.J. Swanger, G.W. Beall and F.K. Dashiell (1993): Knowledge-based interpretation of seismic data in the Intelligent Monitoring System, *Bull. Seism. Soc. Am.*, in press.

Bratt, S.R. and T.C. Bache (1988): Locating events with a sparse network of regional arrays, *Bull. Seism. Soc. Am.*, 78, 780-798.

Kushnir, A.F., V.M. Lapshin, V.I. Pinsky and J. Fyen (1990): Statistically optimal event detection using small array data, *Bull. Seism. Soc. Am.*, 80 Part B, 1934-1950

Kværna, T. and F. Ringdal (1986): Stability of various F-k estimation techniques, in *NORSAR Semiannual Tech. Summ., 1-86/87*, Kjeller, Norway, 29-40.

Kværna, T. and D.J. Doornbos (1986): An integrated approach to slowness analysis with arrays and three-component stations, in *NORSAR Semiannual Tech. Summ., 1-86/87*, NORSAR, Kjeller, 41-50.

Mykkeltveit, S. and H. Bungum (1984): Processing of regional seismic events using data from small-aperture seismic arrays, *Bull. Seism. Soc. Am.*, 74, 2313-2333.

Mykkeltveit, S. (1992): Mining explosions in the Khibiny Massif (Kola Peninsula of Russia) recorded at the Apatity three-component station, Report PL-TR-92-2253, Phillips Laboratory, Hanscom Air Force Base, MA, USA.

Pisarenko, V.F., A.F. Kushnir and I.V.Savin (1987): Statistical adaptive algorithms for estimation of onset moments of seismic phases: *Phys. Earth Planet. Int.*, 47, 4-10.

Sereno, T.J. (1990): Attenuation of regional phases in Fennoscandia and estimates of arrival time and azimuth uncertainty using data recorded by regional arrays, *Semiann. Tech. Rep. No. 3, 1 Jan 89 - 30 Jun 90*, Science Applications International Corp., San Diego, CA, USA.

Mine	Location	
I, Underground	67.6702°N	33.7285°E
I, Open-pit	67.665°N	33.744°E
II	67.647°N	33.761°E
III	67.631°N	33.835°E
IV	67.624°N	33.896°E
V	67.632°N	34.011°E
VI	67.665°N	34.146°E

Table 7.2.1. The table gives the location of the six mines in the Khibiny Massif shown in Fig. 7.2.1.

Event	Mine	ESTON1 P-arrival (APA0)	Size
1	I (U)	1992-312:06.31.49.425	185 tons
2	I (U)	1992-355:07.10.51.931	190 tons
3	I (O)	1992-366:04.35.22.825	14 tons
4	I (O)	1993-017:06.51.15.831	4 tons
5	I (U)	1993-031:04.14.11.263	140 tons
6	I (O)	1993-038:07.13.16.881	7 tons
7	I (U)	1993-045:07.39.45.200	185 tons, double
8	I (O)	1993-052:07.24.49.706	14 tons, double
9	I (O)	1993-059:04.24.01.850	30 tons
10	I (O)	1993-066:06.58.54.356	12 tons
11	I (O)	1993-073:11.28.09.731	10 tons
12	I (O)	1993-080:11.26.36.106	10 tons
13	II	1992-334:04.08.51.725	130 tons
14	II	1992-366:09.41.50.156	100 tons
15	II	1993-024:08.04.48.656	24 tons
16	II	1993-066:04.14.37.475	60 tons
17	III	1992-354:08.38.32.806	15 tons
18	III	1992-361:09.53.07.550	320 tons
19	III	1993-016:09.20.47.756	20 tons
20	III	1993-030:10.16.00.581	20 tons
21	III	1993-030:13.07.15.650	265 tons
22	III	1993-044:12.05.41.725	300 tons
23	III	1993-051:07.28.29.931	16 tons
24	III	1993-058:12.01.17.356	17 tons
25	III	1993-065:08.51.42.356	18 tons
26	III	1993-065:11.00.36.931	130 tons

Event	Mine	ESTON1 P-arrival (APA0)	Size
27	II	1993-065:11.29.46.150	Induced earth-quake, M_L 2.3
28	III	1993-086:10.35.05.925	14 tons
29	IV	1992-353:12.29.32.681	340 tons
30	IV	1992-360:12.37.40.556	380 tons
31	IV	1992-365:11.39.53.300	214 tons
32	IV	1993-006:11.01.24.331	310 tons
33	IV	1993-012:12.04.00.406	130 tons
34	IV	1993-022:12.50.56.806	310 tons
35	IV	1993-036:12.35.08.831	230 tons
36	IV	1993-043:13.37.27.181	350 tons
37	IV	1993-057:12.31.59.475	380 tons
38	IV	1993-064:12.32.40.931	300 tons, double
39	IV	1993-075:12.29.49.650	70 tons
40	IV	1993-082:15.08.34.250	95 tons
41	IV	1993-089:14.44.12.256	100 tons
42	V	1992-346:08.56.58.906	183 tons
43	V	1992-360:08.03.37.581	138 tons
44	V	1993-006:08.18.41.606	101 tons
45	V	1993-015:14.08.51.075	188 tons
46	V	1993-029:10.07.17.831	195 tons
47	V	1993-036:08.05.42.006	unknown size
48	V	1993-050:12.34.53.506	203 tons
49	V	1993-057:10.33.31.006	149 tons
50	V	1993-078:09.45.13.906	260 tons, general
51	V	1993-085:08.59.22.900	146 tons
52	VI	1992-318:06.41.16.250	60 tons
53	VI	1992-332:07.05.26.950	unknown size

Event	Mine	ESTON1 P-arrival (APA0)	Size
54	VI	1992-353:07.35.26.956	73 tons
55	VI	1992-365:07.23.22.631	80 tons
56	VI	1993-022:08.20.09.231	285 tons
57	VI	1993-043:08.13.29.381	140 tons
58	VI	1993-071:07.33.22.906	140 tons, general

Table 7.2.2. This table contains information on the 58 Khibiny Massif events analyzed in this study. For each event, the assigned mine, the automatic P-onset at the Apatity array and the event size are given. I(U) means the underground Mine I, whereas I(O) means the open-pit mine. When the event size is given as "double", the reported charge is distributed between two explosions that are closely separated in time. If the term "general" is used, the reported charge is distributed among several explosions that are closely separated in time.

Mine	APA0		APZ9		ARCESS	
	Delta (km)	Az (deg)	Delta (km)	Az (deg)	Delta (km)	Az (deg)
I(U)	32.0	76.8	17.8	50.4	393.8	118.0
I (O)	32.6	78.0	18.0	53.1	394.7	118.0
II	33.0	81.7	17.5	59.8	396.4	118.2
III	35.9	85.2	19.6	69.0	400.0	118.1
IV	38.4	86.6	21.8	73.3	402.6	118.0
V	43.4	85.7	26.7	74.4	406.0	117.5
VI	49.4	81.8	33.3	70.8	408.6	116.6

Table 7.2.3. Distance and azimuths from the three stations APA0, APZ9 and ARCESS to the mines considered in this study.

	σ_{manual}	$\sigma_{automatic}$
P, Apatity array	0.04 s	0.04 s
P, Apatity 3-comp.	0.06 s	0.05 s
Pn, ARCESS	0.06 s	0.05 s

Table 7.2.4. Estimated standard deviations of manual and automatic (ESTON1) P-onsets at the Apatity array, the Apatity three-component station and at ARCESS.

S-phase	Reference phase	σ_{manual}	$\sigma_{automatic}$
APA0	P at APA0	0.20	0.19
	P at APZ9	0.20	0.19
	Pn at ARCESS	0.18	0.20
APA0	Average	0.19	0.19
APZ9	P at APA0	0.13	0.15
	P at APZ9	0.12	0.14
	Pn at ARCESS	0.13	0.16
APZ9	Average	0.13	0.15

Table 7.2.5. Estimated standard deviations of manual and automatic (ESTON3) S-onsets at APA0 and APZ9. In addition to the average uncertainty, we give for each phase the uncertainty estimates computed using the three different reference phases.

	Mean (°)	σ (°)
P, Apatity array	8.2	3.9
Pn, ARCESS	4.6	0.9
S, Apatity array	-1.0	19.8
Rg, Apatity array	-1.8	3.4

Table 7.2.6. Mean and standard deviation of azimuth residuals relative to Khibiny mine locations.

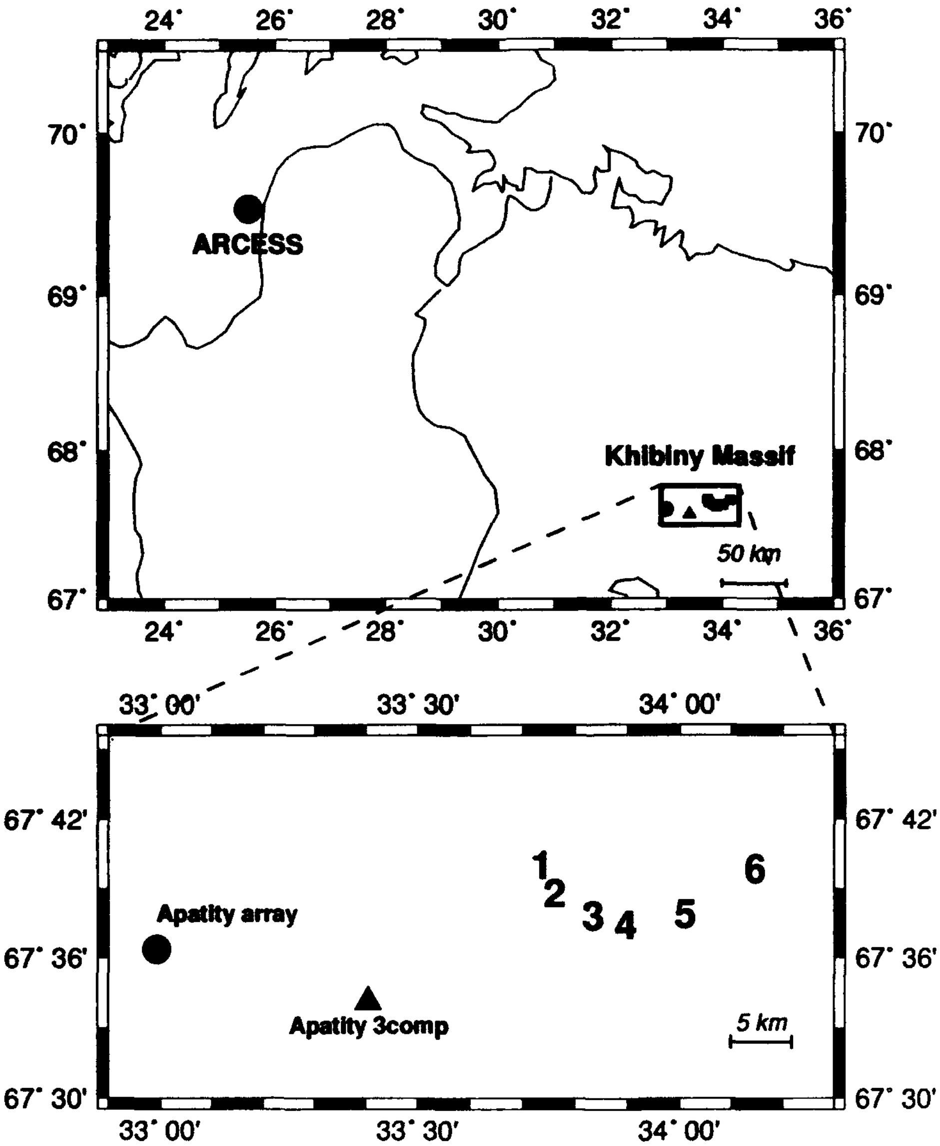

Fig. 7.2.1. In the **upper part**, a large reference area is shown. The location of the ARCESS array is given by a filled circle, and the location of the Khibiny Massif region is shown. The **lower part** shows a detailed picture of the Khibiny Massif region. The locations of the six mining sites are given by large numbers 1-6. The Apatity array is shown as a filled circle and the three-component station in the town of Apatity is shown as a large triangle.

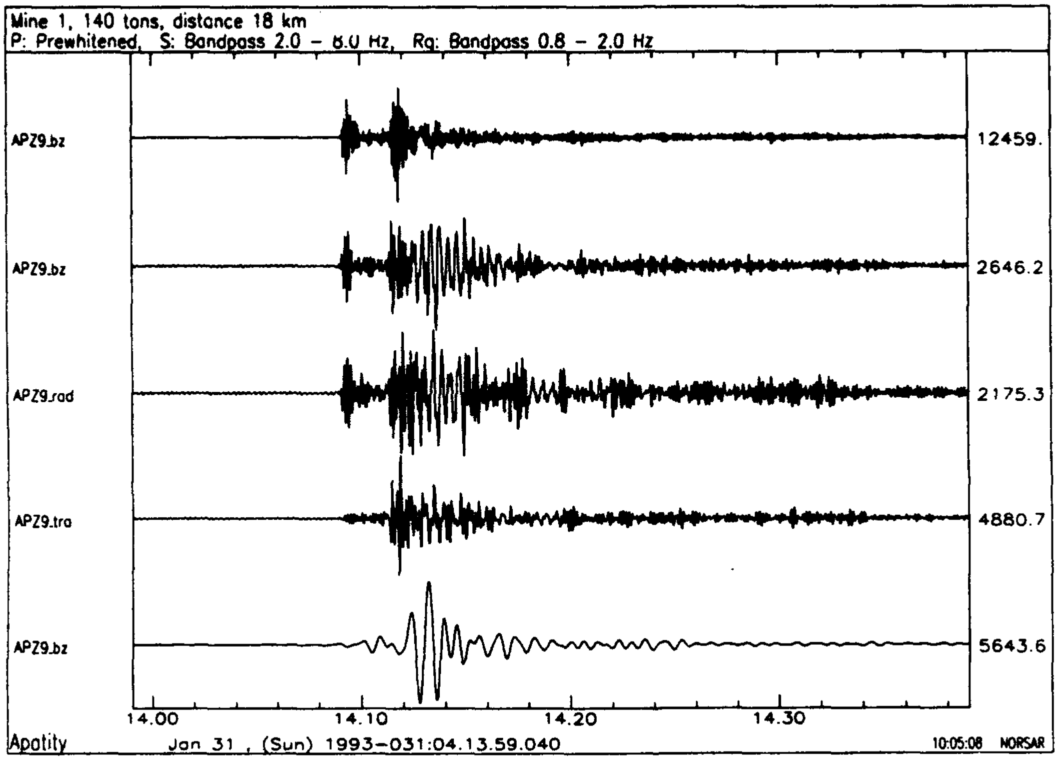

Fig. 7.2.2. Seismograms from an event at the underground Mine I recorded at the Apatity three-component station. The source-receiver distance is 18 km. The upper trace, emphasizing the P-phase, is the z-component prewhitened with a low-order prediction error filter designed from a 25 s noise sample preceding the P-phase. The three-component data rotated with the azimuth to the mine can be seen at traces 2-4. The data are filtered in a relatively wide passband of 2 - 8 Hz, and these three traces clearly show an instantaneous S-phase. The lower trace is bandpass filtered between 0.8 and 2.0 Hz, and clearly illustrate the low-frequency Rg phase.

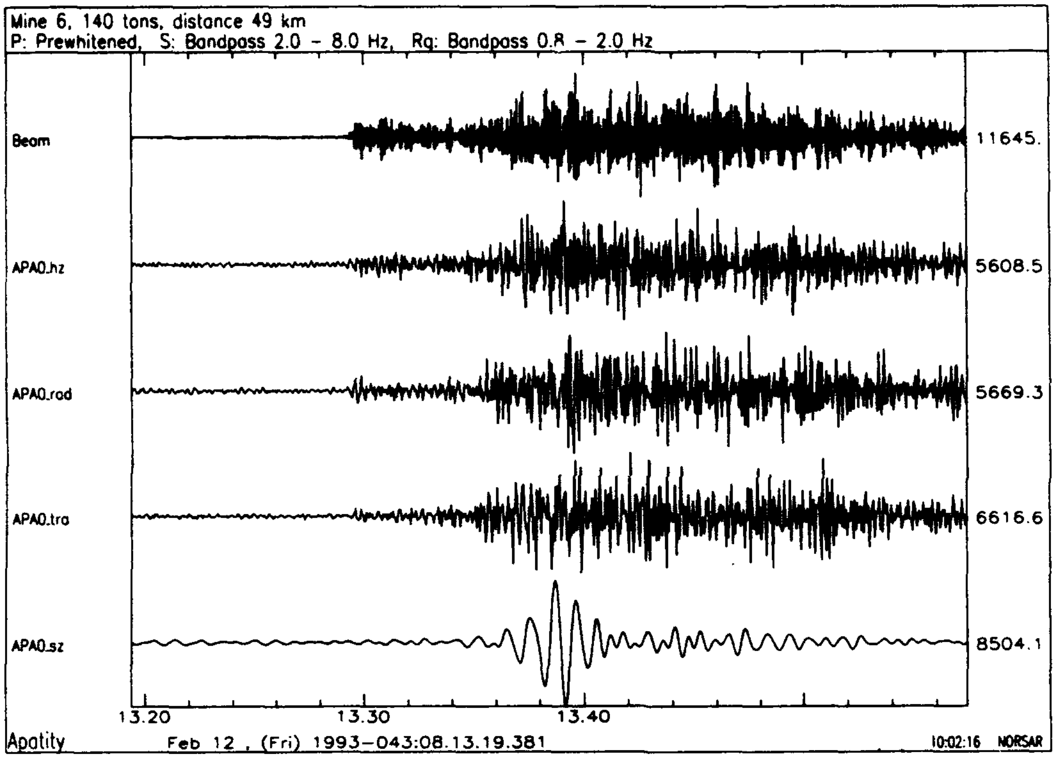

Fig. 7.2.3. Seismograms from an event at mine VI recorded at the Apatity array. The source-receiver distance is 49 km. The only difference from the traces of Fig. 7.2.2 is that the upper trace is the array beam steered with steering delays corresponding to the slowness and azimuth of the P-arrival. Notice that in this case the S-phase is much more emergent than the S-phase of Fig. 7.2.2.

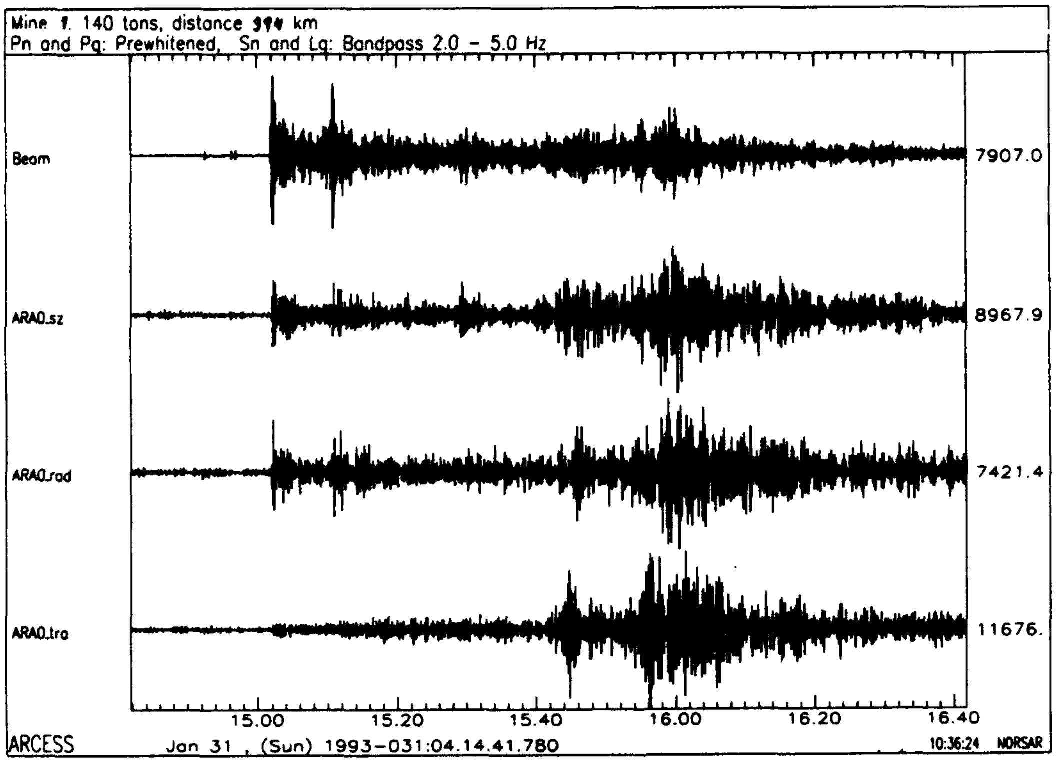

Fig. 7.2.4. ARCESS recording of the event also shown in Fig. 7.2.2. The source-receiver distance is 394 km. The upper trace is the array beam steered with the slowness and azimuth of the P-phase. The beam is prewhitened with a low-order prediction error filter. The lower three traces are the rotated three-component data at the central element (ARA0) of the ARCESS array. The data are bandpass filtered between 2 and 5 Hz. Notice that both Pn, Pg, Sn and Lg are clearly seen, and that Sn and Lg are most prominent on the transverse component.

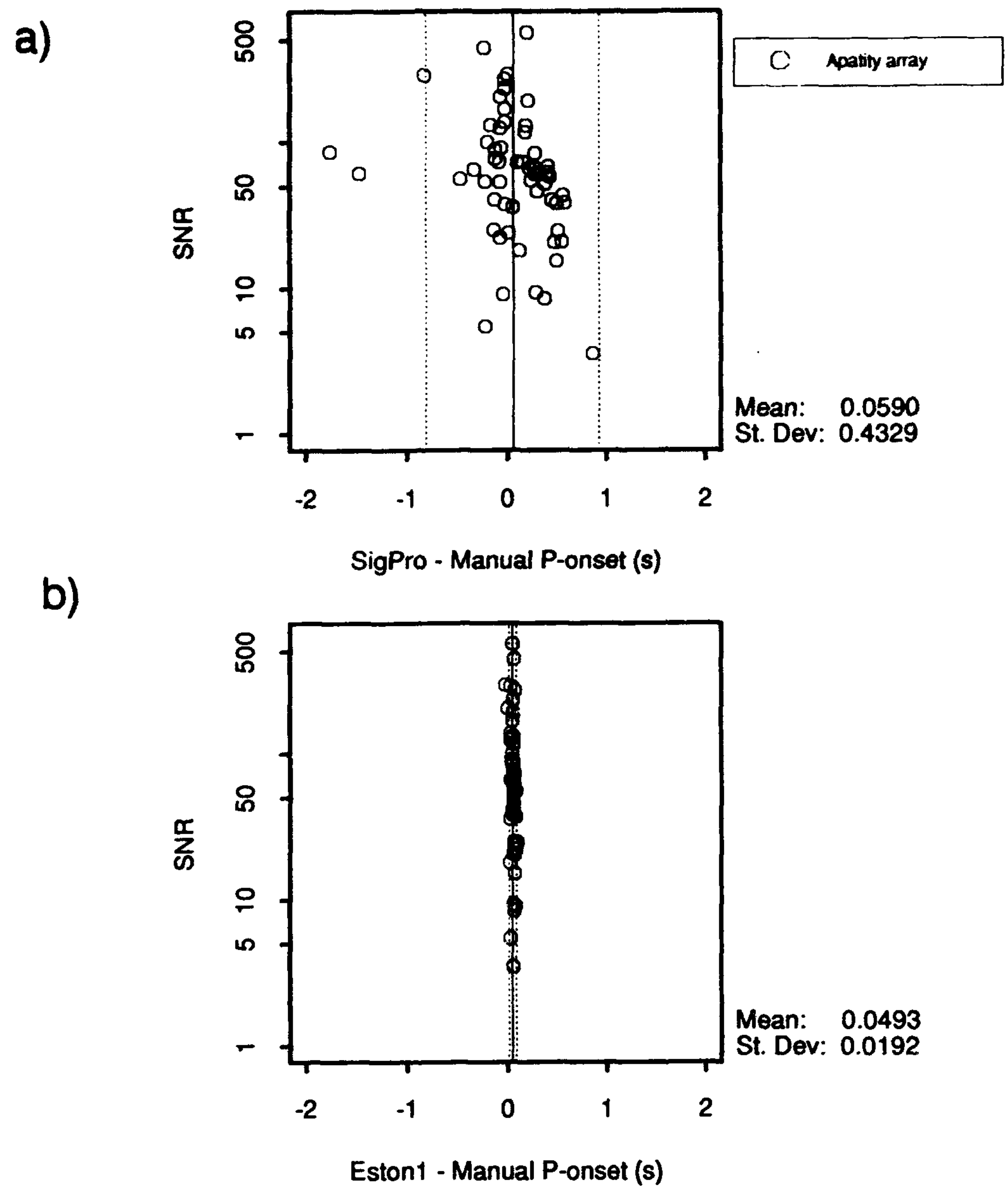

Fig. 7.2.5. These two plots show the time differences between the automatic P-onsets and the manual pick at APA0 as a function of signal-to-noise ratio (SNR) on the prewhitened beam. All 58 P-observations are included. Figure **a)** shows the time differences between the automatic P-onsets from the IMS and the manual picks, whereas figure **b)** shows the time differences between the automatic P-onsets from ESTON1 and the manual picks. The two vertical dotted lines represent $\pm\sigma 2$.

a)

b)

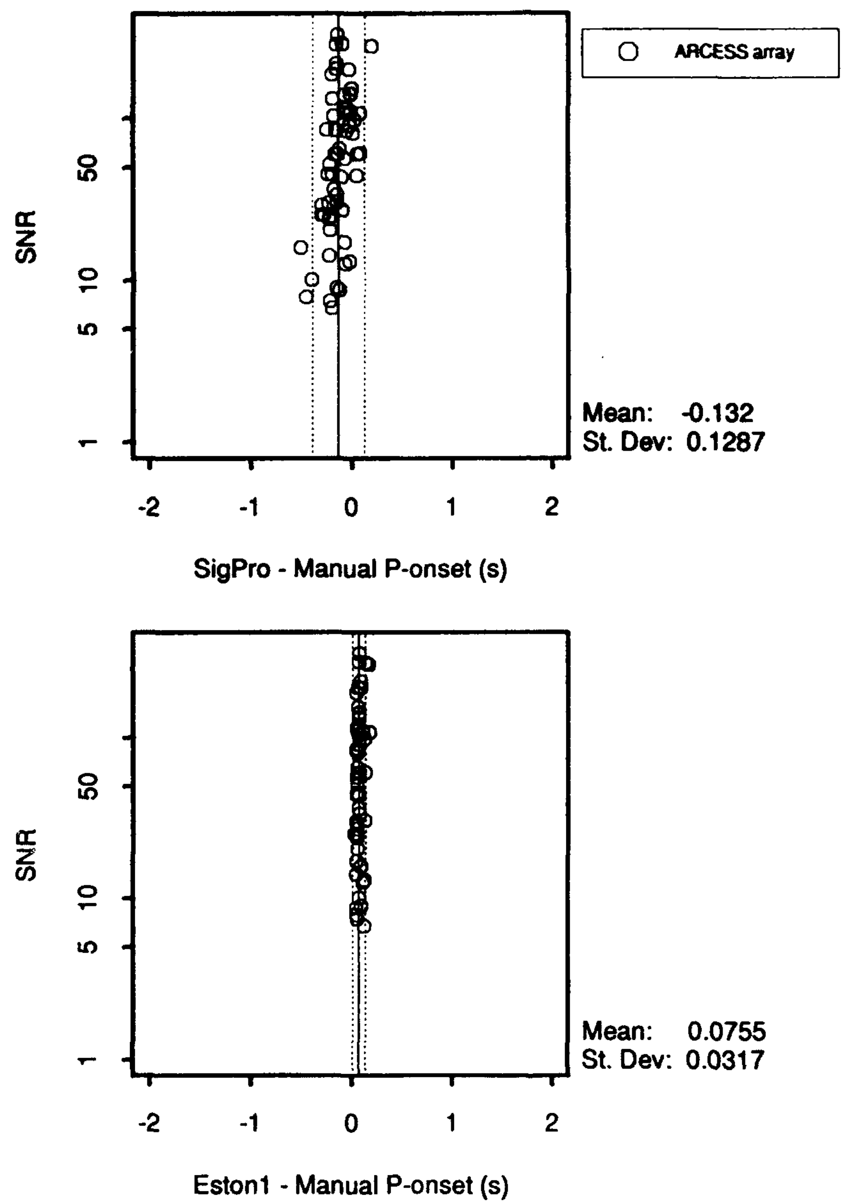

Fig. 7.2.6. Plots similar to those of Fig. 7.2.5, but in this case for Pn-onsets at ARCESS. For one of the Khibiny Massif events, the ARCESS array was not operational, and consequently only 57 P-phases were analyzed.

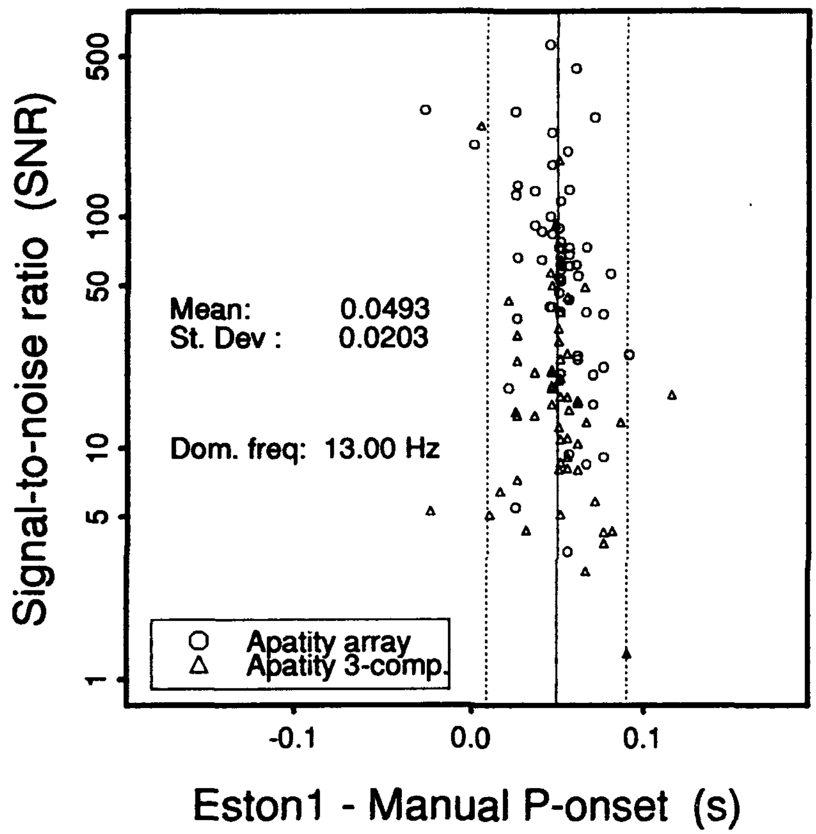

Fig. 7.2.7. This figure show the time differences between the automatic P-onsets from ESTON1 and the manual pick at both Apatity stations (APA0 and APZ9) as a function of signal-to-noise ratio (SNR). Compared to Fig. 7.2.5 the x-axis is strongly expanded. Notice that P-phases at APZ9 (triangles) generally have lower SNR. The average dominant frequency of these P-phases is 13 Hz.

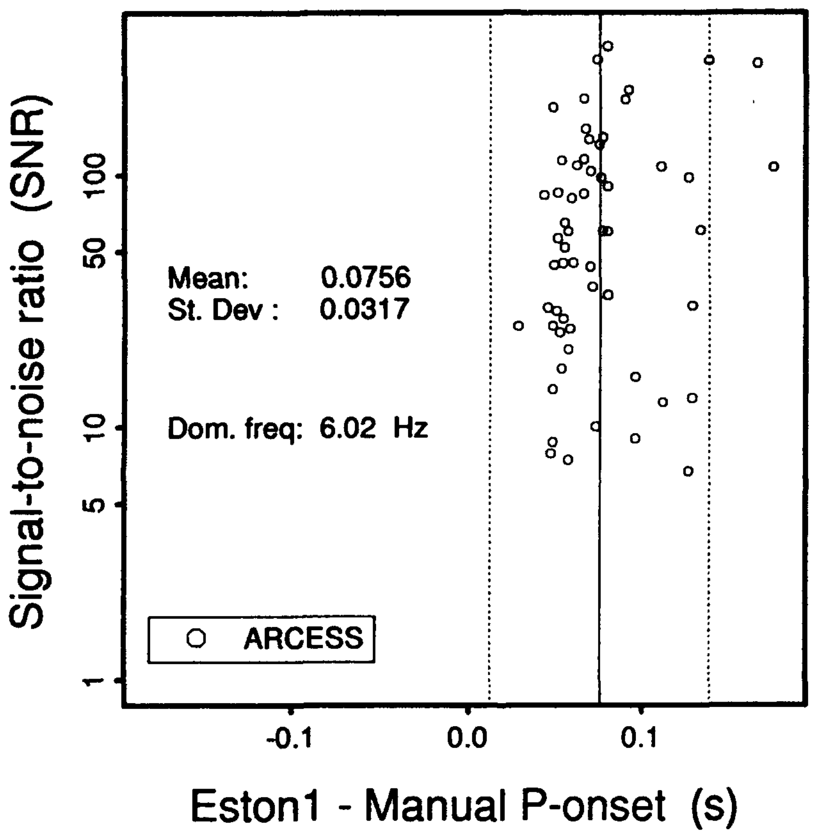

Fig. 7.2.8. Plot similar to Fig. 7.2.7, but in this case for ARCESS P. The average dominant frequency is 6 Hz.

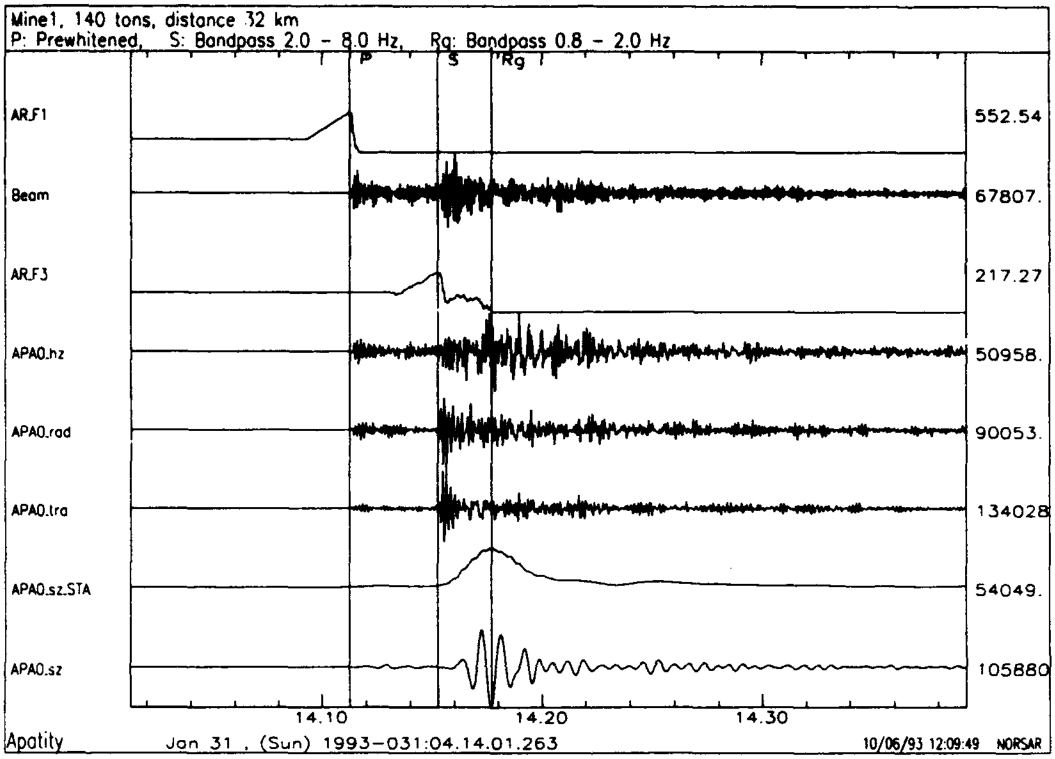

Fig. 7.2.9. The seismograms of this figure are Apatity array (APA0) recordings of the Mine I event also given in Fig. 7.2.2. The source-receiver distance is 32 km. Trace no. 2 is the prewhitened P-beam used for onset-time estimation using ESTON1. The upper trace gives the likelihood function from ESTON1 after processing an interval of ±2 s around the initial P-onset estimate, and the peak of this likelihood function correspond to the estimated onset. The lower trace is the vertical component APA0_sz filtered in a low passband (0.8 - 2.0 Hz) to enhance the Rg phase, and the trace above it is the STA envelope. The peak of this envelope is defined as the peak of the Rg phase. After the P-onset and the Rg maximum is found, we are searching for the S-onset using the three-component ESTON3 estimator. The search interval starts 2 s after the P-onset and stops at the Rg peak, as seen from the ESTON3 likelihood function of trace no. 3. The three-component data processed by ESTON3 are given in traces 4-7. Notice that there is no need to rotate the three-component data before using ESTON3, but to visualize that the S-phase has the largest SNR on the transverse component, we have in this figure rotated the data. Notice that both the ESTON1 and the ESTON3 likelihood functions show clear peaks at the P- and S-onsets.

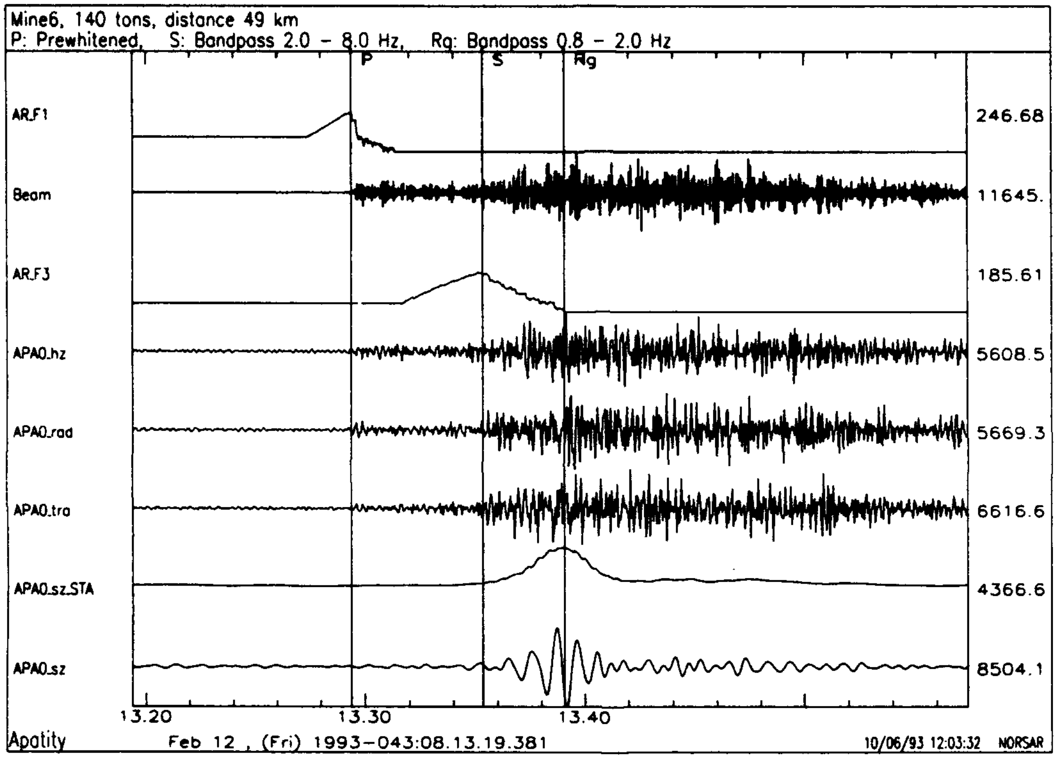

Fig. 7.2.10. The traces of this plot are similar to those of Fig. 7.2.9. The seismograms are Apatity array (APA0) recordings of the Mine VI event also shown in Fig. 7.2.3. The source-receiver distance is 49 km. Notice that the S-phase is much more emergent than the S-phase of Fig. 7.2.9, but the ESTON3 likelihood function still shows a clear peak at the S-onset.

7.3 Intelligent post-processing of seismic events -- Part 3: Precise relocation of events in a known target region

Introduction

From experience with analyst review of events automatically defined by the Intelligent Monitoring System (IMS) (Bache et al, 1993), we have realized that the quality of the automatic event locations can be significantly improved if the event intervals are reprocessed with signal processing parameters tuned to phases from events in the given region. The tuned processing parameters are obtained from off-line analysis of events located in the region of interest. The primary goal of such intelligent post-processing is to provide event definitions of a quality that minimizes the need for subsequent analysis and review.

In this third paper on intelligent post-processing of seismic events we test an event location method that makes use of accurate retiming of seismic phases and accurate re-estimates of azimuth using broad-band analysis of array data. The key to obtaining such accurate estimates is the knowledge, provided by the IMS, of an approximate event location in a known area with good calibration information. Various aspects of generalizing the method and incorporating it into the IMS are also discussed.

Location of regional events

Seismic event location has traditionally relied upon P-wave arrival times from a large number of stations. For small events observed only at regional distances, it has been necessary to include arrival times of later phases as well as arrival azimuths in order to obtain acceptable location accuracy (Bratt and Bache, 1988; Thurber et al, 1989). With a sparse network, the number of arrival time observations may often be so low that azimuth information is given considerable weight in the location scheme. However, as the number of observations increases, the relative importance of the azimuths decreases sharply, in view of the generally large uncertainties (10 degrees or more) that are associated with azimuth estimates (e.g., Suteau-Henson, 1990; Bame et al, 1990).

Kværna and Ringdal (1986) demonstrated that the uncertainty of azimuth estimates from regional arrays can be greatly reduced by applying a broad-band estimation scheme in which the frequency band is kept constant for a given epicentral region. Thus, for NORESS observations from Blåsjø explosions (distance 300 km) with high SNR, they found an azimuth standard deviation of only 1.0 degrees for Pn phases and 1.5 degrees for Sn and Lg phases.

This observation suggests that given an initial (approximate) event epicenter, it should be feasible to determine an optimum frequency band (based upon previous observations) and apply broad-band F-k analysis in order to obtain very accurate azimuth estimates, which can then be used to refine the event location. The basic idea of this paper is to establish and test a method for location refinement which takes into account both the stable azimuth estimates obtained by fixed frequency broad-band analysis and the accurate timing observations described in Section 7.2. We use as an example IMS-reported events in the Khibiny Massif recorded by the nearby Apatity array and the more distant ARCESS array. We show that a significant improvement can be obtained relative to the current IMS processing. Moreover, the method is completely automatic and can easily be incorporated into the IMS, as illustrated in Fig. 7.3.1.

As shown in Section 7.1, the majority of seismic events in Fennoscandia can be associated with mining activity at a few sites. The Khibiny Massif is one of the mining areas with the most events. Obtaining accurate automatic solutions for events from this and other mining areas will lead to a considerably lower workload for the analyst, and will consequently allow more time to be spent analyzing events of particular interest.

Method

The automatic method applied in this study consists of the following steps:

1. The IMS detects and locates a seismic event within a given distance from the target region.
2. For each phase detection by a station in the network, the estimated arrival time is refined using the method of Pisarenko et al (1987) (see Section 7.2). A standard deviation is assigned to each refined estimate.
3. For each phase detection by one of the arrays, an "optimum" frequency band for F-k analysis is extracted from a data base which we assume has been previously established and calibrated.
4. Broad-band F-k analysis is then applied to each phase. The resulting values are corrected for systematic bias and assigned a standard deviation, based upon SNR, phase type and previously observed calibration information.
5. The LocSat program (Bratt and Bache, 1988) is then applied to the revised data set, and a new event location estimate is obtained. In practice, zero depth is assumed a priori in the automatic process.

In the case study discussed in detail in this paper, we will analyze events in the Khibiny Massif recorded by IMS, for which we have independent location information. We will primarily make use of the Apatity array, using arrival times for the P and S phases and azimuths derived from the Rg phase in order to refine the location estimates as described above. In addition, we will consider possible improvement in the location accuracy when using additional available stations.

Data

The data for this study comprises 58 events at 6 mines in the Khibiny Massif. The mines are only a few kilometers apart (Mykkeltveit, 1992), and they each have a dimension ranging from a few hundred meters to about 1 km. These dimensions are small enough so that we ignore the areal extent of each mine. A list of the event parameters is given in Section 7.2.

To obtain an initial location, we have used the automatic IMS epicenter solution for each event. The automatic IMS solution relative to the "true" epicenter for each of the events is displayed graphically in Fig. 7.3.2. Although many of the events are very accurately located (to within a few km), there is a fair amount of scatter in the location estimates. The median "error" is 10.6 km. In a few cases, the location is wrong by several tens of km; this is due to occasional erroneous phase identification by the automatic process.

The Apatity array has been described by Mykkeltveit et al (1992), and initial data analysis results have been presented by Ringdal and Fyen (1992). The latter paper discusses in particular the high stability of azimuth estimates using the Rg phase for shallow events at local distances.

In Section 7.2, some examples of Apatity array recordings of events in the Khibiny Massif are shown. The filtered recordings (0.8-2.0 Hz) are dominated by the Rg phase. In contrast, the P and S phases are far more high-frequent, as is to be expected at such close distances. Because of the low frequency of the Rg phase, this phase has a high coherency across the array and thus provides more stable slowness estimates than are obtained from the other phases.

For the present study, we have used Apatity array recordings for all 58 events. For all but six events, high-frequency three-component data from the array site have been available. Furthermore, all events have associated 3-component broadband recordings from the station installed in the town of Apatity, 15 km from the array site. ARCESS array data have been available for all but one of the events.

Results

In the following, we present results from analyzing the 58 events in the data base under various scenarios. Each scenario assumes that we have an operational situation in which a certain amount of calibration information has been assembled.

a) Use of Apatity array only; P and S arrival times, Rg azimuth, no calibration.

In this scenario, we assume no prior knowledge except for the "optimum" frequency bands for timing and azimuth estimation. The travel-time tables are those that the IMS uses for Fennoscandia in general, with no regional corrections.

The results are displayed in Figs. 7.3.3. We note that there is a small systematic bias, as there seems to be a trend of events being located to the north and east of the sites. This indicates that some improvement could be obtained by introducing a regional velocity model for the Khibiny area, together with regional azimuthal corrections.

Nevertheless, the scatter relative to the 6 mines in this plot (using uncalibrated Apatity array data only) is significantly reduced compared to the IMS results plotted in Fig. 7.3.2.

The improvement can be quantified by considering that the median "error" is only 3.1 km, with a worst case "error" of 6.7 km. This can be compared to the IMS results of 10.6 km and 75.3 km, respectively. Thus the reprocessing, even without regional correction, could significantly improve the precision in the epicenter solutions if incorporated in the automatic IMS processing.

b) Use of Apatity array data only, with a regional P-S travel-time bias correction and a correction for systematic Rg azimuth bias.

The resulting location plot is shown in Fig. 7.3.4. The median error is reduced to 2.1 km, and the "worst case" error is 6.1 km.

c) Use of Apatity array data plus P and S times from the 3-component station in Apatity. Regional corrections have been applied both for the array and the 3-comp. station.

The resulting location plot (Fig. 7.3.5) shows that the median error is 1.4 km, and the maximum error is 5.4 km.

d) This final scenario includes both Apatity array data, Apatity 3-comp. data and ARCESS P arrival times. Regional corrections have been applied for all the data.

The resulting location plot (Fig. 7.3.6) shows a median error of 1.6 km, and a maximum error of 7.1 km. It is interesting to note that this is not quite as good as case c). Thus, it is not necessarily an improvement to add data, even if (as in this case) the additional data are extremely accurate (error $\leq \pm$ 0.05 seconds on P-recordings).

We should note that the travel-time corrections used in this paper are *relative* and based upon the same data set that we have evaluated. In view of the large number of events, the possible bias introduced by this procedure should be negligible. As the origin time of the Khibiny events are unknown, we have fixed the travel-time correction of P at the Apatity three-component station APZ9 to 0. The P phase at APZ0 has travelled a shorter distance and spent less time in the earth than the other phases used in the event locations. Thus, the influence of an erroneous travel-time model is likely to be the least for this phase.

Travel-time corrections:

P	APZ9	0 s (fixed)
P	APA0	-0.10 s
Pn	ARCESS	-0.31 s
S	APZ9	0.22 s
S	APA0	0.09 s

Conclusions

In this study we have conducted extensive off-line analysis of 58 mining explosions in the Khibiny Massif recorded at the Apatity array. Independent locations of these explosions are provided by seismologists from the Kola Science Centre. Most of these events show clear P, S and Rg phases at the nearby Apatity array located 30-50 km away from the mining areas and the events have also been detected by the ARCESS array. By using the onset-time estimator of Pisarenko et al (1987) and comparing to the best manual pick, we have found that P-onsets can be automatically estimated with an accuracy of better than 0.1 seconds, and S-onsets with an accuracy better than 0.5 seconds. In addition, the azimuth estimates from F-k analysis of the P and Rg phases show to be accurate well within $\pm$ 5 degrees after removing the biases. The key to achieving stable azimuth estimates is to process the data in a fixed frequency band, using a fixed time window positioning, as demonstrated by Kværna and Ringdal (1986) for Blåsjø recordings at NORESS.

Our observations suggest that based on data from the Apatity array alone, we are able to locate these events (assuming 0 depth) with a median error of about 3 km relative to the true location. Even better accuracy can be achieved using calibration information, i.e., correcting the azimuth and arrival time observations for systematic bias. The excellent precision of the automatic phase onsets and azimuth estimates also indicate that the need for subsequent manual analysis of these events may be eliminated.

After we have established the tuned processing parameters for events in this region, a natural next step will be to automatically activate such intelligent post-processing every time the IMS locates an event in the Khibiny region. Extensions of the method to other mining areas will also be considered.

T. Kværna
F. Ringdal

References

Bache, T.C., S.R. Bratt, H.J. Swanger, G.W. Beall and F.K. Dashiell (1993): Knowledge-based interpretation of seismic data in the Intelligent Monitoring System, *Bull. Seism. Soc. Am.*, in press.

Bame, D.A., M.C. Walck and K.L. Hiebert-Dodd (1990): Azimuth estimation capabilities of the NORESS regional seismic array, *Bull. Seism. Soc. Am.*, 80, Part B, 1999-2015.

Bratt, S.R. and T.C. Bache (1988): Locating events with a sparse network of regional arrays, *Bull. Seism. Soc. Am.*, 78, 780-798.

Kværna, T. and F. Ringdal (1986): Stability of various F-k estimation techniques, in *NORSAR Semiannual Tech. Summ., 1-86/87*, Kjeller, Norway, 29-40.

Kværna, T. (1987): Wide-band slowness estimation using a small-aperture seismic array, in *NORSAR Semiannual Tech. Summ., 2-86/87*, Kjeller, Norway, 38-45.

Kværna, T. and D.J. Doornbos (1986): An integrated approach to slowness analysis with arrays and three-component stations, in *NORSAR Semiannual Tech. Summ., 1-86/87*, Kjeller, Norway, 41-50.

Mykkeltveit, S. (1992): Mining Explosions in the Khibiny Massif (Kola Peninsula of Russia) Recorded at the Apatity Three-component Station, AFGL Scientific Rep. No. 14, Hanscom AFB, 31 August 92.

Mykkeltveit, S., A. Dahle, J. Fyen, T. Kværna, P.W. Larsen, R. Paulsen, F. Ringdal and I. Kuzmin (1992): Extensions of the Northern Europe Regional Network -- New small-aperture arrays at Apatity, Russia, and on the Arctic island of Spitsbergen, Semiannual Tech. Summ. 1 April - 30 September 1992, Scientif. Rep. 1-92/93, Kjeller, Norway, 58-71.

Pisarenko, V.F., A.F. Kushnir and I.V.Savin (1987): Statistical adaptive algorithms for estimation of onset moments of seismic phases: *Phys. Earth Planet. Int.*, 47, 4-10.

Ringdal, F. and J. Fyen (1992): Initial processing results from the Apatity small-aperture array, Semiannual Tech. Summ. 1 April - 30 September 1992, Scientif. Rep. 1-92/93, Kjeller, Norway, 72-85.

Suteau-Henson, A. (1990): Estimating azimuth and slowness from three-component and array stations, *Bull. Seism. Soc. Am.*, 80, Part B, 1987-1998.

Thurber, C., H. Given and J. Berger (1989): Regional seismic event location with a sparse network: application to Eastern Kazakhstan, USSR, J. Geophys. Res., 94, 17767-17780.

New processing flow:

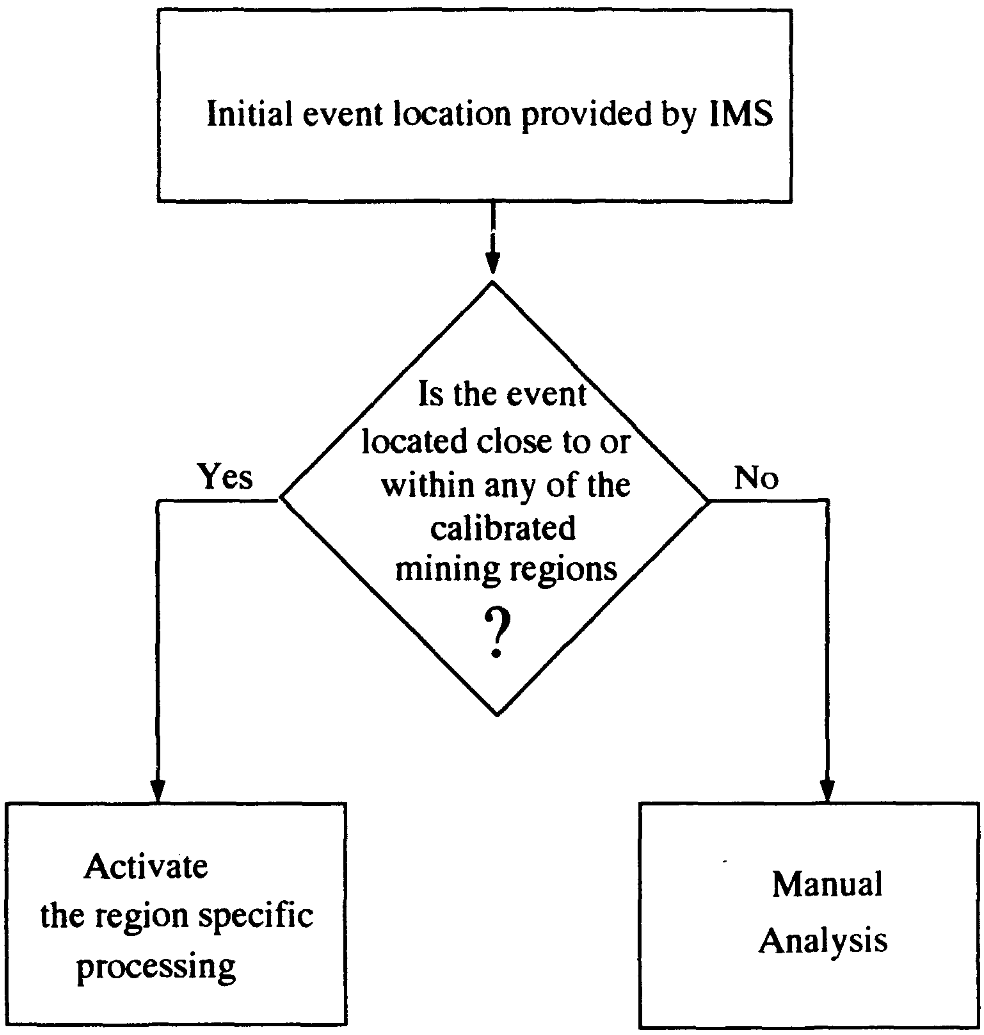

Fig. 7.3.1. Schematic view of the principle behind intelligent post-processing of seismic events.

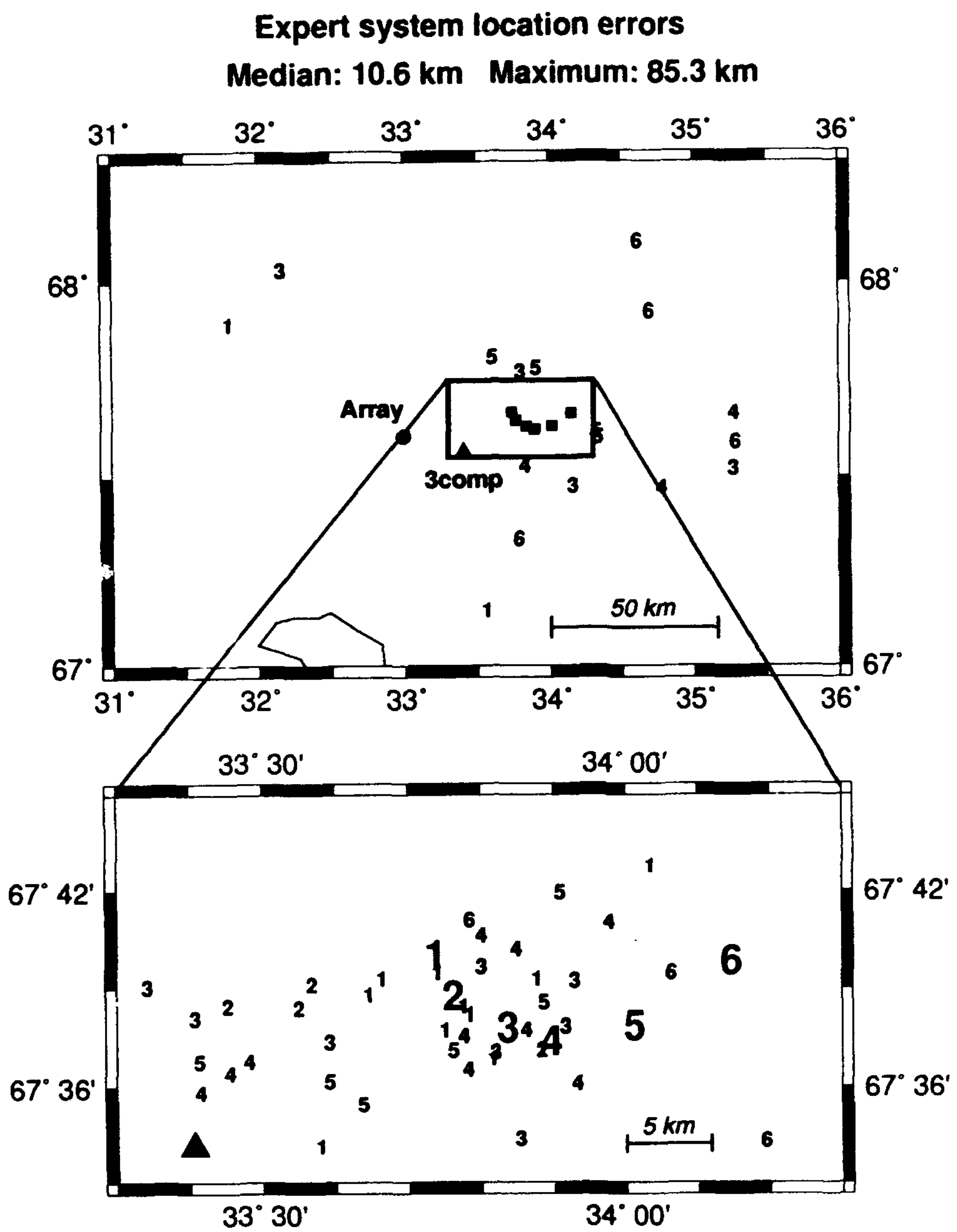

Fig. 7.3.2. Location of the six mining sites in the Khibiny Massif (large numbers 1-6) and the locations of the 58 reference events (small numbers 1-6) as given by the automatic IMS processing. In the **upper part,** a large reference area is shown, with the mines plotted as filled squares. The **lower part** shows a detailed picture for the area near the mines. The small number (1-6) associated with each event represents the mine in which the event actually occurred. The Apatity array is shown as a filled circle and the three-comp. station in the town of Apatity is shown as a filled triangle.

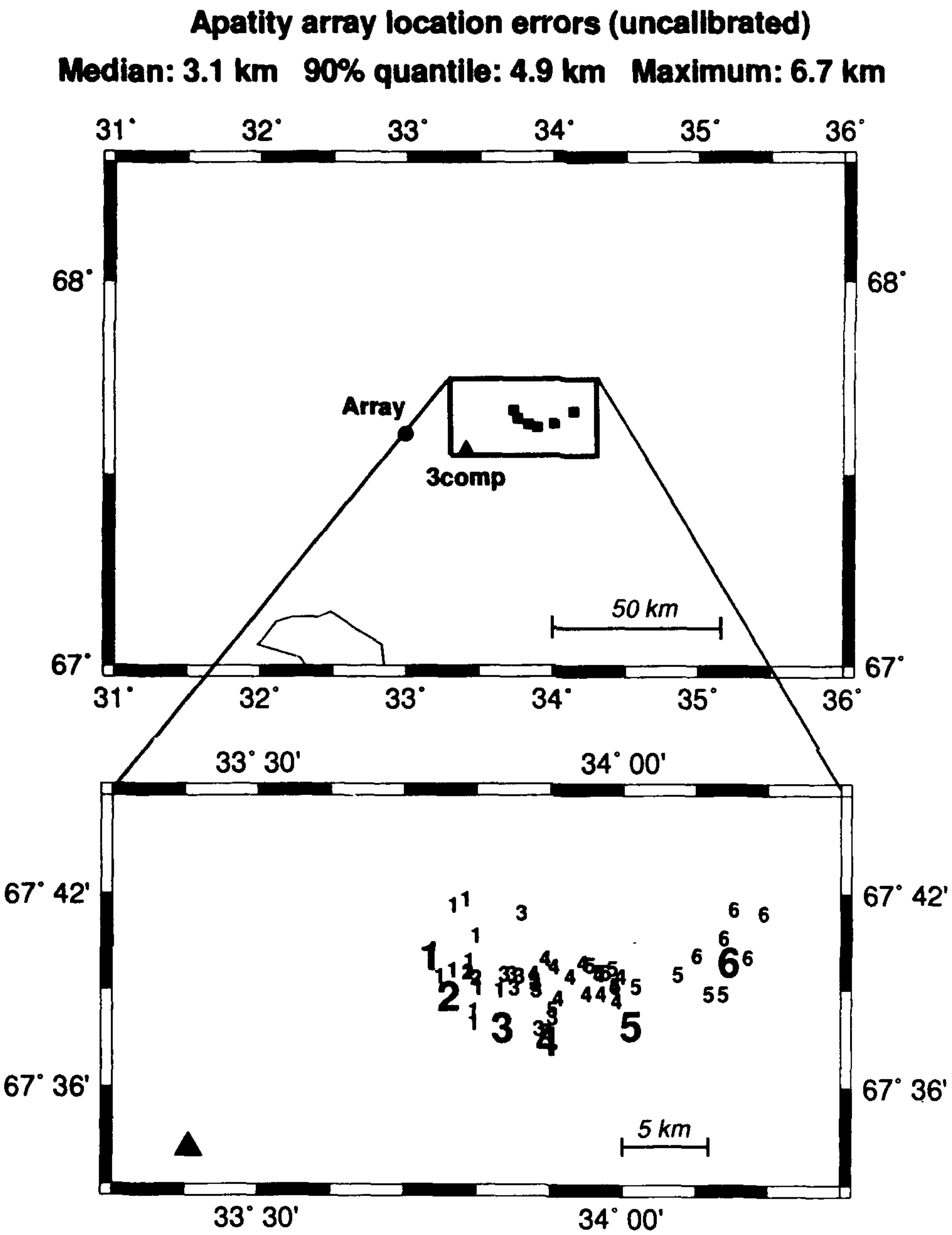

Fig. 7.3.3. Same as Fig. 7.3.2, but the event locations (small numbers) have now been taken from the post-processing results using uncalibrated Apatity array data only.

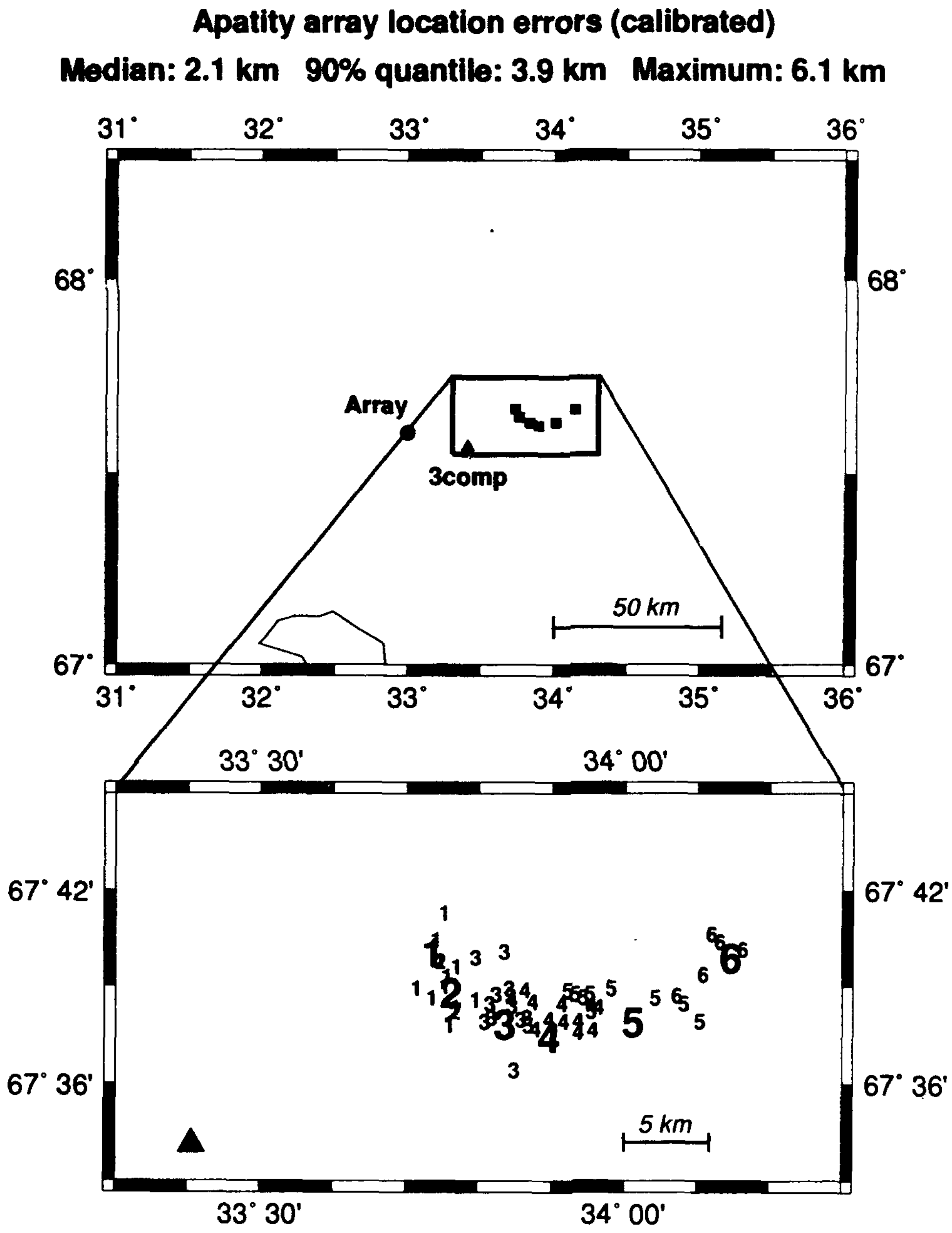

Fig. 7.3.4. Same as Fig. 7.3.2, but with the event locations resulting from post-processing of calibrated Apatity array data (see text for details).

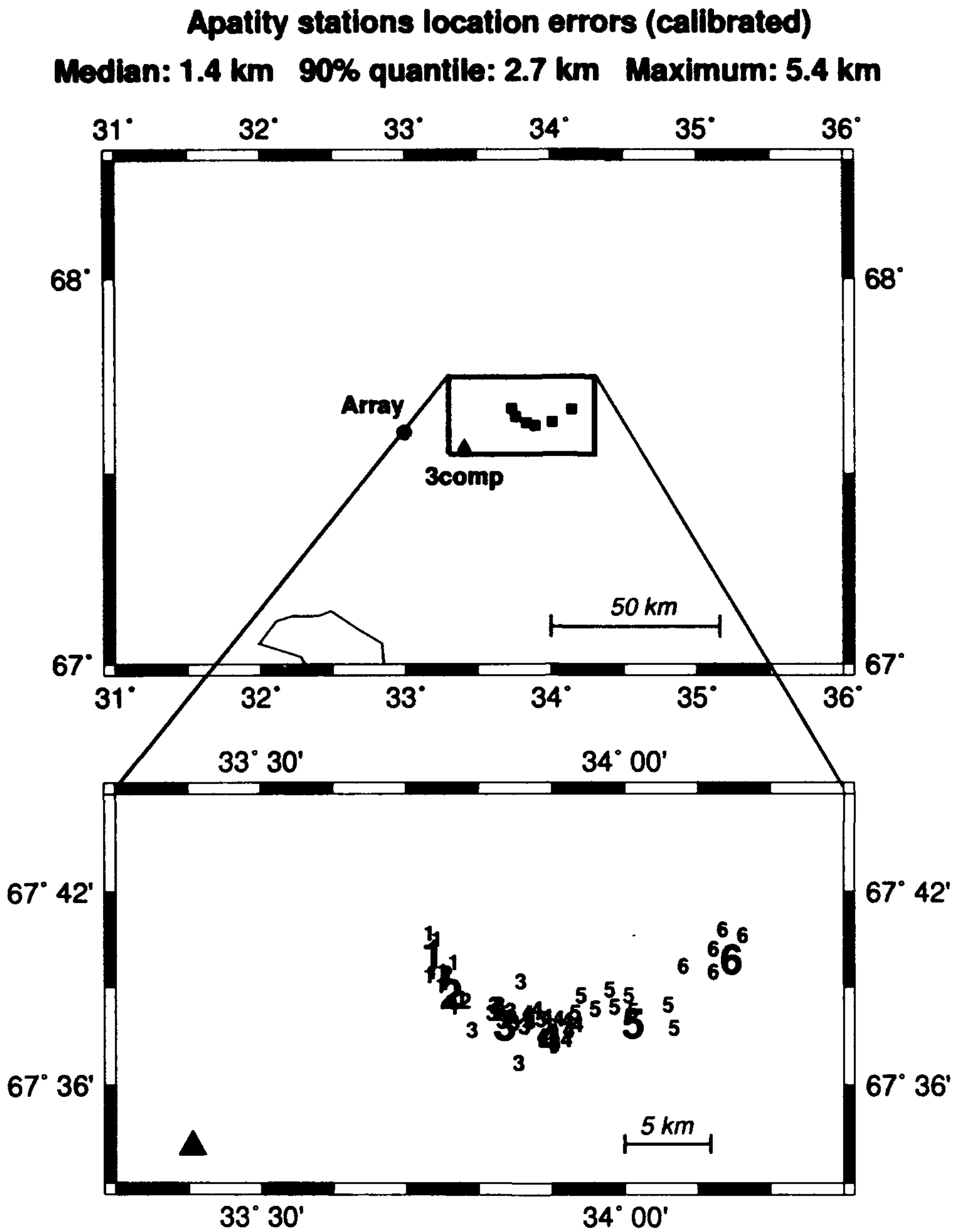

Fig. 7.3.5. Same as Fig. 7.3.2, but with the event locations resulting from combining Apatity array data and 3-comp. data (both calibrated) in the post-processing.

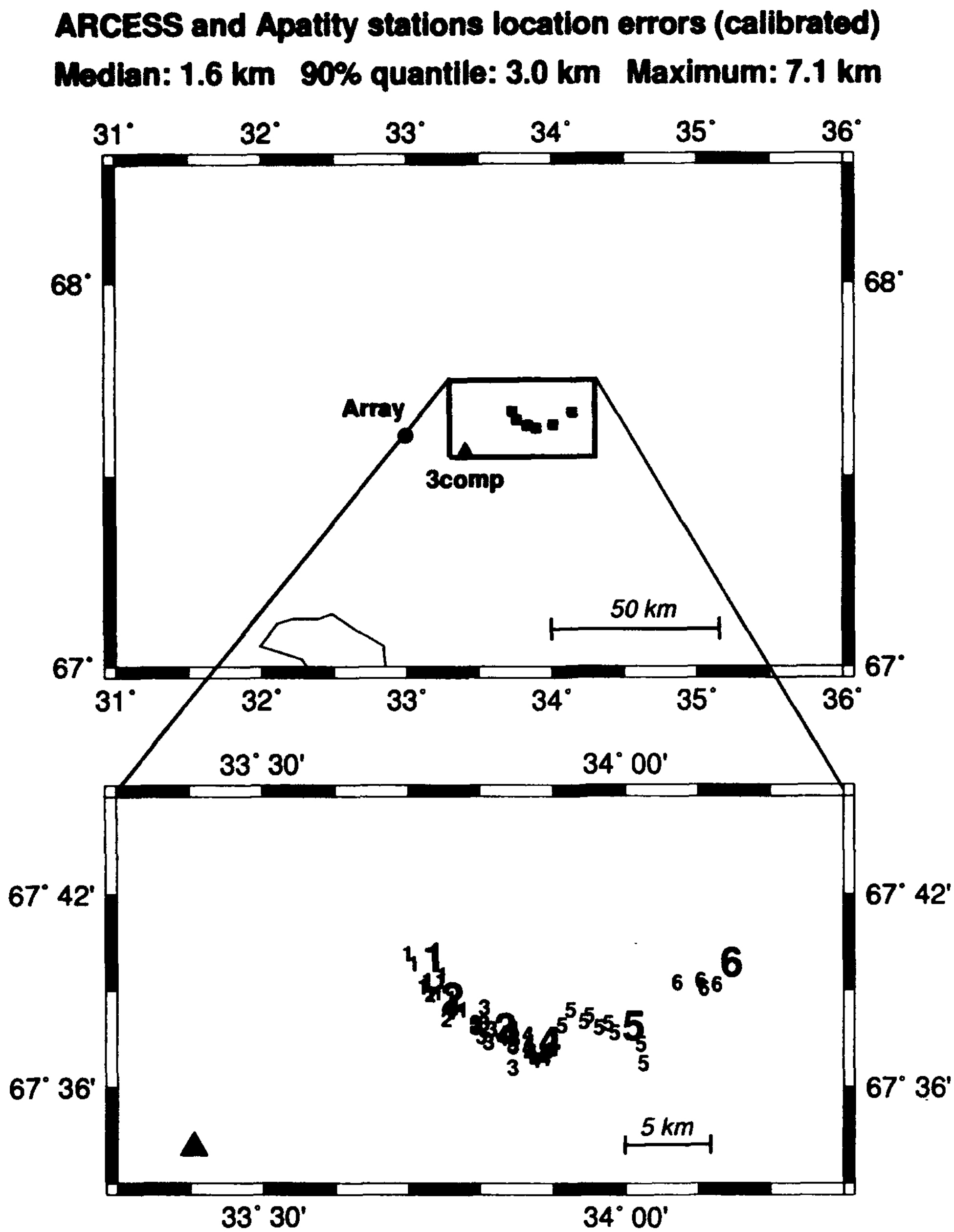

Fig. 7.3.6. Same as Fig. 7.3.2, but with the event locations resulting from combining Apatity array, Apatity 3-comp. and ARCESS array data (all calibrated) in the post-processing.

7.4 Monitoring a moratorium: An experiment in continuous seismic threshold monitoring of the northern Novaya Zemlya test site

Introduction

After 1 October 1992 a moratorium on nuclear testing has been in effect for the US, UK, Russia and France. On this background, we have applied the continuous threshold monitoring technique to the northern Novaya Zemlya test site for a full six-month period (1 October - 31 March 1993), using the NORESS, ARCESS and FINESA regional arrays. Starting 1 December 1992, we have compiled daily statistics of all peaks on the threshold diagram exceeding $m_b = 2.75$, and associated these peaks to regional or teleseismic events whenever possible. In addition, we have analyzed smaller peaks (below $m_b = 2.75$) that can possibly be associated with Novaya Zemlya epicenters.

The theoretical background for and applications of the continuous seismic threshold monitoring metod (CSTM) have been described in several articles. The approach was introduced by Ringdal and Kværna (1989), who showed that by continuously monitoring the seismic amplitude level at several seismic stations or arrays, one can at any time obtain an instant network-based magnitude threshold for a given target region. The magnitude threshold can be interpreted as the maximum magnitude of a possible clandestine explosion, given a predefined level of confidence. In the context of a comprehensive or threshold test ban treaty, the continuous assessment of the magnitude thresholds makes it possible to focus attention upon those specific time intervals when realistic evasion opportunities exist, while retaining confidence that no treaty violation has occurred at other times.

Previous results from experimental monitoring

Kværna (1992) presented results from a one-month experiment of continuously monitoring the northern Novaya Zemlya test site. Data from the Fennoscandian regional array network (ARCESS, FINESA, and NORESS), see Fig. 7.4.1, were used to calculate the magnitude thresholds. It was found that the test site could be consistently monitored at a very low magnitude level (typically $m_b = 2.5$). In fact, every occurrence of the threshold exceeding $m_b = 2.6$ could be explained as resulting from an identified interfering event signal either at teleseismic or regional distance, except for three instances when a short gap in ARCESS recording caused the network threshold to increase.

The excellent capability of the Fennoscandian regional array network to monitor the northern Novaya Zemlya test site was further confirmed by an experiment where recordings of the Novaya Zemlya nuclear test of October 24, 1990 were downscaled to $m_b = 2.6$ and superimposed on different noise intervals (Kværna, 1991).

In the context of using CSTM as a tool in routine monitoring, it is important to determine how the method will work under different conditions. Variability in the seismic noise level, occurrences of large earthquakes and aftershock sequences, station downtimes and data quality problems are all factors that will influence the performance of CSTM.

Analysis of network threshold peaks

Our monitoring experiment was conducted in the same way and with the same parameter settings as used by Kværna (1992). In Kværna (1992) the monitoring results were presented in terms of plots covering one data day each. In Figs. A-1 to A-29 of the Appendix of that report, each covering one day of February, 1992, all time periods where the network magnitude thresholds at the 90% confidence level exceeded $m_b = 2.6$ were identified. A similar approach was used for this experiment.

For the remainder of this paper, the term magnitude threshold implies the magnitude threshold at the 90% confidence level.

Figs. 7.4.2 shows a typical example of a one-day plot. The upper three traces of each figure represent the magnitude thresholds obtained from the three indivitual arrays, whereas the bottom trace illustrates the network threshold. Typically, the individual array traces have a number of significant peaks for each 24-hour period, due to signals from interfering events (regional or teleseismic). On the network trace, the number and sizes of these peaks are significantly reduced, because an interfering event usually will not provide matching signals at all stations. From probabilistic considerations, it can in such cases be inferred that the actual network threshold is lower than these individual peaks might indicate.

The arrows on the one-day threshold plots indicate peaks with network magnitude threshold exceeding $m_b = 2.75$. A **T** at the arrow indicates that the peak is caused by signals from a teleseismic event, whereas an **R** indicates signals from a regional or local event. Fig. 7.4.3 shows summary statistics for one data day, with an explanation of all threshold peaks exceeding 2.75. Such summary statistics were generated for each day during the four-month period, 1 December 1992 - 31 March 1993.

The peaks in the threshold traces are caused by either large teleseismic events or by regional events. The regional events were all processed and located by the Intelligent Monitoring System (IMS) (Bache et al., 1993), and the teleseismic events were located either by the IMS or by the QED service of the USGS.

Fig. 7.4.4 shows a histogram of the number of peaks exceeding given magnitude thresholds. During the entire four-month period, there were only 40 peaks exceeding $m_b = 3.0$. Each of these peaks could be unambiguously associated with either a regional or teleseismic event. Consequently, at the specified confidence level, we can state that no seismic event of $m_b > 3.0$ occurred at the test site during this four-month period.

The event at Novaya Zemlya on 31 December 1992

Figs. 7.4.5 and 7.4.6 show the threshold plots and peak statistics for 31 December 1992. At 0929 GMT that day, a peak occurred corresponding to an event at Novaya Zemlya, located by the IMS. This peak (which is the only one associated to a Novaya Zemlya event during the six-month interval) had an upper magnitude limit of 2.6. The actual event magnitude, according to Carter et al (1993) was 2.5.

This event was detected by ARCESS (P and S), Spitsbergen (P and S), NORESS (P) and Apatity (S). In addition, the Kola Science Centre provided readings for the station Amderma (Pg and Sn) made from analog recordings. Tables 7.4.1 and 7.4.2 summarize the available observations for this event. Table 7.4.3 gives the results of applying the LOCSAT program (Bratt and Bache, 1988) to this parameter set.

Our results indicate that the epicenter was slightly to the north of the test site. However, there are some uncertainties in the travel time tables, and an on-site location cannot entirely be ruled out. We are hesitant to introduce travel-time corrections in this case, since no good reference event is available for some of the key stations.

A plot of the IMS-processed traces is shown in Fig. 7.4.7. Notice in particular the high SNR at the Spitsbergen B2 single sensor (filter band 8-16 Hz) and on the ARCESS array beam. Fig. 7.4.8 shows the IMS solution for this event. The Amderma station is not included in the IMS processing, but adding its data does not cause any significant change in the event location.

Conclusions

This work has documented the practical capability of the Continuous Seismic Threshold Monitoring method to monitor a specific nuclear test site at a very low threshold over an extended time period.

Specifically, we have used the Fennoscandian array network (NORESS, ARCESS and FINESA) to monitor the northern Novaya Zemlya test site for a full four-month period at a threshold of $m_b = 2.75$. We have identified only one instance where an event close to this threshold has occurred near the test site. In fact, the event magnitude (2.5) was below our target threshold, but the peak was still easily identified on the threshold trace.

Recently, additional array stations have been installed or are planned for installation in the Arctic region. These stations would contribute to further improving the CSTM capability, both for Novaya Zemlya and on a general regional basis. This will be the subject for additional studies in the future.

T. Kværna
F. Ringdal

References

Bache, T.C., S.R. Bratt, H.J. Swanger, G.W. Beall and F.K. Dashiell (1993): Knowledge-based interpretation of seismic data in the Intelligent Monitoring System, *Bull. Seism. Soc. Am.*, in press.

Bratt, S.R. and T.C. Bache (1988): Locating events with a sparse network of regional arrays, *Bull. Seism. Soc. Am.*, 78, 780-798.

Carter, J., H. Israelson and V. Ryaboy (1993): Location of the December 31, 1992 Novaya Zemlya Event, Center for Seismic Studies, 12 Apr 93

Kværna, T (1991): Threshold monitoring of Novaya Zemlya: A scaling experiment, *Semi-annual Tech. Summary, 1 Oct 1990 - 31 Mar 1991*, NORSAR Sci. Rep. 2-90/91, NORSAR, Kjeller, Norway.

Kværna, T. (1992): Continuous seismic threshold monitoring of the northern Novaya Zemlya test site; long-term operational characteristics, Report PL-TR-92-2118, Phillips Laboratory, Hanscom Air Force Base, MA, USA.

Kværna, T. and F. Ringdal (1990): Continuous threshold monitoring of the Novaya Zemlya test site, *Semiannual Tech. Summary, 1 Apr - 30 Sep 1990*, NORSAR Sci. Rep. 1-90/91, NORSAR, Kjeller, Norway.

Ringdal, F. and T. Kværna (1989): A multi-channel processing approach to real-time network detection, phase association, and threshold monitoring, *Bull. Seism. Soc. Am.*, 79, 1927-1940.

Station	Lat (°N)	Lon (°E)	Type of Station
AMD (Amderma)	69.742	61.655	3-comp analog
APA (Apatity)	67.600	33.000	Array
ARA0 (ARCESS)	69.535	25.506	Array
FIA0 (FINESA)	61.444	26.079	Array
NRA0 (NORESS)	60.735	11.541	Array
SVA (Spitsbergen)	78.180	16.350	Array

Table 7.4.1. Location of stations used in this study.

Station	Phase	Type[1)]	Arrival time	Azimuth	St. dev.[2)]
AMD	Pg	t	09.30.43.7	-	2.0
AMD	Sn	t	09.31.20.7	-	2.0
APA	Sn	t	09.33.22.0	-	2.0
ARC	Pn	t	09.31.48.7	-	1.0
ARC	Pn	a	-	62.5	15.0
ARC	Sn	t	09.33.37.2	-	2.0
ARC	Sn	a	-	58.4	15.0
NRS	P	t	09.34.04.3	-	1.0
NRS	P	a	-	24.0	15.0
SVA	Pn	t	09.31.50.7	-	1.0
SVA	Sn	t	09.33.41.7	-	2.0

Table 7.4.2. Observed arrivals for the 31 Dec 92 event.

1) t = time, a = azimuth

2) A priori standard deviation in seconds (time) or degrees (azimuth)

```
Final location estimate (+/- S.D.):
      Latitude:   73.620 deg. +/-     6.673 km.
     Longitude:   55.196 deg. +/-     7.177 km.
         Depth:    0.000  km. +/-     0.000 km. (Fixed)
Relative O.T.:   -79.301 sec. +/-     0.849 sec.
Absolute O.T.:   -79.301 sec. +/-     0.849 sec.
              : 1969 12 31 23:58:40.70

Confidence region at 0.90 level:
  Semi-major axis:     18.1  km. =  0.16 deg.
  Semi-minor axis:     10.6  km. =  0.10 deg.
Major-axis strike:     49.3 deg. clockwise from North
 Orig. time error:      1.4 sec.

Standard errors (sigma):
             Prior:  1.00 (  9999 deg. of freedom)
         Posterior:  1.00 ( 10007 deg. of freedom)
         Posterior:  0.65 (Normalized sample S.D.)

     Azimuthal weighting:  1.00
Effective rank of matrix:  2.00
   Maximum azimuthal GAP:  195 deg.
 - No damping required !
```

Ariv ID	Statn	Phase	Data Type	at	Residuals True	Residuals Normalized	Distance (deg.)	Azimuth (deg.)	Data Import	Err
245771	APA	Sn	t	d	-0.087	-0.044	9.417	241.62	0.314	0
245771	AMD	Pg	t	d	0.900	0.450	4.371	149.27	0.319	0
245771	AMD	Sn	t	d	-1.495	-0.748	4.371	149.27	0.455	0
245782	NRS	P	t	d	1.068	1.068	20.495	254.54	0.016	0
245782	NRS	P	a	d	-9.782	-0.652	20.495	254.54	0.000	0
245782	ARC	Pn	t	d	-0.317	-0.317	10.096	261.08	0.055	0
245782	ARC	Pn	a	d	9.672	0.645	10.096	261.08	0.000	0
245782	ARC	Sn	t	d	-1.009	-0.504	10.096	261.08	0.220	0
245782	ARC	Sn	a	d	5.572	0.371	10.096	261.08	0.000	0
245782	SVA	Pn	t	d	-0.320	-0.320	10.244	313.75	0.408	0
245782	SVA	Sn	t	d	-0.033	-0.016	10.244	313.75	0.211	0

Table 7.4.3. Epicenter solution for the 31 Dec 92 event at Novaya Zemlya using the LOCSAT program (Bratt and Bache, 1988). The depth has been constrained to 0. See Table 7.4.1 for station locations and Table 7.4.2 for observed arrival data and assumed a priori standard deviations.

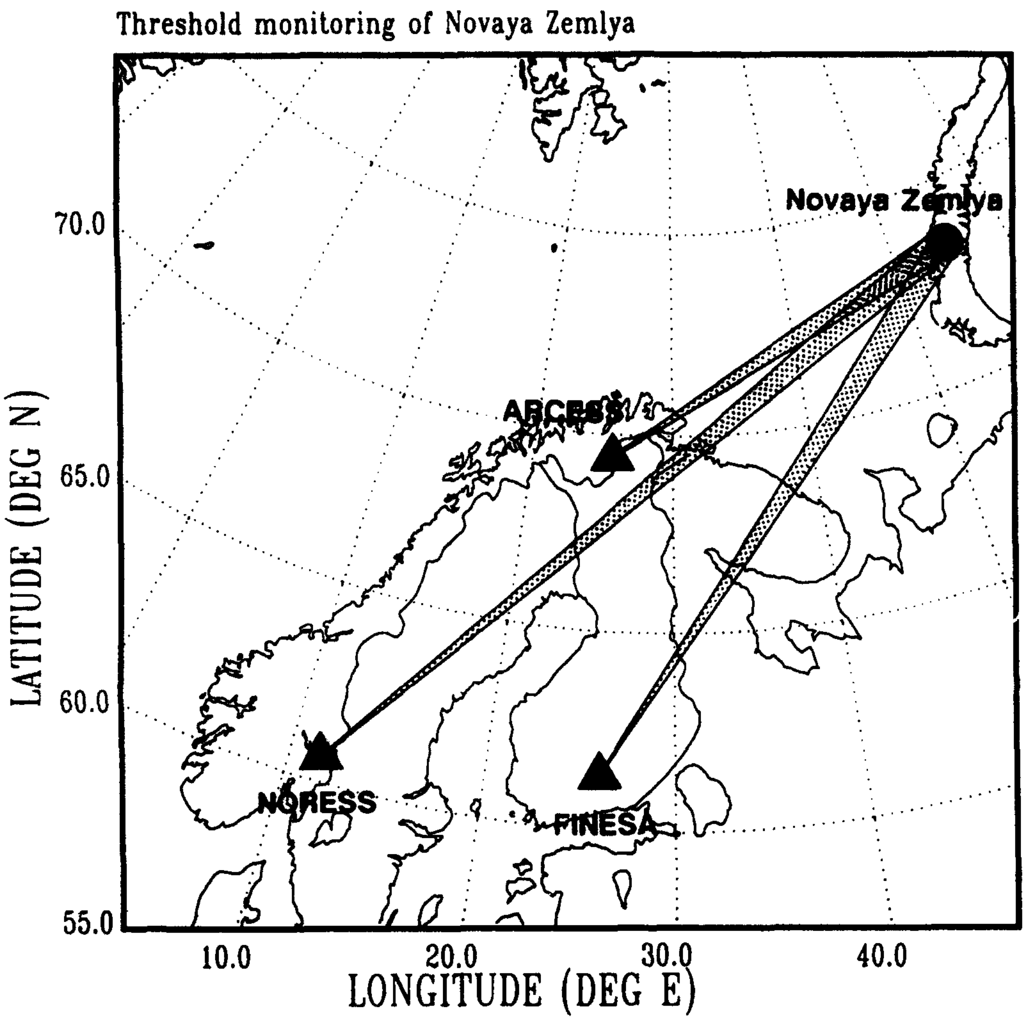

Fig. 7.4.1. Location of the target area (the northern Novaya Zemlya test site) for the monitoring experiment. The locations of the three arrays NORESS (Δ = 2280 km), ARCESS (Δ = 1100 km) and FINESA (Δ = 1780 km) are indicated.

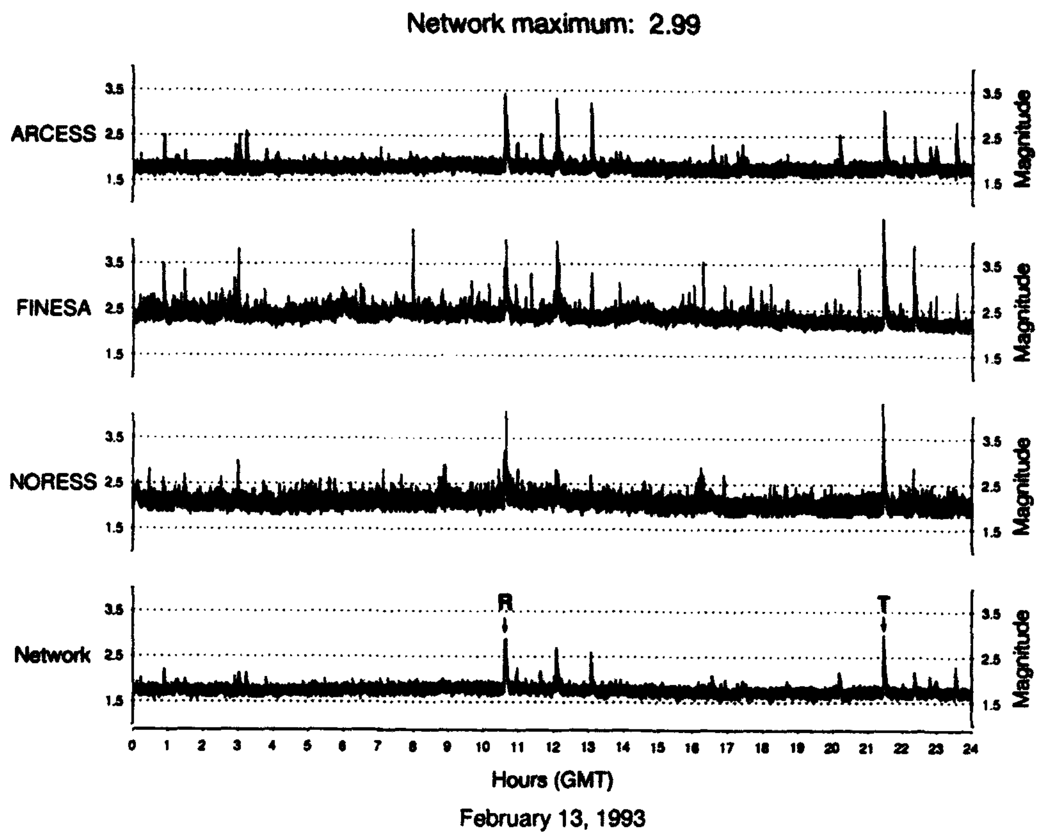

Fig. 7.4.2. Example of continuous threshold monitoring of Novaya Zemlya for one day (13 February 1993). A "threshold trace" is shown for each of the 3 arrays, and the combined network threshold trace is shown at the bottom. Note that the network threshold is well below magnitude 2.5 almost all the time.

Threshold Monitoring - Novaya Zemlya

Date: February 13, 1993 **Day_of_year:** 1993-044

	# peaks	# seconds	% of time
Mag >2.50	4	335	0.39
Mag >2.75	2	67	0.078
Mag >3.00	0	0	0
Mag >3.50	0	0	0

Individual Peaks > 2.75

TM_{max}	TM_{time}	# sec > 2.75	Reg Tele	Or.time	Lat	Lon	Depth	Mag	Agency	Explanation
2.89	10.38.10	27	R	10.37.16	68.1N	32.9E	0	2.4	IMS	Kola Peninsula, Russia, probable explosion
2.99	21.26.57	40	T	21.19.35	51.1N	176.4E	33F	5.4	IMS	Rat Islands, Aleutian Islands, earthquake

Fig. 7.4.3. Characterization of individual peaks in the threshold plot for 13 February 1993 (Fig. 7.4.2). The two peaks exceeding m_b = 2.75 are due to an event in the Kola Peninsula and an earthquake in the Aleutian Islands.

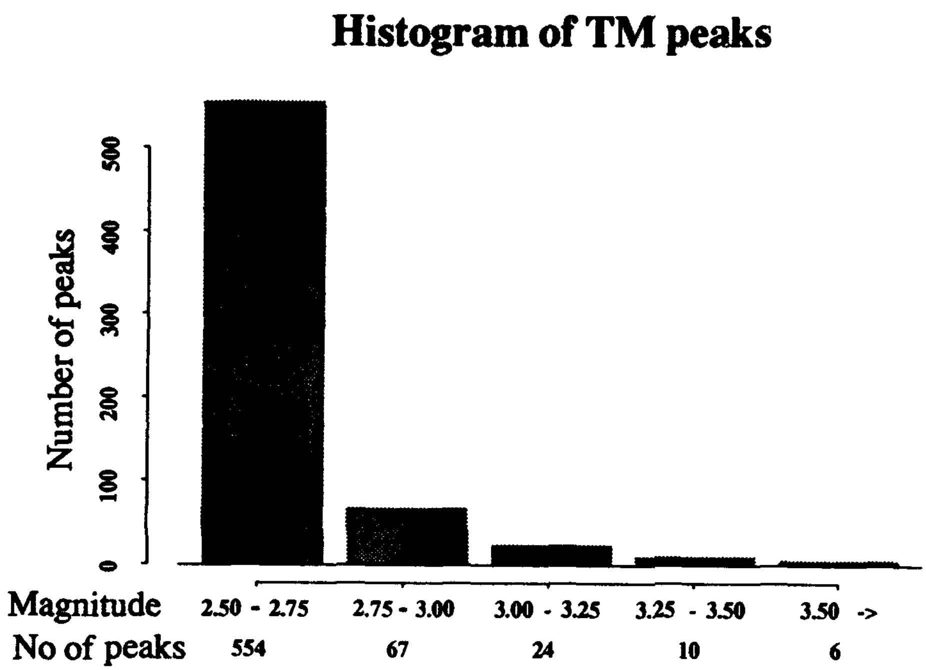

Fig. 7.4.4. Histogram showing the distribution of peaks on the network threshold trace for the four-month monitoring experiment.

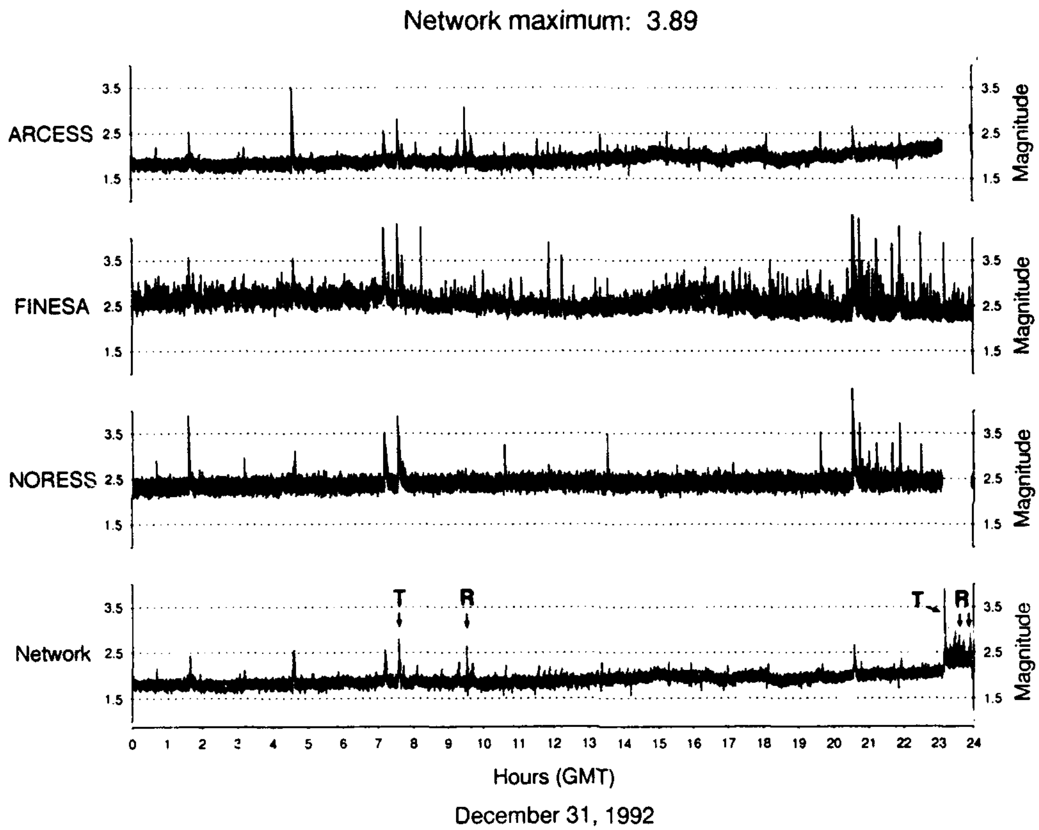

Fig. 7.4.5. Threshold plot for 31 Dec 92 (see Fig. 7.4.3 for explanation). The small Novaya Zemlya event at 09.29 GMT is indicated.

Threshold Monitoring - Novaya Zemlya

Date: December 31, 1992 **Day_of_year:** 1992-366

	# peaks	# seconds	% of time
Mag >2.50	14	648	0.75
Mag >2.75	6	107	0.12
Mag >3.00	2	19	0.022
Mag >3.50	1	7	0.0081

Individual Peaks > 2.75

TM_{max}	TM_{time}	# sec > 2.75	Reg Tele	Or.time	Lat	Lon	Depth	Mag	Agency	Explanation
2.80	07.34.10	8	T	07.25.10	27.4N	138.8E	33F	4.9	IMS	Bonin Islands Region
2.64	09.29.23	0	R	09.29.24	73.6N	55.2E	0F	2.3	IMS	Novaya Zemlya
3.89	23.09.49	38	T	32.01.06	22.3N	146.9E	33F	4.7	IMS	North Pacific Ocean
3.02	23.27.45	31								Gap in ARCESS and NORESS recording. Local noise at FINESA.
2.88	23.34.38	11								Gap in ARCESS and NORESS recording. Local noise at FINESA.
2.79	23.42.23	5	R							Local event at FINESA.
2.92	23.53.35	14	R							Local event at FINESA.

Fig. 7.4.6. Threshold monitoring statistics for 31 Dec 92. Note that there were some data problems just before midnight, causing a rise in the threshold.

Waveforms of Novaya Zemlya Event 31 Dec 1992 - Magnitude 2.5

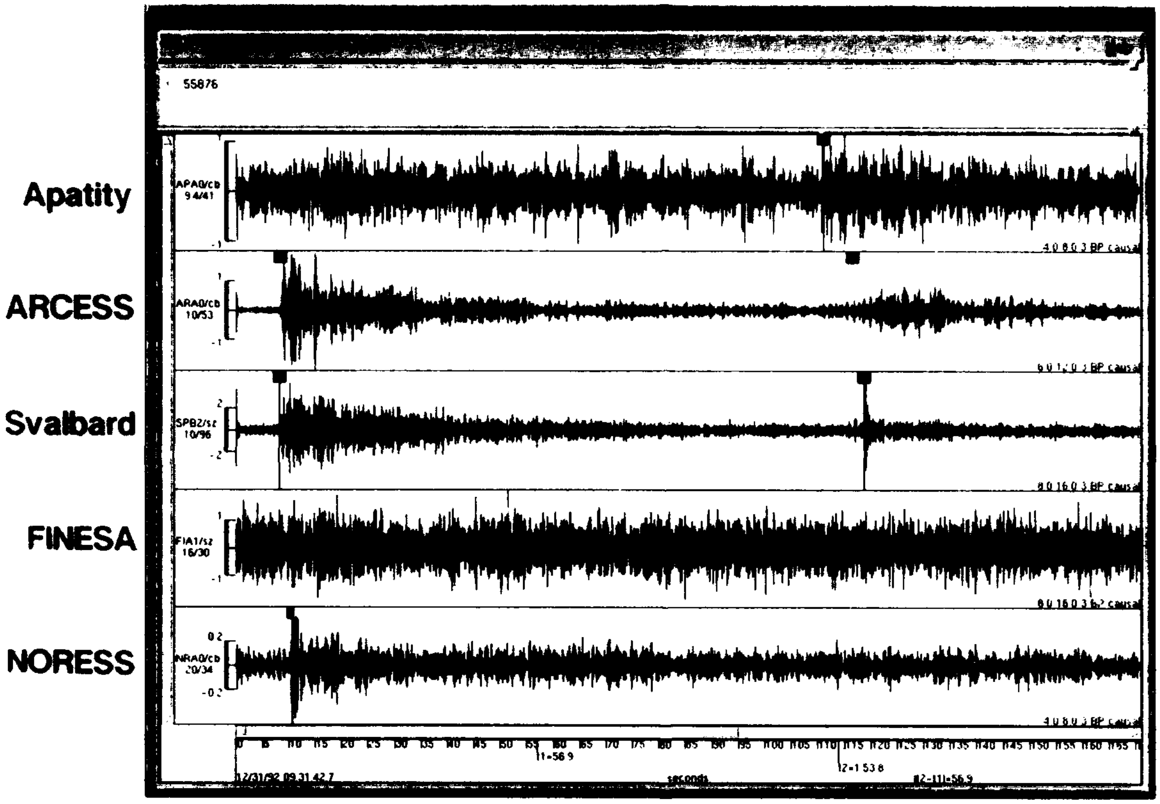

Fig. 7.4.7. Waveform plots for 5 regional arrays for the Novaya Zemlya event on 31 Dec 92. There are P-phase detections at ARCESS, Svalbard (Spitsbergen) and NORESS, and S-phase detections at Apatity, ARCESS and Svalbard.

Novaya Zemlya event 31 Dec 1992

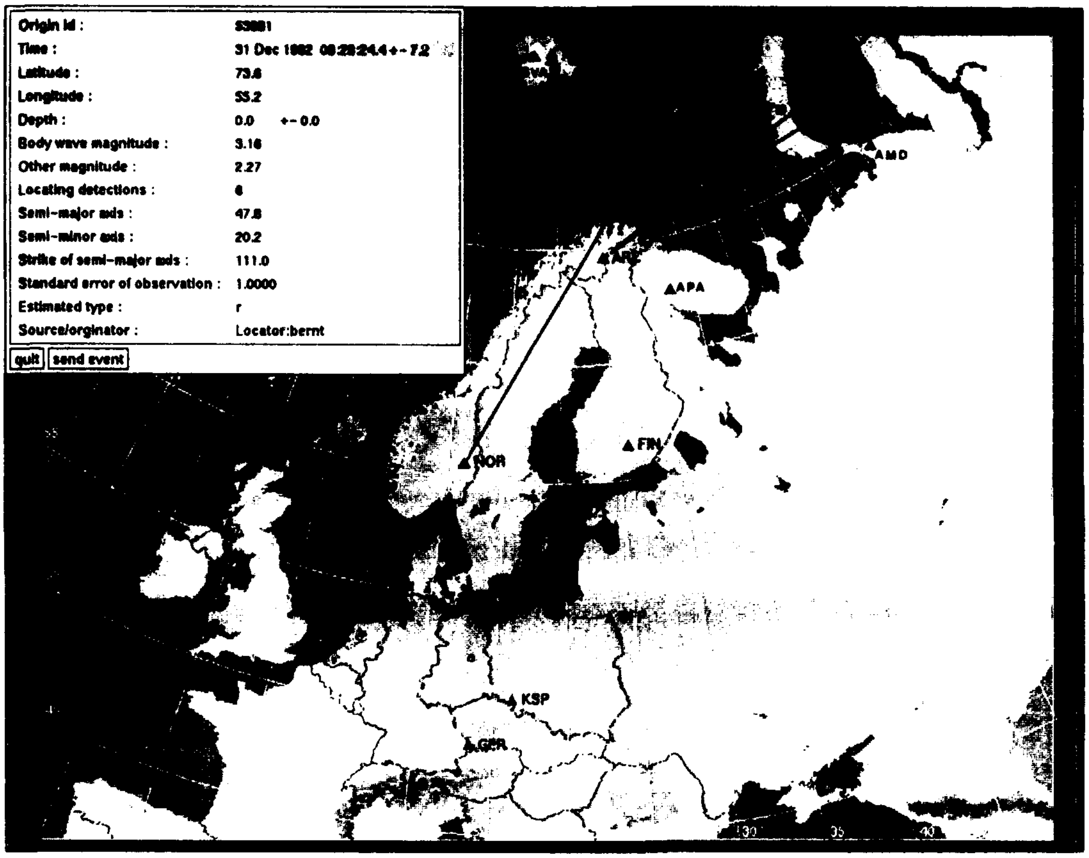

Fig. 7.4.8. IMS solution and associated error ellipse for the Novaya Zemlya event (m_b ~ 2.5) on 31 Dec 92.

7.5 Initial processing results from the Spitsbergen small-aperture array

During the fall of 1992, a new regional array was installed near the town of Longyearbyen on the Arctic island of Spitsbergen (see Mykkeltveit et al, 1992). Fig. 7.5.1 shows the location of this array and Fig. 7.5.2 shows the array geometry. As of early 1993, six of the nine array sites had been finalized, and this study is based on these six instruments.

In the following we report on some initial results from analyzing data from the new array. It is emphasized that these results are preliminary, since the available data cover only a few months, and only a partial array has been installed until now. Thus a more comprehensive assessment must await the collection of more complete array data over a longer time span.

Noise spectra

Fig. 7.5.3a shows an example of corrected noise spectra for the 6 vertical elements of the Spitsbergen array, taken at 00.00 hours (GMT) on day 345, 1992. For comparison, the ARCESS spectra for the same number of channels and taken at the same time are shown in Fig. 7.5.3b. From these figures, it is seen that the Spitsbergen array has practically the same noise level as ARCESS, especially for the "best" Spitsbergen sensor (B2). However, the Spitsbergen array has a much larger variation in noise level than ARCESS, especially at low frequencies.

Fig. 7.5.4a shows 41 corrected noise spectra, taken daily at 00.00 GMT during the period 10 December 1992 - 18 January 1993 for the Spitsbergen array (instrument B2). These spectra represent typical winter conditions. For comparison, a similar set of spectra during summer (23 May - 7 June) is shown in Fig. 7.5.4.b. The range is similar for the two time periods, although the highest noise levels at low frequencies are observed during winter.

Noise suppression

Previous studies have shown that regional arrays are very effective in suppressing seismic noise, thus providing gains that are often of the order of $\sqrt{N}$, or sometimes even in excess of this value (N being the number of sensors). Such better than $\sqrt{N}$ suppression occurs when particular subgeometries are chosen, enhancing the suppression of noise at certain frequencies. As a first check on the capabilities of the Spitsbergen array in this regard, we have computed noise suppression curves for the initial array geometry.

We calculate an uncorrected power density spectrum first by prewhitening 60 seconds of data. Then we estimate the autocorrelation for 6 partially overlapping windows (window length 12 seconds), and compute power density spectra from the average autocorrelation, with compensation for the prewhitening filter.

An average spectrum is obtained by averaging the individual channel spectra for the array. The averaging is done after a logarithmic transform of the spectra, and the standard deviation for each frequency point is calculated. Each spectrum is pointwise compared to the average spectrum. If a value is outside 1.5 standard deviation from the mean value, the point is considered an outlier. If a single channel spectrum has more than 60% outliers, the spectrum is excluded and a new average spectrum is estimated. A beam is calculated using only those channels for which the spectrum was accepted. The suppression is then the beam spectrum divided by the average spectrum.

Fig. 7.5.5 shows noise suppression in the frequency range 0-20 Hz for an infinite-velocity beam (no time delays) for the Spitsbergen array. The figure shows an average of 24 noise samples, taken hourly on day 345, 1992. We note that the noise suppression is between 5 and 10 dB above 2 Hz. This is about the theoretical value (8 dB for 6 sensors). We anticipate further investigations into this subject after the full array is deployed.

Detection processing

Since the array was installed, the Spitsbergen data have been subjected to continuous online detection processing (DP) at NORSAR using the standard small-array detection algorithm. The initial beam deployment is shown in Table 7.5.1.

As an example of a regional seismic event recorded and processed using Apatity data, we show here results for a low-magnitude earthquake ($m_b \sim 2.0$) west of the array (on the North Atlantic Ridge).

Fig. 7.5.6 shows individual recordings for this event. Note the large variations in signal amplitudes across the array. In particular, the B2 instrument shows excellent signal-to-noise ratio for this event as well as for other events we have processed. The reason for this large amplitude variation is as yet unknown. There are two distinct P-onsets and one clear S-onset on the waveforms.

Frequency-wavenumber analysis

Frequency-wavenumber solutions for P and S are shown in Fig. 7.5.7. In spite of the small aperture of the array and the incomplete deployment, the peaks in the F-K diagram are well-defined. However, there is a tendency to side lobes in the plots.

From Fig. 7.5.7 we note that the phase velocities of each of the two phases are reasonably consistent with the phase type, the S phase having the slowest velocity. The estimated azimuths are quite consistent (256 and 260 degrees, respectively).

In conclusion, our preliminary analysis indicates that the Spitsbergen array will be an important supplement to the seismic array network in Northern Europe. Its inclusion into the Intelligent Monitoring System (IMS) will in particular serve to improve the location precision and source characterization of the large number of events in the Barents Sea and adjacent regions. The excellent recordings of this array from the small Novaya Zemlya event on 31 Dec 1992 (see subsection 7.4) is a further illustration of this point. Further evaluation of the array capabilities will be made after the 9-element array has been completed.

J. Fyen
F. Ringdal

References

Mykkeltveit, S., A. Dahle, J. Fyen, T. Kværna, P.W. Larsen, R. Paulsen, F. Ringdal and I. Kuzmin (1992): Extensions of the Northern Europe Regional Array Network -- New small-aperture arrays at Apatity, Russia, and on the Arctic island of Spitsbergen, Semiannual Tech. Summ. , 1 April - 30 September 1992, Scientific Rep. No. 1-92/93, NORSAR, Kjeller, Norway.

BEAM	Velocity	Azimuth	Filter band	Threshold	N	Configuration
S011	99999.9	0.0	0.5 - 1.5	4.4	6	A0B
S021	99999.9	0.0	1.0 - 3.0	4.4	6	A0B
S031	99999.9	0.0	1.5 - 3.5	4.4	6	A0B
S032	11.0	30.0	1.5 - 3.5	4.4	6	A0B
S033	11.0	90.0	1.5 - 3.5	4.4	6	A0B
S034	11.0	150.0	1.5 - 3.5	4.4	6	A0B
S035	11.0	210.0	1.5 - 3.5	4.4	6	A0B
S036	11.0	270.0	1.5 - 3.5	4.4	6	A0B
S037	11.0	330.0	1.5 - 3.5	4.4	6	A0B
S038	15.0	88.0	1.5 - 3.5	3.9	6	A0B
S039	10.0	95.0	1.5 - 3.5	3.9	6	A0B
S041	99999.9	0.0	2.0 - 4.0	4.4	9	A0AB
S042	10.2	30.0	2.0 - 4.0	4.4	9	A0AB
S043	10.2	90.0	2.0 - 4.0	4.4	9	A0AB
S044	10.2	150.0	2.0 - 4.0	4.4	9	A0AB
S045	10.2	210.0	2.0 - 4.0	4.4	9	A0AB
S046	10.2	270.0	2.0 - 4.0	4.4	9	A0AB
S047	10.20	330.0	2.0 - 4.0	4.4	9	A0AB
S048	15.0	88.0	2.0 - 4.0	3.9	9	A0AB
S049	10.0	95.0	2.0 - 4.0	3.9	9	A0AB
S051	99999.9	0.0	2.5 - 4.5	4.4	9	A0AB
S052	8.9	30.0	2.5 - 4.5	4.4	9	A0AB
S053	8.9	90.0	2.5 - 4.5	4.4	9	A0AB
S054	8.9	150.0	2.5 - 4.5	4.4	9	A0AB
S055	8.9	210.0	2.5 - 4.5	4.4	9	A0AB
S056	8.9	270.0	2.5 - 4.5	4.4	9	A0AB
S057	8.9	330.0	2.5 - 4.5	4.4	9	A0AB
S058	15.0	88.0	2.5 - 4.5	3.9	9	A0AB
S059	10.0	95.0	2.5 - 4.5	3.9	9	A0AB
S061	99999.9	0.0	3.0 - 5.0	4.4	9	A0AB
S062	10.5	30.0	3.0 - 5.0	4.4	9	A0AB
S063	10.5	90.0	3.0 - 5.0	4.4	9	A0AB
S064	10.5	150.0	3.0 - 5.0	4.4	9	A0AB
S065	10.5	210.0	3.0 - 5.0	4.4	9	A0AB
S066	10.5	270.0	3.0 - 5.0	4.4	9	A0AB
S067	10.5	330.0	3.0 - 5.0	4.4	9	A0AB
S068	15.0	88.0	3.0 - 5.0	3.9	9	A0AB
S069	10.0	95.0	3.0 - 5.0	3.9	9	A0AB
S071	99999.9	0.0	3.5 - 5.5	4.4	9	A0AB
S072	11.1	30.0	3.5 - 5.5	4.4	9	A0AB
S073	11.1	90.0	3.5 - 5.5	4.4	9	A0AB
S074	11.1	150.0	3.5 - 5.5	4.4	9	A0AB
S075	11.1	210.0	3.5 - 5.5	4.4	9	A0AB
S076	11.1	270.0	3.5 - 5.5	4.4	9	A0AB

Table 7.5.1. Spitsbergen beam table, valid from 1992/328 (23 November 1992). The table shows the name of the beam, velocity (km/sec), azimuth (degrees), filter band (Hz), STA/LTA threshold, and configuration. The configuration is described with number of sensors and a configuration code. Here, A0AB means center A0 SPZ plus A-ring plus B-ring, and A0B means A0 SPZ plus B-ring. SI01 - SI06 are incoherent beams using SPZ channels only. (Page 1 of 2)

S077	11.1	330.0	3.5 - 5.5	4.4	9	A0AB
S081	99999.9	0.0	4.0 - 8.0	4.4	9	A0AB
S082	9.5	30.0	4.0 - 8.0	4.4	9	A0AB
S083	9.5	90.0	4.0 - 8.0	4.4	9	A0AB
S084	9.5	150.0	4.0 - 8.0	4.4	9	A0AB
S085	9.5	210.0	4.0 - 8.0	4.4	9	A0AB
S086	9.5	270.0	4.0 - 8.0	4.4	9	A0AB
S087	9.5	330.0	4.0 - 8.0	4.4	9	A0AB
S091	99999.9	0.0	5.0 - 10.0	4.9	9	A0AB
S092	10.5	30.0	5.0 - 10.0	4.9	9	A0AB
S093	10.5	90.0	5.0 - 10.0	4.9	9	A0AB
S094	10.5	150.0	5.0 - 10.0	4.9	9	A0AB
S095	10.5	210.0	5.0 - 10.0	4.9	9	A0AB
S096	10.5	270.0	5.0 - 10.0	4.9	9	A0AB
S097	10.5	330.0	5.0 - 10.0	4.9	9	A0AB
S101	99999.9	0.0	8.0 - 9.0	4.9	9	A0AB
S102	9.9	30.0	8.0 - 9.0	4.9	9	A0AB
S103	9.9	90.0	8.0 - 9.0	4.9	9	A0AB
S104	9.9	150.0	8.0 - 9.0	4.9	9	A0AB
S105	9.9	210.0	8.0 - 9.0	4.9	9	A0AB
S106	9.9	270.0	8.0 - 9.0	4.9	9	A0AB
S107	9.9	330.0	8.0 - 9.0	4.9	9	A0AB
S201	99999.9	0.0	1.0 - 3.0	4.0	6	A0B
S207	99999.9	0.0	8.0 - 9.0	4.5	6	A0B
S254	99999.9	0.0	2.0 - 4.0	4.0	6	A0B
S282	99999.9	0.0	4.0 - 8.0	4.0	6	A0B
S310	99999.9	0.0	1.0 - 2.0	2.5	6	A0B
S312	99999.9	0.0	2.0 - 4.0	2.4	6	A0B
SI01	99999.9	0.0	0.5 - 1.5	3.2	6	A0B
SI02	99999.9	0.0	1.0 - 2.0	3.2	6	A0B
SI03	99999.9	0.0	1.5 - 2.5	3.0	6	A0B
SI04	99999.9	0.0	2.0 - 4.0	2.6	6	A0B
SI05	99999.9	0.0	3.5 - 5.5	2.6	6	A0B
SI06	99999.9	0.0	5.0 - 10.0	2.8	6	A0B

Table 7.5.1. (Page 2 of 2)

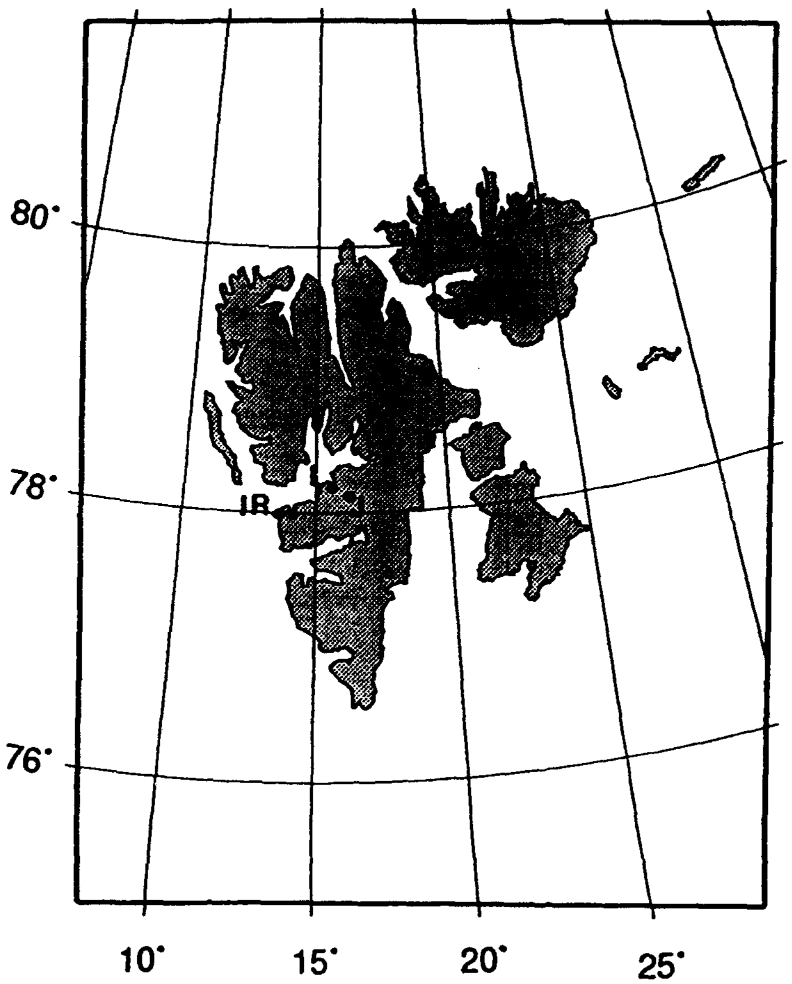

Fig. 7.5.1. This map of the Svalbard archipelago with its main island Spitsbergen shows the location of the array site at Janssonhaugen (J), the location of the array controller at Norwegian Telecom's facility at Longyearbyen (L), and the location of the NOR-SAT B earth station at Isfjord Radio (IR).

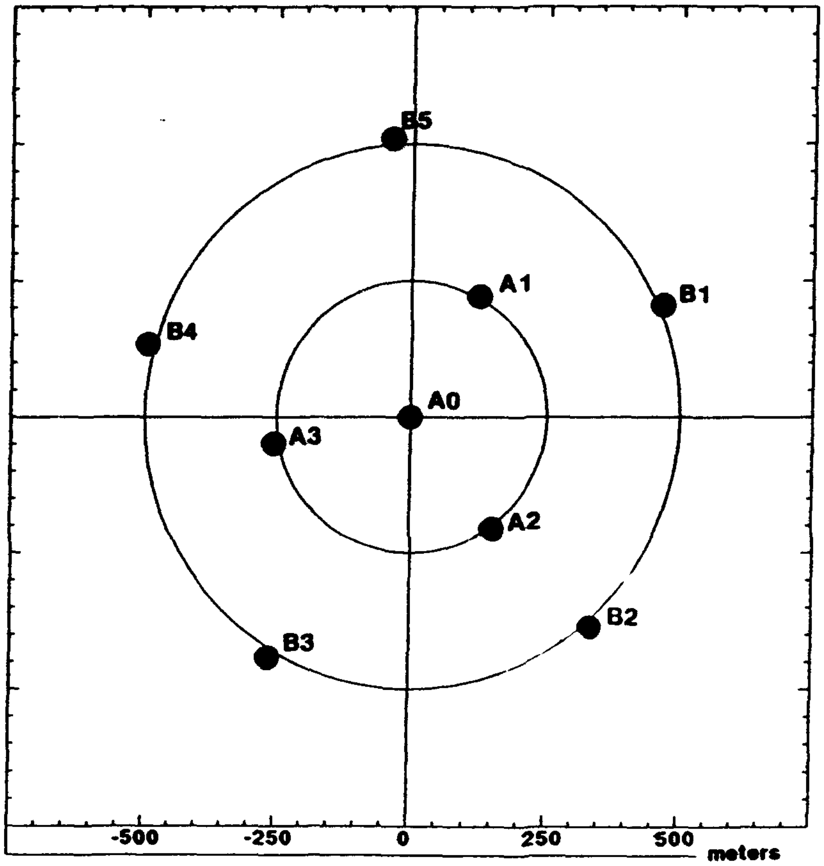

Fig. 7.5.2. Configuration of the new Spitsbergen small-aperture array.

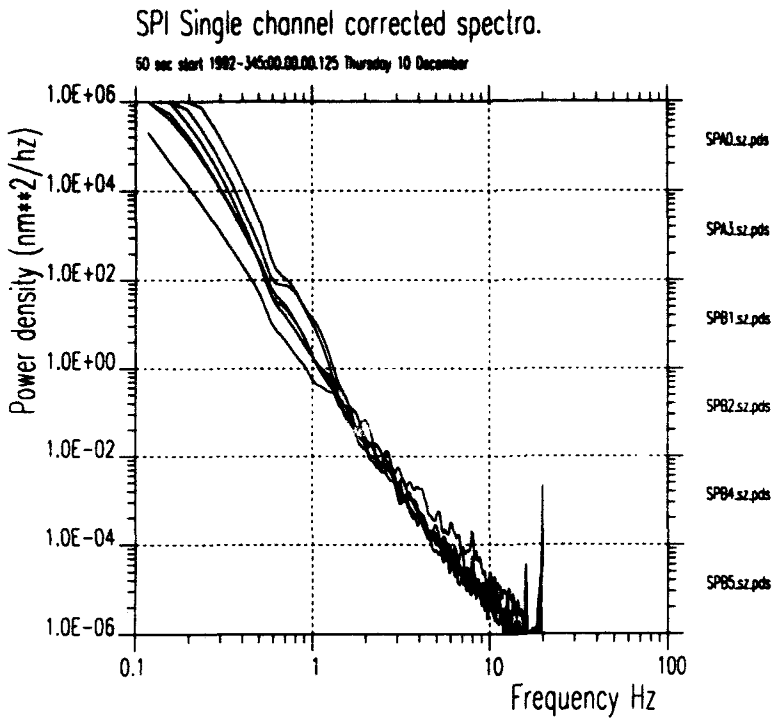

Fig. 7.5.3a. Noise spectra corrected for system response for the Spitsbergen array for 6 vertical channels. The spectra are based on one minute of data at 00.00 hours GMT on day 345, 1992. The power density is in nm^2/Hz.

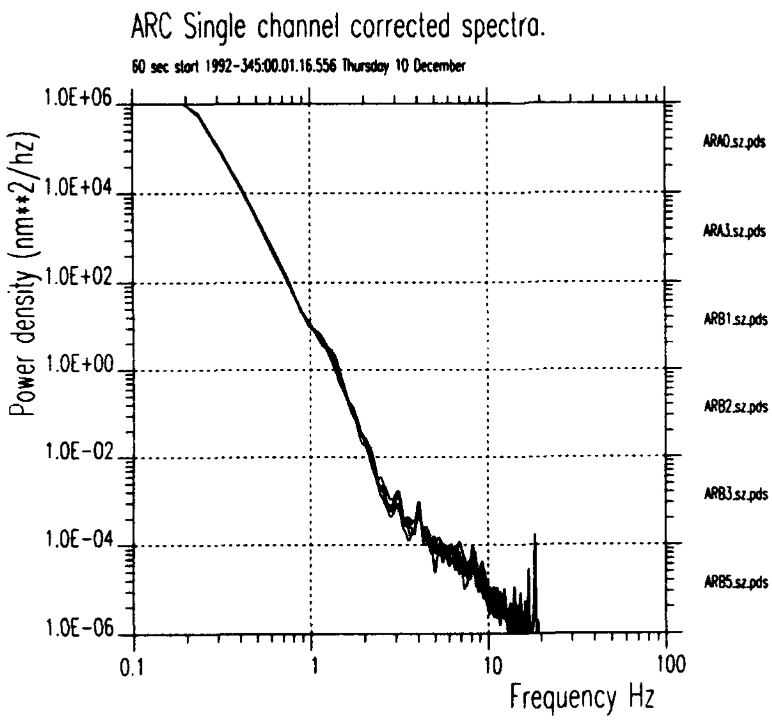

Fig. 7.5.3b. Same as Fig. 7.5.1a, but for ARCESS data taken at 00.00 hours GMT on day 345, 1992.

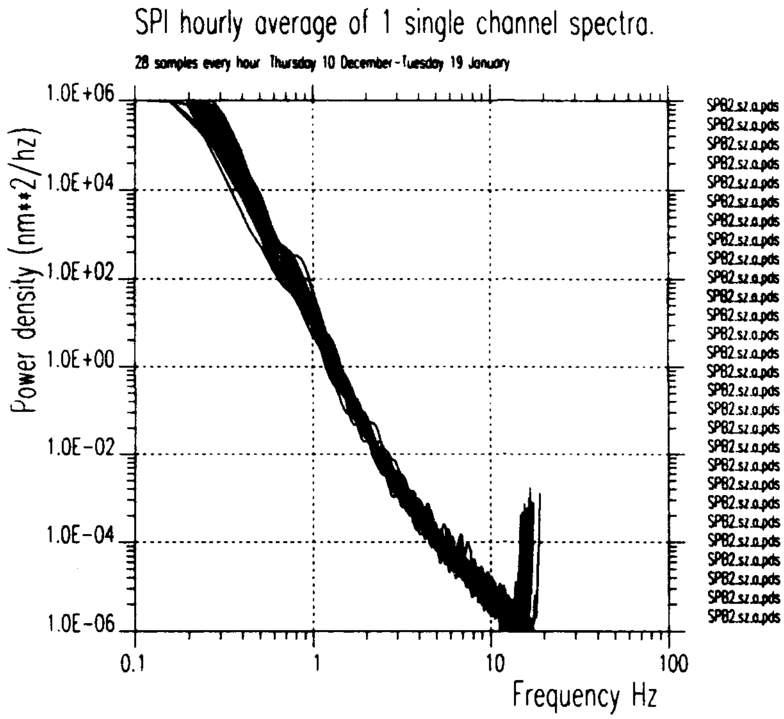

Fig. 7.5.4a. Corrected noise spectra for the Spitsbergen array for 41 one-minute intervals taken daily at 00.00 GMT from 10 December 1992 - 19 January 1993. Each spectrum represents data from the B2 SPZ seismometer.

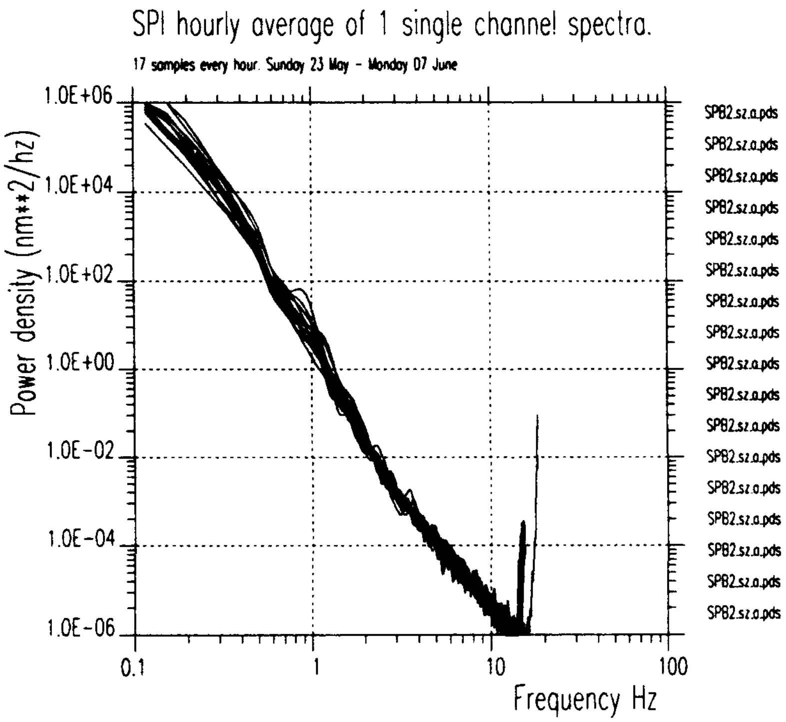

Fig. 7.5.4b. Same as Fig. 7.5.4a but for the time period 23 May - 7 June 1993.

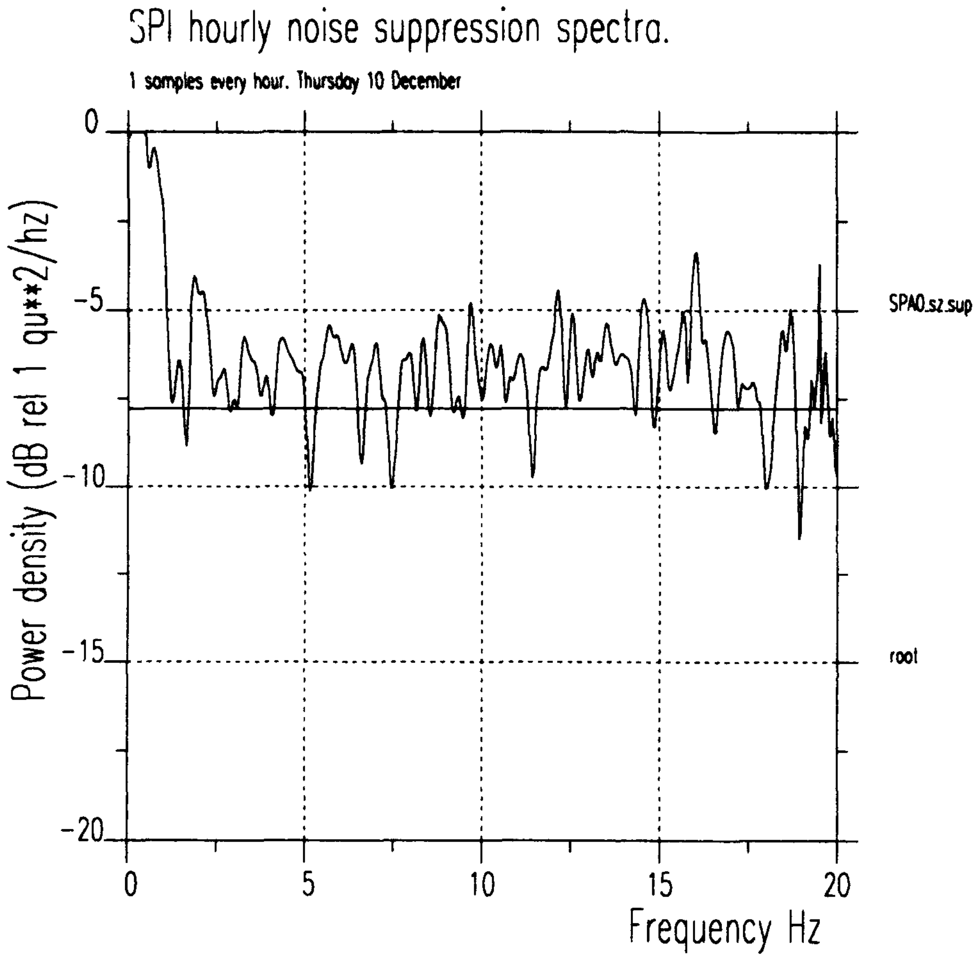

Fig. 7.5.5. Spitsbergen array noise suppression by beamforming for the initial geometry. The plot shows an average of 24 curves. To produce each of these curves, an infinite-velocity beam is formed and the spectrum for this beam is divided by the average of the single sensor spectra. The 24 curves result from one minute of data taken hourly between 00.00 and 23.00 hours GMT on day 345, 1992. The horizontal line at -8 dB represents $\sqrt{N}$ suppression for 6 sensors.

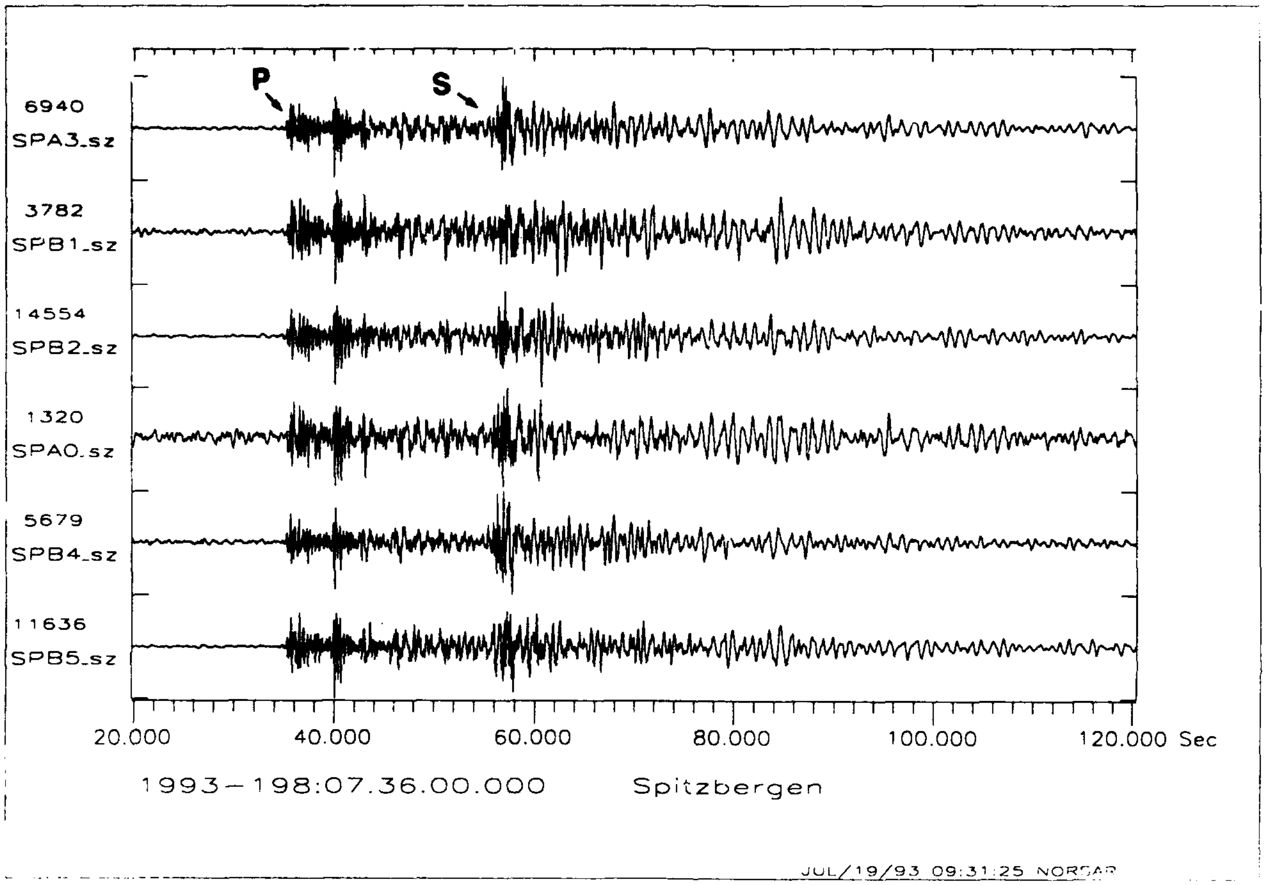

Fig. 7.5.6. Plot of individual Spitsbergen SPZ channels for the event discussed in the text. Note the very prominent amplitude variation across the array, as seen by the scale factors to the left of each trace.

a) P phase

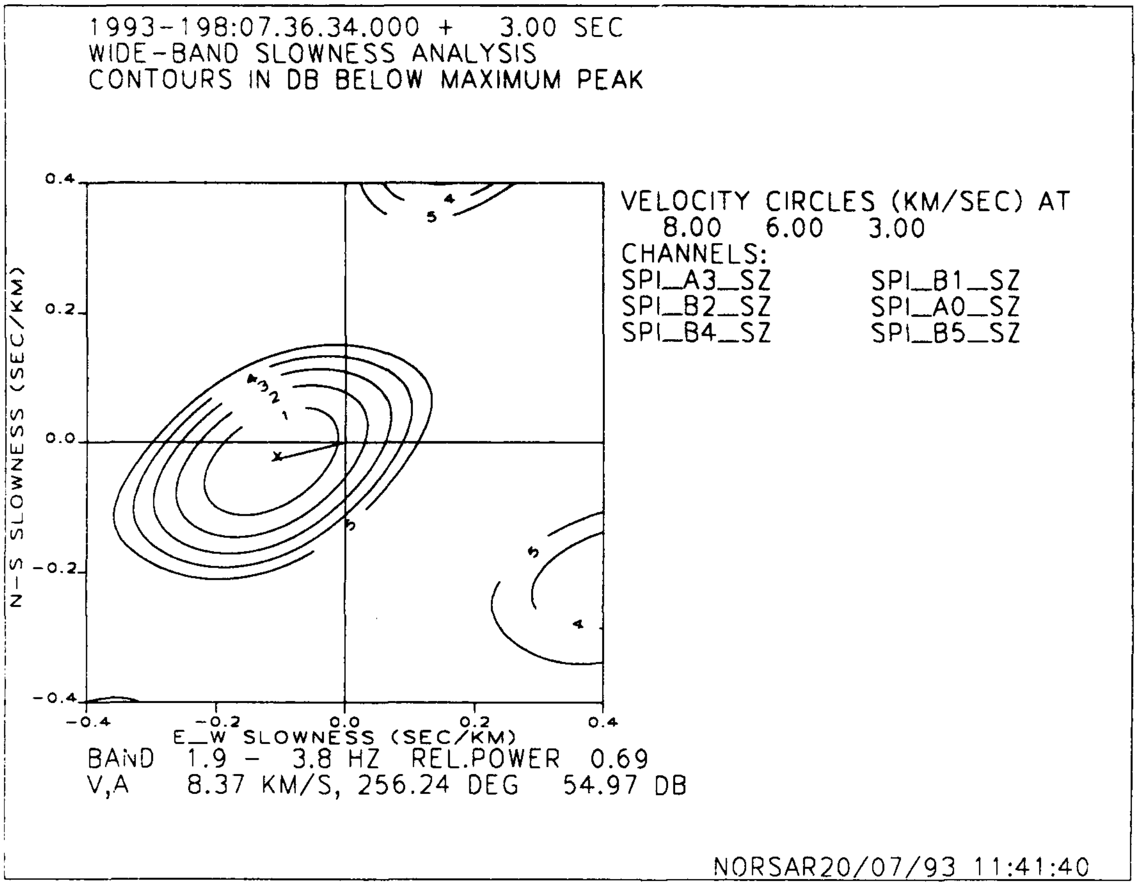

Fig. 7.5.7. Broadband F-K analysis results for the P and S phases of the event shown in Fig. 7.5.6. The figure shows a) the P phase, and b) the S phase. (Page 1 of 2).

b) S phase

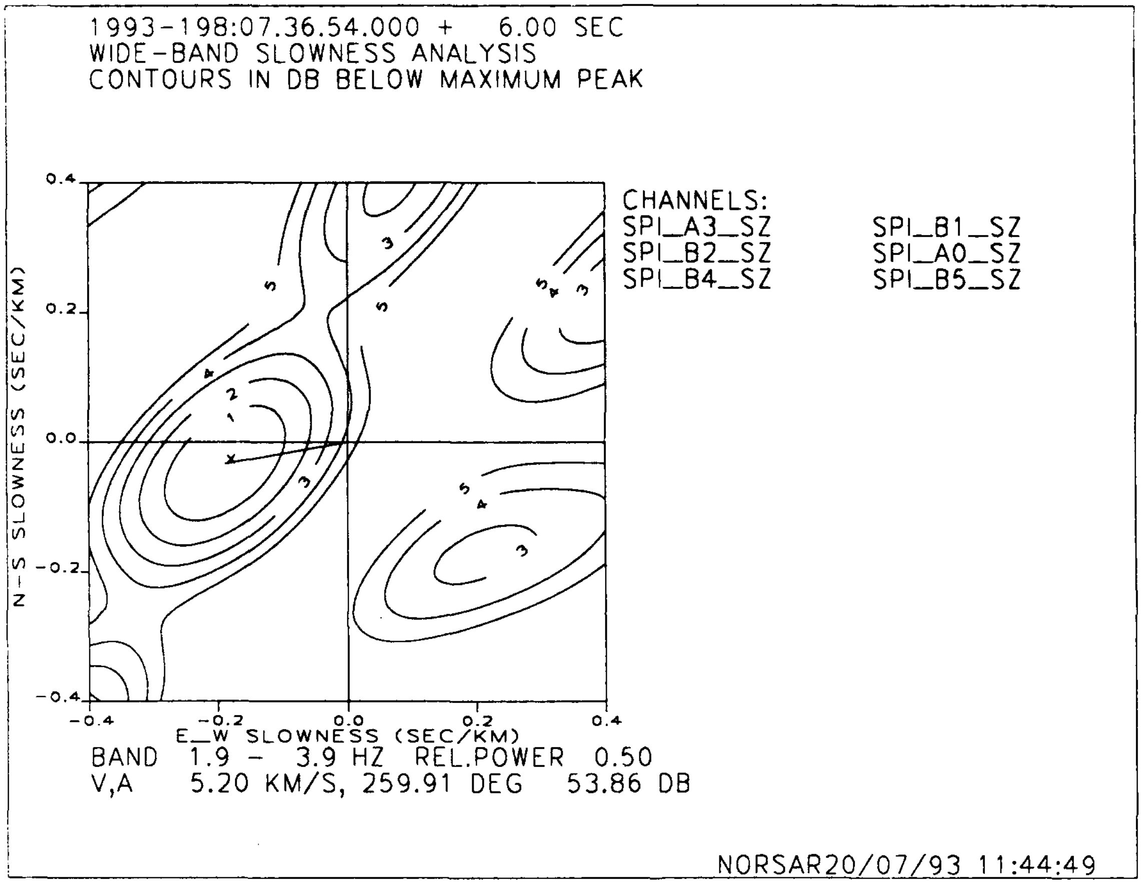

Fig. 7.5.7. (Page 2 of 2)

7.6 An evaluation of the performance of the Intelligent Monitoring System

Introduction

The Intelligent Monitoring System (IMS) is a computer hardware and software system which analyzes data from a network of seismic stations (arrays and three-component stations) to automatically detect and locate seismic events. The events automatically declared by IMS are reviewed by an analyst and modified as appropriate.

The version in current operation at NORSAR is described in Bache et al (1993). This version of IMS provides for joint processing of data from the NORESS and ARCESS arrays in Norway, the FINESA array in Finland, the GERESS array in Germany, and the new (fall of 1992) array near Apatity on the Kola peninsula of Russia (see Fig. 7.6.1). In addition, data from the array installed at Spitsbergen in November 1992 (Mykkeltveit et al, 1992) are made available to IMS for interactive analysis; i.e., detections from this array are not yet automatically associated by IMS. Based on these data sources, IMS automatically produces a bulletin of local, regional and teleseismic events. The key module used by IMS in doing this is ESAL (Expert System for Association and Location). ESAL uses the detection information resulting from the signal processing (the SigPro module, containing automatic signal detection and characterization) performed separately for each array, and forms and locates events using artificial intelligence technologies, notably in the form of rule-based reasoning.

One of the basic objectives of IMS is to provide automatic event definitions of a quality that significantly reduces the burden on the seismic analyst. Operational experience with IMS is thus taken into account to produce enhancements to the system that result in performance improvements. NORSAR has tried to assist in this process by undertaking evaluations of IMS performance following the release of new versions by SAIC, the system developer. The results of such studies are discussed with SAIC, and taken into account in the next set of enhancements to the IMS.

The subject of this study is the outcome of another such evaluation of the IMS. The performance of the system was checked carefully during a recent one-week test period, and the focus was on the performance of ESAL. The performance statistics presented in the following thus basically reflect the quality of the automatic results produced by ESAL, and not the quality of the final event definitions after analyst intervention. In addition to this, we also point to some potential for improvements in SigPro that would enhance the overall performance of IMS.

Evlauation procedure

The evaluation was conducted by NORSAR analyst and seismologist staffs, who analyzed carefully and thoroughly complete IMS data for the 7-day period 26 April - 2 May 1993. The task was threefold, namely, (i) to characterize the automatic IMS event definitions, (ii) to modify these as deemed appropriate, and (iii) to check for missed events, i.e., events that were *not* defined by IMS, but where detections were available from SigPro that should allow ESAL to associate phases and form events. Task (ii) is important in providing information on the performance of various IMS algorithms. Examples here are statistics on retiming of phase onsets and renaming of regional phases. Task (iii) above was performed through various means: The bulletin of the GBF (Generalized Beamforming) processing, which uses the detection information produced by SigPro to locate regional events, was checked to see whether it contained events not declared by IMS. Likewise, the results from the single-array "ep"-processing performed at NORSAR based on the SigPro output was checked. In addition, completely independent bulletins like the NORSAR array bulletin and the PDE bulletin of the USGS were checked, basically to identify teleseismic events that IMS might have failed to catch, even if appropriate detections were available from SigPro.

IMS automatically produces "event plots" like the one shown in Fig. 7.6.2. These plots give a good starting point for the review process, as the inferences made by ESAL in forming and locating the events can be judged from these plots. The actual assessment of all events reviewed for this one-week evaluation period was made on the basis of using the interactive analysis tools offered by the Analyst Review Station.

Each event automatically declared by IMS was assigned to one of the folllowing five categories:

Acceptable events: In addition to events accepted without any modifications, this category includes events where the anlayst made relatively minor changes. The character of these changes was such that the original IMS location was not strongly affected, i.e., the resulting change in location should be less than 50-100 km for regional events. For teleseismic events the requirements on "acceptable" events were more relaxed. The modifications in this category usually amounted to retiming of phases, association and disassociation of phases, as well as renaming of phases, especially for single-array events (e.g., from Sn to Lg or vice versa, from Pg to Px, from Rg to Lg, etc.).

Seriously mislocated events: This category includes events that are real events, but where the event location is too far away from the true location to qualify for the "Acceptable events" category. For these cases, either the phase assignments were wrong, or phases not belonging to the same event were associated.

False events: This category consists of those events declared by the IMS that the analyst rejected, believing they were not real events.

Inconclusive events: For this category, the analyst was not able to reach a definite conclusion whether the events were real or not.

Missed events: This category includes events that were *not* declared by IMS, but where detections were available from SigPro, that should permit ESAL to associate phases and form events. In addition to such events, the analyst occasionally produces events by manually adding signal arrivals that were not detected by SigPro. An example here would be a regional event for which SigPro has detected a P phase but where the S phase, though visible to the analyst during interactive waveform analysis, has gone undetected. Such events are *not* counted as missed in the statistics presented in this report.

All events in these five categories are divided into regional and teleseismic events, based on their epicentral distance from the network:

Regional events: Events where the closest station is within 20 degrees of the epicenter.

Teleseismic events: Events where the distance to the closest detecting station exceeds 20 degrees.

Results and discussion

Table 7.6.1 summarizes the results of the characterization of the events automatically declared by IMS during the one-week test period, and in addition includes statistics on events missed by IMS. As seen from this table, nearly 80% of the events declared are considered to be acceptable, whereas the majority of the remaining ones are considered to be false.

All events in the category "acceptable" were considered by the analyst to be real seismic events with automatic location estimates that were either not changed during the subsequent interactive analysis, or that were slightly modified during this process through minor changes as described in the previous paragraph. Renaming of regional phases is one example of such modifications, and Table 7.6.2 offers statistics in this regard. Only phases for which the original arrival time was changed by less than 2.0 seconds are included in this table. This is done to exclude cases where a change in phase name was accompanied by a substantial change in the phase arrival time. It is noteworthy that only for one single case was a phase changed from P- to S-type by the analyst, and there were no cases where an S-type phase was changed to P. The extent of renaming can thus be characterized as being relatively modest, meaning that the automatic phase identification in ESAL now works very well.

As seen in Table 7.6.1, altogether 105 events automatically declared by IMS were rejected by the analyst as false, based on various kinds of evidence. We have taken a closer look at these events to see if there is parametric or other kind of information available that might permit ESAL to automatically reject these events. The following observations are made:

- For 42 (all regional) of these 105 events, there is, in the judgement of the analyst, parametric information available that might be used by ESAL to preclude the formation of an event. Examples of such parametric evidence are high or low Pn velocities, and frequency content of Pn and Lg phases well outside the expected range for these phases. The formation of these events might be precluded through the addition of new rules in ESAL in the form of consistency checks on the parameters pertaining to phases used in forming these events.
- 15 (also all regional) of the false events were rejected by the analyst because they were located close to an array in the network which showed no sign of any signal arrivals from this event. (It was checked that the closest array was operating nor-

mally in these cases.) This is an expample where contextual information could be used to automatically reject an event hypothesis, and an appropriate consistency check in ESAL might rectify the situation. For several of the events in this category, also parametric information indicated that the events were false.

- Altogether 18 events (both regional and teleseismic in this category) were judged by the analyst to be so-called "split" events, i.e., phase arrivals (often coda detections) belonging to a real event were used to define an additional, false event. Sometimes the arrival azimuth estimates for the phases used to define the split event deviated by 20° or so from those of the phases used to define the real event, and it would be difficult or maybe even inadvisable to preclude formation of the second event.

We find that 27 of the false events originate from detections resulting from bad data (spikes and gaps in the data). For 5 of the events, it is not possible for the analyst to see any signal at all (not even after beamforming) in the traces, and there may be some malfunction of the detector in these cases. Possible remedies for these 32 events would amount to changes in SigPro, but it should be noted that considerable work has already been invested in preventing SigPro from declaring detections when bad data are recorded.

There are a few false regional events at distances around 10° that fall into none of the categories dealt with above. For these events, the only reason for rejecting them is the impression left after close inspection of the waveforms. The S wavetrain is impulsive and of very short duration, and thus does not match the expected shape (emergent onset and a coda of some length). It is of course very difficult to reject such events automatically, at least until the AI technology is able to match the trained eye of a skillful analyst.

As seen in Table 7.6.1, there are 15 regional events that were missed by IMS in the sense that IMS had available detection information that should allow ESAL to associate phases and form and locate events. Only one of these events had detections on more than one array, and this is a small (local magnitude 1.2) Khibiny Massif event recorded at ARCESS and the Apatity array. Three of the missed one-array events were associated with double events (two mine blasts at the same site, 10 seconds or so apart), where IMS only defined one event. For 4 of the remaining 11 missed one-array events, the arrival azimuth estimates for P and S phases differed by more than 20° (they were in the range 22.8-25.9°). This may be the reason why ESAL did not form these 4 events, but it appears that the remaining 7 events (with azimuth differences between P and S phases of less than 16.4°) should all have been formed by ESAL.

Table 7.6.1 shows that 14 teleseismic events were missed by IMS. These were events defined in the reference bulletins, and for which ESAL had detections available (from 2 or more arrays) that apparently should have been associated. It will be necessary to have a closer look at all of these to determine why they were not formed by ESAL.

Conclusions and recommendations

Our main impression after having carefully analyzed one week of data is that the overall performance of IMS is now very satisfactory. For example, the rules used for automatic phase identification in ESAL appear to work very well. It is also observed that problems associated with earlier versions of IMS have now to a large extent been solved. There is, however, still room for some improvement, as discussed above and summarized in the following.

The number of false events may appear a bit high, and we have suggested some possible remedies that might help the IMS to automatically reject some of these. Such changes must, however, be tested very carefully to make sure they do not have unintended effects, like throwing out real events. In fact, in order to make sure that the system does not miss real events, we will just have to cope with a certain number of false events. This number can probably be reduced quite a bit from today's about 20% of the total number of events automatically declared by IMS, and it must remain a goal for IMS to minimize the burden on the analyst by defining as few false events as possible.

Events missed by IMS represent a more serious problem than that of the false events. Due to the large amounts of data processed by the IMS and the limited manpower resources available for interactive analysis of the automatic IMS results, it is unlikely that the analyst review process will pick up the events missed by ESAL. Keeping in mind the basic purpose of IMS, it is therefore of utmost importance that ESAL captures all real events, for which there is a solid basis for phase association and event formation. We have seen in the aforegoing that some of the missed regional events were associated with double mining blasts. Although this is a situation where a trained analyst could pick up the missed event when inspecting the waveform traces, it will certainly present a challenge to capture all such events and at the same time avoid formation of split events. All except one of the other regional events missed were very small one-array events. Still, it is necessary to have a close look at ESAL to rectify this problem, as well as the problem of the missed teleseismic events.

As we have already seen, IMS performance could also be enhanced through certain modifications to SigPro. We will here touch upon another aspect where changes to SigPro might be beneficial: Figs. 7.6.3 and 7.6.4 provide statistics on retiming of the phases Pn and Pg, respectively, during the course of analyst review of the data for the one-week evaluation period. The figures show the differences between the arrival time as automatically determined by SigPro and the arrival time as determined by the analyst during the review process, plotted versus the SNR of the Pn or Pg phase, calculated from the detecting beam. Only phases that after analyst review retained their original, automatic phase assignment (Pn or Pg) and in addition correspond to real seismic events, are included in Figs. 7.6.3 and 7.6.4. The figures show standard deviations of the order of half a second for the differences in the arrival time estimates, and there are appreciable differences even for high SNR phases. This indicates that there should be quite some potential for improvement in the automatic estimation of phase arrival times. Section 7.2 of this Semiannual Technical Summary presents an approach that might be implemented in SigPro and that holds considerable promise to improve the automatic onset times.

The current version of IMS makes use of some region-specific knowledge. Further enhancements to IMS performance are likely to be obtained through introduction of additional such knowledge, and section 7.3 of this Semiannual Technical Summary demonstrates how event locations may be significantly improved using region-specific knowledge.

S. Mykkeltveit **U. Baadshaug** **B.Kr. Hokland**
T. Kværna **L.B. Loughran**

References

Bache, T., S.R. Bratt, H.J. Swanger, G.W. Beall and F.K. Dashiell (1993): Knowledge-based interpretation of seismic data in the Intelligent Monitoring System, *Bull. Seism. Soc. Am.*, in press.

Mykkeltveit, S., A. Dahle, J. Fyen, T. Kværna, P.W. Larsen, R. Paulsen, F. Ringdal and I. Kuzmin (1992): Extensions of the Northern Europe Regional Array Network -- New small-aperture arrays at Apatity, Russia, and on the Arctic island of Spitsbergen, in *Semiannual Technical Summary 1 April - 30 September 1992*, NORSAR Scientific Report No. 1-92/93, Kjeller, Norway.

	Regional	Tele-seismic	Total
Acceptable events	384	67	451
Seriously mislocated events	5	4	9
False events	97	8	105
Inconclusive	0	4	4
Total number of events declared			569
Missed events	15	14	29

Table 7.6.1 Characterization of all events automatically declared by IMS during the seven-day period 26 April - 2 May 1993 (see text for explanation of the various categories). The table also includes statistics on events missed by the IMS.

Analyst

ESAL

	Pn	Pg	Px	Sn	Lg	Rg	Sx
Pn	213	19	2				
Pg	11	203	24	1			
Px	2	2	60				
Sn				34	5		9
Lg				7	325	7	24
Rg					6	30	7
Sx				1	20		75

Table 7.6.2 The table shows the ESAL automatic phase assignments versus analyst assignments made during interactive analysis, for all regional phases that were used by IMS to define regional events during the time period 26 April - 2 May 1993.

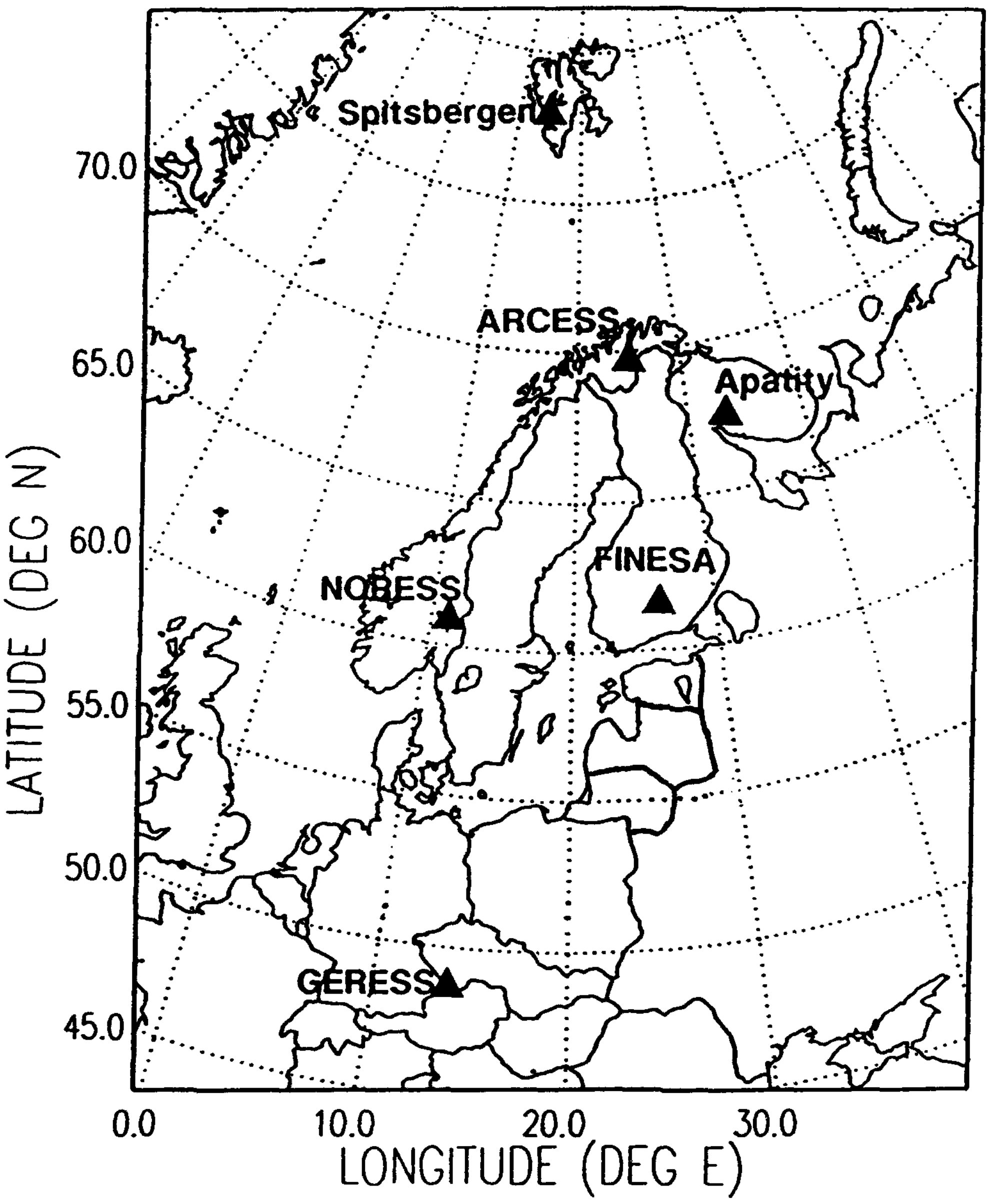

Fig. 7.6.1 The network of six regional arrays in northern Europe.

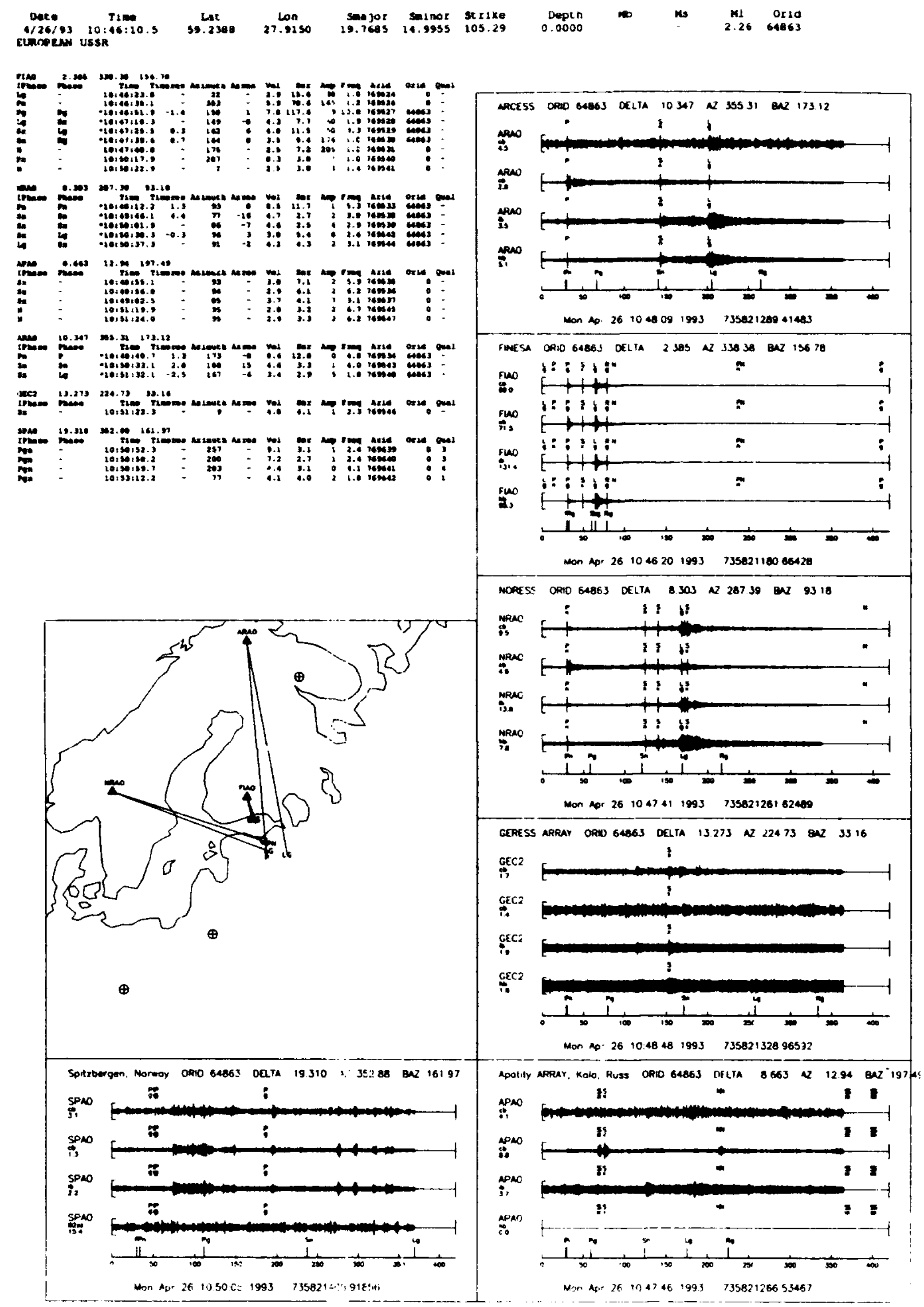

Fig. 7.6.2. A typical example of a plot automatically produced by IMS, basically showing the judgements and inferences made by ESAL in associating phases at the various arrays and forming this event in Estonia.

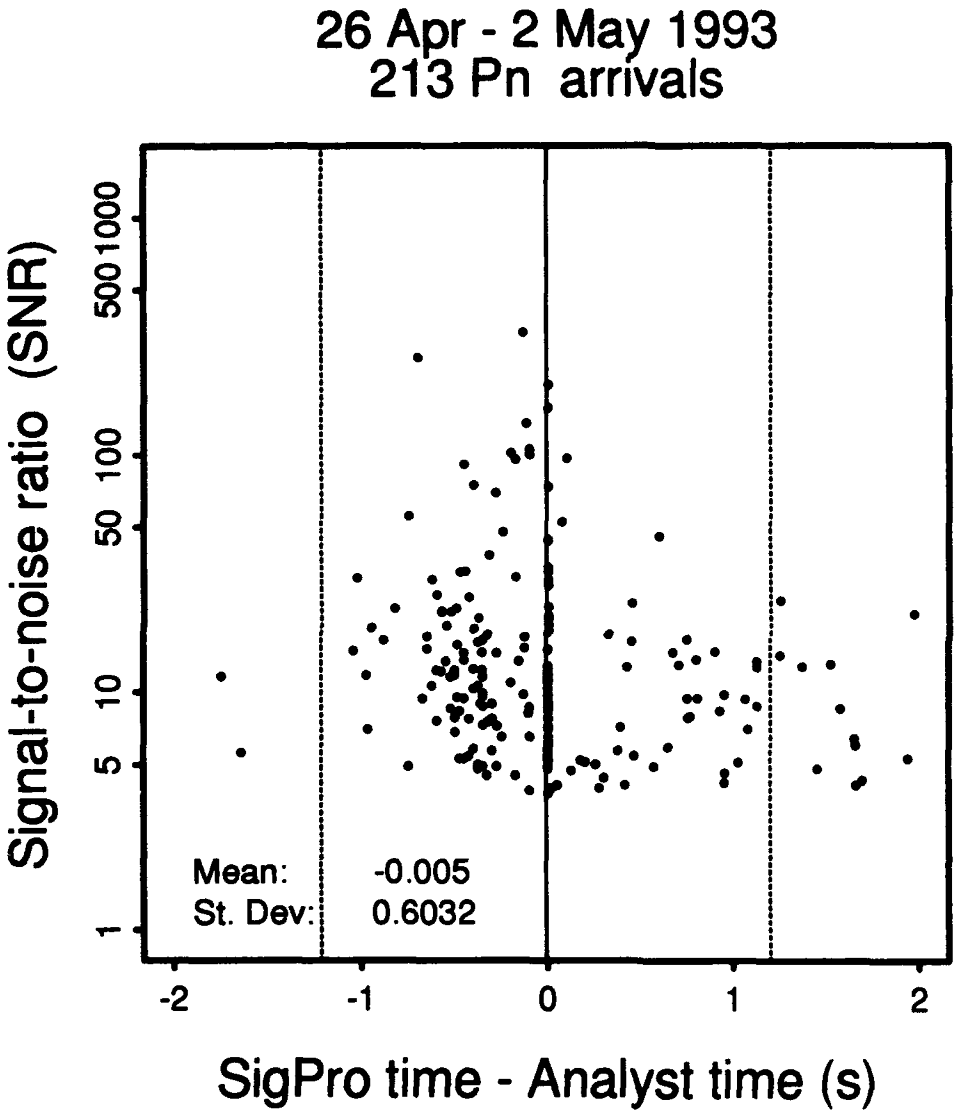

Fig. 7.6.3. The figure shows differences between arrival times as determined by SigPro and arrival times determined by the analyst during review, plotted versus SNR, for Pn phases used by IMS to form events during the evaluation period 26 April - 2 May 1993. The mean value of the arrival time differences is marked by a solid vertical line, whereas the two strippled lines denote ± 2 standard deviations.

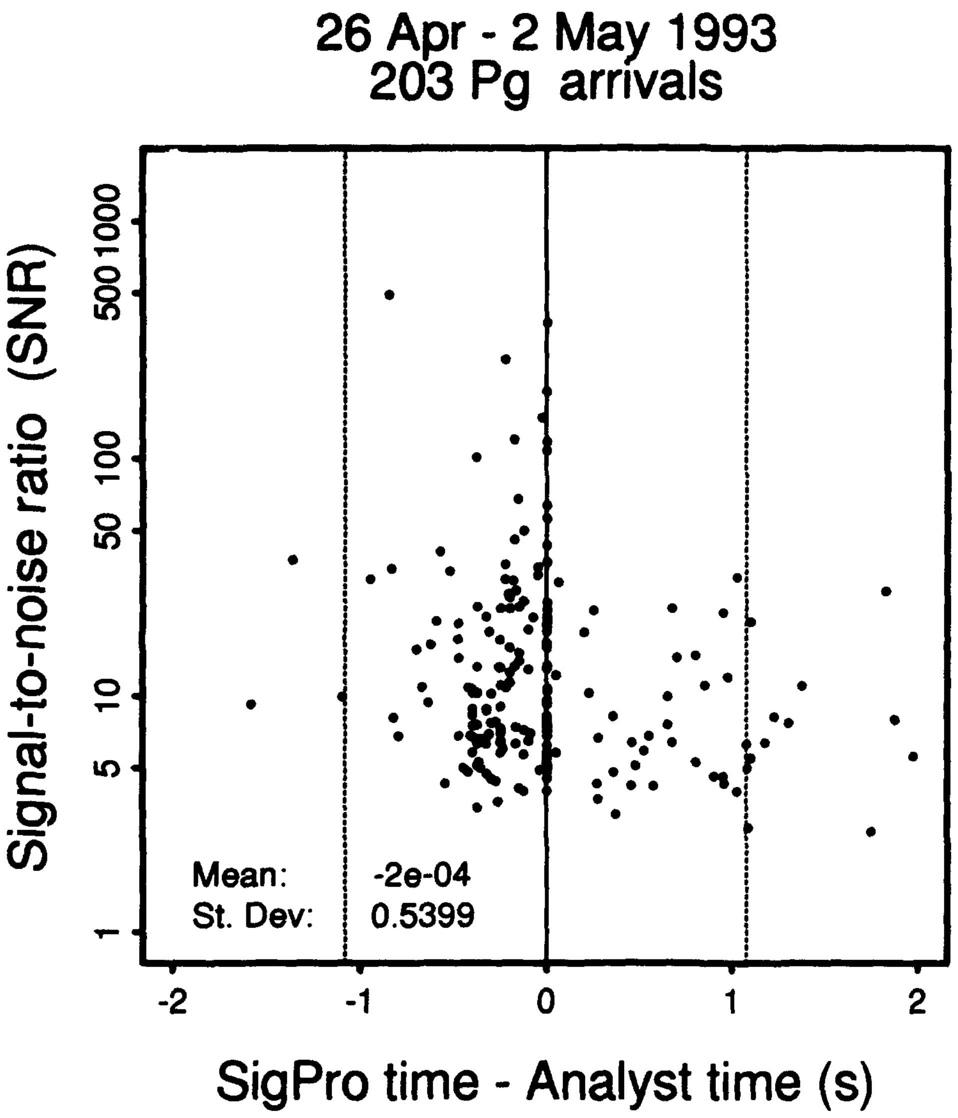

Fig. 7.6.4. Same as Fig. 7.6.3, but for the Pg phase.